CHARLES UNIVERSITY IN PRAGUE

Faculty of Science

Developmental and Cell Biology

Identification and Characterization of Main Genetic Components Involved in Phototransduction and Vision of the Cubozoan Jellyfish *Tripedalia Cystophora*

Ph.D. Thesis

Michaela Liegertová

Supervisor: Zbyněk Kozmik, Ph.D.

Department of Transcriptional Regulation

Institute of Molecular Genetics of the ASCR, v. v. i.

Prague, 2016

DECLARATION

I declare that I wrote the thesis independently and that I cited all the information sources and literature. This work or a substantial part of it was not presented to obtain another academic degree or equivalent.

Prague, 15. 06. 2016 Michaela Liegertová

ACKNOWLEDGEMENTS

I would like to take this opportunity to thank my supervisor, Dr. Zbyněk Kozmik for his excellent leadership and for all the valuable things he taught me – in science and life.

I would like to thank my colleagues from Lab 29, for all the help and support. My special thanks belong to Pavel Vopálenský and Jiří Pergner for their guidance and mental support, and to Chrysa Pantzartzi for her precious advice considering this thesis. My special thanks belong to Ondřej Svoboda, for being my friend all these years at the institute.

Finally, I would like to thank my husband Richard for his great support and patience and for all the hours he had to substitute me as a mother for our kids. Last but not least I would like to thank my whole family for their support during my studies and thesis writing.

FINANCIAL SUPPORT

This work was supported by the Grant Agency of the Czech Republic (P305/10/2141), Ministry of Education, Youth and Sports of the Czech Republic (LO1220) and by IMG institutional support RVO68378050.

TABLE OF CONTENT

LIST OF ABBREVIATIONS

11-cis-Ral	11-cis retinal
454	large-scale parallel pyrosequencing system
A. marsupialis	*Alatina marsupialis*
aa	amino acids
AC	adenylyl cyclase
ad. female	adult female
all-cis-RDH	all-cis-retinol dehydrogenase
all-trans-RDH	all-trans-retinol dehydrogenase
all-trans-R-ester	all-trans-retinyl ester
all-trans-Rol	all-trans retinol
aLRT	approximate likelihood-ratio test
AP1, AP2	nested adapter primers
ARR	arrestin
BL21 DE3-RIPL	high-level protein expression strain of *E. coli*
bp	base pairs
BSA	bovine serum albumin
C. rastonii	*Carybdea rastonii*
C1 – C3	bovine rhodopsin cytoplasmatic loops
cAMP	cyclic adenosine monophosphate
Caryb	*Carybdea rastonii* opsin (homolog of Tcop13)
cDNA	complementary DNA
cGMP	cyclic guanosine monophosphate
Ch. bronzie	*Chiropsela bronzie*
CL	ciliary layer of the retina
CNG	cyclic nucleotide-gated ion channel
CNOP2	*Acropora millepora* opsin
c-opsins	ciliary opsin (opsin from ciliary photoreceptors)
Cp	crossing point values
CRALBP	cellular retinaldehyde-binding protein

CRBP	cellular retinoid-binding proteins (intracellular carrier protein)
Crop	*Cladonema radiatum* opsin
D. melanogaster	*Drosophila melanogaster*
DAG	diacylglycerol
E. coli	*Escherichia coli*
E181	glutamic acid residue at 181 position of the peptide chain
E1-E3	bovine rhodopsin extracellular loops
E-box/M-box	enhancer box – sequences in promotor
G protein	guanine nucleotide-binding protein
G	relative centrifuge force
gastric p.	gastric pouch
GC	guanylyl cyclase
GFP	green fluorescent protein
Gi	G(i) alpha subunit of the heterotrimeric G protein
GMP	guanosine monophosphate
GNA	guanine nucleotide binding protein alpha
GNAI	guanine nucleotide binding protein alpha - inhibiting activity
GNAO	guanine nucleotide-binding protein alpha - “other” activity
GNAQ	guanine nucleotide-binding protein alpha - “q”
GNAS	guanine nucleotide binding protein alpha - stimulating activity
Go	G(o) alpha subunit of the heterotrimeric G protein
GPCR	G protein coupled receptor
Gq	G(q) alpha subunit of the heterotrimeric G protein
GRK1	rhodopsin kinase 1 (rho kinase1)
Gs	G(s) alpha subunit of the heterotrimeric G protein
GSP1, GSP2	nested gene specific primers
GST-Tag	glutathione S-transferase-tag for protein pull-down assay
Gt	G(t) alpha subunit of the heterotrimeric G protein
GTP	guanosine triphosphate
Gx	*T. cystophora* specific variant of G(s)

Gβγ	G protein beta/gamma complex
H. sapiens	*Homo sapiens*
H1 - H8	bovine rhodopsin transmembrane domains
His	histidine
His-tag	polyhistidine-tag
HKQ	histidine-lysine-glutamin residues of the corresponding protein
Hmop	*Hydra magnipapillata* opsin
HP2X1	human purinergic receptor P2X1
IHC	immunohistochemistry
IP_3	inositol-1,4,5-trisphosphate
IPTG	isopropyl-beta-D-thiogalactopyranoside
IRBP	interphotoreceptor retinoid-binding protein
juv. med.	juvenile medusa
K296	lysine residue at position 296 of the peptide chain
L	lens
L. vulgaris	*Loligo vulgaris*
LA	compact layer
LB	lysogeny broth medium
LED	light-emitting diode
LLE	lower lens eye
LRAT	lecithin retinol acyltransferase
LUC	luciferase
LWS	long wave sensitive opsin
M/LWS	medium to long wave sensitive opsin
manb.	manubrium
metam	polyp-to-medusa metamorphosing stages
Mitf	microphthalmia-associated transcription factor
ML	maximum likelihood
MOPS	N-morpholino-propanesulfonic acid fixative
MWS	medium wave sensitive opsin

NF023	subtype-selective P2X1 receptor antagonist
NF449	selective P2X1 receptor antagonist
Ni-NTA	nickel-charged affinity resin used to purify recombinant proteins
NKQ	asparagine-lysine-glutamin tripeptide
np. larva	non-pigmented larva
NRS	asparagine-lysine-histidine tripeptide
NT	not transfected cells used as negative control
Nvop	*Nematostella vectensis* opsin
O. latipes	*Oryzias latipes*
OD600	optical density measured at 600 nm
Otx2	orthodenticle homeobox 2
outer um.	outer umbrella
p	pit eye
p. larva	pigmented larva
P2X1	purinergic receptor P2X1
PBS	phosphate buffer saline
PBT	phosphate-buffered saline with 0.1% Tween
PDE	phosphodiesterase
PDE6	phosphodiesterase subunit 6 (vertebrate visual)
PFA	paraformaldehyde
PIP_2	phosphatidylinositol 4, 5-bisphosphate
PL	pigment layer of the retina
PLC	phospholipase C
PRC1	type-1 photoreceptor
PRC2	type-2 photoreceptor
PTU	phenylthiourea (phenylthiocarbamide)
PVDF	polyvinylidene difluoride membrane
qRT-PCR	quantitative real-time PCR
RACE	rapid amplification of cDNA ends
RCV1	recoverin 1

RGR	retinal G protein coupled receptor
Rh1	rhodopsin
Rh2	rhodopsin 2
Rho kinase	rhodopsin kinase1 (G protein-coupled receptor kinase 1)
RLU	relative light units
r-opsin	rhabdomeric opsin (opsin from rhabdomeric photoreceptors)
RPE	retinal pigment epithelium
RPE65	isomerohydrolase RPE65
Rpl32	ribosomal protein L32
rpm	rotations per minute
s	slit eye
SDS-PAGE	dodecyl sulfate polyacrylamide gel electrophoresis
SKS	histidine-lysine-histidine tripeptide
sub-um.	sub-umbrella
SWS	short wavelength sensitive opsin
Tcop	*T. cystophora* opsin
tentac.	tentacles
TMT	teleost multiple tissue opsin subfamily
TMT	teleost multiple tissue opsins
Tripe	*T. cystophora*
Tris.HCl	Tris(hydroxymethyl)aminomethane chloride
TRP	transient receptor potential channels
ULE	upper lens eye
VAOP	vertebrate ancient opsins
veg. polyp	vegetative polyp

ABSTRACT (English)

Many of the metazoan phyla sense light by an opsin-based photopigment present in a photosensitive receptor cell (photoreceptor), with Cnidaria being arguably the earliest branching phylum containing a well-developed and complex visual system (advanced eyes morphologically similar to those of vertebrate). The evolutionary history of phototransduction and visual components (ranging from light-sensing opsins to structural genes of the lenses) is a long standing question. In this work, we decided to address this issue by applying a comprehensive multidisciplinary approach combining modern molecular biology methods with bioinformatics. Comprehensive genome-wide inspection of a cubozoan jellyfish *Tripedalia cystophora,* was complemented with gene expression analyses, together with functional (cell culture based assays) and behavioural (pharmacogenetics) testing.

First, genome analysis uncovered the presence of a surprisingly large number of opsin genes with distinct tissue- and stage-specific expression. Our extensive phylogenetic analysis classified cubozoan opsins as a sister group to c-type opsins and documented a lineage-specific expansion of opsin gene repertoire. Functional tests in cell cultures provided evidence for the use of Gs-cAMP signalling pathway only in a small subset of opsins, indicating that the majority of cubozoan opsins likely signal by a distinct, yet unidentified pathway. In addition, these functional tests uncovered subtle differences among individual cubozoan opsins, suggesting a possible fine-tuning for specific photoreceptor tasks. The opsin expression data led to identification of two distinct photoreceptors in the retinas of *T. cystophora*, revealing yet another level of complexity of cubozoan advanced eyes. Furthermore, novel opsin expression domains were documented for the first time. Finally, genome analysis revealed the presence of vertebrate-like phototransduction cascade components, together with additional structural proteins of the lenses.

ABSTRAKT (Česky)

Mnoho živočichů vnímá světlo pomocí fotoreceptorů, obsahujících světločivný pigment, jehož základ tvoří protein opsin. Žahavci jsou bezesporu první živočišný kmen, u kterého můžeme nalézt dobře vyvinutý a komplexní zrakový systém (komplexní oči morfologicky podobné očím obratlovců). Evoluční historie fototransdukce a vzniku jednotlivých zrakových komponent (od světločivných opsinů po strukturální geny čoček) zůstává dodnes sporná. V této práci jsme se rozhodli k tématu přistoupit s využitím širokého multidisciplinárního přístupu, kombinujícího moderní metody molekulární biologie a bioinformatiky. Podrobná celogenomová analýza čtyřhranky trojité (*Tripedalia cystophora*), byla doplněna analýzami genové exprese, funkčními testy v buněčných kulturách a farmakogenetickým testováním (behaviorální testy).

Za prvé, v genomu byl odhalen překvapivě velký počet genů pro opsiny se zřetelnou tkáňově a vývojově specifickou expresí. Rozsáhlá fylogenetická analýza vedla k vymezení opsinů čtyřhranek jako sesterské větve k c-opsinům a ke zmapování expanze opsinů v této živočišné linii. Funkční testy v buněčných kulturách odhalily, že Gs-cAMP signalizace je typická pouze pro malou podskupinu opsinů a naznačily, že většina opsinů čtyřhranek signalizuje odlišnou a doposud neidentifikovanou kaskádou. Dále funkční testy odhalily jemné rozdíly mezi jednotlivými opsiny, což naznačuje možné "vylaďovaní" pro specifické úlohy daných fotoreceptorů. Analýzy exprese genů vedly k identifikaci dvou odlišných fotoreceptorů v sítnici *T. cystophora* a poukázaly tak na další úroveň komplexity jejích očí. Data, získaná z výzkumu exprese genů vedla také k odhalení zcela nových domén exprese opsinů. V neposlední řadě studium genomu vedlo k odhalení dalších fototransdukčních komponent (připomínajících fototransdukční kaskádu obratlovců) a nových strukturních proteinů čoček.

INTRODUCTION AND BACKGROUND

Many of the metazoan species sense light for vision and nonvisual photoreceptions. The importance of the ability to detect spatial differences in ambient light levels could be documented by the fact that 96% of the known species alive today possess image-forming eyes. These species represent six of over 30 extant metazoan phyla, namely Cnidaria, Mollusca, Onychophora, Annelida, Arthropoda, and Chordata (Land and Fernald 1992, Land and Nilsson 2002).

To talk about vision one must clearly define the "minimal" eye – a photoreceptor in the close vicinity of a shading pigment. This concept could be exemplified by dorsal ocelli of the cephalochordate *Branchiostoma floridae* (Lacalli 2004) or paired larval eyes of the annelid *Platynereis dumerilii* (Arendt et al. 2004). This minimal eye consists of either a single photoreceptor cell containing photosensitive molecules and a pigment cell which redirects the incoming light to a certain direction (two-cell eye prototype – Fig.1), or both these functions could be performed by a single photosensitive cell housing both a photopigment and a shading pigment (as defined by Arendt and Wittbrodt 2001).

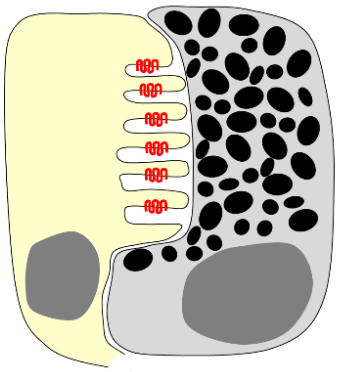

Fig. 1: **Concept of the minimal eye.**

a) Schematic representation of the two-cell prototype eye as seen in larvae of the annelid *Platynereis dumerilii* (Arendt et al. 2002). The eye is composed of a single photoreceptor cell (photosensitive neuron - photopigment shown in red) adjacent to a dark pigment bearing cell.

Such a minimal eye enables the distinction of light from dark, without the ability to utilize complex light patterns. During the course of evolution, invagination of such eyespot into a pit would add the capacity to detect the directionality of the incoming

light. In the next steps, the addition of more photoreceptors leading to a chambered eye and addition of an optical system (e.g. lenses - to achieve sufficient refractive power for underwater vision) that could increase light collection and produce an image, increased the usefulness of an eye substantially. Advanced eyes deliver more sophisticated information about wavelength, contrast, and light polarization (as argued and reviewed by Land and Fernald 1992, Nilsson and Pelger 1994, Arendt and Wittbrodt 2001, Land and Nilsson 2002, Fernald 2006).

A common indispensable basis of all animal eyes are the photoreceptor cells, containing a photopigment connected to a downstream phototransduction cascade. Based on their morphology they could be classified into rhabdomeric or ciliary photoreceptors (Fig. 2).

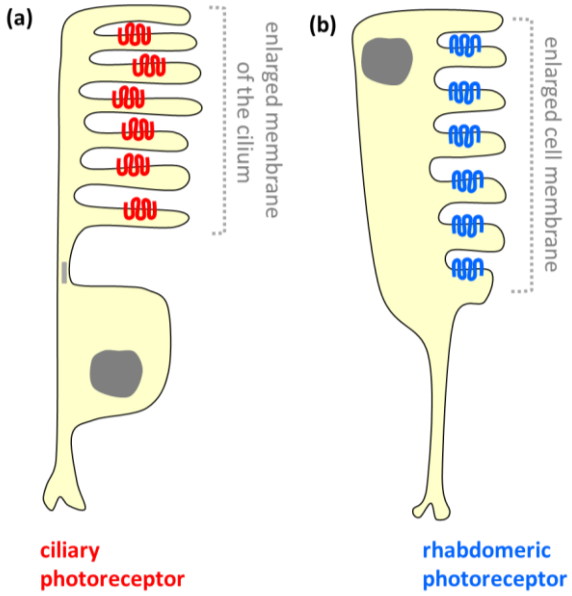

Fig. 2: Simplified representation of the two basic types of photoreceptors.

a) Ciliary photoreceptor cell type, where the photopigment (in red) is contained in many membrane discs of highly specialized sensory cilia. b) Rhabdomeric photoreceptor cell type, where photoreceptive area housing the photopigment (in blue) is derived from microvilli.

Rhabdomeric photoreceptors bear visual pigments in the membrane protrusions as a part of the apical cell surface, while the ciliary photoreceptors fold the membrane of the cilium (Eakin 1982, Yamada 1982, Arendt 2003). The two photoreceptor types are considered „sister cell types“ and seem to share common evolutionary history as they probably evolved from one common precursor by cell type diversification (Arendt 2003).

On the molecular level, both types of photoreceptors use a vitamin-A-based light sensitive photopigment, comprising of a chromophore retinal and of the apoprotein opsin. The process of phototransduction activation always requires the binding of a photoactivated opsin to the corresponding G alpha subunit of a G protein (Kuhn et al. 1981), as well as the subsequent deactivation of the involved cascade by e.g. rhodopsin kinase, which phosphorylates the photoactivated opsin, or by arrestin which competes with the G alpha subunit of the corresponding G protein for binding to opsin (Pfister et al. 1985, Krupnick et al. 1997).

Rhabdomeric photoreceptors have been repeatedly shown to mediate vision in the various eyes of invertebrates, in contrast to the exclusive ciliary mode found in the eyes of vertebrates (as discussed and reviewed in Land and Fernald 1992, Arendt and Wittbrodt 2001, Land and Nilsson 2002). The physiological responses of these two types of photoreceptors also differ substantially. The rhabdomeric receptors of arthropods and molluscs activate Gq type of G protein alpha subunits as the first step and depolarize in reaction to light, whereas receptors of vertebrates activate Gt type (called transducin) and hyperpolarize to light (Fig. 3).

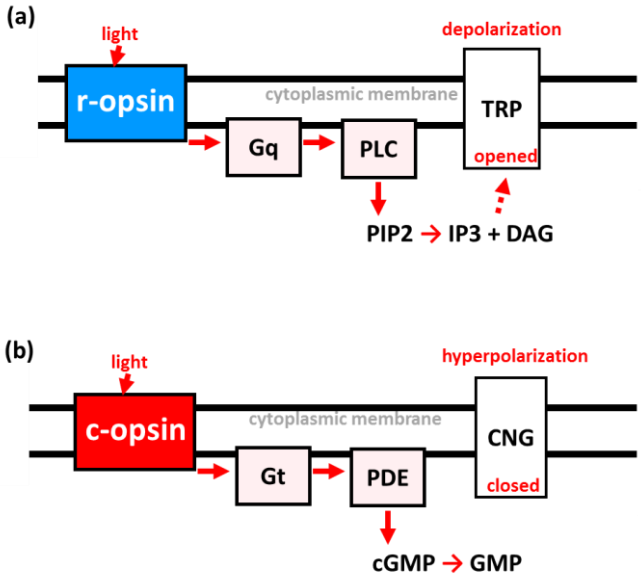

Fig. 3: Simplified scheme of invertebrate and vertebrate phototransduction cascades.

a) In *Drosophila melanogaster*, light activated r-opsin activates the Gq type alpha subunit of the corresponding G protein, which in turn activates phospholipase C (PLC). Phospholipase C catalyses the hydrolysis of phosphatidylinositol 4, 5-bisphosphate (PIP_2) into diacylglycerol (DAG) and inositol 1,4,5-trisphosphate (IP_3). The subsequent influx of Ca^{2+} ions activates transient receptor potential channels (TRP) leading to depolarization (as reviewed in Hardie and Juusola 2015) b) In human and other vertebrates light activated c-opsin activates transducin (Gt), leading into stimulation of phosphodiesterase (PDE), which breaks down cGMP to GMP. The drop in the concentration of cGMP causes the closure of cyclic nucleotide-gated ion channels (CNG) and hence leads to hyperpolarization (as reviewd in Koch and Dell'Orco 2015).

The transducin subfamily of G alpha subunits is not present in invertebrates and probably originated during vertebrate-specific whole-genome duplications from the Gi type protein subfamily (Nordstrom et al. 2004, Milligan and Kostenis 2006). Consistently with this assumption, a Gi type alpha subunit is expressed in the ciliary photoreceptors of tunicate *Ciona intestinalis* (Yoshida et al. 2002). cGMP and inositol trisphosphate are used as second messenger systems for phototransduction, by vertebrate and invertebrate photoreceptors, respectively.

As important as the processes leading to phototransduction activation are, it is necessary to address the issue regarding the transduction shut off as well. The deactivation of phototransduction is a complex process, still being investigated (for review see Burns and Arshavsky 2005, Luo et al. 2008, Koch and Dell'Orco 2015). For

complete deactivation in vertebrate-like cascades, each of the components must shut down. Activated rhodopsin (metarhodopsin II) is phosphorylated by a rhodopsin kinase (GRK1) (Bownds et al. 1972, Sakurai et al. 2015) in a Ca^{2+} dependent manner via the Ca^{2+} binding protein recoverin (RVC1) (Chen et al. 1995, Zang et al. 2015), followed rapidly by the binding of arrestin (ARR) (Kuhn et al. 1984, Pfister et al. 1985, Chatterjee et al. 2015, Deming et al. 2015). Eventually, after decay, rhodopsin loses the bound arrestin and is dephosphorylated by a generic phosphatase (Palczewski et al. 1989). Another protein – phosducin (PDC) - serves for modulation of the activation cascade by direct interaction with the beta and gamma subunits of the involved trimeric G protein, leaving the Gt alpha subunit (transducin) active for longer period to increase the amount of time for visual excitation (Fig. 4) (Watanabe et al. 1990, Belcastro et al. 2012).

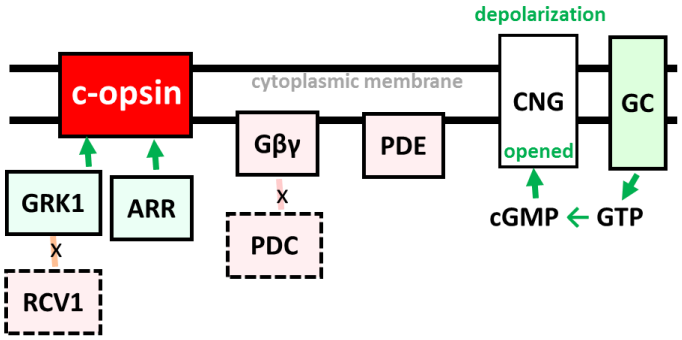

Fig. 4: Phototransduction inhibition in vertebrates.

When the calcium levels drop during phototransduction activation, calcium dissociates from recoverin 1 (RCV1) followed by release of the bound rhodopsin kinase 1 (GRK1). GRK1 phosphorylates the activated c-opsin, lowering its affinity to transducin (not depicted in the figure). The phosphorylated opsin is completely deactivated by binding of arrestin (ARR). Dissociation of phosducin (PDC) from beta/gamma complex (Gβγ) of the G protein promotes re-association of all the subunits, modulating the amount of the free active transducin. Guanylyl cyclase (GC) transforms GTP to cGMP to allow the reopening of the cyclic nucleotide-gated ion channels (CNG) leading to depolarization. PDE – phosphodiesterase.

The mode of the photopigment regeneration/re-izomeration differs substantially between the vertebrate and invertebrate types of phototransduction (for review see Travis et al. 2007, Yau and Hardie 2009, Hardie 2014, Hardie and Juusola 2015, Koch and Dell'Orco 2015, Molday and Moritz 2015, Yang et al. 2015). In vertebrate-like cascades activation of the photopigment leads to the release of its chromophore, which is then

recycled in a multi-enzymatic pathway – the visual (retinoid) cycle. This is in contrast with the situation in invertebrates, e.g. *D. melanogaster*, where the chromophore is bistable (light-activated chromophore is not released after photoisomerization, but the absorption of a second photon promotes the regeneration to the active form; for review see Hardie and Juusola 2015).

In the vertebrate rod, light isomerizes 11-cis-retinal to all-trans-retinal. Thereafter, all-trans-retinal is reduced to all-trans-retinol, which is transported (with help of an extracellular carrier) to the overlying retinal pigment epithelial (RPE) cell. In these cells, all-trans-retinol is re-converted into 11-cis-retinol, subsequently to 11-cis-retinal, and then returned back into the photoreceptor for recombination with opsin protein to reform the visual pigment (for review see Rando 2001, Travis et al. 2007). Some of the key enzymes needed for complete retinal regeneration for vertebrate rod and cones are the retinyl isomerohydrolase (RPE65), lecithin-retinol acyl transferase (LRAT) and retinol dehydrogenase (RDH) (for review see Yau and Hardie 2009, Koch and Dell'Orco 2015) (Fig. 5).

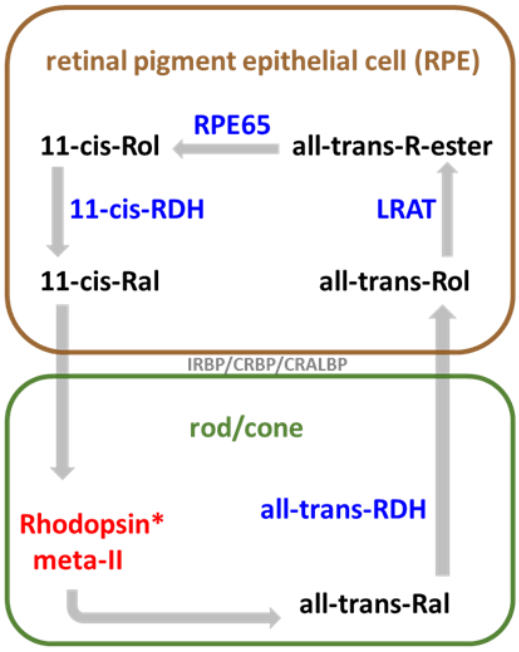

Fig. 5: Schematic representation of the vertebrate visual cycle.

Visual cycle in the retinal pigment epithelial cell (RPE) is used by vertebrate rod and cones. When struck by a photon (*), 11-cis retinal (11-cis-Ral) undergoes photoisomerization to all-trans

retinal (all-trans-Ral) and is released from the opsin. All-trans retinal is reduced to all-trans retinol (all-trans-Rol) by all-trans retinol dehydrogenase (all-trans-RDH). All-trans retinol is then transported from the retina to the RPE by an extracellular carrier protein the interphotoreceptor retinoid-binding protein (IRBP), to the adjacent RPE cell. In the RPE, all-trans retinol undergoes esterification (all-trans-R-ester) by the lecithin retinol acyltransferase (LRAT) to be subsequently converted to 11-cis retinol (11-cis-Rol) by the isomerohydrolase RPE65 (RPE65). 11-cis retinol is converted to 11-cis retinal by 11-cis retinol dehydrogenase (all-cis-RDH). The regenerated chromophore is carried back to the rod/cone cell with the help of intracellular carrier proteins (CRBP and CRALBP) (as reviewed in Yau and Hardie 2009, Koch and Dell'Orco 2015). Adapted from Yau and Hardie (2009).

Using molecular and morphological data it has been well-documented, that both photoreceptor types do coexist in Bilateria, with the non-visual photoreceptor type employed in a rather different type of photosensitivity e.g. as deep brain photoreceptors of vertebrates involved in photoperiodicity perception (Kang and Kuenzel 2015), or as optic ganglion cells of onychophorans (Beckmann et al. 2015; for other examples see Gomez and Nasi 2000, Velarde et al. 2005, Graham et al. 2008).

The protein moiety of the photopigments are opsins. They are members of the G protein coupled receptor (GPCR) superfamily of proteins, with seven transmembrane helices that are involved in a diverse set of signalling functions. All opsins form a large monophyletic subclass within the GPCR superfamily and are characterized by the presence of a lysine in the seventh transmembrane helix, which serves as the attachment site for the chromophore, thus enabling the photosensitivity of functional opsins. These essential molecules mediate the ability of diverse metazoan species to detect and proceed light signals for many diverse biological functions. Opsins have been discovered in a wide variety of tissues and cell types, where they also serve functions other than image formation (for review see Terakita 2005, Porter et al. 2012). Consistent differences in the structure between photoreceptors, as well as in the corresponding opsins primary sequences (plus subsequent transduction components) between vertebrates and invertebrates led to the conceptual division of opsins into two distinct classes: rhabdomeric type - r-opsin and ciliary type - c-opsins (Arendt and Wittbrodt 2001, Arendt 2003, Fernald 2006). This division reflects the types of photoreceptor cells that house these corresponding pigments.

Due to the increasing number of sequenced animal genomes across the phylogenetic tree, there are hundreds of annotated opsin sequences available to date. Recent molecular and phylogenetic analyses suggest that opsin diversity is even greater than previously assumed and that at least four major monophyletic subgroups can be recognized, namely the c-type, the cnidopsins, the r-type and group 4 opsins (Kojima et al. 1997, Sun et al. 1997, Koyanagi et al. 2002, Tarttelin et al. 2003, Terakita 2005, Porter et al. 2012) (Fig. 6).

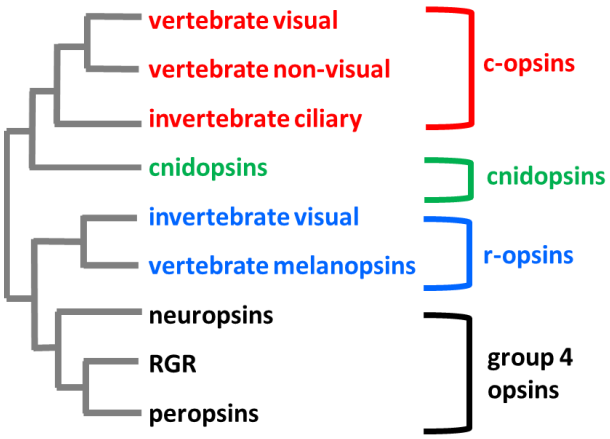

Fig. 6: Four major sub-families of opsins. Schematic representation of the possible phylogenetic relationships between the four sub-groups of opsins. Adapted from Porter et al. (2012).

C-type opsin group comprises the vertebrate visual (Gt coupled) and non-visual opsin subfamilies: the pinopsins, paprapinopsins, encephalopsins, parietopsins, teleost multiple tissue (TMT) opsin subfamily and invertebrate ciliary opsins. Cnidopsins were exclusively found among cnidarians. The r-type group consists of the Gq-coupled invertebrate visual opsins and invertebrate and vertebrate melanopsins. Group 4 contains relatively poorly characterized opsin types - neuropsins, peropsins and retinal G protein coupled receptors (RGR). Analysis of intron arrangement and insertion/deletion events (Porter et al. 2012) support the distribution of opsins into these four major groups. All four groups contain genes found in multiple tissues (photoreceptors and/or other tissues). However, two recently published studies of opsin phylogeny (Feuda et al. 2012 and Feuda et al. 2014) argued against the findings of the majority of studies (Arendt et al. 2004, Suga et.al 2008, Plachetzki et al. 2007, Plachetzki et al. 2010, Porter et al. 2012), in regard to the fact that cnidarian opsins, might not be

of monophyletic origin, but can be divided into three groups, each more closely related to either the c-, r- or group 4 opsin sub-groups.

The covalently bound chromophore - 11-cis retinal - responsible for the light sensitivity of the visual photopigment, is one of the opsin's most defining features. The photopigment is activated when the chromophore undergoes a photo-isomerization from 11-cis to all-trans retinal after an exposure to light. The amino acids on certain positions of the opsins binding pocket can shift the absorbance range of the pigment from around 380 nm (for the free cis-retinal) to sensitivities ranging from 400–650 nm (Nathans 1990, Robinson et al. 1992, Nickle et al. 2006).

11-cis retinal is attached to the universally conserved lysine in the last of the seven transmembrane helices via a Schiff base linkage (Fig. 7).

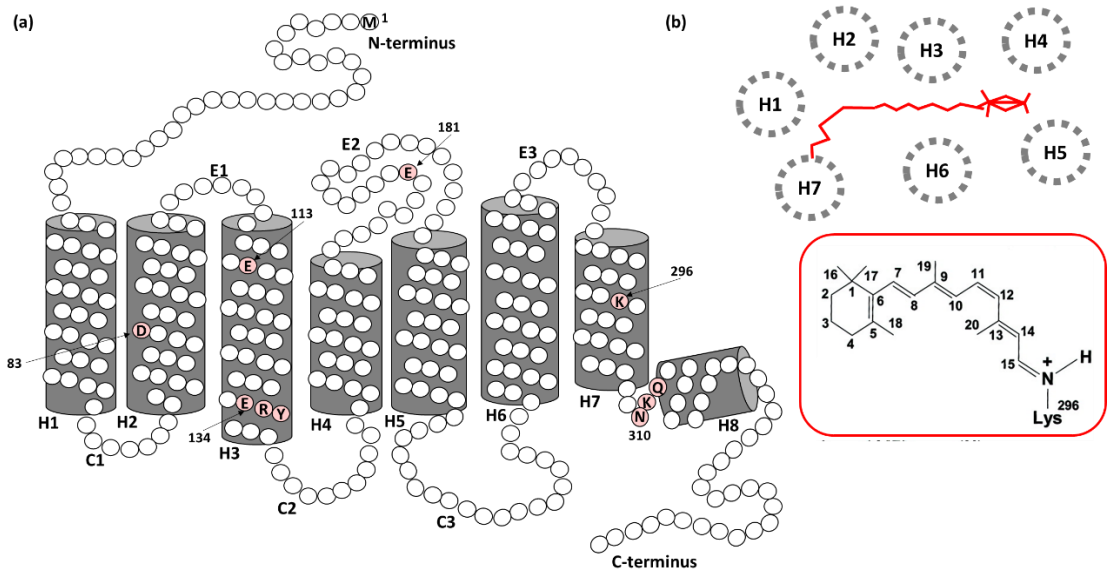

Fig. 7: Schematic structure of the bovine rhodopsin.

a) Simplified scheme of bovine rhodopsin secondary structure. Single amino acid residues are symbolised as circles. Residues with key importance are depicted in single letter code (in red) with a number corresponding to the position in the peptide chain. 11-cis retinal is attached via a Schiff base linkage to a universally conserved lysine (K296) in the last of the seven transmembrane helices (H7) of the opsin protein. Transmembrane domains H1-H7 and H8 domain (parallel to the membrane surface) are depicted as grey cylinders. C1 – C3 are the cytoplasmatic loops and E1-E3 extracellular loops of bovine rhodopsin. Adapted from Sakmar et al. (2002). b) Schematic representation of the rhodopsin structure. H1-H7 are the opsin seven transmembrane domains. The chromophore is depicted in red. *Inset:* Structure of the 11-cis-

retinylidene chromophore. 1-20 are numbered carbon atoms. Adapted from Baldwin (1993) and Davies et al. (2007).

Generally, a counterion (negatively charged amino acid) is required to stabilize the Schiff base linkage, which is protonated (Terakita et al. 2004). In bovine rhodopsin, the counterion has been identified as glutamic acid at the position 113 (E113) of the rhodopsin protein chain in the third transmembrane helix (Terakita et al. 2004). As opposed to bovine rhodopsin, experimental evidence suggests that the residue corresponding to the bovine E181 acts as the counterion in some of the group 4 opsins - peropsins, the squid retinochrome and *B. floridae* opsin (Terakita et al. 2000, Terakita et al. 2004). It is very difficult to express functional photopigments in tissue culture, other than vertebrate c-type opsins. As a result, spectral studies investigating counterions in many photopigments are very limited.

Marin et al. (2000) provided evidence to support the hypothesis that substitutions of some of the amino acid in the fourth cytoplasmic loop of duplicated opsins were involved in the origins of interactions with other G alpha subunits (leading to distinct phototransduction cascades). Using site-directed mutagenesis, it has been shown that a tripeptide region (corresponding to positions 310-312 of bovine rhodopsin protein chain) mediates opsin-G protein interaction in ciliary opsins (Marin et al. 2000), and these data were later verified by correlation analyses (Plachetzki et al. 2007).

In recent years, a new promising biological technique – optogenetics, which involves the use of light to control cells (typically neurons) in living tissues was developed. It is a method for neuromodulation combining techniques from optics and genetics to monitor and control individual cells in living tissues or free-moving animals (for review see Cho and Li 2016). Various opsin based-pigments (and especially the non-conventional visual pigments with characteristics distinct from those traditional vertebrate or insect opsins) became of extreme interest, since these molecules could be used for development of new promising optogenetic tools for modulating GPCR-signalling (Koyanagi and Terakita 2014). In fact, one of the cubozoan opsins is already

being used to control cellular processes with unprecedented spatiotemporal resolution (Bailes et al. 2012).

Cubozoa (box jellyfish) belong to the phylum Cnidaria, probably the earliest branching phylum containing a well-developed visual system. Light is known to affect many behavioural activities of cubozoans and other cnidaria, including diel vertical migration and responses to shifts in light intensity and reproduction (Martin 2002). Their phylogenetic position, simple nervous system and elaborate set of many eyes (Nilsson et al. 2005) render their visual system important for understanding the early evolution of vision as well as the basic biology of box jellyfish (Coates 2003, Garm et al. 2007, O'Connor et al. 2009, Garm and Mori 2009, Garm et al. 2011, Petie et al. 2011).

Surprisingly, eyes of box jellyfish share many features with those of vertebrates. Morphologically, by the overall design comprising ciliary photoreceptors, retina, lens (Land and Nilsson 2002, Nilsson et al. 2005) and based on recent characterisation of some of the molecular components, it was suggested that the box jellyfish visual system could be more closely related to vertebrate than to that of invertebrates (Kozmik et al. 2003, Piatigorsky and Kozmik 2004, Kozmik 2008, Kozmik et al. 2008a).

Photoreceptive organs in Cnidaria have diverse structures, not only between the different classes (O'Connor et al. 2009) but within the same animal as well (Ekstrom et al. 2008, Garm et al. 2008, O'Connor et al. 2010a, O'Connor et al. 2010b). The box jellyfish investigated in our study, *Tripedalia cystophora* (Conant 1897), has four equally spaced rhopalia (sensory structures), hanging from stalks and situated within open cavities surrounding the bell. Each of the rhopalia bears six separate eyes.

There are two large complex eyes containing spherical lenses (upper lens eye – ULE - and the larger lower lens eye – LLE), situated at right angles to each other accompanied with one pair of pit shaped and one pair of slit-shaped simple ocelli comprising photoreceptors laterally to the complex eyes (Parkefelt et al. 2005, Garm et al. 2008) (Fig. 8).

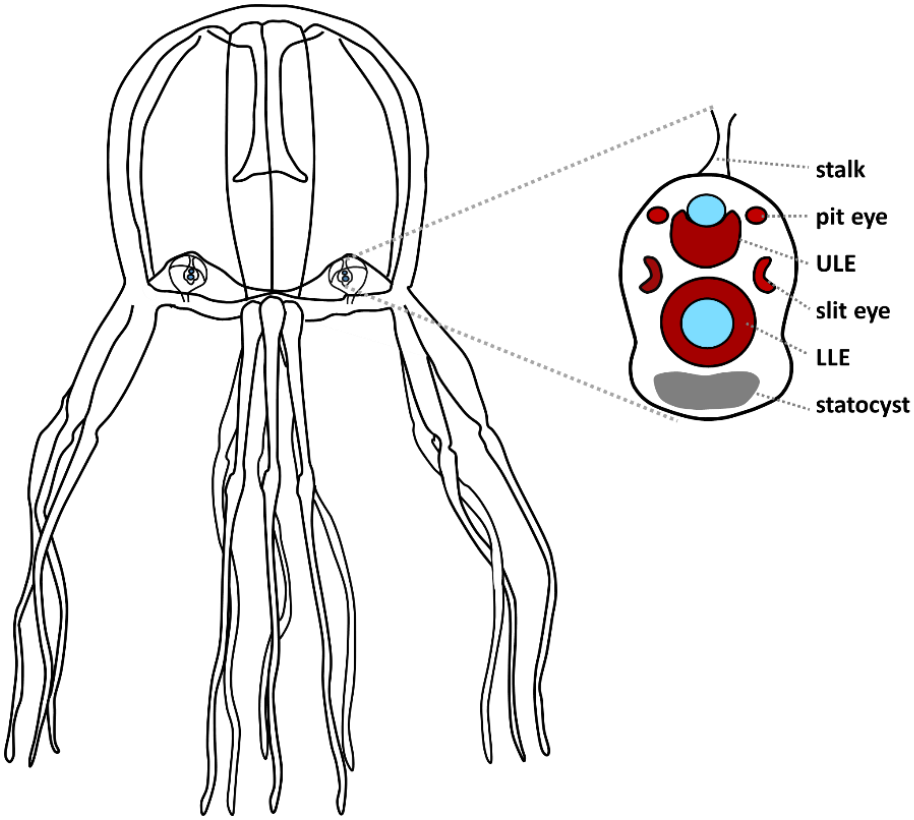

Fig. 8: Visual organs of *T. cystophora.*

Schematic drawing of *T. cystophora* (adapted from Conant 1897) with a detailed view of the rhopalium on the right. The smaller upper lens eye (ULE) and larger lower lens eye (LLE) lie medially, while the simpler paired pit and slit eyes lie laterally to those complex eyes. Each of the four rhopalia houses six eyes (24 eyes all together). Rhopalia hang on stalks and are kept in constant orientation to the horizon by the weight of the statocyst, while the jellyfish moves. Lenses of the complex eyes are depicted in blue.

The visual fields of all the individual eyes partly overlap, leading to almost complete view of *T. cystophora* surroundings. The lens containing eyes have sophisticated visual optics as do molluscs and vertebrates (Land and Nilsson 2002, Nilsson et al. 2005). Two opsin genes have been identified so far in cubozoans, one in *T. cystophora* (Kozmik et al. 2008a), and one in *Carybdea rastonii* (Koyanagi et al. 2008). *C. rastonii* opsin was furthermore shown to transfer light stimuli via Gs signalling pathway.

MOTIVATION AND AIMS OF THE STUDY

Vision is one of the most crucial senses in many animals and perhaps the most important sense for humans. Eye morphogenesis and phototransduction have been studied for a long time, however the function of involved genes began to be elucidated in the last two decades. One of the most striking findings over the past few years is the discovery of vertebrate-like components (e.g. ciliary-type opsin) in the phototransduction of the non-vertebrate cnidarian box jellyfish, *T. cystophora.*

The aim of this study is the identification and characterization of the main genetic components of *T. cystophora* phototransduction cascade and vision, with the main focus on opsins, and inspection of the putative similarities to phototransduction of other species, particularly vertebrates. Elucidation of the biological role and function of *T. cystophora* opsins and other phototransduction genes used for its "pioneer vision" will enhance our knowledge of specific aspects of eye and phototransduction evolution. Last but not least, this study aims to identify and characterize novel cnidarian opsins sequences as a potential source for novel optogenetic tools development.

To solve these questions a comprehensive multidisciplinary approach combining modern molecular biology methods with bioinformatics was applied.

1. Identification and cloning of *T. cystophora* opsin genes

The aim was to mine out opsin genes from the *T. cystophora* "in-house" 454-generated genomic library. The newly identified opsins were subsequently cloned in full lengths and used for following *in silico, in vitro* and *in vivo* analyses.

2. Sequence analysis of *T. cystophora* opsin genes

We tried to identify and characterize the key functional and structural features of the novel *T. cystophora* opsin sequences through comparison (alignment) with other well characterized and annotated metazoan opsins.

3. Phylogenetic analysis of *T. cystophora* opsin genes

We aimed for a detailed and precise phylogenetic analysis of all metazoan opsins. Adding a set of novel opsin sequences from *T. cystophora* (the earliest branching phylum

containing eyes) to the currently used set of various annotated sequences available from public databases could help to resolve the long-lasting discrepancy in opsin gene phylogeny, as well as shed light onto a possible scenario of cnidarian photoreception evolution.

4. Analysis of *T. cystophora* opsin genes expression patterns and dynamics

We aimed to characterize the spatiotemporal expression patterns of the novel opsin genes in *T. cystophora.* Expression of these genes was analysed on mRNA level by extensive quantitative real-time PCR analysis (qRT-PCR), as well as on the protein level by immunohistochemistry (IHC) to demonstrate various utilization of opsins for ocular and extra-ocular functions, with a special focus on characterization of the cnidarian visual photoreceptors. In addition, we decided to take advantage of having a culture of a related box jellyfish, *Alatina marsupialis,* and inspected the possible presence of the main *T. cystophora* opsin homologs by IHC of the developing eyes of this species (for comparison between these two species).

5. Identification and functional testing of a possible *T. cystophora* opsin coupling partner

To enable comparative studies and hypotheses about photoreception evolution, it was of special interest to identify the direct *T. cystophora* coupling partner between opsins and the G alpha subunit types of the corresponding trimeric G protein partner. Coupling to each of the G alphas subunit variants (Gi, Gs, Gq, Go) defines the type of subsequent cascade and corresponding physiological reaction of the photoreceptor cell (depolarization or hyperpolarization to light signal). We searched the *T. cystophora* genomic database for these variants of G protein alpha subunits (known to be used in vision in different animals) and verified their actual presence in the photoreceptors using commercially available antibodies for cross-species IHC (use of antibodies originally generated for other organisms e. g. mouse or human). Furthermore, we aimed to confirm the direct coupling partner of *T. cystophora* opsins by designing a novel *in vitro* light-response assay in cell culture.

6. Behavioural testing of *T. cystophora* visual navigation ability after treatments with pharmacological inhibitors of the opsin´s coupling partner

Using highly selective pharmacological inhibitors for the selected G alpha subunits, we wanted to test the functional association of these two crucial components of the phototransduction cascade by designing simple behavioural experiments with living animals.

7. Identification of other possible phototransduction cascade components by *T. cystophora* genome analysis *in silico*, complemented with IHC screening with commercially available antibodies *in situ*

We thoroughly searched the *T. cystophora* genomic library for other genes essential for effective visual perception, e.g. phototransduction activators, modulators and de-activators. We performed a parallel IHC screening of cryo-dissected rhopalia with commercially available antibodies generated against various candidate proteins of the phototransduction cascade (cross-species IHC) to complement the *in silico* approach with *in situ* data.

8. Identification of novel crystallin genes in *T. cystophora* genomic library

Since the addition of lenses as a refracting unit significantly enhances the quality of vision in Bilateria with advanced eyes, we searched the *T. cystophora* genomic library for additional crystallin genes (five crystallin genes were identified previously) as candidates for expression in the complex lens eyes.

MATERIAL AND METHODS

1. *T. cystophora* collection and culture

Adult and larvae *T. cystophora* were manually collected from the mangroves outside Isla Magueyes marine station in La Parguera, Puerto Rico (17.974932, -67.065042) and were either used directly for culture establishment or were fixed in 4% paraformaldehyde (PFA) in phosphate buffer saline (PBS) or in RNAlater stabilizing solution (for qRT-PCR analyses). The laboratory culture was established by releasing adult *T. cystophora* females together with matured larvae into a glass aquarium (20x20x40 cm) provided with artificial sea water and preserved at 26°C. After settling, larvae metamorphosed into young polyps. Polyps were stimulated into transformation to asexually reproducing polyps by feeding them with brine shrimp nauplii (*Artemia salina*) several times per week. Metamorphosis into free swimming medusa was promoted by increasing the water temperature to 28°C for several days. Samples were collected from all of the aforementioned stages and used for opsin expression pattern analysis by qRT-PCR. Adults and juvenile medusae were used for rhopalium IHC. Three days old, actively swimming medusae (selection based on convenient size of the jellyfish for the testing chamber) were used for behavioural testing after pharmacological inhibition.

A. marsupialis culture was established from vegetative polyps, kindly provided by Professor Gerhardt Jarms of the University of Hamburg. All animals were kept under the same conditions.

2. *T. cystophora* genome sequencing and *in silico* analysis

2.1 Generation of the *T. cystophora* genomic database

A *T. cystophora* genomic database was generated by DNA shotgun sequencing performed on the GS FLX Titanium platform (454 Life Sciences, Roche). Pyrosequencing resulted in 1, 952, 068 reads with an average read length of 360 bp (about 7×10^8 bases). Assembly generated 134, 683 contigs containing 40.5% (790, 111 reads) of the reads.

Assembly was done using Newbler - version 2.3 (Roche). Resulting contigs were combined with individual reads to produce a complete contig database (Fig. 9a).

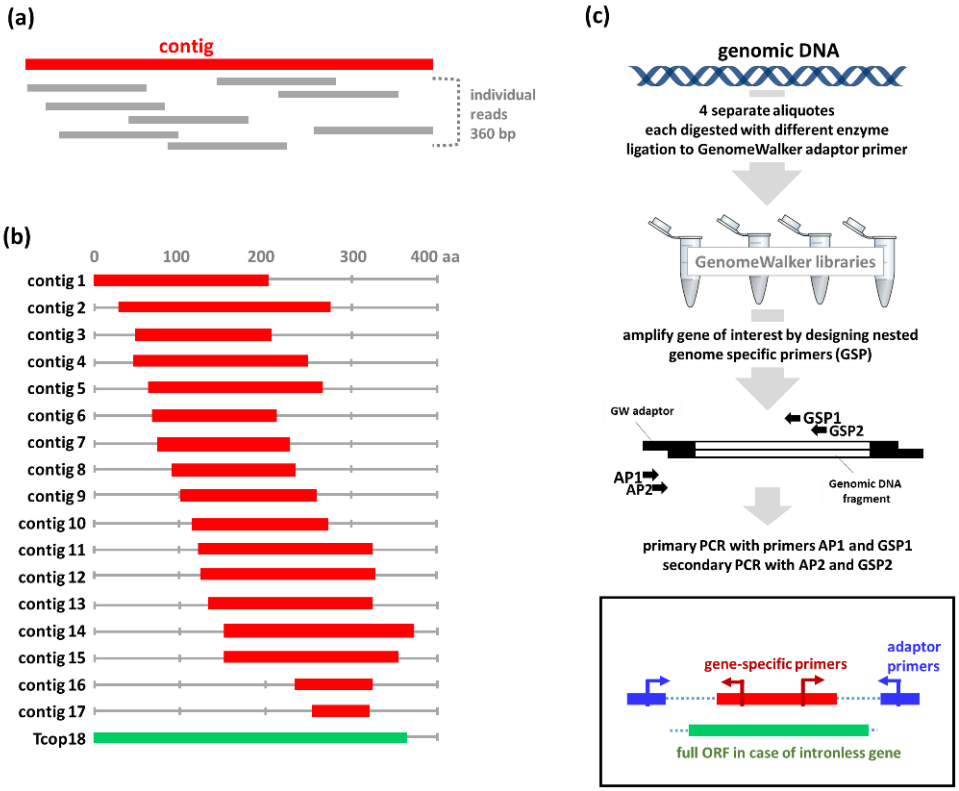

Fig. 9: Scheme of the opsin identification and cloning strategy.

a) Visualization of the assembly of single reads (in grey) into a contig (red), based on identical overlapping parts of the individual reads. b) Map of the identified contigs (red). Each contig (1-17) corresponds to the partial sequence of a novel *T. cystophora* opsin found in the genomic library and its position according to the sequence of the previously annotated *T. cystophora* opsin 18 (Tcop18) (Kozmik et. al. 2008a) in green. c) GenomeWalker method visualization. Nested gene specific primers (GSP1, GSP2) are used to clone the sequence between the known stretch of DNA and nested adaptor primers (AP1, AP2). *Inset:* If the cloned genes are intronless, by "walking" in both direction (upstream/downstream) from a known stretch of a DNA sequence, the whole open reading frame could be recovered. Contigs in red, full open reading frames (ORF) in green.

2.2 *In silico* data mining

The 454 generated *T. cystophora* genomic database was subjected to similarity searches using the FASTA (Pearson and Lipman 1988, Pearson 2016) algorithm. A wide range of homologous opsin (Table 1) and other phototransduction cascade candidate as well as structural genes from cnidarian and bilaterian species (summarized in Table 2)

were used as queries (protein queries were used to search the translated nucleotide database under default parameters).

Table 1: List of opsin protein sequences used as queries for the FASTA search of *T. cystophora* 454 generated genomic library.

Columns: Sequence ID - refers to the nomenclature used in the phylogenetic tree; Major Lineage - refers to the four opsin sub-families; Phylum of the source organism; Genus of the source organism; Gene/protein ID refers to accession number for the given sequence (genomic, transcript or protein).

Sequence ID	Major Lineage	Phylum	Genus	Gene/protein ID
>LWS.takRub	C-type	Chordata	*Takifugu*	AAT38456.1
>PARIE.anoCar	C-type	Chordata	*Anolis*	AAD32622.1
>PIN.podSic	C-type	Chordata	*Podarcis*	DQ013042
>Rh1.Canfam	C-type	Chordata	*Canis*	X71380.1
>Rh1.Musmus	C-type	Chordata	*Mus*	BC031766.1
>RH2.Notang	C-type	Chordata	*Notothenia*	AY771354
>RHO1.bosTau	C-type	Chordata	*Bos*	NM_001014890
>RHO2b.danRer	C-type	Chordata	*Danio*	NM_182891
>SWS1.Botau	C-type	Chordata	*Bos*	NP_776992
>SWS2.Orylat1	C-type	Chordata	*Oryzias*	BAE78650
>VAOP.Salsal	C-type	Chordata	*Salmo*	NM 001123626
>ENCEPH.musMus	C-type	Chordata	*Mus*	AF140241
>TMT.danRer	C-type	Chordata	*Danio*	NP_001112371.1
>TMT1.plaDum	C-type	Annelida	*Platynereis*	CT030681
>TMT.triCas	C-type	Arthropoda	*Tribolium*	NP_001138950.1
>TMTPIN.stoPur	C-type	Echinodermata	*Strongylocentrotus*	XM_001177470
>CNID.CropB1	Cnidops	Cnidaria	*Cladonema*	AB332416
>CNID.CropC	Cnidops	Cnidaria	*Cladonema*	AB332420
>CNID.CropD	Cnidops	Cnidaria	*Cladonema*	AB332422
>CNID.CropE	Cnidops	Cnidaria	*Cladonema*	AB332421
>CNID.CropF	Cnidops	Cnidaria	*Cladonema*	AB332426
>CNID.CropH	Cnidops	Cnidaria	*Cladonema*	AB332423
>CNID.CropI	Cnidops	Cnidaria	*Cladonema*	AB332424
>CNID.PcopB (2)	Cnidops	Cnidaria	*Podocoryna*	AB332434
>CNID.PcopcC (1)	Cnidops	Cnidaria	*Podocoryna*	AB332435
>CNOPa1.hydMag	Cnidops	Cnidaria	*Hydra*	ACZU01000679
>CNOPa2.hydMag	Cnidops	Cnidaria	*Hydra*	ACZU01004988
>Nvop1	Cnidops	Cnidaria	*Nematostella*	FAA00408.1
>Nvop2	Cnidops	Cnidaria	*Nematostella*	FAA00400.1
>Caryb	Cnidops	Cnidaria	*Carybdea*	BAG80696
>Tcop18	Cnidops	Cnidaria	*Tripedalia*	EU310498
>PER1a.sacKol	Group 4	Hemichordata	*Saccoglossus*	ACQM01133041
>NEUR.strPur	Group 4	Echinodermata	*Strongylocentrotus*	XM_001197837
>NEUR1.galGal	Group 4	Chordata	*Gallus*	NP_001124215
>NEUR1.homSap	Group 4	Chordata	*Homo*	NP_859528
>PER2.braFlo	Group 4	Chordata	*Branchiostoma*	AB050607
>PER1.aplCal	Group 4	Mollusca	*Aplysia*	EB338056
>RGR.Bostau	Group 4	Chordata	*Bos*	NP_786969
>RGR2.danRer	Group 4	Chordata	*Danio*	NM_001024436
>PER1a.sacKol	Group 4	Hemichordata	*Saccoglossus*	ACQM01133041
>NEUR.strPur	Group 4	Echinodermata	*Strongylocentrotus*	XM_001197837
>BCR.limPol	R-type	Arthropoda	*Limulus*	ACO05013
>BCR.triGra	R-type	Arthropoda	*Triops*	BAG80976
>DIP.Bacdor	R-type	Arthropoda	*Bactrocera*	NP_001291902.1
>LMSa.apiMel	R-type	Arthropoda	*Apis*	NM_001077825
>LMSa.nasVit	R-type	Arthropoda	*Nasonia*	NM_001170908.1
>LWS.Pierap	R-type	Arthropoda	*Pieris*	BAD06459
>UV5B.droMel	R-type	Arthropoda	*Drosophila*	AAC47426.1
>UV7.aedAeg	R-type	Arthropoda	*Aedes*	XM_001650694
>CEPH.Eupsco1	R-type	Mollusca	*Euprymna*	ACB05673.1
>MEL1.bosTau	R-type	Chordata	*Bos*	NP_001179328.1

Table 2: List of the inspected phototransduction candidates used as queries for the *T. cystophora* FASTA search.

Columns: Inspected candidate genes - names of inspected genes; Gene/protein ID refers to accession number for the given sequence (genomic, transcript or protein); Phylum of the source organism; Genus of the source organism; Common name of the source organism.

Inspected candidate genes:	Gene/protein ID	Phylum	*Genus*	Common name
Gs alpha subunit	NW_001834410.1	Cnidaria	*Nematostella*	sea anemone
(**GNAS**)	XP_002154528.3	Cnidaria	*Hydra*	hydrozoan
	BAG80697.1	Cnidaria	*Carybdea*	jellyfish
	JAQ12855.1	Arthropoda	*Lygus*	insect
	NP_001095223.1	Chordata	*Xenopus*	frog
	XP_007882614.1	Chordata	*Callorhinchus*	shark
	NP_000507.1	Chordata	*Homo*	human
Gi alpha subunit	NW_001834412.1	Cnidaria	*Nematostella*	sea anemone
(**GNAI**)	XP_012557495.1	Cnidaria	*Hydra*	hydrozoan
	CAD91433.1	Mollusca	*Crassostrea*	oyster
	BAO00908.1	Echinodermata	*Patiria*	starfish
	JAP62513.1	Platyhelminthes	*Schistocephalus*	flatworm
	BAO00908.1	Echinodermata	*Patiria*	starfish
	EFX86353.1	Arthropoda	*Daphnia*	water flea
	P38412	Mollusca	*Loligo*	squid
	NP_002060.4	Chordata	*Homo*	human
Gq alpha subunit	NW_001834343.1	Cnidaria	*Nematostella*	sea anemone
(**GNAQ**)	XP_012554580.1	Cnidaria	*Hydra*	hydrozoan
	AFZ78090.1	Cnidaria	*Acropora*	coral
	JAP41286.1	Platyhelminthes	*Schistocephalus*	flatworm
	NP_999835.1	Echinodermata	*Strongylocentrotus*	sea urchins
	ADD38851.1	Arthropoda	*Lepeophtheirus*	sea lice
	KHN71322.1	Nematoda	*Toxocara*	parasitic nematode
	JAO96793.1	Chordata	*Poeciliopsis*	fish
	NP_002063.2	Chordata	*Homo*	human
Go alpha subunit	JAP45842.1	Platyhelminthes	*Schistocephalus*	tapeworm
(**GNAO**)	AFZ78089.1	Cnidaria	*Acropora*	coral
	KFB50440.1	Arthropoda	*Anopheles*	mosquito
	NP_001016995.1	Chordata	*Xenopus*	frog
	NP_066268.1	Chordata	*homo*	human
Arrestin	AAA28380.1	Arthropoda	*Drosophila*	fruit fly
(**ARR**)	BAR90777.1	Mollusca	*Idiosepius*	bobtail squid
	BAJ83617.1	Chordata	*Lethenteron*	lamprey
	ABF59484.1	Chordata	*Danio*	zebrafish
	NP_033144.1	Chordata	*Mus*	mouse
Recoverin	P42325.2	Arthropoda	*Drosophila*	fruit fly
(**RCV**)	P36608.2	Nematoda	*Caenorhabditis*	
	Q16982	Mollusca	*Aplysia*	sea hare
	NP_001025419.1	Chordata	*Danio*	zebrafish
	NP_036011.3	Chordata	*Mus*	mouse
Rhodopsin kinase	AAR19398.1	Mollusca	*Loligo*	sguid
(**GRK**)	NP_001036438.1	Arthropoda	*Drosophila*	fruit fly
	NP_001188419.1	Chordata	*Oryzias*	medaka
	NP_001131051.1	Chordata	*Xenopus*	frog
	NP_776598.1	Chordata	*Bos*	cow
	NP_002920.1	Chordata	*homo*	human
Lecithin retinol acyltransferase	EDO37343.1	Cnidaria	*Nematostella*	sea anemone
(**LRAT**)	XP_014769676.1	Mollusca	*Octopus*	
	EFX73255.1	Arthropoda	*Daphnia*	water flea
	NP_001134398.1	Chordata	*Salmo*	salmon
	AAI09505.1	Chordata	*Bos*	cow
Retinol dehydrogenase	AGN03869.1	Cnidaria	*Aurelia*	moon jellyfish
(**RDH**)	XP_015780449.1	Cnidaria	*Acropora*	coral
	XP_014786541.1	Mollusca	*Octopus*	
	ACI67415.1	Chordata	*Salmo*	salmon
	NP_001011363.1	Chordata	*Xenopus*	frog
	O55240.1	Chordata	*Mus*	mouse
	NP_002896.2	Chordata	*Homo*	human
RPE65 isomerase	AAL01119.1	Chordata	*Mus*	mouse
(**RPE65**)	Q9YGX2.1	Chordata	*Gallus*	chicken
	Q9YI25.3	Chordata	*Ambystoma*	salamander
	NP_000320.1	Chordata	*Homo*	human
CNG channel	BAG80699.1	Cnidaria	*Carybdea*	jellyfish
(**CNG**)	A7RI02	Cnidaria	*Nematostella*	sea anemone
	NP_001038211.1	Chordata	*Danio*	zebrafish
	NP_001268939.1	Chordata	*Mus*	mouse
	Q28181.1	Chordata	*Bos*	cow
	NP_001136036.1	Chordata	*Homo*	human
Cubozoan crystallins	AAA30106.1	Cnidaria	*Tripedalia*	jellyfish
(**J1A-C,J2, J3**)	AAA30107.1	Cnidaria	*Tripedalia*	jellyfish
	AAA30108.1	Cnidaria	*Tripedalia*	jellyfish
	ABQ12778.1	Cnidaria	*Tripedalia*	jellyfish
	AAG09203.1	Cnidaria	*Tripedalia*	jellyfish

FASTA searches provided Hits corresponding to short stretches (individual contigs) of assumed *T. cystophora* protein sequences (as depicted for *T. cystophora* opsin Hits in Fig. 9b).

2.3 Molecular phylogeny

For investigation of the relationships between the cnidarian and bilaterian opsins, we inferred a molecular phylogenetic tree using the maximum likelihood (ML) method implemented in PhyML 3.0 (Guindon et al. 2010) applying the LG substitution model (Le and Gascuel 2008) to count the substitution probabilities along phylogeny branches. Support for internal nodes was assessed using the Approximate Likelihood-Ratio Test for Branches (aLRT) (Anisimova and Gascuel 2006).

2.4 Dataset for phylogenetic analysis

All available annotated opsin protein or transcript sequences were mined from Genbank or acquired from the UCSC genome browser (as described in Porter et al. 2012). However, incomplete sequences were discarded from the analysis.

In order to root the phylogenetic tree, 22 non-opsin GPCRs from the human genome were used as outgroup (Table 3).

Table 3: Complete list of sequences used as outgroup for the opsins phylogenetic analysis.

Columns: Sequence ID - refers to the nomenclature used in the phylogenetic tree; Gene name; Gene/protein ID - refers to accession number for the given sequence (genomic, transcript or protein). Source organism – human.

	Sequence ID	Gene	Gene/protein ID
1	>OG.TSHR	thyroid stimulating hormone receptor	AAB87990
2	>OG.ADORA3	A3 adenosine receptor	AAA16365.1
3	>OG.TRHR	thyrotropin-releasing hormone receptor	NP_003292.1
4	>OG.ADRA1D	alpha-1A-adrenergic receptor	AAA35496.1
5	>OG.GPR161	G-protein coupled receptor isoform 2	NP_722561.1
6	>OG.PRLHR	prolactin-releasing peptide receptor	NP_004239.1
7	>OG.NPY1R	neuropeptide Y receptor type 1	NP_000900.1
8	>OG.PPYR1	neuropeptide Y receptor type 4	NP_005963.3
9	>OG.GPR19	G-protein coupled receptor 19	NP_006134.1
10	>OG.QRFPR	QRFP receptor	BAC98938.1
11	>OG.NMUR2	neuromedin U receptor 2	AAF82755.1
12	>OG.TACR2	neurokinin-2 receptor	AAB05897.1
13	>OG.HCRTR1	orexin receptor 1	AAC39601.1
14	>OG.P2RY8	P2Y purinoceptor 8	NP_835230.1
15	>OG.CYSLTR1	cysteinyl leukotriene receptor 1	NP_006630.1
16	>OG.GPR17	G protein-coupled receptor 17	AEP43758.1
17	>OG.BDKRB2	B2 bradykinin receptor	NP_000614.1
18	>OG.CCR4	C-C chemokine receptor type 4	NP_005499.1
19	>OG.GALR1	galanin receptor	AAC51936.1
20	>OG.OPRM1	opioid receptor, mu 1	CAI20458.1
21	>OG.OPRL1	nociceptin receptor	NP_000904.1
22	>OG.SSTR1	somatostatin receptor type 1	NP_001040.1

This selection was based on previous phylogenetic studies of opsin and GPCR evolution (Fredriksson et al. 2003, Suga et al. 2008, Davies et al. 2010, Plachetzki et al. 2010). The resulting dataset of 801 (779 opsin plus the 22 non-opsin) transcript sequences was aligned using Clustal (Thompson et al. 1997, Larkin et al. 2007) under default parameters and trimmed after careful inspection in BioEdit (Hall 1999). For phylogenetic analysis, only the 7-transmembrane region (H1-H7 transmembrane domains) and the intervening intra-cellular and extra-cellular domains were included. N- and C- termini were trimmed out due to sequence length variation and lack of conservation in this area across all the genes. The resulting opsin phylogenetic tree was inferred from a 226 amino acids alignment of the inspected opsin protein sequences. For the full list of the used 801 sequences used see Liegertova et al. (2015).

3. Molecular cloning and vectors

All commonly used molecular cloning methods were performed according to Ausubel et al. 2003.

3.1 Amplification by PCR and ligation of the inserts into vectors

Advantage 2 polymerase (Clontech), which has the most sensitive and robust capabilities of any of the Taq-derived polymerases, was preferentially used for genome-walking (GenomeWalker, Clontech), 3´ RACE (Rapid Amplification of cDNA Ends) cloning and in cases that high fidelity was necessary for successful subsequent processing of PCR products, e.g. molecular cloning of opsins into expression vectors. All PCR products were purified using QIAquick PCR Purification Kit (Qiagen) and cloned into pJET vector (CloneJET PCR Cloning Kit, Thermo Scientific) or into expression vectors pET42a (+) (Novagen) for recombinant protein production in *E. coli*, into EGFP_C1 (Clontech) and pcDNA3.1 (Clontech) for protein expression in mammalian cell lines for western blotting and functional analyses (light-response assay), respectively (Table 4).

Table 4: List of vectors used in this study.

GW – genome-walking. RACE – 3´RACE cloning approach. deg. PCR – cloning with degenerate primers. Tcop – *T. cystophora* opsins. Caryb – *C. rastonii* opsin. ORF – open reading frame. WB – western blot analysis.

Vector	Insert	Use
pJET	all products of clonning (GW, RACE, deg. PCR)	verification of PCR products, sequencing
pET42a (+)	C-terminus of Tcop1 and Tcop13	protein production for immunization
EGFP_C1	C-terminus of Tcop1 and Tcop13	immunogenicity verification (WB)
pcDNA3.1 + 1D4	all Tcops (1-18) full ORF + Caryb	light-response assay

The expression vector pcDNA3.1 + 1D4 was prepared by introducing the recognition site for BamHI restriction enzyme followed by 1D4 epitope tag (sequence from bovine rhodopsin for latter verification of successful construct expression in the cells by IHC with anti-1D4 antibody) into the multiple cloning site of pcDNA 3.1 vector using KpnI and EcoRI sites. cDNA of opsin from the box jellyfish *C. rastonii* (GenBank AB435549; the vector was kindly provided Dr. Koyanagi), was amplified from the vector by standard PCR and re-cloned into the pcDNA3.1 + 1D4 vector using BamHI and HindIII restriction sites. The opsins of box jellyfish *T. cystophora* (all single exon/intronless genes), were amplified by PCR from genomic DNA and cloned into the pcDNA 3.1 + 1D4

vector either via BamHI/ HindIII or BamHI/KpnI cloning sites. All the constructs were verified by standard sequencing techniques before use.

3.2 Cloning of full-length genes and partial sequences

The full length sequences of *T. cystophora* opsin genes (which are all intronless/single-exon genes) were obtained by a genome-walking strategy using adaptor-ligated genomic DNA library as a template (for method overview see Fig. 9c). The products of genome-walking were cloned into the pJET vector and sequenced for validation. Obtained opsin sequences were deposited in GenBank under accession numbers: JQ968416 -JQ968432.

In the case of genes bearing introns, a different strategy was applied. To obtain the complete terminal sequences of the identified candidate genes, the RACE approach was used (Fig. 10), a technique that can provide the complete sequence of an RNA transcript from only a small known part within the transcript all the way to the 5' end (5' RACE-PCR) or 3' end (3' RACE-PCR) of the RNA.

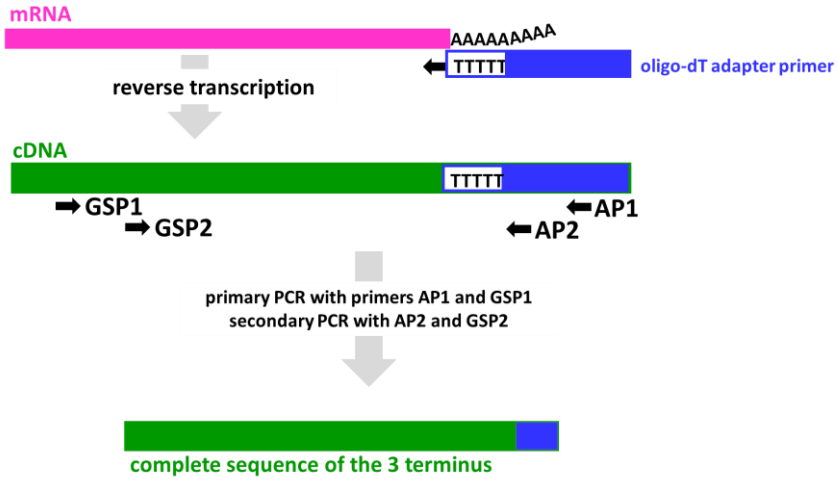

Fig. 10: Schematic representation of 3´ RACE cloning approach.

mRNAs extracted from rhopalia were converted into complementary DNA (cDNA) using reverse transcriptase and an oligo-dT adapter primer. The resulting cDNA had the adapter sequence incorporated at the 3´terminus, which serves as a priming site for nested adapter primers (AP1, AP2). The complete 3´ends were then recovered by nested PCR using two gene specific (forward) primers (GSP1, GSP2) and the adapter primers.

For the G alpha subunits and crystallin genes identified in the genome, nested gene-specific forward RACE primers were designed using Primer3 (Rozen and Skaletsky 2000, Untergasser et al. 2012) and rhopalia derived RACE cDNA library (prepared according to manufacturer´s protocol) was used as a template for the PCR reaction.

In the case of CNG channel and arrestin (where the corresponding Hits provided only a short stretch of sequences within a single exon) we used highly conserved domains among bilaterian orthologues of arrestin and CNG channel genes to design degenerate primers and partially cloned these genes using the rhopalia derived RACE cDNA library as a template. PCR products were gel-purified, cloned into pJET vector and sequenced. All primers used in this study are listed in Appendix - Table 1.

3.3 Plasmid cloning

Prior to cell transformation, concentration of plasmid DNA was determined using Spectrofotometer NanoDrop ND-1000 (Thermo Scientific). In the case of "sticky-ends" cloning (e.g. into expression vectors) 1 µg of plasmid DNA was digested with 10 U of the appropriate restriction enzyme (or combination of enzymes) for 1 hour at 37 °C. If necessary, plasmid DNA was dephosphorylated by 1 U of alkaline phosphatase (Thermo Scientific) for 1 hour at 37 °C, followed by deactivation of the phosphatase for 15 minutes at 65 °C. Digested plasmid was resolved on 1% agarose gel and DNA was purified from the gel using QIAquick Gel Extraction Kit (Qiagen) according to the manufacturer´s protocol. Plasmid DNA and inserts were ligated using T4 ligase (Fermentas) for 1 hour at room temperature. A 2 µl aliquot of ligation mixture was added to 50 µl of chemically competent *Escherichia coli* cells (TOP 10, Life Technologies), and the mixture was incubated for 30 min on ice, followed by heat shock at 42 °C for 45 seconds and 10 minutes incubation on ice. Transformed cells were transferred to plastic test tubes with lysogeny broth (LB) medium, were vigorously shaken for 1 h at 37 °C, and then plated on LB agar plates supplemented with appropriate selection antibiotics (ampicillin, kanamycin, chloramphenicol). Following overnight incubation at 37 °C, individual colonies were picked from the plate and used for inoculation of media for plasmid DNA isolation. Plasmids isolated by minipreparation were verified for the presence of desired insert by PCR and sequencing.

4. Analysis of key positions of the *T. cystophora* opsin protein sequences

All *T. cystophora* opsin protein sequences were aligned (ClustalX) to bovine rhodopsin and other well characterised opsin sequences to identify the key amino acids, which are supposed to be determinative for the opsin function.

5. Gene expression analyses

5.1 *T. cystophora* opsins expression analysis by qRT-PCR

RNA from larvae, polyps and medusae, or dissected adult *T. cystophora* body parts was isolated using TRIZOL reagent (Invitrogen). DNAse digestion was used to remove contaminating genomic DNA and the RNA was re-purified on RNeasy Micro columns (Qiagen) according to the manufacturer's protocol.

The same volumes of RNA from each of the samples were used for reverse transcription by VILO cDNA kit (Invitrogen). Primers for the qRT-PCR analysis were designed using the Primer-3 software. The qRT-PCR was performed in the LightCycler 2.0 System, using the LightCycler 480 DNA SYBR Green I Master kit (Roche) according to the standard manufacturer's protocol. Targeted opsin genes (Tcop1-Tcop18) and the ribosomal protein L32 (Rpl32) (housekeeping gene used for normalization) were measured under the same conditions from the same cDNA template in triplicates.

LightCycler software was used to analyse the results. Crossing point (Cp) values were calculated as an average of Cp values from the triplicates and normalized by Cp values of the Rpl32 housekeeping gene (deltaCp values). The results represent relative normalized gene expression levels. Student´s t-test was used to calculate the statistical significance of changes in the mRNA level of the targeted genes between different samples.

In addition, a heat map from the standard scores (Z-scores) of deltaCp values for targeted opsin genes expression in different *T. cystophora* stages and tissues was constructed in R statistical environment with Bioconductor package (R-project.org).

5.2 *T. cystophora* opsins and other candidate genes expression patterns analysis by IHC

5.2.1 Preparation of T. cystophora specific antibodies

pET system, designed for cloning and high-level expression of peptide sequences fused with the 220 aa GST-Tag (Novagen) was used for overexpression of desired protein fragments.

Antibodies directed against Tcop1 and Tcop13 opsins were prepared by the immunization of mice as follows. The C-terminal sequence regions of Tcop1 and Tcop13 (see Appendix Table 2 for the source sequences) were cloned into the pET42a (+) vector to create fused proteins containing 6xHis-GST. The resulting recombinant vectors were used for transformation of *E. coli* strain BL21 DE3-RIPL (high-level protein expression system utilising the T7 RNA polymerase promoter to direct high-level expression - Stratagene). Successfully transformed and verified clones were used for large scale protein production.

5.2.2 Expression and purification of protein fragments for mice immunization

A total volume of 500ml LB medium was inoculated by overnight BL21-pET42 culture (transformed with a verified clone), which was grown in LB medium supplemented with chloramphenicol (12,5 µg/ml) and kanamycin (30 µg/ml). Transformed cells were grown at 37°C, 200 rotations per minute (rpm) until optical density measured at 600 nm (OD600) reached 0.6 and thereafter induced by 0.5 mM isopropyl-beta-D-thiogalactopyranoside (IPTG) - used to induce expression of cloned genes under control of the lac operon, and grown under the same conditions for three more hours. Cells were harvested by spinning in a large capacity centrifuge at 6000G for 20 minutes, the pellet was collected and re-suspended in lysis buffer (0.1M NaH_2PO_4, 6M guanidine hydrochloride, 0.01M Tris.HCl, β-mercaptoethanol added to final concentration of 20mM, with pH adjusted to 8.0). Suspended cells were lysed via sonication using an ultrasonic bath (Elmasonic S150) for 6x20 seconds and incubated for 3 hours at 22°C. The resulting cell lysate was centrifuged at 10 000G for 10 minutes, the supernatant was carefully collected and mixed with pre-equilibrated Ni-NTA agarose beads (QiaGen). Ni-NTA beads, commonly used for purification of His-tagged proteins

by gravity-flow chromatography, were pre-equilibrated using urea buffer (50 mM NaH_2PO_4, 8M urea, 20 mM Tris.HCl, 100 mM NaCl, β-mercaptoethanol supplemented to a final concentration of 20mM, with pH adjusted to 8.0).

Cell lysate supernatant and the pre-equilibrated beads were incubated on a mildly rotating platform overnight at 22°C. The Ni-NTA beads with the desired His-tag bound proteins were washed twice with 40 ml of the urea buffer and loaded onto empty disposable gravity-flow columns (Bio-Rad). The gravity-flow columns were washed several times with urea buffer with decreasing pH ranging from 8.0 to 6.8. After extensive washing the His-tag bound proteins were eluted by urea buffer with pH 4.2 and collected. Immediately after the elution, pH was adjusted to 7.5 by 1M Tris.HCl (pH 8). Protein concentration was calculated by Protein Assay Reagent (Bio-Rad). Purified proteins were stored at -20°C for later use as antigen for mouse immunization.

5.2.3 Mice immunization and sera collection

For immunization with the purified protein fragments, virgin female mice strain B10A-H2 x BALB/CJ were used. Mice were immunized 3-4 times in one month intervals by peritoneal injections using 50-100 µg of purified protein mixed with Freund's adjuvant (Sigma) in each of the immunization step. After immunization mice were sacrificed and blood samples were collected into 2ml test tubes. The blood was allowed to coagulate for 3 hours at 22°C, followed by incubation at 4°C overnight. The clear and slightly yellow supernatant was carefully collected with a syringe. Obtained sera were diluted 1:1 with sterile glycerol, divided into several aliquots and stored at -20°C until used for IHC (as the source for polyclonal antibodies).

5.2.4 Western blotting of mouse polyclonal sera

To verify the immunogenicity of the generated polyclonal antibodies, HEK293T cell line was transfected with the expression vectors EGFP_C1-Tcop1 and EGFP_C1-Tcop13 using the FuGENE 6 reagent (Roche). Two days after transfection, the whole-cell extract was obtained by cell lysis and tested by western blot analysis. The cell lysate was resolved by 6% sodium dodecyl sulphate-polyacrylamide gel electrophoresis (SDS-PAGE) and semi-dry transferred onto polyvinylidene difluoride (PVDF) membrane. The

membrane was submerged into blocking buffer (150 mM NaCl, 20 mM Tris, 0.02% Tween 20.5% non-fat dry milk, with pH adjusted to 7.5) for 30 minutes on a rotating platform at 22°C. The mice antisera were diluted in the blocking buffer to 1:500, applied on the membrane and incubated overnight at 4 °C. The excess of the primary antibodies was washed out 3x10 minutes with blocking buffer (at room temperature) and horse radish peroxidase-conjugated secondary antibody was added and mildly shaken for another 45 minutes at room temperature. The excess of the secondary antibody was washed out 3x10 minutes with TTBS buffer (20 mM Tris, 150 mM NaCl, 0.02% Tween 20, with pH adjusted to 7.5), and the signal was developed using the chemiluminescent detection kit (Pierce).

5.2.5 Tissue collection and histology

Rhopalia were collected from several fixed *T. cystophora* specimens (adult and/or juvenile), cryoprotected in 30% sucrose overnight at 4°C and thereafter immersed in OCT (Tissue Freezing Medium, Jung) and frozen in minus 30°C. Horizontal frozen sections with an 8–12 µm thickness prepared by Cryostat Leica CM3050 S, were transferred onto microscopy slides. These cryosections were washed three times in PBS, re-fixed by 4% PFA and subsequently immuno-stained with an antibody.

5.2.6 Immunolabelling of cryosections

Cryosections were refixed in 4% PFA for 10 minutes, washed three times with PBS, permeabilized with PBT (PBS + 0.1% Tween 20) for 15 minutes, and blocked in 10% BSA in PBT for 30 minutes. The primary antibodies for Tcop1 and Tcop13 (paragraphs 5.2.1 - 5.2.3) along with the commercially available antibodies used for the phototransduction cascade screening, were diluted in 1% BSA in PBT to 1:50, 1:500, 1:1000, 1:2000. For complete list of antibodies used in this study see Table 5.

Table 5: List of primary antibodies used for IHC in this study.

ML – generated by the author, ZK – generated for Kozmik et al. (2008a). Sc – Santa Cruz, sa - Enzo Life Sciences, ab – Abcam, AB – Chemicon, R - Sigma-Aldrich, MA- Invitrogen [1) 2)] Antibodies raised against distinct domains within the corresponding G alpha subunit, [3)] Abrahams and Gregerson (1983), [4)] Antibody used to verify opsin expression in mammalian cell line for the light-response analysis.

	Candidate genes:	Antibody:
1	Tcop1	ML
2	Tcop13	ML
3	Tcop18	ZK
4	Gs (GNAS)	sc-383
5	Gi (GNAI)	sc-393, sa-128 [1)]
6	Gq (GNAQ)	sc-392, , sc-393 [2)]
7	Go (GNAO)	sc-387
8	arrestin (ARR1)	S-antigen Gregerson[3)]
9	recoverin (RCV1)	AB5585
10	rhodopsin kinase (GRK1)	R3151
12	lecithin retinol acyltransferase (LRAT)	ab166784
13	retinol dehydrogenase (RDH5)	ab106738
14	rhodopsin 1D4-antibody (1D4)	MA1-722 [4)]

Each dilution was applied on at least two glass slides (each slide housing several sections of rhopalia from different specimens). The slides were incubated overnight at 4 °C, washed three times with PBS, followed by incubation with secondary antibodies (Alexa Fluor 488- or 594-conjugated goat anti-mouse or anti-rabbit IgG - Molecular Probes) in 1% BSA in PBT (1:500). The sections were counterstained with DAPI and mounted in Mowiol (Sigma) or Vectashield (Vector Laboratories).

Fluorescence and bright-field light images were acquired on Nikon Diaphot 300 with objectives 4x/0.1 and 10x/0.25. Confocal scans were acquired on a Leica Inverted and Upright TCS SP5 Confocal Microscopy System, with a four fluorescent channel detection system. Images were captured and processed in Leica Application Suite 1.8.0 software.

6. Light response assay experimental set-up

A light-response assay for opsin-Gs-cAMP pathway stimulation according to that used by Bailes et al. (2012) was established. This assay is highly specific for inspected receptors (opsins in this case) signalling via the Gs-cAMP pathway, but insensitive to signalling via Gi (or any other G protein alpha subunit sub-type).

GloSensor cAMP HEK293 cells constitutively express a biosensor encoding luciferase. This luciferase is modified to carry a cAMP binding domain (from the RIIb

subunit of cAMP-dependent protein kinase A), which in case of increase in the cAMP levels in these cells leads to strong luciferase activity, which is measured by a luminescence reader.

6.2 Immunofluorescent staining of GloSensor cAMP HEK293 cells for opsin expression verification

We introduced the cDNAs encoding all of the *T. cystophora* opsins into pcDNA3.1 vector in-frame with the epitope tag 1D4 from bovine rhodopsin, together with the *C. rastonii* opsin (shown to activate the Gs-cAMP pathway by Koyanagi et al. 2008) as a positive control. As heterologous protein expression in cell lines may sometimes prove difficult or even impossible (Koyanagi et al. 2005), we decided to verify the expression of individual opsin genes in the GloSensor cAMP HEK293 cells (Promega) by immunofluorescent labelling using antibody against the introduced 1D4 epitope tag. All of the *T. cystophora* full length opsins and Caryb (GenBank AB435549, opsin cDNA for *C. rastonii* kindly provided by Dr. Koyanagi) were amplified and cloned into pcDNA3.1 + 1D4 and verified before further use.

GloSensor cAMP HEK293 cells were seeded on glass cover-slides (submerged in well plate with media) followed by transfection with the pcDNA3.1 + 1D4 recombinant plasmids using the FuGene HD (ROCHE) and were grown over night at 37 °C. The transfected cells were then washed with PBS, fixed with 4% paraformaldehyde (PFA) for 10 minutes and permeabilized with 0.1% Triton X-100 for another 10 minutes, followed by blocking in 10% BSA in 1x PBS with 0.1% Tween 20 for an hour. In order to immuno-stain the expressed opsins, a mouse monoclonal anti-rhodopsin antibody against the last 9 amino acids - the 1D4 epitope (Millipore Chemicon MAB5356), was used at a dilution of 1:250 in combination with a secondary antibody conjugated with Alexa Fluor 488. Cells were mounted in Mowiol and fluorescent images were captured using a Leica SP5 confocal microscope.

6.3 Light-response assays

GloSensor cAMP HEK293 cells were plated onto a plastic 96-well plate in the Leibovitz's (L-15) Medium, provided with phenol red (Gibco) and 10% serum, and

incubated overnight at 37 °C with 0.3% CO_2. Thereafter, cells were transfected with plasmids expressing inspected opsin genes (Fig. 11) using the FuGENE HD Transfection Reagent (ROCHE).

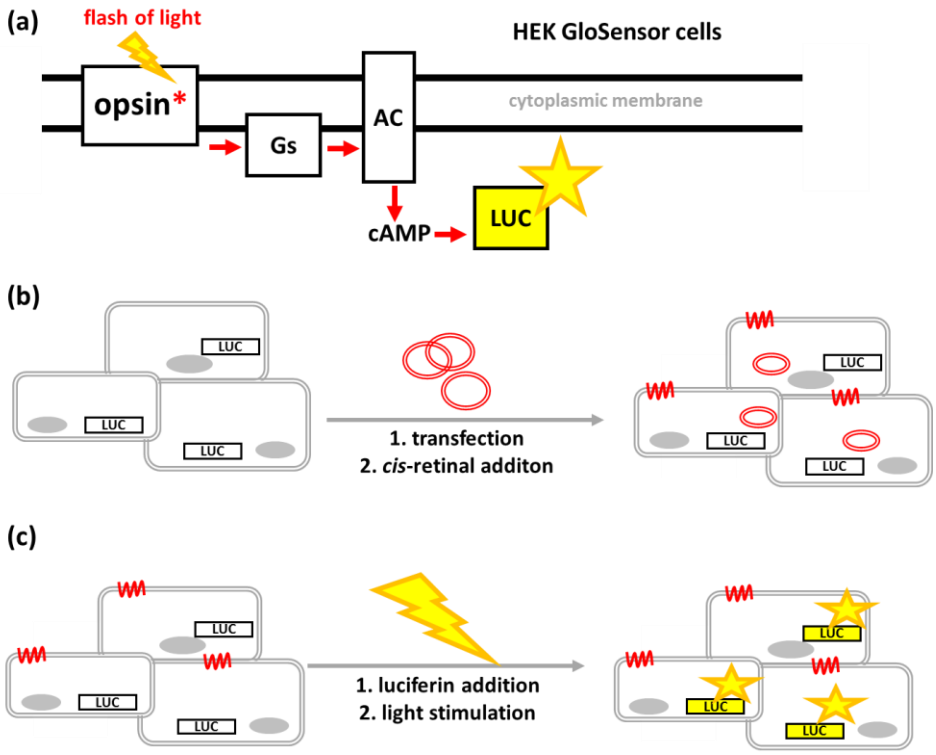

Fig. 11: Schematic illustration of the light-response assay.

a) Basic scheme of the assay. HEK Glosensor cells express genetically modified form of luciferase (LUC) with inserted cAMP-binding protein moiety. Stimulation of inspected G protein coupled receptors (opsins in our assay) leads to the activation of Gs mediated signalling cascade and a rise in cAMP via adenylyl cyclase (AC) stimulation by the Gs alpha subunit of the trimeric G protein. cAMP binding to the modified luciferase leads to conformational change resulting in an increased light output (luminescence), which is measured. b) HEK Glosensor cells were transfected with various opsin expressing vectors (pcDNA3.1+1D4; red circles) and were incubated at 37 °C for several hours to allow transient expression of the receptors (red squiggles on the membranes) in the cells. The cells were then treated with 9-cis retinal and incubated overnight at 37 °C, to allow the reconstitution of the chromophore and opsin into functional photopigment. c) Prepared cells were treated with luciferin and tested in the assay by light stimulation. The response was then measured in ultra-sensitive luminescence reader.

All subsequent procedures were carried out under dim red light. Six hours after the transfection, 9-cis retinal (Sigma-Aldrich) was added to the medium (final

concentration of 10 mM) and the cells were incubated overnight at 37 °C with 0.3% CO_2. On the next day, the transfected cells were equilibrated for 30 minutes at room temperature. Beetle luciferin potassium salt (Synchem), was reconstituted in 10 mM HEPES buffer and added to the cells (final concentration of 3 mM). The cells were then inspected using ultra-sensitive luminescence model in the EnVision Multilabel Plate Reader (PerkinElmer). The activity of luciferase was measured for 2 hours with 0.1 second resolution and 1-minute cycle intervals for determination of the luciferin uptake.

Cells were then stimulated with three pulses of light, using repeated flashes from a Nikon speedlight SB-600 electronic camera external flash (5 flashes, 1 flash/second in each pulse, approximately 40000 lumen/m^2 per single flash), followed by recovery periods of 30 minutes during which the raw luminescence units (RLU) were recorded. After the third round of measurement, the cells were stimulated again with seven light pulses with 3-minute duration (5 flashes, 1 flash/second in each pulse). Luminescence was recorded between the pulses (0.1 second resolution, 15 seconds per cycle) and 120 minutes after the last pulse (0.1 seconds resolution, 30 seconds per cycle).

To investigate the role of the tripeptide (contact between bovine rhodopsin and the corresponding G alpha subunit; see Marin et al. 2000) in cnidopsin signalling, we replaced the HKQ tripeptide region in Tcop13 DNA sequence with tripeptides NKQ (Tcop1 and bovine rhodopsin), SKS (Tcop14) and NRS (Tcop18). Light-response assay experiment for the mutated tripeptides was performed analogically to the aforementioned set-up (with only minor changes – the experiment was performed at 37 °C, leading to faster response of cells to the light stimulation). In all of the experiments cells were plated and treated in triplicate. Luminescence recordings were analysed in Microsoft Office Excel. Prism (Graphpad) software was used for all statistical analyses.

7. Phototaxis inhibition experimental set-up

Behavioural testing of *T. cystophora* visual navigation ability after treatment with pharmacological inhibitors of the G protein alpha subunits was performed in an aquarium-like testing chamber, with a size of 20×5×5 cm with one side illuminated by white light emitted by a light-emitting diode (LED) diode (Fig. 12).

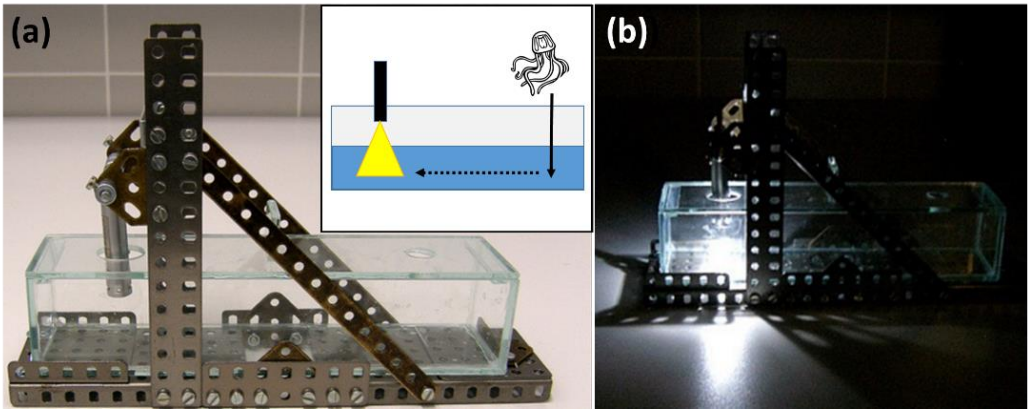

Fig. 12: Experimental set up for behavioural testing of *T. cystophora*.

a-b) Testing chamber (size of 20×5×5 cm) with a diode holder constructed form Merkur. *Inset:* Tested medusae were placed into the testing chamber into artificial seawater. After a short adaptation in the dark, the diode was switched on (b) and the number of medusae reaching the illuminated side of the chamber was counted in time intervals ranging from 5 minutes to 24 hours.

To test the effect of the two selected pharmacological inhibitors (Fig. 13), namely NF449 and NF023 (Calbiochemon), on the phototactic behaviour, we incubated actively swimming juvenile medusa (three days old) in 1 ml of artificial seawater with NF449 or NF023 in concentrations of 0 µM, 100 µM and 1 mM for 30 minutes).

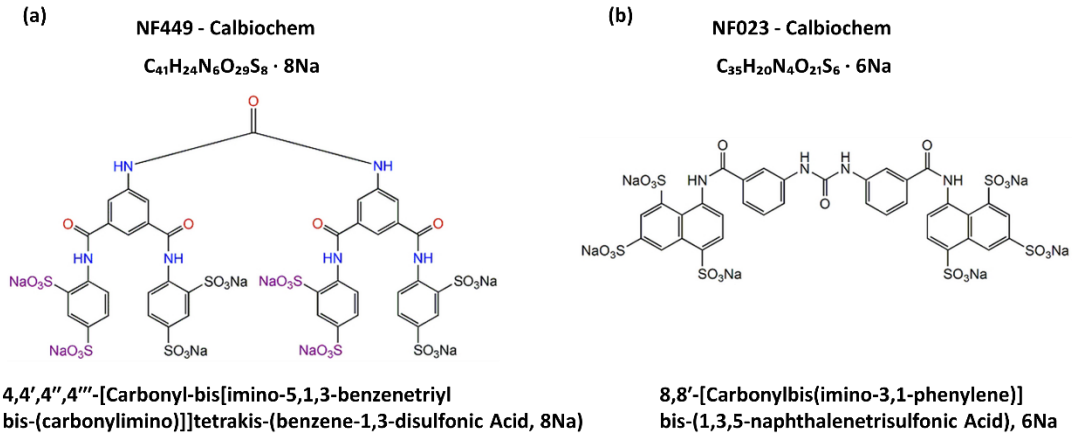

Fig. 13: Pharmacological inhibitors used in the behavioural assay.

The product ID, molecular formula, structural formula and chemical name of the highly selective inhibitor; a) HP2X1 receptor antagonist - NF449 (selectively inhibits G alpha s subunit). b) P2X1 receptor antagonist – N023 (selectively inhibits G alpha i subunit).

Medusae were carefully washed with untreated artificial seawater and gently placed into the non-illuminated side of the testing chamber with a plastic dropper and observed for phototactic behaviour. The number of medusae that reached the illuminated region of the chamber in the intervals of 5 minutes, 3 and 24 hours, was recorded and compared to the number of jellyfish from the untreated control group. All experiments were performed at 22 °C.

RESULTS

Most of the results presented in this chapter were published in:

Liegertová M, Pergner J, Kozmiková I, Fabian P, Pombinho AR, Strnad H, Pačes J, Vlček Č, Bartůněk P, Kozmik Z. (2015). Cubozoan genome illuminates functional diversification of opsins and photoreceptor evolution. Sci Rep. 5:11885.

1. Identification and cloning of *T. cystophora* opsin genes

In addition to the previously annotated *T. cystophora* c-opsin (Kozmik et al. 2008a) another 17 opsin sequences (named Tcop1-Tcop17) were identified in the *T. cystophora* genomic library (for visualization of the identified contigs Hits see Fig. 9b). Complete coding sequences were cloned from the genomic DNA (GenomeWalker) and submitted to GenBank under the accession numbers JQ968416-JQ968432. One of these novel sequences (named as Tcop13) was identified as the ortholog (with 93% sequence identity) of the annotated box jellyfish *C. rastonii* opsin - Caryb (Koyanagi et al. 2008) (Fig. 14).

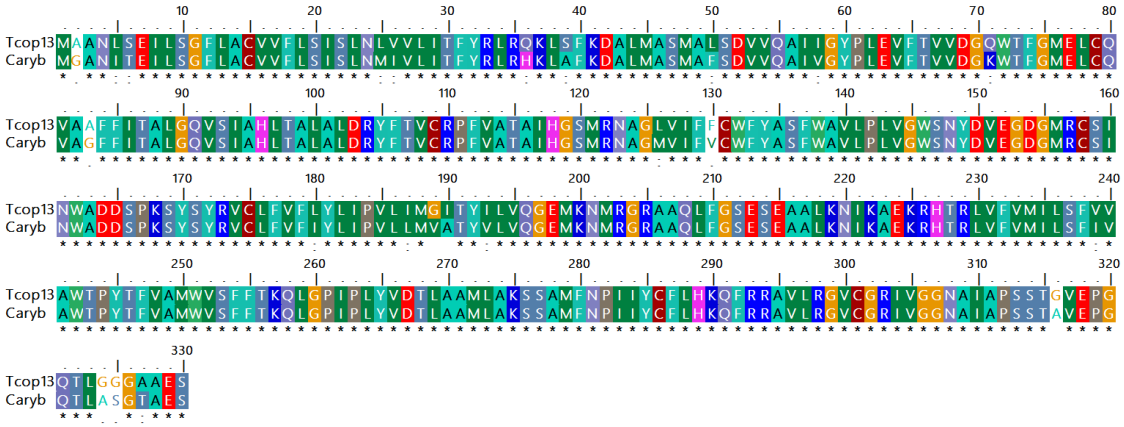

Fig. 14: Pairwise sequence alignment of Tcop13 and *C. rastonii* opsin Caryb.

Alignment depicting homology between Tcop13 and Caryb opsins, overall sequence identity is 93%. * Identical amino acids position.

All of the seventeen novel opsins are intronless genes, showing overall sequence homologies to other cnidarian opsins as well as to bilaterian rhodopsins. The conserved

lysine to which the chromophore 11-cis-retinal binds was confirmed in each of the cloned opsins.

Author´s contribution: *In silico* data mining, identification, cloning and characterization of 17 novel genes.

2. Sequence analysis of *T. cystophora* opsin genes

We focused on the identification of residues within three potential counterion sites 83, 113, 181 (numbering according to bovine rhodopsin amino acid chain) within the Tcops and other cnidopsins (Fig. 15).

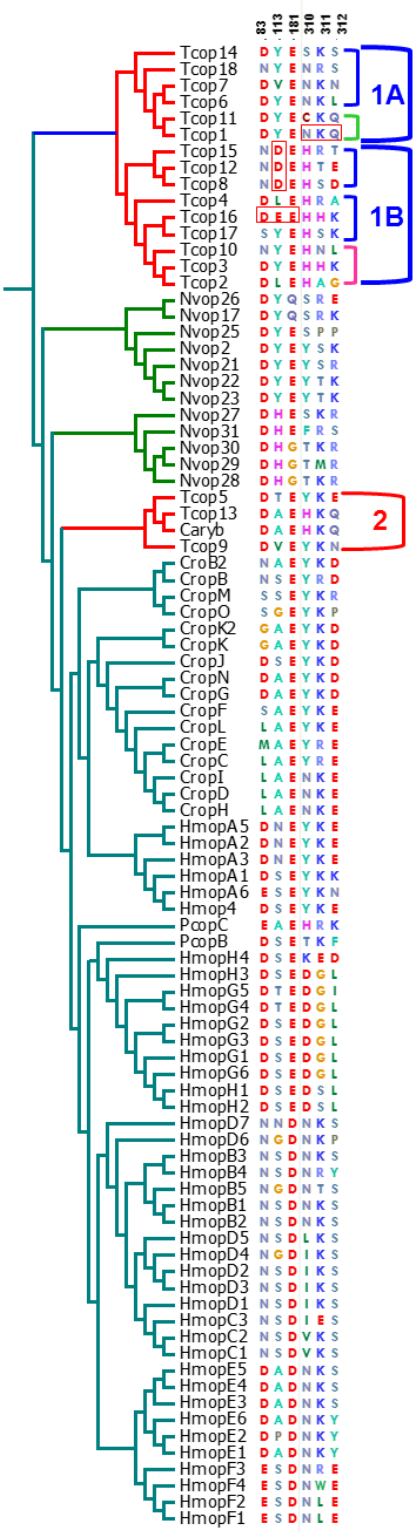

Fig. 15: Comparison of putative counterion and tripeptide diversity within cnidopsins.

Partial sequence alignment of amino acid residues at the three potential counterion sites 83, 113, 181 (amino acid position according to bovine rhodopsin) and the G protein binding tripeptide at position 310-312 within the cnidopsins in respect to their phylogenetic position (branching at left). Red boxes: NKQ - tripeptide also found in vertebrate rhodopsin; DDD - D at position 113 found only in chordates; DEE at 83, 113, 181 common in vertebrate opsins. Brackets at the right side highlight phylogenetically closely related subgroups of Tcops. For details see phylogenetic analysis and discussion. Tcop – *Tripedalia cystophora* (Cubozoa) opsin; Nvop – *Nematostella vectensis* (Anthozoa); Crop – *Cladonema radiatum* (Hydrozoa); Hmop – *Hydra magnipapillata* (Hydrozoa); Caryb – *Carybdea rastonii* (Cubozoa). Adapted from Liegertova et al. (2015).

A negatively charged amino acid (E/D) at position 83 was found in more than 50 % of all the cnidarian opsins, more than 95 % have E/D at position 181, in contrast to E/D

at position 113, which was found only in four of the Tcops (Tcop16, Tcop15, Tcop12, and Tcop8) (Fig. 15 – red box). Next, we focused on the residues of the putative G protein binding tripeptide (positions 310-312 according to bovine rhodopsin) of the cnidarian opsins. The tripeptides have shown to be conserved between closely related opsin branches within each species (Fig. 15) but are apparently not conserved between the species across cnidarian lineages. Furthermore, Tcop1 tripeptide was found to be identical with vertebrate rhodopsin NKQ motive.

Author´s contribution: Novel opsin sequences characterization.

3. Phylogenetic analysis of *T. cystophora* opsin genes

Our phylogenetic analysis of a large and diverse set of 779 opsin sequences recovered the four major clades described in earlier studies (Plachetzki et al. 2007, Suga et al. 2008, Plachetzki et al. 2010, Porter et al. 2012) – the c-type opsins, cnidopsins, r-type opsins and group 4 opsins (Fig. 16).

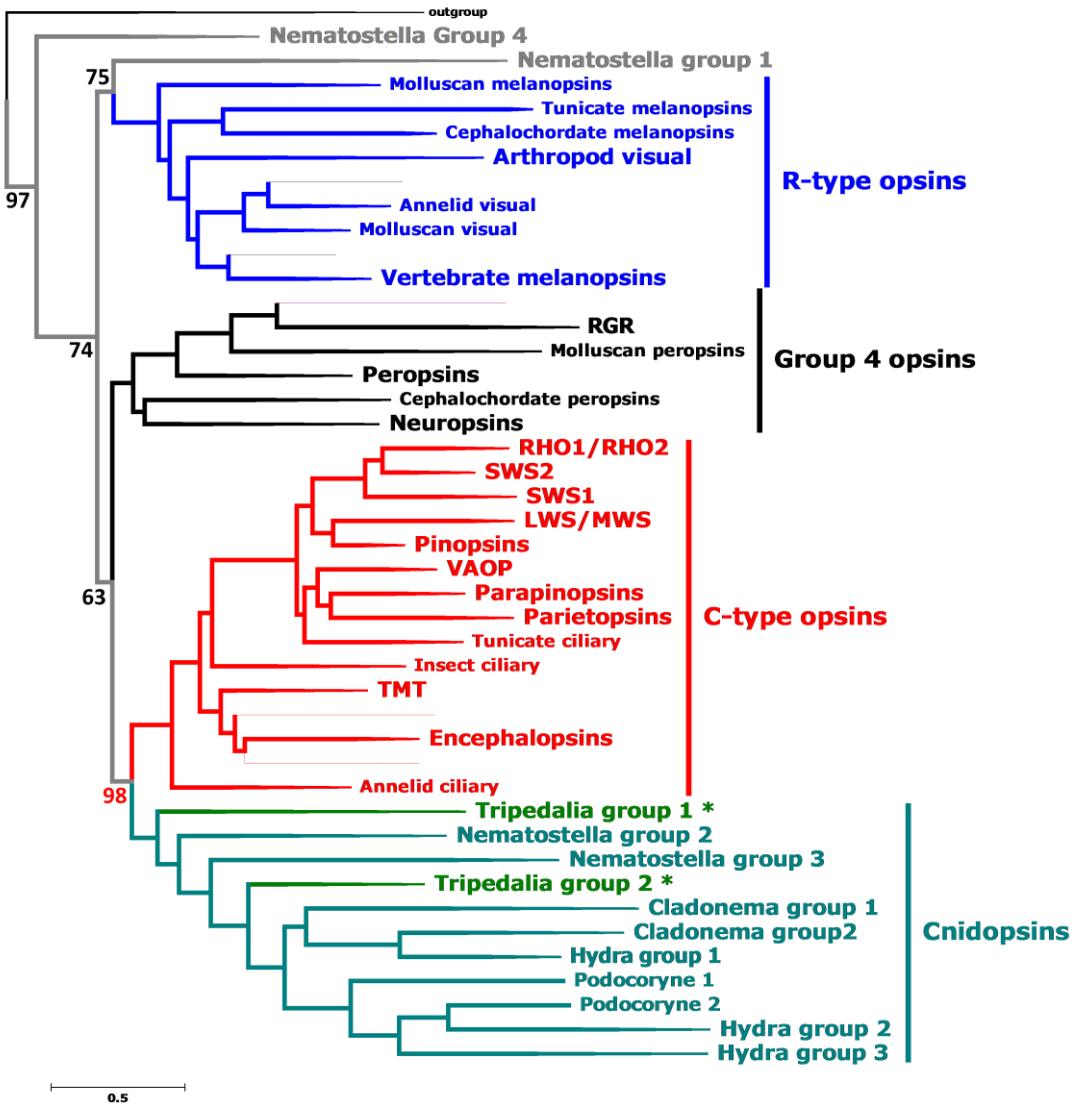

Fig. 16: Compressed Maximum-likelihood tree of the opsin family.

The maximum-likelihood tree inferred from 801 protein sequences (779 opsin sequences + 22 non-opsin outgroup sequences) with the branches compressed into individual clades. Approximate Likelihood-Ratio Test (aLRT) branch support values in % are shown for the major opsin subfamilies, which have been labelled at the right. R-type opsins: arthropod visual pigments (M/LWS, SWS); annelid and molluscan visual pigments; vertebrate melanopsins; uncharacterized tunicate, cephalochordate and molluscan opsins. Group 4 opsins: neuropsins; peropsins; RGR and uncharacterized cephalochordate and molluscan peropsins. C-type opsins: vertebrate visual pigments (Rh1, Rh2, SWS1, SWS2, M/LWS); pinopsins; parapinopsins; vertebrate ancient opsins (VAOP); parietal opsins; teleost multiple tissue opsins (TMTs); encephalopsins; tunicate ciliary opsins; ptersopsins and insect ciliary opsins; uncharacterized annelid ciliary opsins. Cnidopsins: cnidarian opsins including representatives from hydrozoans, anthozoans and cubozoans. Nematostella group 4 and 1 are novel cnidarian opsin subfamilies which are the only cnidarian opsins not clustering within the cnidopsins. Adapted from Liegertova et al. (2015).

Nevertheless, the statistical support for some of the relationships was not that strong. Due to the weaker branch support, we were unable to exclude the scenario where group 4 and r-type opsins cluster together as sister groups, opposing the c-type opsin and cnidopsin subgroups as suggested by Porter et al. 2012 (based on the phylogeny and presence of bistable pigments in arthropod/cephalopod visual r-type opsins and chicken group 4 neuropsin; see Panda et al. 2005, Yamashita et al. 2010).

The relationship between cnidopsins and the c-type opsin subfamily had the strongest support. Most of the cnidarian opsins fell within cnidopsins, with the exception of Nematostella group 4 and group 1. All Tcops fell into the cnidopsins subfamily (Fig. 17), clustering with the hydrozoan opsins, which was consistent with the relationship among cnidarian classes (Bridge et al. 1992).

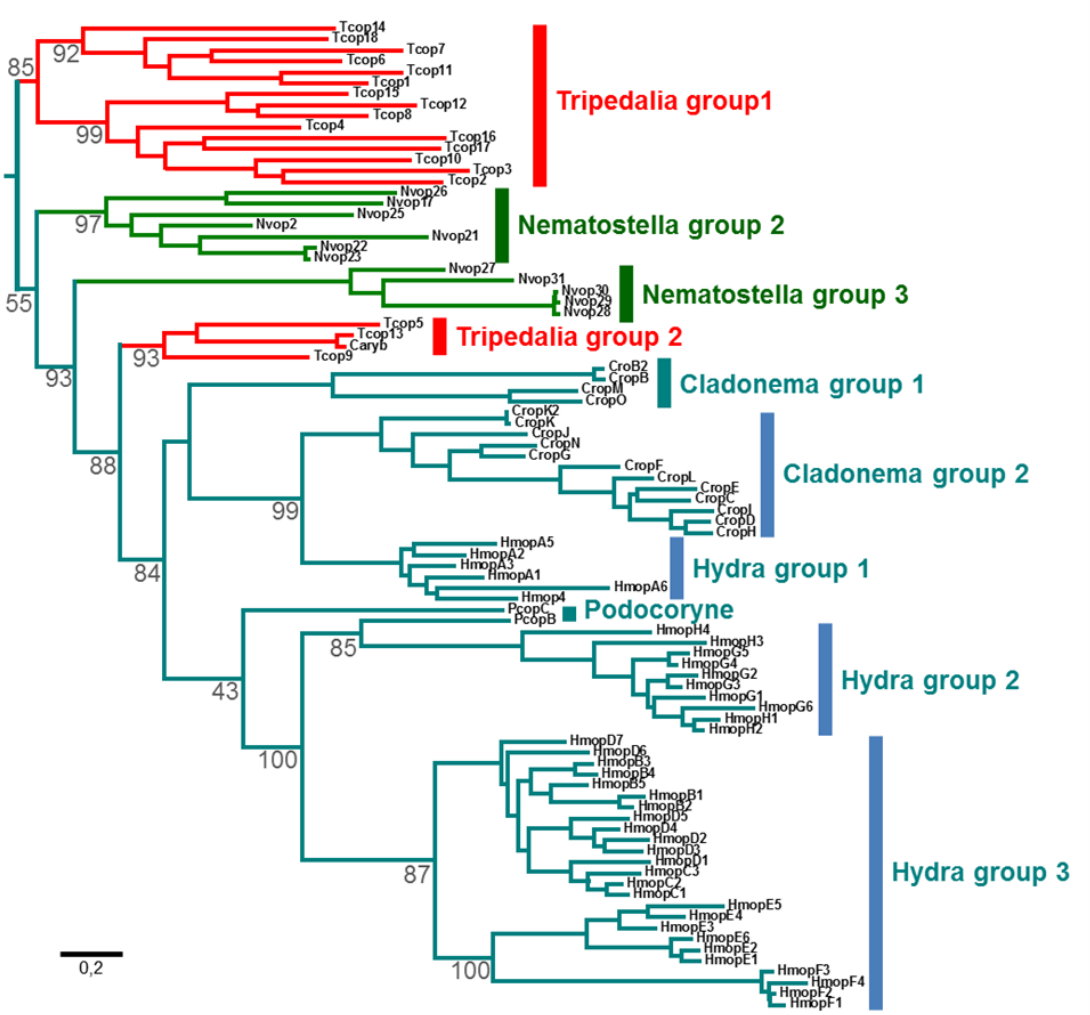

Fig. 17: The cnidopsin branch of the opsin family maximum-likelihood tree.

The major cnidopsin clades have been labelled. aLRT branch support values in % are shown for major groups. Tcop – *Tripedalia cystophora* (Cubozoa); Nvop – *Nematostella vectensis* (Anthozoa); Crop – *Cladonema radiatum* (Hydrozoa); Hmop – *Hydra magnipapillata* (Hydrozoa); Caryb – *Carybdea rastonii*. Nematostella group 1 and 4 not shown here. Adapted from Liegertova et al. (2015).

In the phylogenetic tree Tcops clearly fell into two distinct groups: Tc-group-1 and Tc-group-2.

Author´s contribution: Dataset preparation and complete phylogenetic analysis (performed under supervision from Jan Pačes, Ph.D.)

4. Analysis of *T. cystophora* opsin genes expression patterns and dynamics

To inspect the expression patterns of Tcops, qRT-PCR analysis on mRNA isolated from different jellyfish life stages and various adult tissues was performed. The expression level of each Tcop in each of the inspected body parts (Fig. 18a) of the adult medusa relative to the rhopalium expression (set to 1.0) was calculated and normalized to that of the housekeeping gene Rpl32 (Fig. 18b-s).

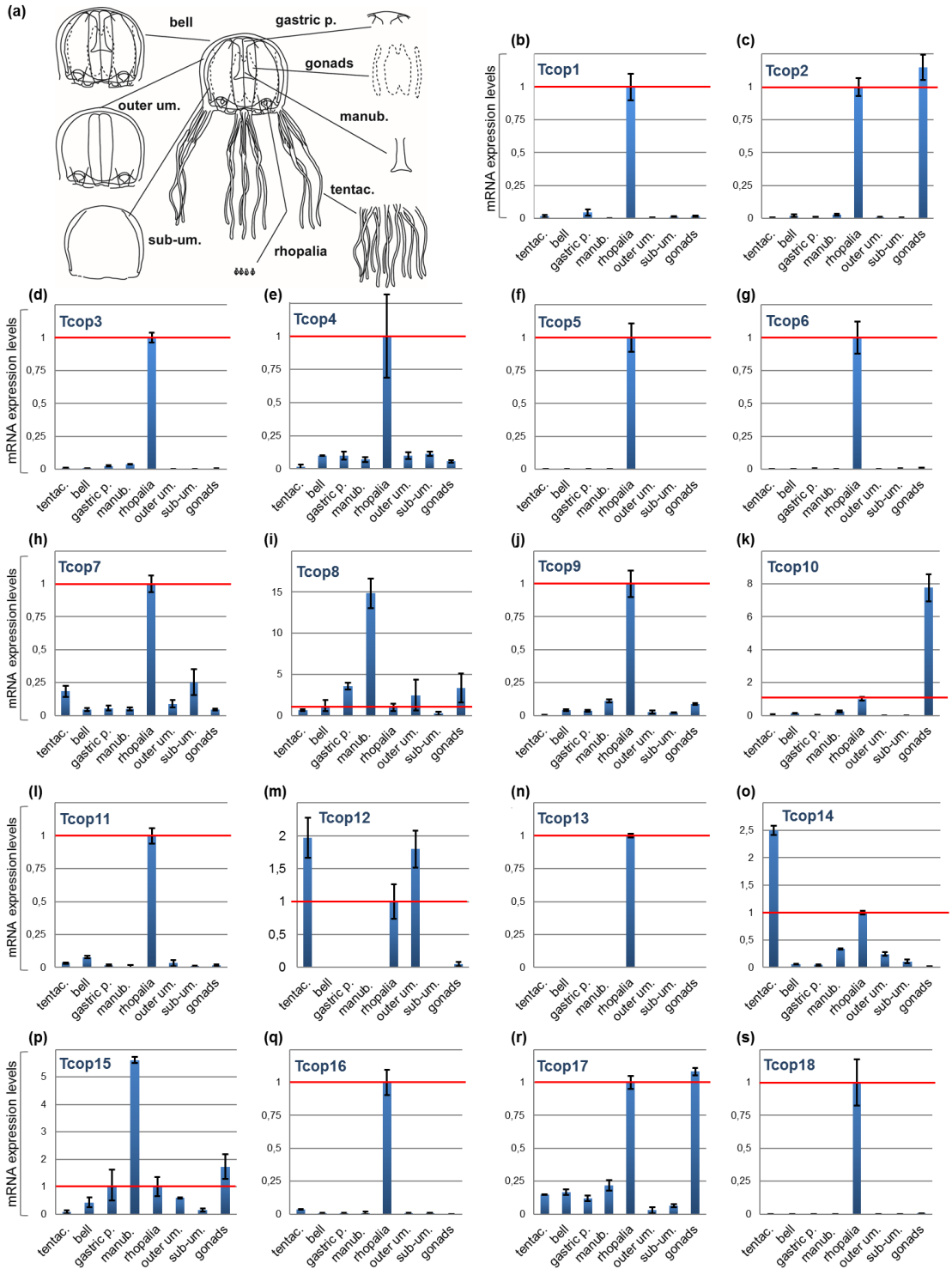

Fig. 18: mRNA expression levels of individual Tcops in various tissues of adult medusa.

a) Body parts of adult medusa dissected for the qRT-PCR analysis: tentacles (tentac.), manubrium (manb.), male gonads, gastric pouch (gastric p.), bell, outer umbrella (outer um.), sub-umbrella (sub-um.) and rhopalia. b-s) mRNA expression levels of Tcops for each inspected body part relative to the rhopalium expression (set to 1.0 – red line), normalized to Rpl32. x –

axis: analysed body parts, y – axis: relative mRNA expression level. Adapted from Liegertova et al. (2015).

Most of the Tcops were detected in the rhopalium at least in small amounts (Fig. 18, 19a).

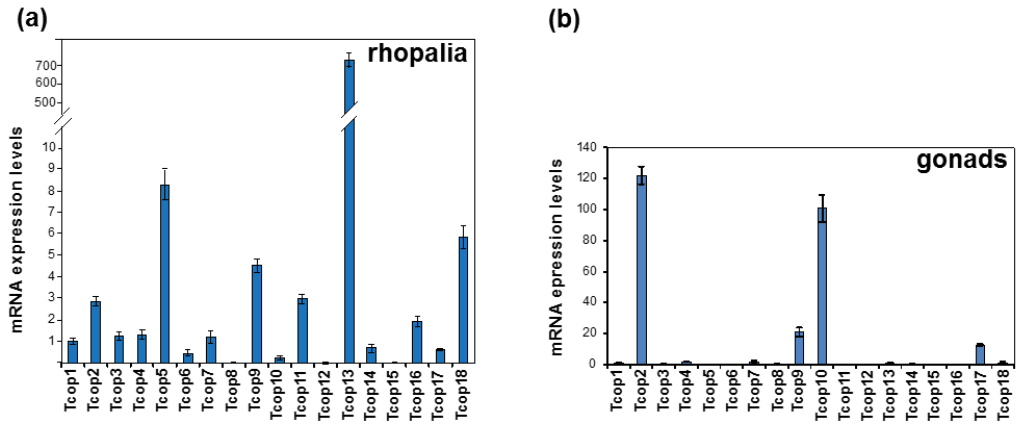

Fig. 19: Comparison of Tcops mRNA expression levels within selected tissues.

qRT-PCR results for a) rhopalium and b) male gonads, normalized to Rpl32 and plotted separately to enable better gene-to-gene comparison. Adapted from Liegertova et al. (2015).

Moreover, for the majority of Tcops (Tcop1, 3, 4, 5, 6, 7, 9, 11, 13, 16, 18 = 11 out of 18), rhopalium was the tissue with the highest expression detected. Other Tcops shown to be mainly expressed in male gonads (Tcop2, Tcop10, Tcop17), manumbrium (Tcop8, Tcop15) or tentacles (Tcop12, Tcop14). For a better gene-to-gene comparison within an individual tissue, the results were plotted separately for rhopalium and male gonads (Fig. 19).

Next, we investigated Tcops gene expression during the life cycle of *T. cystophora.* For this purpose, mRNAs from two stages of larvae - non-pigmented and pigmented (larval eye-containing stage), vegetatively grown polyp, four stages of a metamorphosing polyp (where stage 3 and 4 contain developing rhopalia) and juvenile medusae were isolated and subjected to qRT-PCR (Fig. 20a).

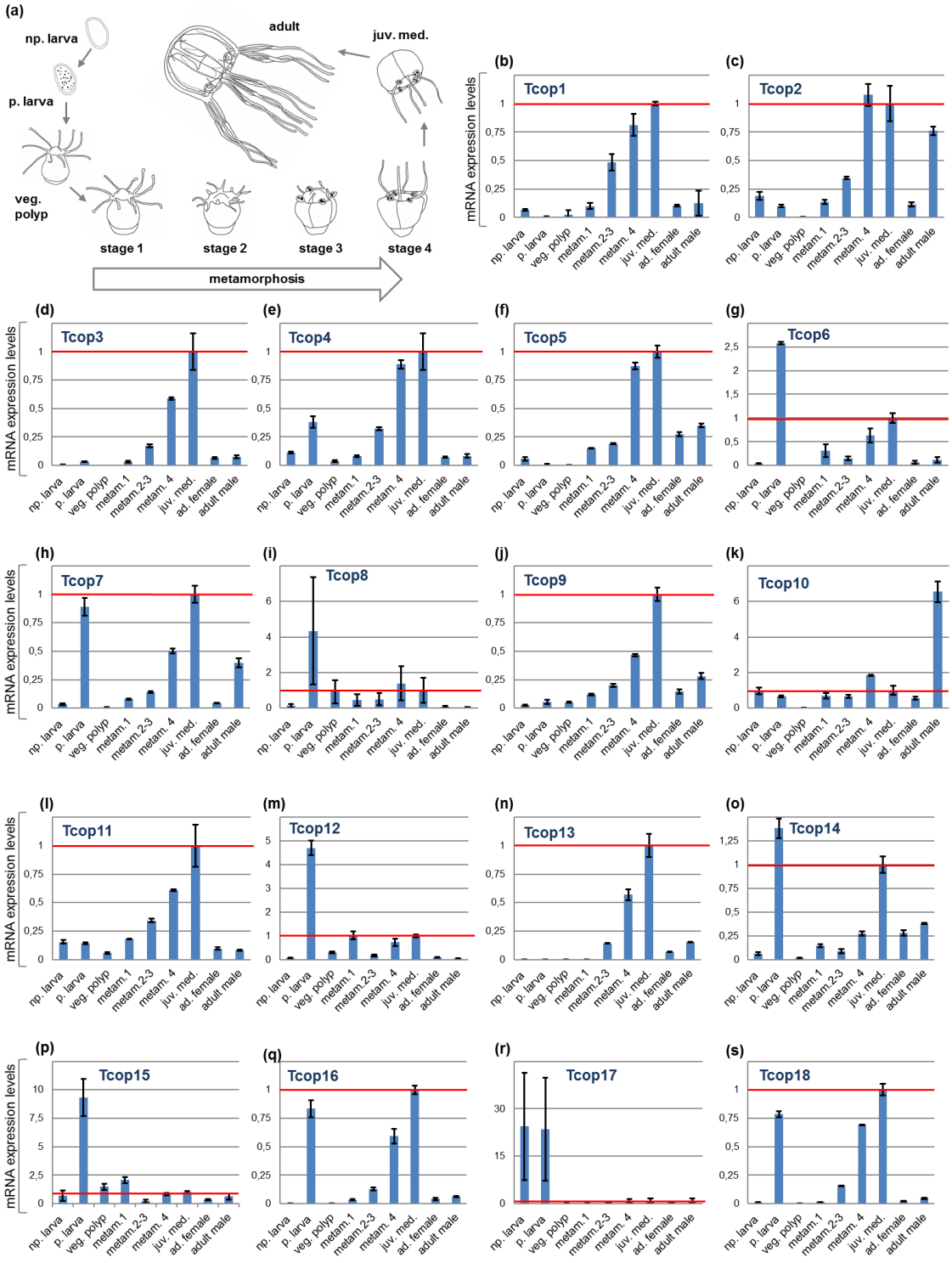

Fig. 20: mRNA expression levels of Tcops in different *T. cystophora* life stages.

a) For the qRT-PCR analysis, mRNA samples from nine subsequent life stages were isolated: non-pigmented larva (np. larva), pigmented larva (p. larva), vegetative polyp (veg. polyp), three polyp-to-medusa metamorphosing stages (metam1, 2-3, 4), juvenile medusa (juv. med.), adult female (ad. female) and adult male. b-s) mRNA expression levels of the individual Tcops of the inspected life stage relative to the juvenile medusa expression (set to 1.0 – red line), normalized

to Rpl32. x – axis: analysed stages, y – axis: relative mRNA expression level. Adapted from Liegertova et al. (2015).

Expression levels of all individual Tcops for each *T. cystophora* life stage relative to the juvenile medusa expression (set to 1.0) were calculated and normalized to Rpl32 (Fig. 20b-s). Two consistent features were revealed in the results. First, Tcops with highest expression in the adult rhopalium (e.g. Tcop5, Tcop9, Tcop13 and Tcop18), significantly increased their expression during the metamorphosis into medusa stage (when the rhopalia emerge and develop). Second, many group-1 Tcops (Tcop6, 12, 14, 15, 17) were highly expressed in the pigmented (eye-containing) larval stage, in contrast to group-2 Tcops (established as Gs-coupled receptors with a major role in adult lens-containing eyes – see further), whose expression was absent at this stage. All of the qRT-PCR data are schematically summarized in Fig. 21.

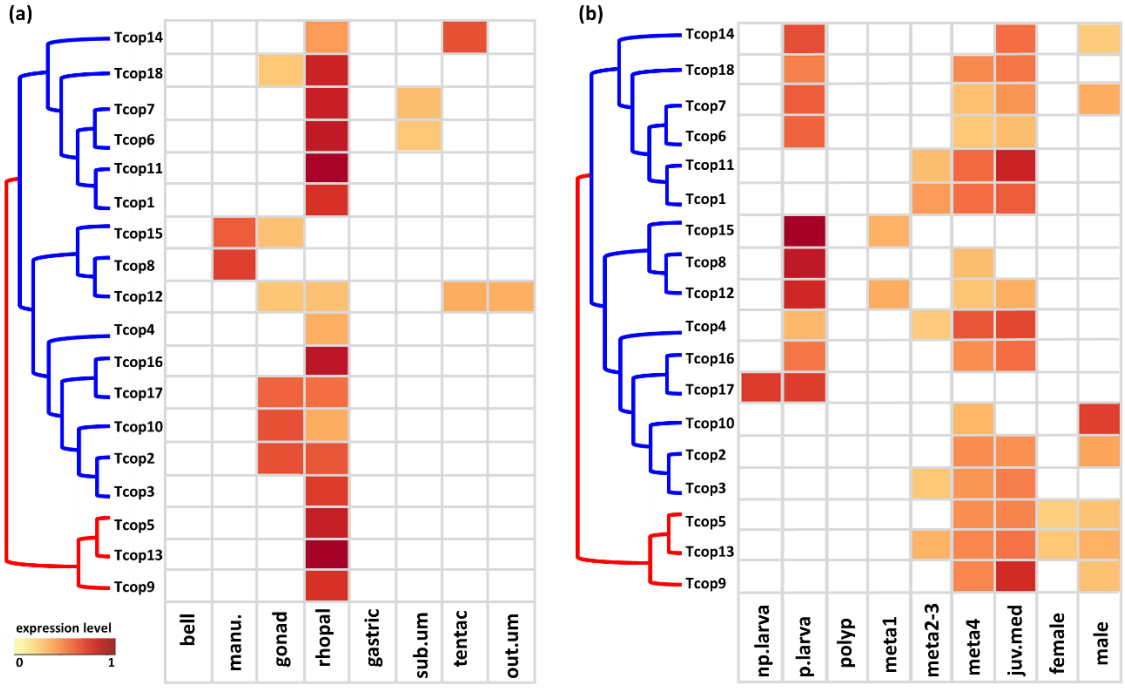

Fig. 21: Summary of the qRT-PCR data for individual Tcops according to their phylogenetic relationship.

The expression levels of individual Tcops derived from a Z-score heat map generated from the qRT-PCR data. Intensity of the shading corresponds to expression levels when normalized to expression of Rpl32. a) qRT-PCR results of individual Tcops expression in *T. cystophora* body

parts. manu – manumbrium, rhopal – rhopalium, gastric - gastric pouch, sub. um – sub-umbrella, out.um - outer umbrella. b) qRT-PCR results of Tcops expression during *T. cystophora* life cycle. np. larva - non-pigmented larva, p. larva - pigmented larva, polyp - vegetative polyp, meta1, meta2-3, meta4 - three polyp-to-medusa metamorphosing stages, juv. med. - juvenile medusa, female - adult female and male - adult male. Adapted from Liegertova et al. (2015).

To gain further insight into the possibly diverse roles of group-1 and group-2 Tcops in *T. cystophora* eyes, we analysed expression of key representatives of each of the Tcops sub-group (Tcop13/group-2; Tcop1/group-1, Tcop18/group-1) by immunohistochemical staining of the rhopalia cryosections *in situ* (Fig. 22a-c).

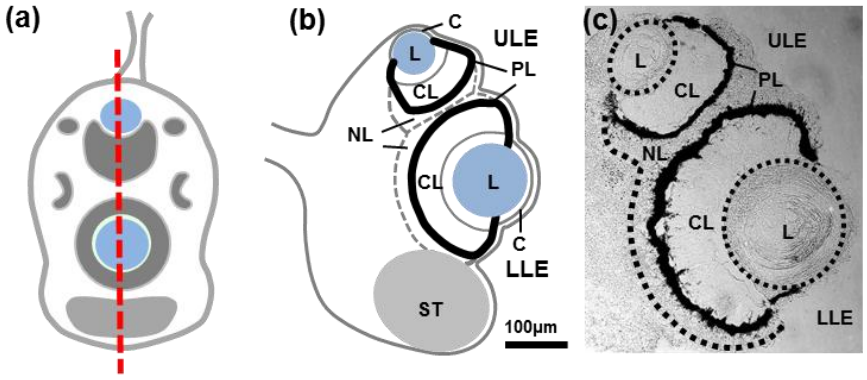

Fig. 22: Anatomy of the adult rhopalium.

a) For IHC analysis of the major lens eyes, rhopalia were sectioned preferentially along the medial line (red line). b) Scheme of the section plane. c) Detail of the same section plane under microscope for comparison. ULE - upper lens eye; LLE - lower lens eye; CL - ciliary layer; PL – pigment layer; NL - neural layer; L – lens; C – cornea; ST – statocyst.

To this end we generated specific antibodies against Tcop1 and Tcop13 (members of group-1 and group-2, respectively). Staining for Tcop1 did not provide any detectable specific signal in the retinas of *T. cystophora* eyes, whereas clear signal was observed for Tcop13. We performed co-staining of Tcop13 with previously identified Tcop18 (Kozmik et al. 2008a) on the cryosectioned rhopalia to inspect the possible co-expression. Indeed, Tcop13 and Tcop18 were found to be expressed in the retinas of ULE and LLE in distinct patterns (Fig. 23a-l).

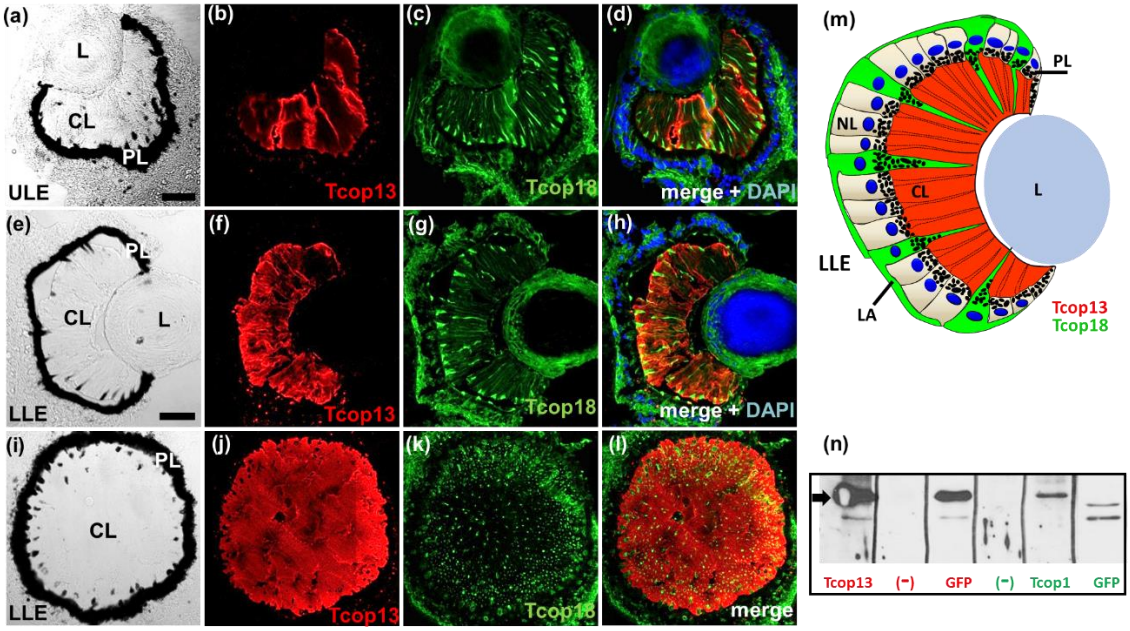

Fig. 23: Immunohistochemically detected localization of Tcop13 and Tcop18 in the retinas of *T. cystophora* lens eyes.

a-d) Sagittal section through the upper lens eye (ULE); e-h) Sagittal section through the lower lens eye; (LLE); i-l) Retina transverse section of the LLE. L - lens, CL - ciliary layer, PL - pigment layer. Tcop13 (red) is expressed in the ciliary layer of the retina in both ULE and LLE. Tcop18 (in green) expression in the CL of ULE and LLE retinas is more restricted (when compared to Tcop13) and extends into the PL. In the merge of both signals in panel (l), it is visible that both Tcops are expressed in distinct cells (with Tcop13 positive cells being more abundant); Blue – DAPI. m) Schematic representation of LLE. The CL is dominated by the ciliary segments (in red) of type-1 photoreceptor cells (PRC1). Scattered among the PRC1 are the cone shaped projections (in green) of type-2 photoreceptor cells (PRC2). In the neural layer (NL) both receptor types have their cell bodies with nuclei (dark blue), with only PRC2 cell bodies positive for Tcop18 signal. Projections of PRC2 cell bodies create a compact layer (LA) surrounding the whole retina. n) Western blot analysis of Tcop1 and Tcop13 antibodies. Antibodies were tested on a triple-lane blot containing the appropriate protein (Tcop1 and Tcop13) and protein of the other Tcop as a negative control (-). Both proteins, tagged with GFP, were recognised by the anti-EGFP antibody (GFP). The lower bands in the positive lanes are likely caused by protein degradation. Scale bar: 50 µm. Adapted from Liegertova et al. (2015).

According to analysis of the immunolabelled rhopalia sections, *T. cystophora* retinas contain at least two morphologically distinct photoreceptor cell types: ciliary photoreceptor type-1 (PRC1), expressing Tcop13 in the receptor cell cilia of the ciliary layer, and photoreceptor type-2 (PRC2) expressing Tcop18, not restricted only to the ciliary layer of the retina but expressed within the whole cell body (Fig. 23m, 24).

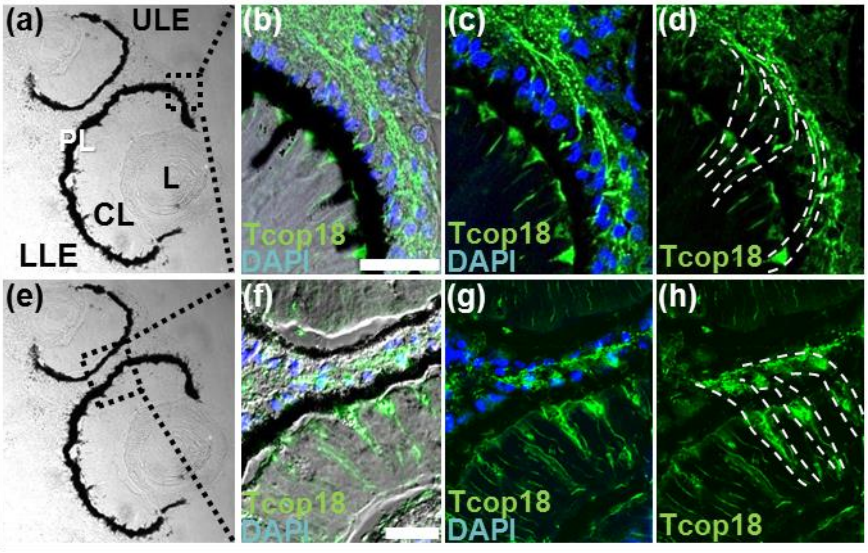

Fig. 24: Detailed morphology of type-2 photoreceptors (PRC2) in the retinas of ULE and LLE.

a-h) Confocal images showing IHC signal for Tcop18 (in green) in selected part of retinas of the lens eyes (bright field). d, h) Dotted white line indicates the probable shape of the PRC2 extending into cone-like projections towards the lens. Blue – DAPI. Scale bar 20 µm. Adapted from Liegertova et al. (2015).

Both Tcops were also distinctly expressed in the retinas of developing lens eyes of the newly metamorphosed *T. cystophora* medusa (Fig. 25a-d).

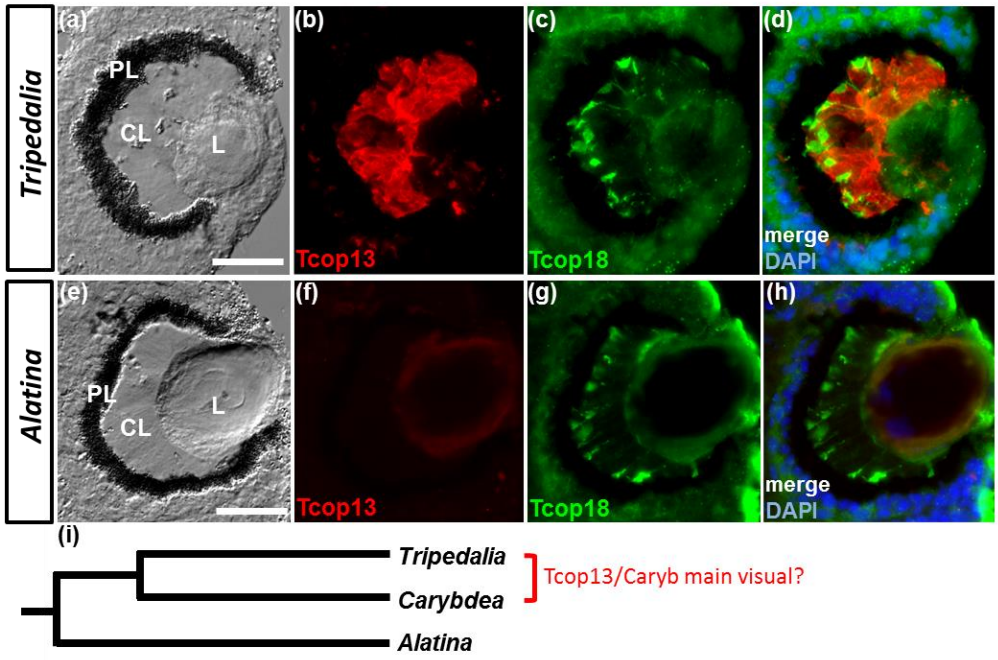

Fig. 25: Comparison of Tcop13 and Tcop18 expression in the retinas of lens eye between Tripedaliidae and Alatinidae

Confocal images of immunohistochemical staining for Tcop13 (red), Tcop18 (green) in the developing LLE of a-d) *T. cystophora* and e-h) *Alatina marsupialis* juvenile medusa. Note the absence of Tcop13 signal in the retina of *A. marsupialis* (f). i) Phylogenetic relationship between Carybdeid families. Blue – DAPI. Scale bars: 20 µm. Adapted from Liegertova et al. (2015).

We took advantage of having a culture of another box jellyfish *A. marsupialis* and performed IHC with both Tcops antibodies on the freshly metamorphosed medusa rhopalial sections (Fig. 25e-h). Only Tcop18 was detected in the developing eyes of this species.

Analysis of the staining for the two lesser eye types, slit and pit eyes (Fig. 26) revealed another difference in the expression of both the group-1 and group-2 Tcops representatives.

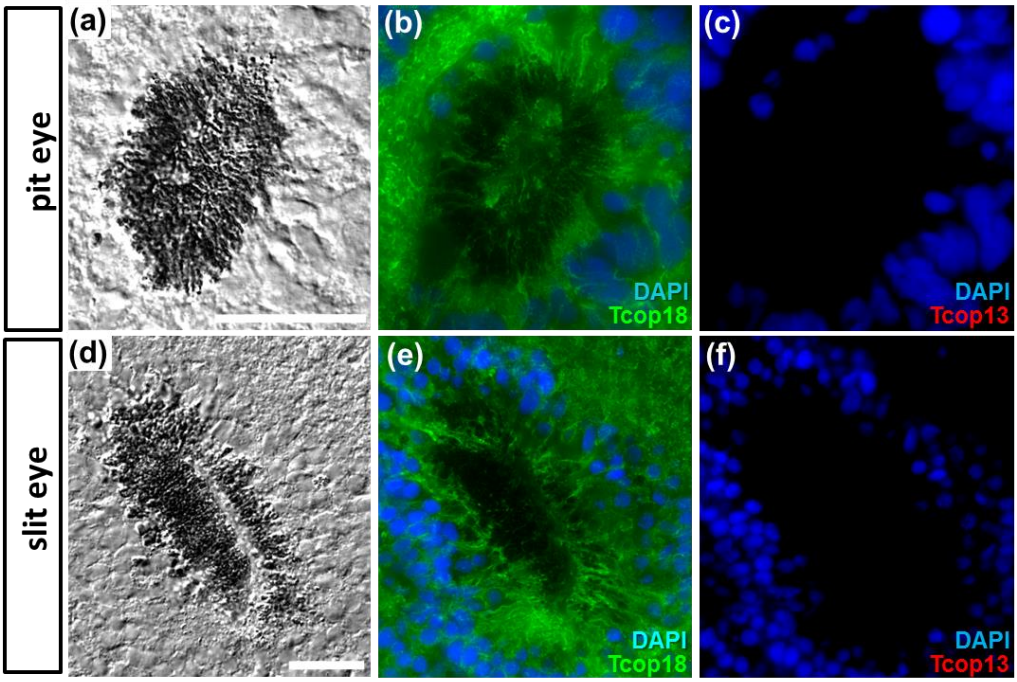

Fig. 26: Expression patterns of Tcop13 and Tcop18 in the pit and slit eyes of *T. cystophora*.

a-f) Confocal images of the pit and slit eyes. a) Pit eye as seen in bright field. b) Immunohistochemical staining for Tcop18 (green). c) Staining for Tcop13 (red). d) Slit eye as seen in bright field. e) Immunohistochemical staining for Tcop18 (green) and DAPI (blue). f) Staining for Tcop13 (red) and DAPI (blue). Note that Tcop13 was not detected in the retina of neither the pit nor the slit eye. Both minor eye types seem to be completely missing PRC1-like cells expressing Tcop13. Scale bars: Blue – DAPI. 20 µm. Adapted from Liegertova et al. (2015).

In this case only Tcop18 (not Tcop13) was found to be expressed in the pit and slit eyes of *T. cystophora* and is the only known opsin to be expressed in the lesser eyes so far. Both types of these ocelli seem to be formed exclusively from PRC2-like cells (based on the broader expression of Tcop18 as seen in the photoreceptors of major eyes). Some other molecular features are shared by the photoreceptor cells of lesser eye types with those of the complex lensed eyes (PRC1 and PRC2), e.g. all contain at least two different screening pigments (dark and "white"), first described in *Chiropsella bronzie* (O'Connor et al. 2009), which becomes observable in polarization microscopy (Fig. 27).

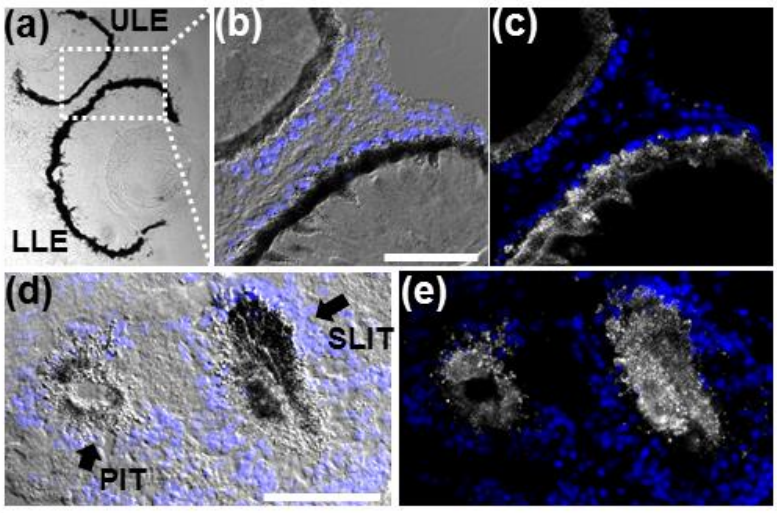

Fig. 27: Types of shading pigment granules in the eyes of *T. cystophora.*

a-c) Detailed view of the pigmented areas of ULE and LLE retinas. a-b) In bright field both types of pigment granules appear dark. c) The same view in polarized light. Part of the granules alter the plane of polarization and appear white. d-e) Both types of pigment granules are present in retinas of pit and slit eyes, in bright field (d) and polarized light (e). Blue - DAPI. Scale bars: 50 µm. Adapted from Liegertova et al. (2015).

Author´s contribution: qRT-PCR data processing and visualisation (experiment performed by Irina Kozmikova, Ph.D.). Antibodies design, generation and complete IHC analysis; data analyses, evaluation and visualisation performed by the author.

5. Identification and functional testing of the possible *T. cystophora* opsins coupling partner

In silico search for G protein alpha subunits in the sequenced *T. cystophora* genomic library resulted in identification of four putative genes, representing three distinct G alpha subunit guanine nucleotide binding protein alpha (GNA) subfamilies – GNAI, GNAS, GNAQ. Given the fact that C-terminus is highly conserved in between the members of the four GNA sub-families (hence the most defining feature), we used a 3´ RACE cloning approach to isolate the complete 3´ends of these genes. Sequencing and subsequent analysis confirmed the presence of – Gi (GNAI), Gq (GNAQ) and two genes corresponding to Gs (GNAS) – with one of the alternatives named Gx (Fig. 28a-b).

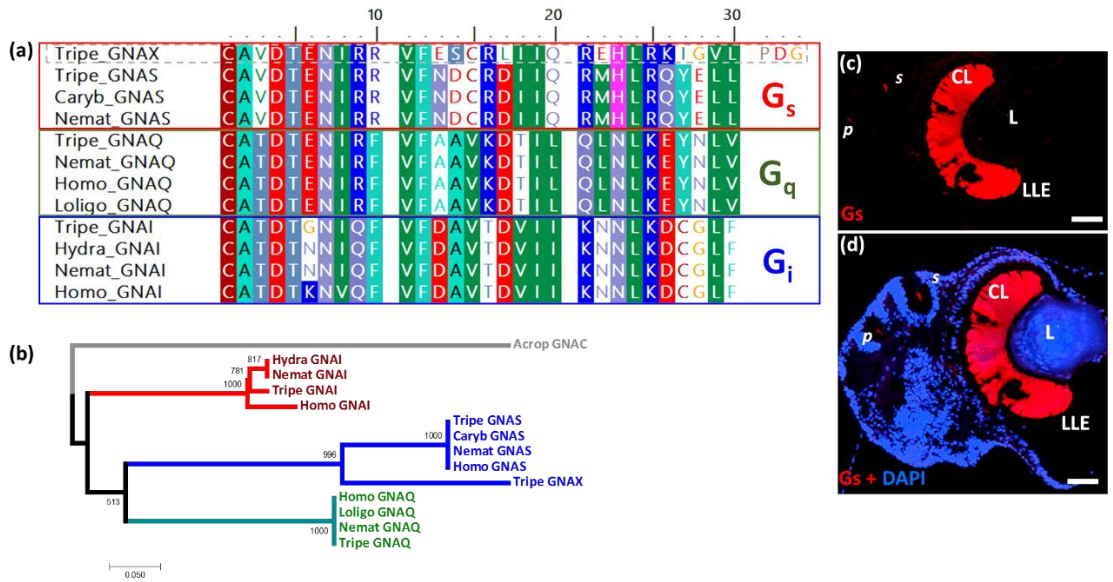

Fig. 28: G protein alpha subunit identification in *T. cystophora*.

a) Partial alignment of the 30 C-terminal amino acids (distinctive for each of the sub-families) of the newly identified G alpha subunit sub-types in *T. cystophora*. b) Phylogenetic tree showing clustering of the newly identified genes into GNA subfamilies. c-d) Cross-species IHC staining of the cryosectioned rhopalia with anti-Gs antibody (in red). Strong signal in all the retinas (major and minor eyes) was detected. Gs - GNAS subf.; Gq - GNAQ subf.; Gi- GNAI subf. Tripe – *T. cystophora*; Caryb – *C. rastonii*; Nemat – *N. vectensis*, Homo – *H. sapiens*, Loligo – *L. vulgaris*; Hydra – *H. magnipapillata*; p – pit eye; s – slit eye; CL – ciliary layer; L – lens. Blue – DAPI. Scale bar: 50µm

To inspect the possibility of expression of these genes in the retinas of *T. cystophora* eyes, we performed cross-species IHC staining of the rhopalia sections with

six commercially available antibodies - against Gs, Go and two different antibodies against each Gi and Gq (antibodies raised against different domains of the corresponding subunit). The only detectable signal was obtained for the Gs subunit in the retinas of major and minor *T. cystophora* eyes (Fig. 28c-d). This corresponds with data shown by Koyanagi et al. (2008) for the related cubozoan species *C. marsupialis*. IHC staining for other G alpha subunit types provided no detectable signal.

In order to get a deeper insight into the functional diversification of opsins identified in *T. cystophora* we used a Gs protein-coupled signalling assay to investigate their biochemical properties**.** The activity of luciferase in GloSensor cAMP HEK293 cells, transfected with individual opsin constructs (pre-incubated in the dark with 9-cis retinal), was determined before and after repeated light stimulations (Fig. 29).

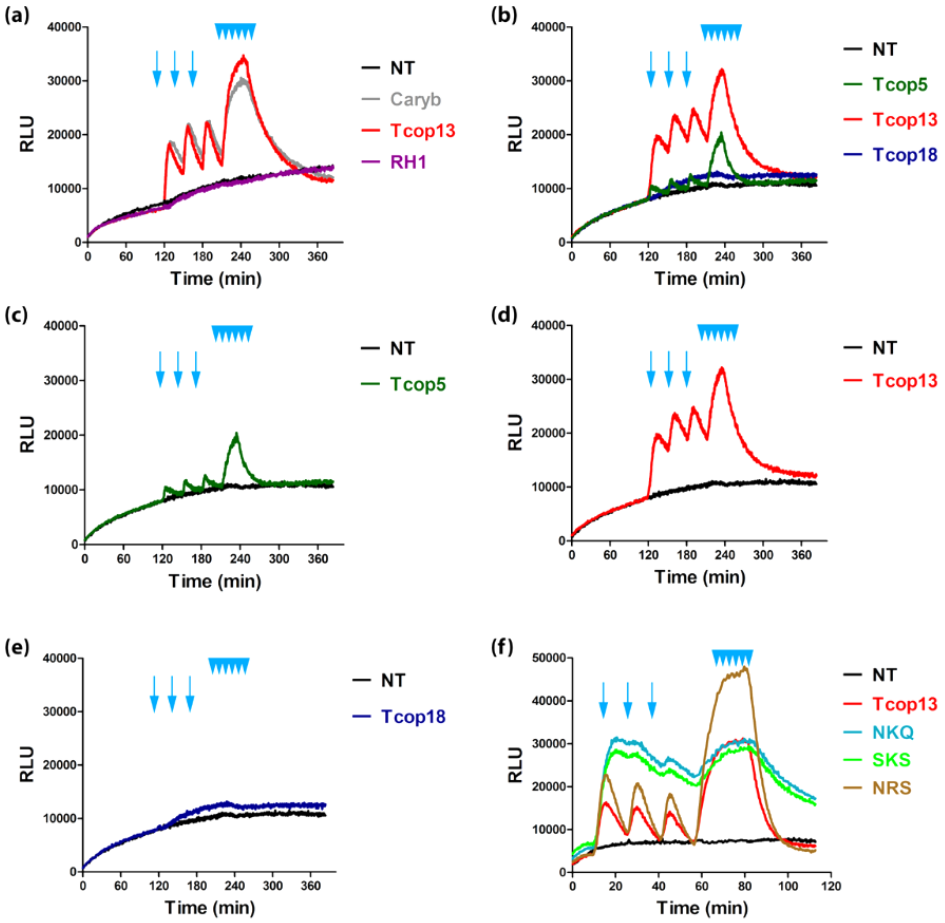

Fig. 29: Light-response Opsin-Gs-cAMP assay.

Light activation of opsin-Gs-cAMP pathway by selected opsins. GloSensor cAMP HEK293 cells were transfected with expression vectors containing the coding sequences of different opsins and stimulated with light. Long blue arrows represent simple light pulse; multiple connected arrowheads represent repeated stimulation. Each graph represents a mean of triplicates for every sample. a) Previously reported Gs-cAMP pathway stimulating opsin from *C. rastonii* - Caryb (Koyanagi et al. 2008) showed ability to increase cAMP level in our set-up (visualized with cAMP dependent luciferase activity). Exact homologue of Caryb from *T. cystophora* Tcop13 showed highly similar response in our assay. Opsin RH1 from medaka fish (*Oryzias latipes*), expected to signal via Gt leading to cGMP decrease, showed no change in luciferase activity (negative control). b-e) Examples of different Tcops light response. Tcop5 showed faster and weaker activation of Gs-cAMP pathway in comparison with Tcop13. Tcop18 did not activate Gs-cAMP pathway. NT – not transfected cells used as negative control; Caryb – signal for cells transfected with vector expressing the opsin from *C. rastonii*, used as positive control; RH1 – signal for cells transfected with vector expressing opsin RH1 from *O. latipes*, used as negative control; Tcop5, Tcop13, Tcop18 – signal for cells transfected with vectors expressing respective opsins from *T. cystophora*. f) The altered response of Tcop13, where its tripeptide region (HKQ) was replaced by those of Tcop1 and bovine rhodopsin (NKQ), Tcop14 (SKS), and Tcop18 (NRS). None of these Tcops activated the assay by itself, surprisingly the introduction of their respective tripeptides to Tcop13 led to an enhanced response in the assay. Adapted from Liegertova et al. (2015).

Each light stimulation of cells was immediately followed by increased luciferase activity reaching the maximum in around 10 minutes, plateauing for several minutes and decreasing to levels before irradiation (Tcop5) or higher (Caryb, Tcop13). Comparison of the Caryb response with its ortholog from *T. cystophora*, Tcop13, revealed that both opsins show similar light responses (Fig 29a). As anticipated, RH1 opsin from medaka fish (*O. latipes*), used as negative control (signals via a distinct pathway leading to a cGMP decrease), elicited no increase of luciferase activity in the assay. IHC staining of the transfected cells confirmed that all examined opsins were expressed at comparable levels (transfection efficiency using the FuGENE HD transfection reagent was about 50%), and that the signal for opsin was detectable on the cell membranes (Fig. 30).

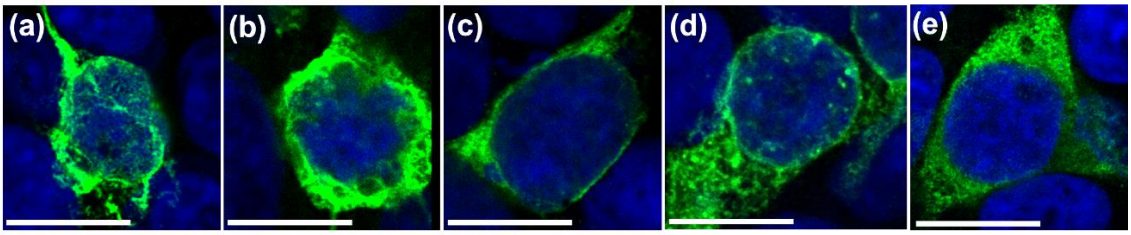

Fig. 30: **Expression of recombinant *T. cystophora* opsins in GloSensor cAMP HEK293 cells.**

a-d) Recombinant Tcops tagged with 1D4 tag were expressed in GloSensor cAMP HEK293 cells stained blue (DAPI) and green (1D4 tag). The signal localizes to the cell membrane. a) Tcop5. b) Tcop13. c) Tcop18. d) Tcop9. e) *O. latipes* rhodopsin (RH1) used as negative control. Scale bars: 10 µm. Adapted from Liegertova et al. (2015).

The light-response assay was performed for the entire set of Tcops. Only Tcop5 and Tcop13 (both group-2) activated the Gs-cAMP signalling pathway (Fig. 29b-e), showing increased signalling after repeated light stimulation. However, Tcop5 responded to light faster with lower intensity (Fig. 29c), while the response of Tcop13 was considerably slower, but with higher signalling values (Fig. 29d). The remaining Tcops were unable to mediate light-dependent activation in the assay.

To investigate the role of the tripeptide (contact between bovine rhodopsin and G protein – see Marin et al. 2000) in cnidopsin signalling, we replaced the HKQ tripeptide region in Tcop13 with tripeptides NKQ (Tcop1 and bovine rhodopsin), SKS (Tcop14) and NRS (Tcop18) - none of these Tcops activated the Gs signalling cascade in the light-response assay by itself. Surprisingly, the mutation of Tcop13 tripeptide did not disrupt Gs activation (as expected), but rather modulated the response of Tcop13 to the light stimulation. Introduction of NKQ and SKS tripeptides led to enhanced and prolonged responses, while introduction of NRS led to an enhanced response and a sharp increment of light response after single stimulation and repeated stimulation, respectively, in regard to Tcop13 (Fig. 29f).

Author´s contribution: *In silico* data mining, identification, cloning and characterization of G alpha subunits, IHC screening and data analysis. Light-response assay designed and performed by Jiří Pergner, Mgr. and Antonio Pombinho, Ph.D. under supervision of Petr Bartůněk, Ph.D.

6. Behavioural testing of *T. cystophora* visual navigation ability after treatments with pharmacological inhibitors for opsins coupling partners

(data published only for NF449)

The only opsin identified so far in retinas of lens eyes of box jellyfish *C. rastonii* – Caryb, was previously shown to transfer the light stimuli via the Gs signalling pathway (Koyanagi et al. 2008). To investigate whether group-2 Tcops, that signal via Gs (see above) serve as the main visual pigments, we performed a behavioural assay focused on the positively phototactic behaviour of the medusae in the absence or presence of the pharmacological compounds NF449 (G protein antagonist - supresses the binding to Gs type subunit) and NF023 (Suramin analog – supresses Gi,o types subunits). NF449 was identified as a selective suppressor of the Gs signalling pathway, whereas its effect on prototypical Gi/Go- and Gq-coupled receptors is limited (Hohenegger et al. 1998). NF023 was identified as a selective suppressor of the Gi/o signalling pathways without effect on Gs signalling (Soto et al. 1999). Positive phototaxis in *T. cystophora* was significantly decreased after treatment with NF449, although a variable response was detected to white light depending on NF449 concentration and time after the treatments (Fig. 31 and video at nature.com/article-assets/npg/srep/2015/150708/srep11885/extref/srep 11885-s1.avi), most likely due to the reversible nature of the inhibition of Gs signalling pathway by NF449.

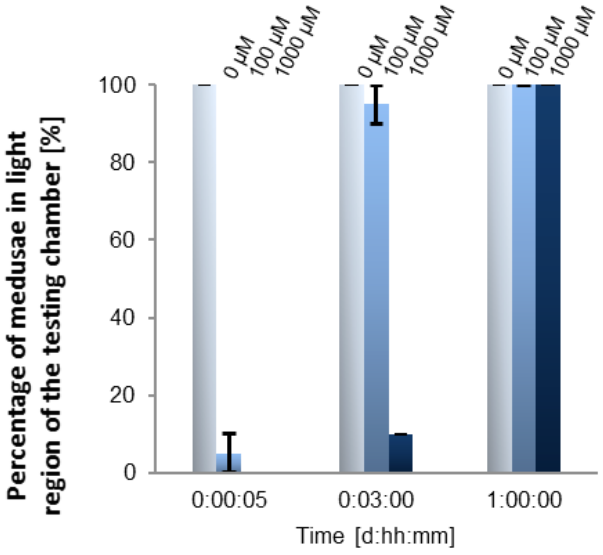

Fig. 31: Testing of *T. cystophora* phototaxis after NF449 treatment.

a) Statistical analysis of light response of *T. cystophora* after NF449 treatments (0 µM, 100 µM, 1000 µM). Bars represent percentage of phototactic medusae (animals reaching the light shaft)

in given time points. x - axis: time (represented as day: hour: minute), y – axis: percentage of medusae reaching the illuminated side of the testing chamber. Adapted from Liegertova et al. (2015).

Phototactic behaviour was not altered after treatment with NF023 (data not shown). The percentage of treated animals with phototactic response 5 minutes post-treatment was 5 ± 5 % in samples treated with 100 µM NF449 and 0 % in samples with 1000 µM. In the case of animals treated with 100 µM NF449, the percentage of responding medusae after 3 hours rose to 95 ± 5 % and in the case of 1000 µM NF449 it rose to 10 %. However, 24 hours later, the decrease in photosensory response was no longer present. The response in untreated animals (0 µM NF449) was 100% phototactic as in animals treated with any concentration of NF023 after 5 minutes, 3 and 24 hours intervals. Thus, the pharmacological inhibition of group-2 opsins transiently abolishes positive phototactic movement of the medusae. In summary, phototactic behaviour of *T. cystophora* medusa is dependent on Gs signalling.

Author´s contribution: Original experiment design, testing chamber design, preliminary testing with both inhibitors to verify possible effect. The final experiment with NF449 was performed by Peter Fabian, Ph.D.

7. Identification of other putative phototransduction cascade components by *in silico* analysis of the *T. cystophora* genome, complemented with IHC screening with commercially available antibodies

(unpublished data)

We screened the sequenced *T. cystophora* genomic library for seven other candidate phototransduction components – visual arrestin, recoverin, rhodopsin kinase, Rpe65 isomerase, lecithin retinol acyltransferase (LRAT), retinol dehydrogenase (RDH) and CNG channel, previously identified as a part of the vertebrate phototransduction cascade or involved in photopigment regeneration (Table 6).

Table 6: List of the inspected phototransduction genes.

Columns: Candidates genes - all the inspected genes; Genome - *in silico* search outcome, where (+) means the sequence was present in the 454 derived genomic library of *T. cystophora* and (-) where there was not a high score producing Hit; IHC signal - represents the outcome of IHC staining, where (+) in green means that specific signal was detected in the retinas of *T. cystophora* eyes, as opposed to (-) in red, where no signal was observed. *n.d.* stands for not determined in this study (these antibodies were not available in our collection).

	Candidate genes	Genome	IHC signal
1	Arrestin (ARR)	+	+
2	CNG channel (CNG)	+	n.d.
3	Recoverin (RCV)	-	-
4	Rhodopsin kinase (GRK)	-	-
5	Lecithin retinol acyltransferase (LRAT)	-	-
6	Retinol dehydrogenase (RDH)	-	-
7	RPE65 isomerase (RPE65)	-	n.d.

To combine this *in silico* approach with *in situ* data, we took advantage of the various commercially available antibodies for phototransduction components (our laboratory´s collection of commercially generated antibodies from previous projects on other model animals) and performed parallel IHC staining on rhopalia cryosections with: anti-arrestin, anti-recoverin, anti-rhodopsin kinase 1A, anti-LRAT antibody, anti-RDH5 antibody (see Table 5 for details).

In the genome, we successfully identified a partial sequence with high similarity to known visual arrestins (Fig. 32a-b).

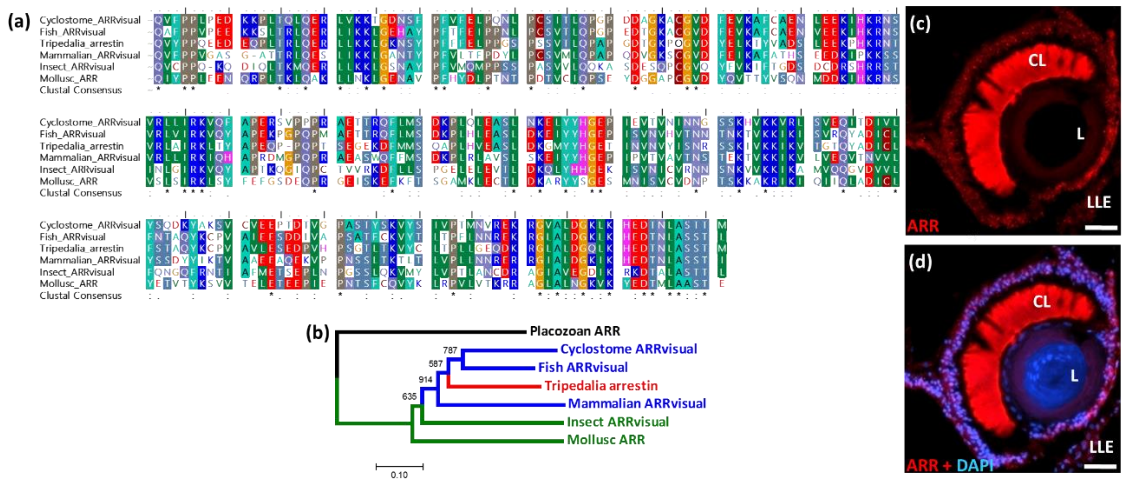

Fig. 32: Arrestin homolog in *T. cystophora.*

a) *T. cystophora* arrestin´s partial alignment showing similarity to other visual arrestins across animal phyla; b) When placozoan arrestin is used as an outgroup, the novel *T. cystophora* arrestin clusters within vertebrate visual arrestins. c-d) Cross-species IHC staining of rhopalia cryosections showing signal for anti-bovine visual-arrestin antibody in the retina of the ULE.

Because only a short stretch (from a single exon) of the arrestin sequence was found in the genome (and many introns were expected based on e.g. the cnidarian *N. vectensis* predicted arrestin-like protein), we used the degenerate primer PCR approach, using rhopalia derived cDNA library as a template, and successfully recovered most of the *T. cystophora* arrestin sequence (220aa). Because the newly identified arrestin shows a high degree of similarity to vertebrate visual arrestins we inspected the possible expression pattern by cross-species IHC using anti-bovine visual-arrestin antibody and indeed obtained a strong signal in the retinas of *T. cystophora* major lens eyes (Fig. 32c-d). Arrestin is the first of the phototransduction deactivation components identified in cnidarian eyes so far.

Furthermore, we identified a CNG channel homolog sequence (Fig. 33), but the possible expression in the *T. cystophora* photoreceptors was not further investigated in this study.

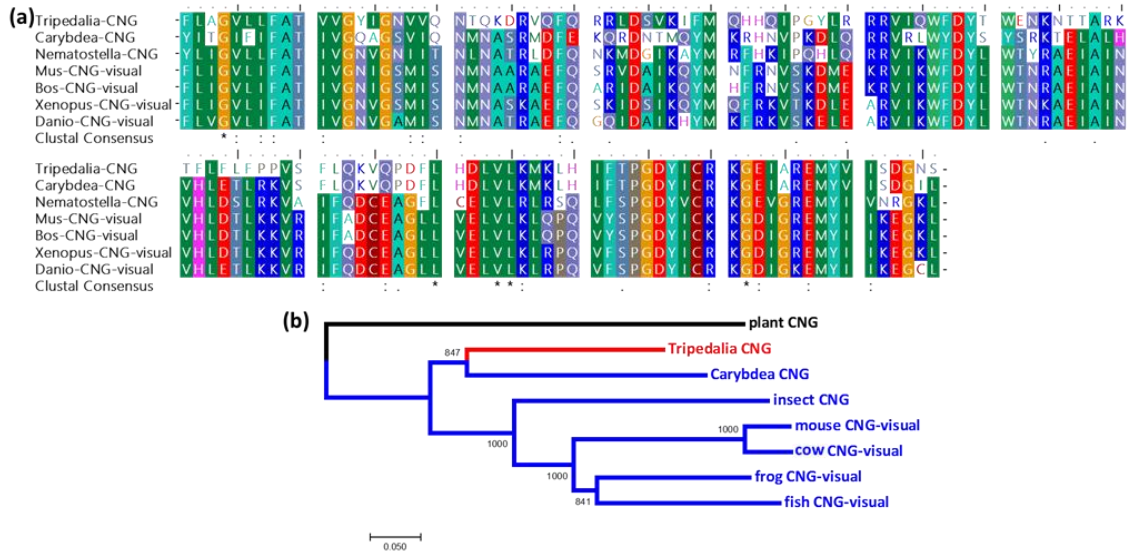

Fig. 33: CNG channel homolog in *T. cystophora.*

a) Partial alignment of CNG channels across animal phyla; b) Phylogenetic tree of the CNG channel homologs with a plant CNG channel used as outgroup.

We were unable to find any considerable hits for the other candidate genes – Recoverin, Rho kinase 1A, LRAT, RDH and Rpe65 isomerase in the genome. Accordingly, the IHC staining did not provide any detectable expression signal for Recoverin, Rho kinase 1A, LRAT, ARAT and RDH (data summarized in Table 6).

Author´s contribution: *In silico* data mining, identification, cloning and characterization of 2 novel genes (arrestin and CNG channel), IHC screening and data analysis.

8. Identification of novel crystallins in the *T. cystophora* genomic library

(unpublished data - manuscript in preparation*)

We screened the *T. cystophora* genomic database for the structural proteins of the lenses – crystallins. Three partial putative crystallin genes, namely J1D, J1E (Fig. 34a) and J2B (Fig. 34b), were identified.

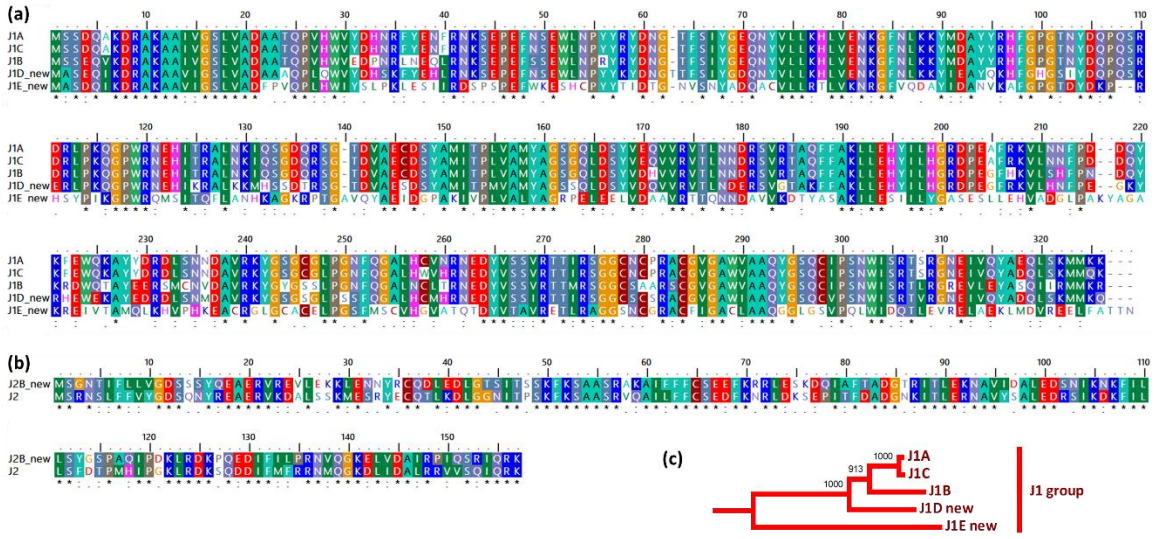

Fig. 34: Identification of crystallins in *T. cystophora.*

a) Alignment of the previously annotated *T. cystophora* crystallins (Piatigorsky et al. 1993) – J1A, J1B, J1C with the newly identified genes J1D and J1E, showing high similarity between crystallins from this sub-family. b) Alignment of another crystallin J2 (the same study) with the new variant J2B. c) Phylogenetic tree showing relations in between the J1 crystallins.

We took advantage of the fact, that complete 5´ends were already included in all of the three significant Hits, and cloned these genes from the rhopalia derived cDNA library using a 3´ RACE approach to recover the full open reading frames. The novel crystallins strongly cluster with the previously reported and annotated sequences in *T. cystophora* – J1 and J2 respectively (Fig. 34c), whose expression was confirmed in the lenses (Piatigorsky et al. 1993). Repeated cloning from genomic DNA (and subsequent sequencing) revealed their single exon nature, which correlates with the intronless structure of the previously annotated *T. cystophora* crystallins (J1A, B, C and J2). Our preliminary data from IHC stainings with *T. cystophora* specific antibodies generated against anti-J1 crystallins (designed against a highly conserved domain between the three J1 genes – J1A, B, C) and anti-J2 crystallins show J1 and J2 are co-expressed in the lenses of ULE and LLE (creating a putative protein gradient), as well as in the opening of the slit eye. Screening for the J1 and J2 expression patterns in other tissues also revealed "extra-lens" expression in the gastric cavity, statolith and nematocyses (data not shown).

Author´s contribution: *In silico* data mining, identification, cloning and characterization of 3 novel genes (J1D, J1E, J2B).

* Data used for manuscript in preparation:

The lenses of box jellyfish in space and time: Crystallins as lens creators.

Kristýna Marková, Juraj Sekereš, Viktor Goliáš, Čestmír Vlček, Michaela Liegertová, Zbyněk Kozmik

DISCUSSION

Scenario for cnidarian opsins rapid expansion and retro-gene origin.

It has been shown, that gene duplications and subsequent divergence play a key role in the evolution of a novel gene function (Innan and Kondrashov 2010). In *T. cystophora*, each of the Tcops seem to be a result of a duplication event and several of the variants seem to have undergone multiple rounds of duplication as could be inferred from the phylogenetic relations between these genes.

Duplicated genes can be lost rapidly (Lynch and Conery 2000), but the spectrally rich and diverse aquatic environment provides strong selective pressures on photoreception evolution, as shown in fish (Hofmann et al. 2012, Cortesi et al. 2015), where the opsin gene diversity in the genome is similarly high as in the genome of *T. cystophora*. The large complement of opsins found in freely swimming species seems to be a result of sensory adaptation to this spectrally diverse environment. In the genomes of medaka fish (*O. latipes*) or zebrafish (*Danio rerio*) the subtype opsins are closely linked and are considered to be the outcome of local gene duplications (Matsumoto et al. 2006). The diverse set of fish opsins was generated by duplications followed by amino acid substitutions at key sites, which provided the opsins with subtle tuning capacity (Rennison et al. 2012). Since the same selective pressures acted during the evolution of cnidaria, we can assume that similar mechanisms of opsin gene repertoire expansion occurred in this case (evolutionary convergence). Once the duplicated variant (paralogue) of a gene is present in the genome, it could become advantageous by either partitioning the function of the original gene between the two duplicates (subfunctionalization) or gaining a novel function (neofunctionalization) (Lynch and Conery 2000, Lynch and Force 2000). In the case of subfunctionalization, each variant of the gene performs multiple but only subtly distinct functions. Separating these functions between the duplicated (multiplicated) copies may increase the fitness of the animal by removing the conflict between two or more functions and could lead to the segregation of spatio-temporal expression patterns of the individual copies (Hurles 2004, Fernandez et al. 2011).

Taking into account the intronless nature of cnidarian opsins even more rapid duplication events and subsequent diversification could be anticipated, as documented by our analyses. A similar situation of lineage-specific extensive expansions of many gene families is documented in other cnidarians with sequenced genomes (Steele et al. 2011) with opsins being a perfect example (more than 30 and 60 annotated or predicted opsin sequences in *N. vectensis* and *H. magnipapillata*, respectively).

Studies in vertebrates suggest that intronless genes are evolutionary innovations and that the generation of these "single-exon" genes via reverse transcription/retrotransposition is important for the evolution of novel tissue-specific functions in animals (Brosius and Gould 1992, Shabalina et al. 2010, Zou et al. 2011). Interestingly, intronless genes in vertebrates often encode components of signalling pathways (Hill and Sorscher 2006). In fact, the lack of introns is typical for most members of the giant G protein-coupled receptors gene family and it has been proposed that many GPCRs are derived and amplified from a single intronless common progenitor that was encoded by a gene copied into the genome by reverse transcription of its mRNA (Brosius 1999, Gentles and Karlin 1999).

Such an intronless "retrogene" is formed by homologous recombination between the genomic copy of a gene and its cDNA and it has been reported that many retrogenes exist in eukaryotic genomes (Betran et al. 2002, Agarwal and Gupta 2005, Kabza et al. 2014, Zhou et al. 2015, Zhong et al. 2016). It has been proposed (at least for the extensively studied mammalian genomes) that intronless genes are expressed at lower levels, tend to be tissue specific, and evolve significantly faster than spliced genes (Fridmanis et al. 2007). Since the intronless state of a gene is considered to be an indicator that a particular gene family is undergoing active changes, the families of predominantly intronless genes, as in the case of GPCRs, are perfect candidates for investigation of intron gain and loss (Fridmanis et al. 2007).

Interestingly, even though many of the rhodopsin GPCRs in mammals are intronless, most GPCRs from invertebrates contain at least one intron (Fridmanis et al. 2007). Previous studies have proposed an explanation which has resulted in two very different conclusions. Earlier classic studies already suggested that the low number of

introns in mammalian GPCRs is related to gene multiplication via retrotransposition (Brosius 1999, Gentles and Karlin 1999), while more recent data provided a rather controversial conclusion, suggesting a major loss of introns within the rhodopsin GPCR family (since the majority of genes lost an “ancient” intron located in the conservative DRY motif of Rhodopsin GPCR) (Bryson-Richardson et al. 2004).

It has been shown that many intronless GPCR genes are located very close to each other in the genomes of mouse (Zylka et al. 2003) and zebrafish (Gloriam et al. 2005), and for most of the olfactory receptors (Newman and Trask 2003), this could have resulted from local DNA-based duplication mechanisms. The possible scenario is that mRNA-based duplication generates new intronless variants of receptor genes while DNA-based duplications multiply these new variants via local, block- or genome-wide duplications; subsequently, additional gain of introns may occur in the evolutionary history (Roy 2004, Fridmanis et al. 2007). Once a new intronless copy is established in the genome, it consequently increases the likelihood of replacing the intron-containing region in the original variant of the gene with its corresponding intronless region via homologous recombination (and conversely the intronless region in the new gene could be replaced by an intron-containing region from the source gene). It has been shown that intron losses are more frequent than intron gains across many eukaryotic lineages and that early eukaryotic gene structure was rather highly complex, with subsequent simplification during the course of evolution (Roy et al. 2003, Roy and Gilbert 2005a, Roy and Gilbert 2005b).

For a long time, it seemed that all of the identified and annotated cnidarian opsins are intronless genes. However, thanks to authors of the genomewiki project (genomewiki.ucsc.edu), we were able to identify one opsin in anthozoan *Acropora digitifera* genome - CNOP2, which has two introns (Fig. 35).

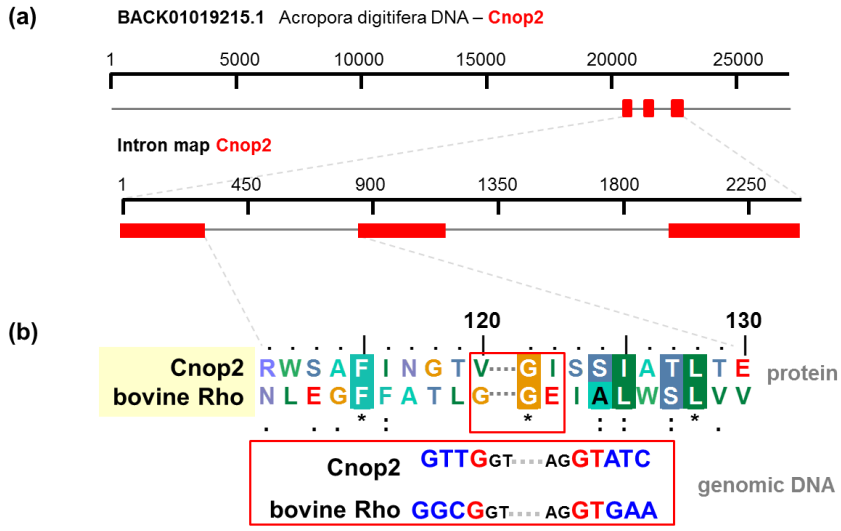

Fig. 35: Intron characterization of CNOP2 opsin from anthozoan *Acropora digitifera*.

a) CNOP2 genomic localization and intron map (mined from *A. digitifera* whole genome database - Shinzato et al. 2011). b) Partial protein alignment of bovine rhodopsin and CNOP2. Positions of the first intron in both genes are highlighted by red box. Introns from both species match in position and in phase (as shown in the *inset* for genomic DNA). Adapted from Liegertova et al. (2015).

These are the first introns to be detected in cnidarian opsins. They are moderately long and have a typical GT-AG donor and acceptor splicing sites. Intriguingly, the first intron of CNOP2 matches, in position and in phase, with the highly conserved first intron between vertebrates, implying that this intron was already present in an ancient opsin gene in the last common ancestor of Eumetazoa. The presence of this “scarce” intron-bearing variant (along with the predominantly intronless opsins) in basal anthozoans indicates, that intronless opsins could be a cnidarian innovation with the “original” variant being lost in medusozoans (Fig. 36).

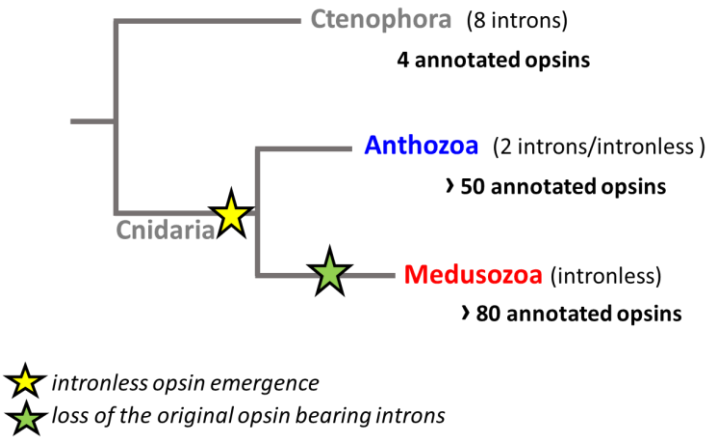

Fig. 36: Simplified phylogenetic tree showing the presence of introns in opsins from Ctenophora and Cnidaria.

In Ctenophora, all hitherto annotated opsins have 8 introns. In Cnidaria, intronless opsins are predominant, with Anthozoa having an opsin variant bearing two introns. In Medusozoa, all of the so far annotated opsins are intronless. We propose that, the intronless opsins are a cnidarian innovation, with the original intron-containing opsin being lost in all medusozoans. Data collected from genomewiki.ucsc.edu.

Interestingly, some intronless opsins were previously identified in two mollusc species (Morris et al. 1993) and in a teleost fish genome (Fitzgibbon et al. 1995), probably derived from intron-containing opsin genes by retrotransposition (convergent evolution). This seems to be, at least in part, a “common” mechanism of novel opsin generation.

Taking in account the fact, that only intronless opsins are found in *T. cystophora* and in most other cnidarians, we could propose a scenario describing the fate of the original intron-containing opsin variant in these animals. As mentioned above, the duplicated gene variants tend to “homogenize” over time via the process of possible reciprocal (mutual) conversions of the paralogous sequences. This process retards their divergence, obscures the possible resolution of their true common history and probably lasts until both variants of the duplicated gene achieve a similar intron–exon structure or until their coding sequences diverge through acquired mutations to the point of being too distinct for homologous recombination to act (Hurles 2004). Based on this, a deduction could be made, that the more intronless variants of one gene are formed, the higher the chance for the original variant of losing its introns too (Fridmanis et al. 2007),

as seems to be true for at least *T. cystophora*. Based on our data, confirming once again the clustering of cnidopsins as sister clade to c-opsins, we conclude that cnidarian intronless opsin genes are derived via retrotransposition from an ancient eumetazoan ciliary opsin with introns (Fig. 37).

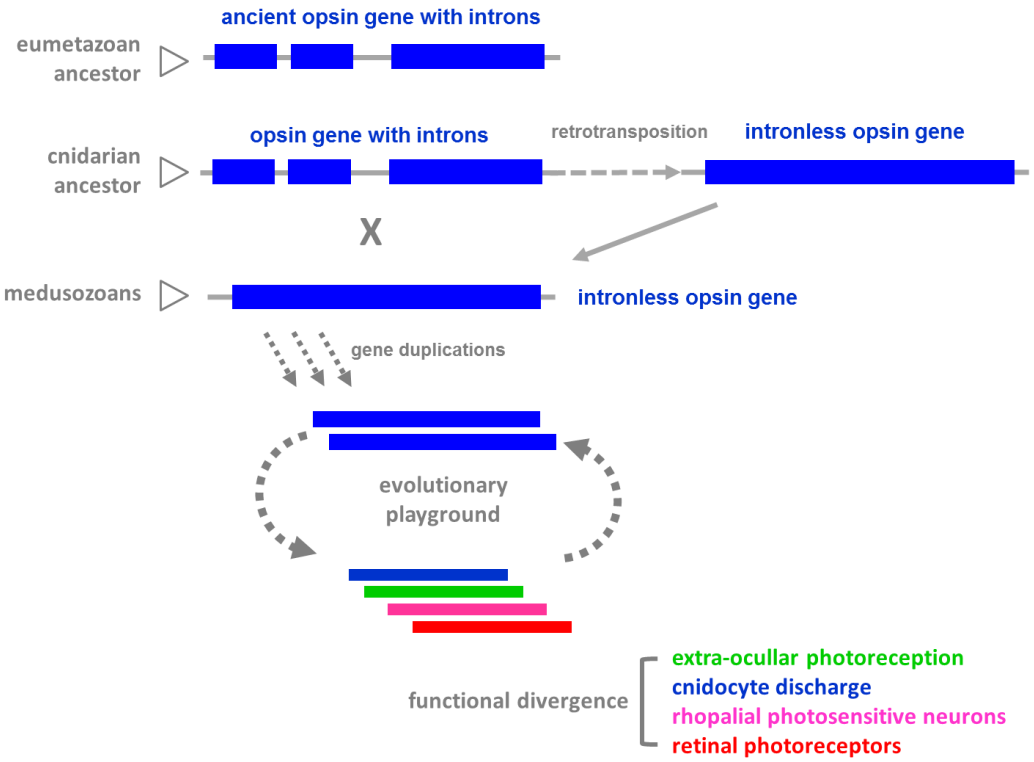

Fig. 37: Possible scenario for intronless opsin emergence and subsequent expansion in *T. cystophora*.

Our scenario suggests that cnidarian intronless opsins genes are derived from an ancient eumetazoan ciliary-like opsin containing introns by retro-transposition and that the original variant (still present in Anthozoa) was probably lost in the medusozoan sub-phylum. Once the intronless copy was present in the cnidarian ancestor it was repeatedly duplicated in many subphyla and subsequently within individual classes (as demonstrated for cubozoan *T. cystophora* in this study), generating the wide and diverse opsin subfamily of cnidopsins. In *T. cystophora* the individual Tcops are results of many rounds of duplication followed by sub-functionalisation and differ in stage- or tissue-expression, primary structure and also in the subsequent cellular signalling (either via Gs-cAMP pathway or other G protein pathways). Adapted from Liegertova et al. (2015).

Once the intronless variant appeared in the genome, it was subjected to rapid duplications across cnidarian lineages, followed by subsequent species-specific duplication resulting in the present diversity of cnidopsins, with modified subfunctions and spatio-temporal expression within the individual species. This diversity provided a substrate for the evolution of cnidarian photoreception (either extraocular or in the sophisticated cubozoan eyes).

Rhopalia-specific opsin expression in *T. cystophora.*

Cubozoan jellyfish have relatively simple nervous systems consisting of a nerve net and a ring nerve. A major part of this neural ring is most likely involved in the communication between the four rhopalia. The visual organs of *T. cystophora* (including eight optically advanced eyes) operate with only this "rudimentary" and simple nervous system. Various anatomical and functional studies suggest that the processing and integration of information takes place in the rhopalial nervous system (Parkefelt et al. 2005, Garm et al. 2006, Skogh et al. 2006, Garm and Mori 2009, Parkefelt and Ekstrom 2009). Moreover, a high number of neurites and synapses leaving the rhopalial stalk is suggestive of the possibility that the visual information leaving single rhopalium has not been completely processed. These observed connections possibly serve for integration of visual input from two adjacent rhopalia (Garm et al. 2006, Skogh et al. 2006) and thus the behavioural outcome of the regulatory system is probably influenced by the visual input to each rhopalium (Stockl et al. 2011).

The presence of eyes directly embedded in the CNS somehow resembles the situation in vertebrates, where the retina develops as a part of the CNS. In addition to the photoreceptors within the retinas of all the *T. cystophora* eyes, each rhopalium accommodates over a thousand various neurons (approximately half of them being retina-associated). The complex system of rhopalial neurons of *T. cystophora* was thoroughly described (Parkefelt et al. 2005, Skogh et al. 2006). Each of the four rhopalia contains a cluster of "pacemaker" neurons, regulating movements of the animal through the direct control of the motor nerve net. Thus, each of the rhopalia mediates various modes of behaviour, such as the typical obstacle avoidance or light attraction (Garm and Bielecki 2008, Stockl et al. 2011). It has been proposed that in Cubozoa multiple

photoreceptor systems (three out of the four eye types and rhopalial neuropil) directly affect the swim pacemaker. When stimulated with light, the lower lens eye (LLE) inhibits the pacemaker and when light is turned off the effect is opposite (the pacemaker gets activated), as opposed to the upper lens eye (ULE) and both pit eyes, which all were show to have the opposite effect (Garm and Bielecki 2008, Garm and Mori 2009, Garm and Ekstrom 2010).

Based on our mRNA and protein expression profiles (summarized in Fig. 38) for all *T. cystophora* opsins most of the Tcops identified are indeed expressed in rhopalia.

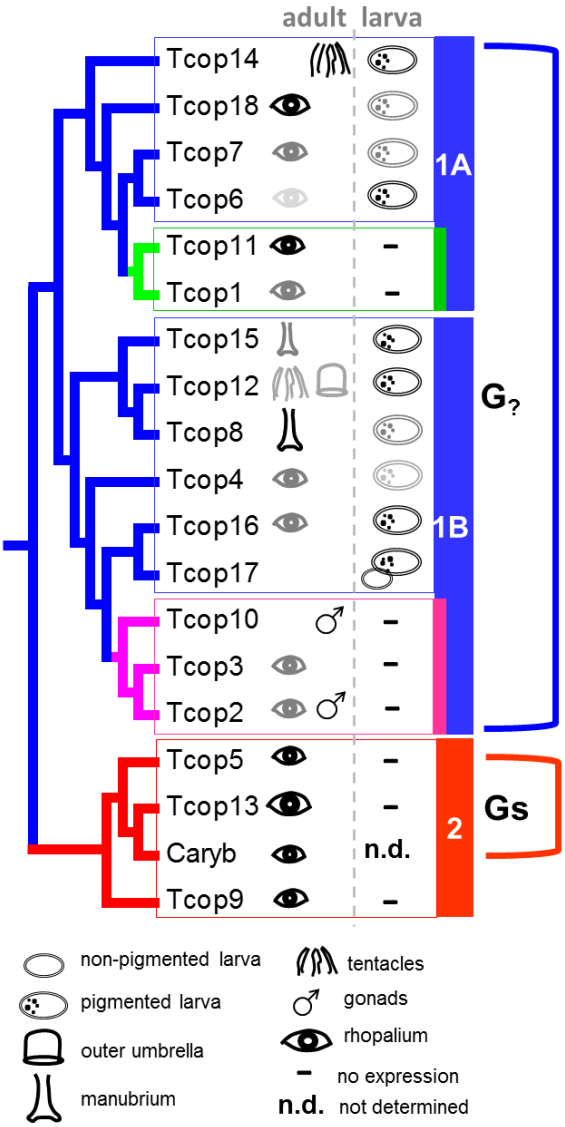

Fig. 38: Schematic representation of the Tcops expression patterns according to their phylogenetic relationship.

Tcops can be classified into two groups, a probable more ancient group-1, with a broader expression patterns, and group-2 – rhopalium-specific Tcops (with Tcop13 being retina-specific). The size and shade intensity of the symbols corresponds to the expression level. Green coloured box and branches (Tcop1 and Tcop11) represent rhopalia specific Tcops forming sub-group-1A. Pink coloured box and branches (Tcop2, Tcop3, Tcop10) represent male specific Tcops from sub-group-1B. Red coloured box and branches (Tcop5, Tcop9, Tcop13) represent rhopalia specific Tcops from group-2. Red bracket - Tcops for which Gs signalling was demonstrated in the light-response assay. Blue bracket – is pointing out that there is a yet unidentified signalling pathway distinct to group-2 Gs signalling. Caryb – Tcop13 ortholog from *C. rastonii.*

Our data suggest that all group-2 Tcops and at least one Tcop from each of the group-1 sub-groups (group-1A and 1B) are rhopalium-specific. This fact is supported by the qRT-PCR analysis, which has revealed that all of the rhopalium-expressed Tcops are greatly up-regulated during the polyp-to-medusa metamorphosis when the rhopalia are formed. The expression of rhopalium-specific Tcops goes far beyond the expression in the retinas of the eyes, as many of retina-associated neurons already proved to be photosensitive as well (Garm and Mori 2009). We thus confirmed that the rhopalium is a complex organ, which serves for integration and processing of diverse light cues (enabled by the diverse set of opsins) and transformation of these signals into various behavioural responses. In order to understand visual processing in the rhopalium, identification of its functional units is crucial, especially in the terms of the possible presence of multiple types of photosensitive neurons, expressing different Tcops. It would be of highest interest to inspect the expression patterns of all the Tcops orthologues found to be expressed in rhopalia by extensive IHC analysis, performed preferentially on whole mount rhopalia. A thorough confocal analysis to enable the mapping of individual Tcops into the supposedly photosensitive rhopalial neurons would uncover the complexity of this photoreceptive organ.

Retina-specific opsin expression in *T. cystophora.*

In more complex Bilateria, multiple photopigments present in the retina mediate the basis of colour vision. However, in simple animals the same multiple photopigments can be used for simpler responses like wavelength-specific behaviour and ambient light tuning (Land and Nilsson 2002). Sets of multiple photopigment systems may also serve the purpose of extending the sensitivity range and give different temporal

characteristics (as reviewed for the case of vertebrate rods and cones in Kawamura and Tachibanaki 2008).

To address the question of possible presence of distinct photopigments used for the cubozoan advanced vision, we carefully inspected retinas of *T. cystophora* eyes by IHC staining. The major complex eyes (ULE and LLE) comprise of a hemisphere-shaped retina with ciliary photoreceptors (bearing the dark pigment within cell bodies), a small vitreous space, a spherical cellular lens and a thin cornea from monociliated epithelial cells (Yamasu and Yoshida 1976, Laska and Hundgen 1982, O'Connor et al. 2009).

The retinal ultrastructure has previously been investigated in four cubozoan species with rather ambiguous conclusions with respect to the number of photoreceptor types. For the cubozoan *Tamoya bursaria* a single type of photoreceptor - the "pigmented sensory cells" in LLE was reported, being interspersed with long pigment cells, which bear no ciliary specialization (Yamasu and Yoshida 1976). However, another study described three types of photoreceptors in the lens eyes of *T. cystophora* on the basis of differences in the morphology of their sensory cilium and microvillar organization (Laska and Hundgen 1982). All three types were observed in the lower lens eye: long pigment, pyramid and prism cells, whereas the upper lens eye contained only pyramid and prism cells. This same study did recognize a fourth sensory cell type contained within the pit ocelli and slit minor eyes. No specialized pigment cells were recognized, the long pigment cells were reported to be ciliary and considered photosensory at the same time.

Some of the more recent studies (Ekstrom et al. 2008, O'Connor et al. 2009, Garm and Ekstrom 2010) supported the interpretation that there was only a single basic morphological type of a dark-pigment-bearing photoreceptor in the cubozoan major eyes. Our IHC analysis strongly supports the "multi-receptor" interpretation of Laska and Hundgen (1982), by showing that there are at least two types of photoreceptors (PRC1 and PRC2 - each expressing distinct opsin) in both of the lens eyes of *T. cystophora*.

T. cystophora retina has three distinct layers, adjacent to the vitreous space and lens is the ciliary layer: a thick layer of the photoreceptor cilia formed mainly from PRC1

cells (probably equivalent to Laska´s prism cells) interspersed with cone-shaped projections from PRC2 cells (equivalent to pyramid cells); next to the ciliary layer is a thin pigmented layer, where both cells types are densely pigmented, and a neural layer containing cell bodies with nuclei of both types of photoreceptors.

The ciliary segments of PRC1 cells (expressing Tcop13) dominate the ciliary layer and the cilia extend from the pigment layer to the vitreous space. As shown in microstructural studies (Laska and Hundgen 1982, O'Connor et al. 2009), microvilli extend from the ciliary membrane and make up the mass of the ciliary layer (PRC1 cells). The cone-shaped projections of PRC2 cells (expressing Tcop18) are partially filled with screening pigment granules and run parallel to the cilia of the PRC1, among which they are scattered. In the neural layer, PRC2 cells have their cell bodies with nuclei (also positive for Tcop18 protein expression) and long projections creating a compact layer, surrounding the whole retina. However, we cannot exclude the possibility that a third (or even more) photoreceptor expressing yet another Tcop will be identified in the retina by more detailed analyses, recovering Laska´s morphological study.

According to our data (dominant mRNA and protein levels and strict retinal specificity) Tcop13 serves as the main visual opsin in *T. cystophora* major lens eyes. It was argued recently by Bielecki et al. (2014), that Tcop18 expression is restricted only to the neutropil of the rhopalia, since their RNA *in situ* data did not provide clear signal in the retinas of *T. cystophora* eyes. The authors discussed the possibility that the Tcop18 expression pattern obtained by IHC and published in one of our previous studies (Kozmik et al. 2008a), was obtained by non-specific antibody staining in the lens eyes, such that our antibody probed the Caryb homolog (Tcop13) rather than Tcop18. Our more detailed IHC co-expression analysis clearly shows that not only is Tcop18 expressed in the retinas of all the eyes (major or minor), but clearly localizes to a distinct PRC cell type in the lens eyes and is not even co-expressed with Tcop13 in the same photoreceptors. Moreover, Tcop18 is the only known opsin to be expressed in the minor (pit and slit) eyes so far. Our IHC data indicate, that retinas of both eye types (major with lenses and minor) express different Tcops combinations according to their task, providing another level for visual tuning. Interestingly, in the major eyes of box jellyfish *A. marsupialis* only

Tcop18 (and not Tcop13) was detected in the developing retinas, suggesting, that Tcop18 is more conserved (and probably more ancient) within the Carybdeid families (which is consistent with our suggestion of Tcop group-1 being more ancient than the group-2).

Arguments for colour vision in Cubozoa.

It has long been suggested (Pichaud et al. 1999) that a primitive colour vision system could have been composed of just two types of photopigments (as seen in Chelicerata). Presence of different pigments with specific wavelength sensitivity is essential for colour vision, but it is the subsequent neural wiring that determines whether the organism has merely wavelength-specific behaviour, or true colour vision.

Interestingly, colour-photosensitivity and preference for substrates of particular colour during settlement of coral larvae was recently shown to exist (Mason and Cohen 2012, Strader et al. 2015). It has been argued, that coral larvae of various species may use coloured light cues as a mean not only to measure the depth (Mundy 1998), but also as an indicator of settlement surface orientation via its colour detection (Mason et al. 2011, Strader et al. 2015). Mason et al. (2012) identified and mapped the expression of three novel opsins from another cnidarian – the coral *Acropora palmata* - and hypothesized, that the photopigments form functional rhodopsin-based photoreceptors and potentially may have a role in colour preference observed during settlement in the larvae of this anthozoan. Two of these opsins were shown to activate distinct phototransduction pathways, thus the presence of two photosystems could be used as an indicator for possible capability of colour discrimination in these eyeless animals.

Taking into account our identification of the two types of photoreceptors in the retinas of lens eyes of *T. cystophora*, with restricted expression of two distinct photopigments and the complex wiring of the rhopalial nerve net, it is tempting to hypothesize that cubozoan jellyfish are in fact able to discriminate colours to some extent. This would coincide with the proposed scenario, that colour vision evolved very early in animals inhabiting shallow water to improve contrast of the ambient environment (Maximov 2000). In fact, avoidance of red colour by the freely swimming

medusae was observed in our own culture, but was not further inspected. It would be interesting to investigate this observation by some behavioural tests in the future.

Larval and tissue-specific opsins.

Extraocular photosensitivity is widespread throughout the animal kingdom, in both invertebrates and vertebrates. Majority of metazoan species have supplementary non-visual photosensitive cells that regulate the organism's temporal physiology (Yoshida 1979, Arikawa et al. 1980, Foster et al. 1994, Taddei-Ferretti 1997, Taddei-Ferretti and Musio 2000, Foster and Hankins 2002). These photosensitive cells are not organized into functional organs, lack the typical structural specialization (microvilli or specialized cilia) as well as distinct morphology commonly seen in photoreceptors and might be scattered throughout the animal body therefore they are often difficult to identify (Taddei-Ferretti and Musio 2000, Musio et al. 2001). It has been long known that the muscle cells in sea anemones are light-sensitive and contract upon a light stimulus (Marks 1976), while in other cnidarians neurons and epithelial cells have been shown to be photosensitive as well (Yoshida 1979, Arkett and Spencer 1986, Sawyer et al. 1994, Musio et al. 2001). In *Hydra magnipapillata*, it was quite recently shown that the cnidocyte discharge is controlled by an opsin mediated signalling cascade (Plachetzki et al. 2012). The function of these photosensitive cells lies in mediating the simplest physiological processes, such as informing about the presence or intensity of light (simple light detectors) or activators of photoperiodic behaviour. There is a clear tendency in the extraocular photoreceptors to make use of distinct opsins than those conventionally used in vision (Kumbalasiri and Provencio 2005).

Our gene expression analyses imply that cnidarians indeed utilize opsins extensively, not only for visual but also for extraocular photosensitivity. By analysing all the Tcops expression in various body parts and live stages by qRT-PCR and with clear support from the phylogenetic data, it was revealed that all the Tcops could be classified into two subgroups. Group-2 Tcops (Tcop5, Tcop9, Tcop13), all of which are rhopalia specific with Tcop13 as the main visual opsin for the major lens eyes, and group-1 Tcops. The group-1 Tcops, being probably more ancient, have broad expression ranging from larvae to male gonads, however a trend for specialization and increased tissue or organ

specificity could be observed in the 1A and 1B subgroups (the same seems true for the relation between the main groups 1 and 2), being in agreement with the proposed scenario of subfunctionalization after subsequent duplication events (Fig. 39).

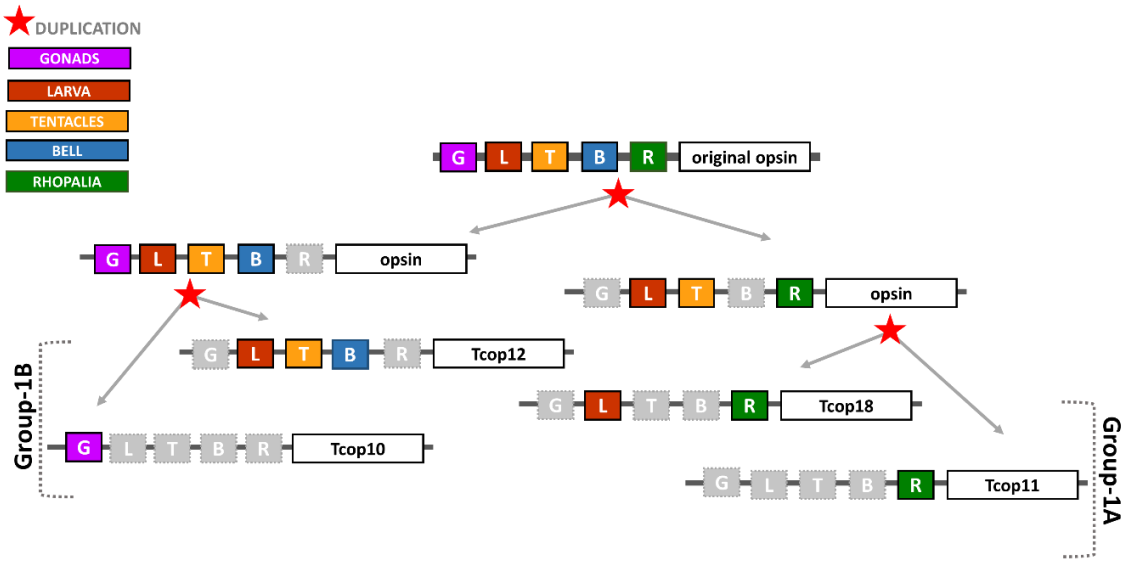

Fig. 39: Evolutionary scenario for group-1 Tcops expansion.

Within group-1, some of the Tcops have broad expression ranging from larvae to male gonads, however a clear tendency for increased tissue or organ specificity could be observed in the 1A and 1B subgroups. The original "mother gene" probably had a broad expression pattern. After its multiplication via subsequent duplications, descendant genes have subdivided the expression domains and eventually broadened the functional repertoire of the original opsin. Over time, acquisition of substitutions in key regions of the novel opsin proteins, led to partial functional divergence e.g. subtle tuning of the individual Tcops response to light stimulation. Hypothetical regulatory elements (for tissue-specific expression of opsins) are depicted by coloured boxes with a letter symbol of the corresponding expression site. Genes are depicted as rectangles with the name of gene within.

Expression data from adult tissues identified common sites of expression (likely reflecting a common gene origin), yet a clear tendency for specialization is apparent, as huge differences in expression levels and unique sites of expression were identified.

For the first time, we identified opsins being expressed in the planula larvae. Interestingly, more than half of the group-1 Tcops were detected in the planula, with Tcop17 and probably Tcop6 being larva-specific. Such diversity in larval opsin was

surprising, since only three larval opsins have been reported from cnidarian (for the reef corals) so far (Mason et al. 2012). Cubozoan planula larvae were shown to have an extremely simple anatomy lacking any nervous system at all (Nordstrom et al. 2003). The presence of several pigment-cup ocelli, with rhabdomeric-like photosensitive cells without visible neural connections to any other cell, could be considered the only advanced feature of this life stage. The behaviour of the larvae is most likely controlled by a motor-cilium extending from these cells (Nordstrom et al. 2003). In such a simple system, tuning to light stimuli must be crucial at least for a successful substrate selection and settlement. It would be of extreme interest to inspect the expression pattern of at least the larvae-specific Tcops by IHC in the future.

In addition, an even more detailed analysis revisiting the possible diversity of Tcops expression in combination with physiological studies to address the use of various Tcops for various behavioural tasks should be considered.

Phototransduction by cubozoan opsins.

If we closely inspect invertebrate and vertebrate phototransduction cascades, one principle becomes evident - ciliary photoreceptors invariably use a cyclic-nucleotide motif in the phototransduction cascade, whereas rhabdomeric photoreceptors use the phospholipase C (PLC) motif (Garen-Fazio et al. 1991, Yau 1994, Kojima et al. 1997, Finn et al. 1997, Xiong et al. 1998, Pugh et al. 1999, Gomez and Nasi 2000). As reviewed in Yau and Hardie (2009), the Gq and Gt (a photoreceptor-specific member of the Gi alpha type subunit family) alpha subunits mediate the absolute majority of visual cascades in invertebrates and vertebrates, respectively. Activated Gt(i) stimulates PDE, which hydrolyses cyclic GMP to GMP. This results in the closing of CNG channels leading to hyperpolarization of the photoreceptor. In contrast, PLC activation by Gq is followed by the opening of the TRP and TRPL ion channels, resulting in depolarization of the photoreceptor cell. For ciliary mode of phototransduction, there are three recognised “submotifs” to date, mediated by Gt(i), Go and cnidarian Gs (as summarized in Fig 40).

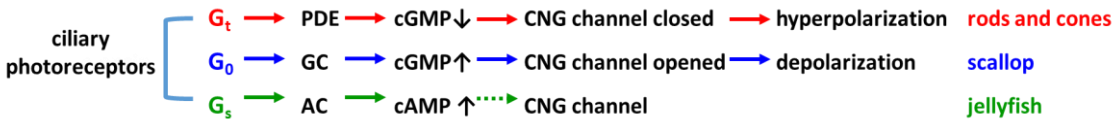

Fig. 40: Modes of ciliary phototransduction.

The Gt(i) pathway comprises stimulation of phosphodiesterase (PDE), leading to cGMP decrease, followed by closing of the CNG channel and hyperpolarization of the photoreceptor as seen in vertebrate rod and cones. The Go pathway leads to guanylyl cyclase (GC) stimulation leading to cGMP increase and hence to depolarization of the receptor as found in molluscs. The Gs pathway leads to a rise in cAMP levels, probably by direct adenylyl cyclase (AC) stimulation, but the nature of this motif is not yet fully resolved (depicted by a dotted green arrow). For review see Yau and Hardie (2009).

Gt(i) invariably activates a PDE and hence cGMP hydrolysis. Go activates a guanylyl cyclase (GC) resulting in a rise in cGMP. Alternatively, Gs seems to stimulate adenylyl cyclase (AC) resulting in the rise of cAMP. Downstream from these second messengers (either cGMP or cAMP), is in all cases a light-transducing CNG ion channel, with the open channel leading to depolarization or hyperpolarization, respectively.

There are currently two hypotheses considering the evolution and split of the two main phototransduction cascades (rhabdomeric vs. ciliary). One suggests that phototransduction evolved from a non-opsin G protein coupled receptor using the CNG pathway (Porter et al. 2012) and that the Gq mediated phototransduction evolved after the cnidarian-bilaterian split (Plachetzki et al. 2010). The second hypothesis (based mainly on the sequence diversity and phylogenetic position of anthozoan opsins) suggests even earlier divergence of the two pathways, predating the split of Cnidaria and Bilateria (Suga et al. 2008).

Interestingly, in a recent study (Mason et al. 2012) a Gq cascade coupled to the coral *Acropora palmata* larval opsin (Acropsin 3) was identified. This opsin was shown to interact specifically with the coral ortholog of mammalian Gq. Additionally, phospholipase C (PLC) and protein kinase C (PKC) genes (involved in the Gq cascade) were identified in poriferans and *Hydra* (Koyanagi et al. 1998), indicating that origin of

Gq cascade indeed predates the parazoan-eumetazoan split, favouring the second hypothesis and providing yet a deeper insight into the evolution of phototransduction.

The identification of a Gs-AC-cAMP cascade provided the first example of phototransduction where an opsin-based photoreceptor signals via neither cGMP nor PLC (but note that the CNG principle for ciliary phototransduction still holds). Considering all the information mentioned above, it comes almost as a surprise, that the Gs is the only G protein alpha subunit identified so far in photoreceptors of cubozoan eyes. The lack of signal in our IHC analysis for the different G alpha subunits might be a result of limited cross-species interaction capacity/reactivity of the commercial antibodies used. There is also a hypothetical possibility that the *T. cystophora* specific variant to the Gs, the Gx (clusters to Gs, but has distinct C-terminus), recovered from the genome, might itself represent a novel phototransduction pathway. We propose generation of *T. cystophora* specific anti-G alpha antibodies directed against the last 30 amino acids of the C-terminus of each of the identified variants and repeat the IHC analysis to confirm our results. To investigate if the Gs activation is true for all of the Tcops, we performed a light-response assay for opsin-Gs coupling confirmation and revealed that the Gs-cAMP is used only by a small set of Tcops from group-2 (Tcop13 and Tcop5) and the majority of cubozoan opsins likely signal by a distinct pathway.

Our behavioural assay confirmed that visually guided behaviour is impaired after Gs pharmacological inhibition, confirming the conclusion that Tcop13 (group-2) is the main visual pigment. The mode of transduction remains unknown for all the group-1 Tcops, which did not provide any light-mediated activation in our light-response assay. It is very likely that this group of Tcops uses a different signalling cascade. The identification and functional testing of the potential G alpha subunit type coupled to group-1 Tcops is necessary to conclude that *T. cystophora* possess at least two independent photosystems, indicating yet another level for the functional divergence of the identified opsins.

From our data, we assume that variable sensitivity and bleaching properties of the individual Tcops depend on their primary amino acid sequence and further structural-functional studies of Tcops are highly required, mainly to inspect if the vertebrate-like

E/D counterions are indeed used by the corresponding Tcops and to investigate the significance of the various tripeptide variants found among *T. cystophora* opsins. We anticipated a complete loss of Gs cascade signalling after the tripeptide mutation, but in fact the corresponding substitutions in this region led to distinct light response modulation. Our data indicate that tripeptide mutation in cnidopsins might contribute to subtle tuning of the opsin response to light stimulation, rather than being determinative for the G alpha subunit coupling. These non-conventional properties and distinct characteristics of Tcops make these opsins valuable potential candidates for novel optogenetic tools development.

As aforementioned, some of the Tcops show some intriguing similarities to vertebrate visual opsins, this resemblance is intensified by some of the previously identified necessary intermediary vertebrate-like cascade components in *T. cystophora.* Kozmik et al. (2008a) identified (by qRT-PCR on cDNA derived from rhopalia) a catalytic and an inhibitory subunit of PDE (phylogenetically clusters with vertebrate rod- and cone-specific PDE6), a phosducin and a guanylyl cyclase, suggesting a possible presence of vertebrate-like phototransduction cascade. In agreement with this scenario, we identified a CNG channel partial sequence in the genome of *T. cystophora*. However, possible expression of the CNG channel in the photoreceptors was not further investigated in this study and should be addressed in the future research (at least by anti-CNG channel IHC staining). Nevertheless, in a study of another cnidarian *H. magnipalpiata,* CNG channel was reported to be co-expressed with a previously described member of the cnidopsins clade hmOps2 (Plachetzki et al. 2007), with this connection being supported by behavioural testing with the CNG channel inhibitor (Plachetzki et al. 2012). Accordingly, it is tempting to hypothesise, that group-1 Tcops and (hence the PRC2 cells) may in fact use vertebrate type signalling, as supported by the presence of these vertebrate-like components in the rhopalia and furthermore by the presence of vertebrate-like arrestin in the retinas of the major eyes.

Based on Koyanagi et al. (2008) the photoproduct of illuminated Caryb (exact ortholog of Tcop13 – PRC1) did not show photoregeneration by subsequent light absorption, leading to the assumption that the Caryb opsin does not have the true

bistable nature (the chromophore is not re-isomerized by a second photon as seen in e.g. *D. melanogaster*), which bilaterian invertebrate visual pigments exhibit (Tsukamoto et al. 2005, Koyanagi and Terakita 2008). Since there is no true retinal pigment epithelium overlying the photoreceptors in the major eyes of *T. cystophora*, the mechanism for pigment regeneration is unclear. However, we were unable to identify any significant Hits for any of the enzymes necessary for pigment regeneration or transduction shut-down, known from other vertebrate or invertebrate animals. This could be caused either by the fact that cnidarian orthologues of these genes already diverged too much in sequence to provide us with corresponding Hits, or there could be yet another undiscovered mode of pigment regeneration and phototransduction shut-down. We could even "wildly" speculate the possibility of PRC2 cells acting in the photopigment regeneration process rather than being true photoreceptors, meaning Tcop18 would act as an isomerase for the Tcop13 chromophore. This possibility could be inspected by functional testing in a modified light-response assay in cell lines involving coexpression of Tcop13 and Tcop18 in these cells.

The cnidarian Gs-cAMP phototransduction is the first cascade identified in a prebilaterian phylum, to be distinct from known phototransduction cascades, but nevertheless exhibits significant similarity with those in vertebrate and invertebrate ciliary photoreceptors in CNG channel employment. This fact could imply monophyletic origin of ciliary phototransduction. Moreover, this "unusual" cnidarian Gs-mediated signal transduction quite resembles the vertebrate olfactory signalling cascade, which is also composed of Gs activating adenylyl cyclase, resulting in increase in cAMP and activation of CNG channels (Breer 1991, Breer 1993, Kaupp 2010). Since the olfactory sensory neurons display ciliary morphology, it is tempting to speculate about the possible common evolutionary origin with ciliary photoreceptors, as already hypothesised by Koyanagi et al. (2008).

Novel lens crystallins.

Cubozoan eyes are very complex, but the quality of the image produced by these eyes is a long-standing question. The cornea of the lens eyes forms a part of a single layer covering the entire rhopalium and has no refractive capacity, yet the high quality

of the lenses of *T. cystophora* was as a surprising finding (Nilsson et al. 2005). Interference microscopy revealed graded refractive indices creating almost an aberration free image. This study also revealed that the position of the retina does not coincide with the sharp image (the focal length exceeds the distance to the retina), resulting in unfocused images with poor spatial resolution. Authors propose that most likely the eyes are under-focused on purpose, probably to remove finer image details from the retinal view, as it would help the animals to detect large stationary objects, rather than the smaller particles floating around (Nilsson et al. 2005). Such "filter" would help the animal to remain in nearshore area of the mangroves and to avoid obstacles while swimming, which was shown to be typical behaviour of *T. cystophora* (Garm et al. 2007, Garm et al. 2011, Garm et al. 2013).

The lenses of *T. cystophora* consist of closely spaced cells with few organelles (cellular lenses). The lens is situated next to the retina, with a thin acellular layer separating it from the photoreceptors. The lenses of *T. cystophora* differ in size, shape and distribution of refractive index gradient between the two eyes; lens of the smaller eye is drop-shaped while the second one is biconvex corresponding to differences in development from de-differentiated myoepithelia cells of polyp (Laska-Mehnert 1985). Both eyes are equipped with refractive gradient as described for aquatic animals such as squid or trout (Jagger and Sands 1999). The lens of the smaller upper eye works with continuous gradient through the entire lens (maximum in the centre, minimum at the periphery) while the lens of the large eye has an almost homogenous core and the gradient falls just on its periphery. Changing the light intensity revealed that the larger LLE eye has a mobile pupil (Nilsson et al. 2005).

The gradient is especially essential for the aquatic lenses to compensate for underwater ineffective refractivity of cornea. For example, the refractive index in the centre of human lenses is 1.41 (comprising 35% of proteins), whereas in squid lenses it reaches up to 1.55 comprising almost 100% protein concentration (Sweeney et al. 2007). *T. cystophora* lenses were shown to reach up to 1.48 in the centre and the index falls to 1.34 at the periphery (Nilsson et al. 2005). A lens-like structure, a "pseudolens" with a

probably negligible optical power, was discovered within the slit eye of *T. cystophora* (Garm et al. 2008).

Crystallins are common water-soluble proteins, known to be responsible for the optical properties of the transparent lenses. In contrast to the highly similar and conserved opsins in the retinas, crystallins are a rather highly diverse group of molecules (different proteins function as crystallins in different species), multifunctional and often taxon- or species-specific (Wistow and Piatigorsky 1988, Piatigorsky et al. 1989, Piatigorsky and Wistow 1989, de Jong et al. 1993), in contrast to the general/overall conservation of opsins as the visual pigments in the photoreceptors.

Most of the crystallins are identical or related to abundant, ubiquitously expressed cytoplasmatic enzymes or stress proteins. These proteins, when expressed at low levels function as enzymes in many tissues, but when massively expressed in the eye, “pile up” and thus form lenses (de Jong et al. 1993, D'Alessio 2002). The abundance parameter is crucial, since the protein must be expressed at excessive levels to affect the refractive properties of the lens (for review see Piatigorsky 2007, Jonasova and Kozmik 2008). Thus, crystallins from different species could be characterized by the massive, lens-preferred expression rather than their structure alone (Piatigorsky et al. 1993, Carosa et al. 2002). They also serve non-lens functions in the organism, in a process called “gene sharing” (Piatigorsky and Wistow 1991) or “protein moonlighting” (Jeffery 1999, Henderson and Martin 2014).

An important implication of gene sharing (with crystallins as an excellent example) is that a protein can evolve a new role, without losing its original function, only by a change/modification in gene expression. Some “moonlighting proteins” perform both functions simultaneously, others can alter their function in reaction to changes in the environment (Piatigorsky and Wistow 1991, Piatigorsky 2003). It has become apparent over time that gene sharing and repeated use of proteins for new tasks in general represents a common evolutionary strategy (Piatigorsky 2007).

As aforementioned, gene duplications have been recognized as a major force of molecular evolution (Magadum et al. 2013), however the lens crystallins seem to have

taken an evolutionary “detour”, were acquisition of a new function of a particular gene precedes gene duplication and hence represents a model situation where changes in expression (and function) occur before the gene is duplicated.

Our genomic search in the *T. cystophora* 454 derived library recovered all of the previously reported crystallins and confirmed the single-exon structure of the J1 and J2 sub-families. Moreover, we identified three new potential crystallins, clustering to either J1 or J2 group. None of the crystallins have a sequence/phylogenetic relationship with crystallins of any other species and are used by *T. cystophora* exclusively. With addition of the three newly identified genes, at least eight crystallin genes are present in *T. cystophora* genome (with J1 and J2 derived crystallins being intronless). J1A, J1B, J1C, J2 and J3 were previously confirmed to be expressed in the lenses (by peptide isolation and sequencing, qRT-PCR analyses and mRNA *in situ* hybridization, but not IHC) (Piatigorsky et al. 1989, Piatigorsky et al. 1993, Kozmik et al. 2008b). The crystallin groups J1 and J2, were shown to represent the majority of crystallins within the lens of both the small and large eye (Piatigorsky et al. 1993), while the mRNA *in situ* hybridisation data confirmed expression outside the lens for all the previously identified *T. cystophora* crystallins. The J1 crystallins show similarity to ADP-ribosylglycohydrolases (Piatigorsky and Kozmik 2004, Castellano et al. 2005). J3 crystallin is encoded by a single gene and shows homology to vertebrate saposins (Piatigorsky et al. 2001). The J2 crystallin gene has no apparent homology to known proteins from other species, but was found to be expressed in other tissues as well (performing non-optical function simultaneously).

IHC staining data with anti-J1 (generated against common domain between all the J1 members, since these genes are too conserved to be recognised by distinct antibodies respectively) and anti-J2 generated antibodies (unpublished data, manuscript in preparation) suggest that the inner part of both lenses is composed mainly of J1 crystallins while the outer is enriched by J2 crystallins. The extra-lens expression of both groups of crystallins was also confirmed in the gastric and statolith cavity and in nematocytes for J1 and for J2 solely in the statolith. The screening for J1 and J2

expression in lesser eyes revealed J1 crystallin in the slit eye pseudolens but not in the pit eye opening.

Based on the above mentioned studies and our preliminary data we propose, that the observed specific distribution and combination of crystallins in the lenses could serve a role in maintenance of the correct lens state (e.g. transparency) and it can represent an example of functional distribution of diverse crystallins as in the case of squid lens (Sweeney et al. 2007).

Since several variants of J1 and J2 crystallin genes were found in the genome of *T. cystophora*, multiplication (most likely via DNA based duplications) might be perceived as an important step for the highly up-regulated lens-specific expression in the present-day lenses. The presence of the newly acquired "copies" in the genome probably released the original selective pressure on maintenance of both the functions and led to the establishment of new regulation resulting in high ocular expression, via the process of superfunctionalization (van Straalen and Roelofs 2012) (Fig. 41).

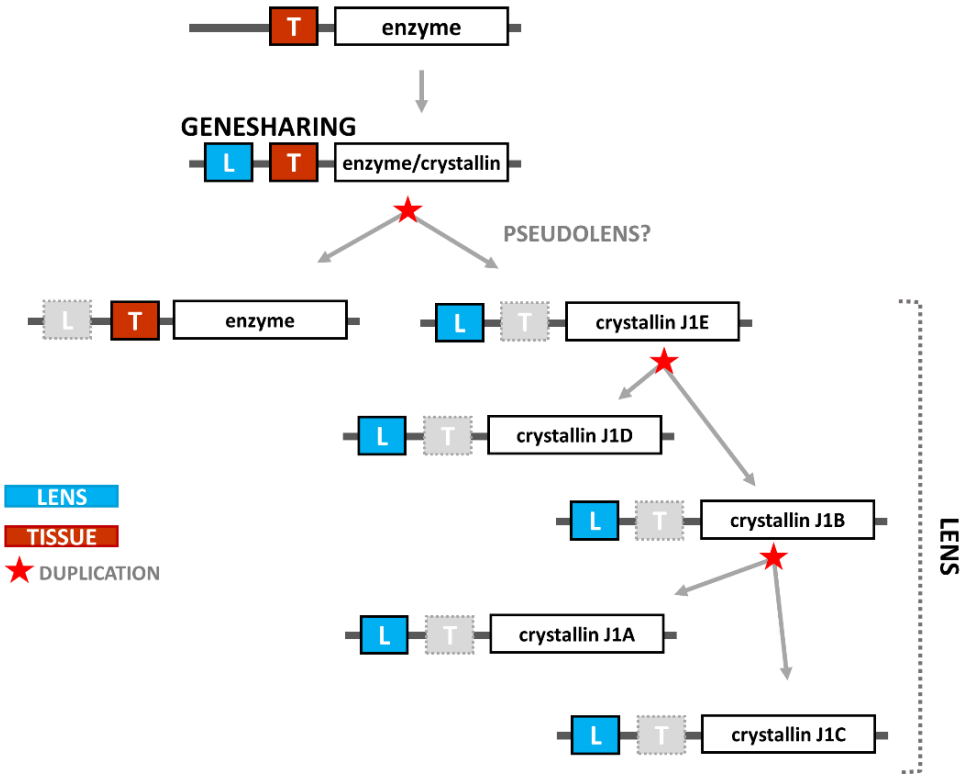

Fig. 41: Evolutionary scenario for J1 crystallin family emergence and expansion.

A common enzyme (ADP-ribosylglycohydrolase) established a new function by acquisition of a new regulatory element (depicted by coloured boxes with a letter symbol of the corresponding expression site), leading to expression of this enzyme in cells of the eye (probably forming a pseudolens-like structure). This gene underwent duplication and one of the new variants (preferentially expressed in the lens) was multiplicated in subsequent DNA based duplication events. These new copies remained active and together produced a large amount of crystallin mRNA (superfunctialization), which was maintained as a selective advantage for the lens, where the protein abundancy is the crucial factor.

The observed extra-ocular expression (in gastroderm around gastric cavity and in statocyst) may refer to the original site of expression and function.

The pit cup eyes are frequent among cnidarians and obviously an ancestral type. The so far identified single photoreceptor type of the lesser eye seems to be identical with PRC2 cells of the major eyes and this is suggestive of gradual cell differentiation which ended up with numerous cell types of the large lens eye. Despite the presence of a “pseudolens” in the slit eye, this structure seems not to gather light directly but it was proposed that it serves as UV light filter (Garm et al. 2008). The expression of J1 and J2 crystallins in the almost “perfect” *T. cystophora* lenses had to be preceded by numerous events accompanying the pit to complex lens eye transition. Highlighting the evidence of J1 in slit pseudolens, we suggest a scenario for the genesis of large complex eye. Introduction of new regulatory sites into the promoter area of J1 (originally a common enzyme - ADP-ribosyl glycosylhydrolase), enabled high expression in cells neighbouring the photoreceptor cells or directly in a group of photoreceptors. Thereafter, J1 crystallin underwent several rounds of subsequent duplications (DNA based duplication including the promoter region). Once these cells, with a substantial amount of protein expressed, appeared anteriorly to the photosensitive cells and such connection proved to be beneficial for vision, it has been maintained and developed further, probably up to the lenses of complex eyes.

In summary, the case of *T. cystophora* provides an example where recruitment of crystallins for structural function (via gene sharing) was probably followed by gene duplication and subsequent partial separation of both functions, as clearly documented by multiplication within members of the two unrelated groups of J1 and J2 crystallins.

From this view gene sharing strategy seems to be universally applicable throughout the animal kingdom and probably represents a common evolutionary strategy, as is well documented by the example of lens history shared between Cubomedusae and other invertebrates and vertebrates (Piatigorsky et al. 1993, Kozmik et al. 2008b).

CONCLUSION

None of the present-day animals represent the real ancestral node, since evolution at the DNA level is a continuous process and changes happen and accumulate even if the outward morphology seems rather constant. Cnidarians have been evolving over enormous timescale under selective pressure on their huge populations. Rather than “frozen in time” in some primitive state as often portrayed, they are rather fast evolving creatures that have had enormous time to “perfect” their genes and expression systems and thus provide an attractive model for studying the evolution of genes and complexity (for review see Steele et al. 2011).

Only within the last 20 years (with accumulating genomic data) have biologists realized that many molecular and morphological innovations previously attributed to chordates (or to more “basal” bilateralia) actually date back much earlier to their common ancestor with Cnidaria (Eumetazoa). Elements of the phototransduction machinery are shared between cnidarians and bilaterian animals and were supposedly already present at the origin of opsin-based photosensitivity phenotypes in animals. Cnidaria constitute the earliest branching phylum containing a well-developed visual system and hence are a perfect model to study evolution of photoreception and vision.

In this work we integrated approaches of phylogenetics, gene expression analyses, functional studies in cell cultures and behavioural pharmacogenetics to provide compelling evidence for the existence of multiple general- and visual-photosystems (photopigments coupled to at least two distinct phototransduction pathways) in cubozoan jellyfish *T. cystophora.* In addition, we identified 17 novel non-conventional opsins with a potential to be co-opted in optogenetics.

The key conclusions of our study and my thesis, focused on identification and characterization of the genetic components necessary for cubozoan phototransduction and vision, are summarized as follows:

* A surprisingly large number of functional opsin genes is present in the *T. cystophora* genome.

* Some of these opsins show intriguing sequence similarities to vertebrate opsins.

* Extensive phylogenetic analysis clearly classifies cubozoan opsins as a sister group to c-type opsins and documents lineage-specific expansion of the opsin gene repertoire in the cubozoan genome.

* Detailed opsin expression analyses uncovered both redundancy and specialization in the use of the opsin gene repertoire. Multiple opsins with presumably similar molecular characteristics are apparently utilized in the same stage/tissue while a clear tendency to establish unique expression patterns exists both within the opsin subfamilies (group-1 and group-2) and between the two subfamilies.

* There are at least two types of photoreceptors in the retinas of the major lens eyes of *T. cystophora*, expressing distinct opsins.

* Gs type alpha subunit is expressed in the photoreceptors of the major and minor eyes and probably serves as a direct coupling partner at least for the main visual opsin (based on IHC data and functional tests in cell cultures), however most of the cubozoan opsins probably signal via distinct yet unidentified phototransduction cascade.

* Pharmacological inhibition by Gs antagonist abrogates visual navigation in *T. cystophora in vivo*.

* Vertebrate-like arrestin mediates phototransduction quenching in the eyes of *T. cystophora*.

* The crystallin repertoire of *T. cystophora* is even larger than anticipated, as documented by identification of three novel crystalline genes.

Taking into account our data and studies presented here, one can assume an early evolutionary origin of the key genes associated with photoreception and their regulation, with frequent subsequent lineage-specific upgrading (or reduction) of the details, with deuterostomes being rather the late-comers with imaging vision. I could

simply not conclude this work without considering the classic question Darwin asked, of how many times did an eye evolve. Supposedly, the essential photoreception genes (with opsins as a perfect example) and their developmental regulation arose just once (monophyly on the genetic and molecular level). Once this “molecular connection” was established, it was repeatedly subjected to numerous gene duplications and morphological variations in deployment, accompanied with independent (convergent) recruitment of other genes (as in the case of crystallins of the lenses), leading to the clearly polyphyletic view on the eye evolution on the organ level.

SIDE-PROJECT: Molecular analysis of the frontal eye pigmented cells in cephalochordate *Branchiostoma floridae*

Data from this co-project were published in:

Vopalensky P, Pergner J, **Liegertova M**, Benito-Gutierrez E, Arendt D, Kozmik Z. (2012). **Molecular analysis of the amphioxus frontal eye unravels the evolutionary origin of the retina and pigment cells of the vertebrate eye.** *Proc Natl Acad Sci U S A.* 109(38):15383-8.

SHORT INTRODUCTION

B. floridae belongs to the subphylum Cephalochordata, considered to be the earliest branching group belonging to phylum Chordata (Bertrand and Escriva 2011). It has a simple body plan, while it exhibits many features of a hypothetical vertebrate ancestor - notochord, dorsal nerve cord and pharyngeal gill slits (Holland et al. 2004). Its relatively simple body plan and simple genome organisation (lacks the vertebrate-specific whole-genome duplications) make *B. floridae* a unique model animal for understanding the evolution of characteristic vertebrate features (Koop and Holland 2008).

Interestingly, *B. floridae* bears four morphologically distinct light-sensing structures (Fig. 1), from which the un-paired frontal eye was long considered the possible vertebrate paired-eyes homolog.

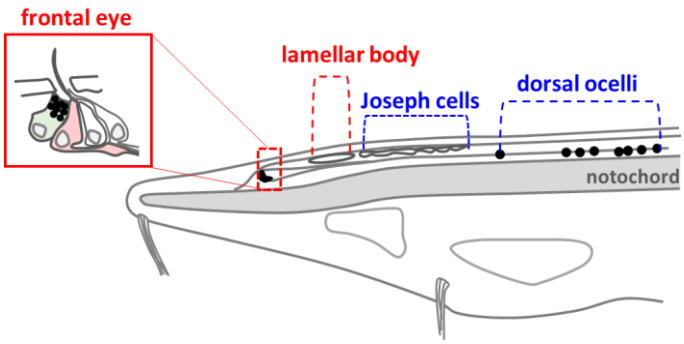

Fig.1: Schematic representation of *B. floridae* photosensitive structures in a 12.5 day old larvae.

The family of Branchiostomidae possess four types of light-sensitive structures. The dorsal ocelli (Hesse organs) and Joseph-cells are rhabdomeric-type photoreceptors embedded in the neural tube, that use melanopsins (r-opsin) as photopigment (Gomez et al. 2009). The dorsal ocelli photoreceptors are half enveloped by a cup-shaped pigment cell, which was shown to express Mitf together with melanogenic pathway enzymes tyrosinase and tyrosinase-related proteins (Yu et al. 2008). The lamellar body is formed from putative ciliary photoreceptors (and is accepted as the homologue of vertebrate pineal body; see Ruiz and Anadon 1991, Lacalli 2004) and is well developed in larvae, but its role in adults is not known. The frontal eye consists of a group of photoreceptor cells adjacent to several pigment cup-shaped cells (*Inset:* Photoreceptor pink, pigment cell green). These ciliary photoreceptors (termed Row 1) use c-opsin as photopigment, form a row symmetrically to the ventral midline and are in contact with neurons, which send projections to putative locomotor control regions (Lacalli 2004). Adapted from Lacalli (2004).

The frontal eye is located anteriorly in the tip of the neural tube and consists of several simple photoreceptors with few adjacent pigment cells (Lacalli 2004). For many years *B. floridae*, was a suspect for possessing the earliest vertebrate eye type. However, the retinal structure of its simple unpaired ocellus differs substantially from that of other vertebrates and led to long-lasting uncertainty about homology between this two structures. Specifically, the photoreceptors of *B. floridae* are only simply ciliated cells in contrast to the more sophisticated elaborate structures extending from the cilia in vertebrate retinas (axonemal projections forming membrane stacks of rod and cones) (Lacalli 2004).

In addition to photoreceptors, the second essential component of a postulated minimal eye is the dark shielding pigment (Arendt and Wittbrodt 2001). Partial shielding from the coming light provides the animal with additional information about light direction. As opposed to opsins, the distribution of molecules used as screening pigments in different animal phyla does not follow any obvious rule neither correlates with a certain photoreceptor cell type (ciliary or rhabdomeric). However, in most animal eyes - pterins, ommochromes or melanins serve as shielding pigments (Vopalensky and Kozmik 2009). It seems that the combination of the dark pigment and photoreceptor cannot be traced to any ancestral condition, but might be a result of independent assembly of these two components in different animal phyla, or the pigments might already have coexisted in an ancient “precursor” pigmented photoreceptor cell and were lost in some of the extant animal lineages (Vopalensky and Kozmik 2009).

In vertebrates, retinal pigmented epithelial (RPE) cells are one of the two major melanin-producing pigment cell types (together with melanocytes) (Strauss 2005). The development and pigmentation of these cells depend critically on the microphthalmia-associated transcription factor (Mitf) - a basic-helix-loop-helix-leucine-zipper transcription factor (Adijanto et al. 2012). It has been shown (Yu et al. 2008) by mRNA *in situ* hybridization, that transcripts of Mitf, along with melanin synthesizing enzymes (tyrosinase and tyrosinase-related proteins) are co-expressed during *B. floridae* embryogenesis (late gastrula and early neurula stages) in the primary pigment spot in the neural tube, which eventually becomes the first pigment cell of the dorsal ocelli. However, any expression data considering the frontal eye region were missing.

AIMS OF THE CO-PROJECT

The aim of this research co-project was to analyse and describe the possible expression patterns of Mitf in the frontal eye of *B. floridae* in an attempt to finally determine the relevancy of the homology between the pigmented cells of cephalochordates and retinal pigment epithelium in vertebrates. The strategy was to inspect the molecular fingerprint of the frontal eye pigmented cells by immunohistochemical staining with “in-house” generated antibody raised against *B. floridae* Mitf orthologue and to compare the data between the two phyla (cephalochordates and vertebrates).

MATERIAL AND METHODS (author´s contribution)

Collection of adult animals

Adult *B. floridae* specimens were collected by sieving sand of the shallow waters of Tampa Bay beaches (Tampa Florida) during the 2010 spawning season (June-August).

Laboratory spawning and larvae culturing

Adult males and females were kept separately in plastic dishes containing 50ml of sea-water. Eggs and sperm were obtained by applying a brief nonlethal shock (direct current - 50V) with an electric stimulator, which triggers gamete releasement in these animals. The gametes were collected using plastic droppers and released into a clean plastic Petri dish with filtered sea-water for the *in vitro* fertilization to occur. After several minutes the presence of fertilised eggs was confirmed by observation of an elevated fertilization membrane (a step preceding the first cleavage). About 10 to 12 hours post fertilization, hatching of the freely swimming neurula from the fertilization membrane occurred. Inspected stages of *B. floridae* larvae were collected using a plastic dropper and fixed in MOPS (N-morpholino-propanesulfonic acid Fixative).

Mitf antibody design

The sequence selected for antigen production corresponds to the position 206-408 of the *B. floridae* Mitf amino acid chain (see Appendix Table 2 for the source sequence). Expression and protein purification were performed according to the chapter Materials and Methods in the previous section. For antibody production, rabbits were immunized with 300–500 µg of purified protein mixed with Freund's adjuvant (Sigma) three times in subsequent months, thereafter rabbits were sacrificed and the sera were collected. The final sera were tested for immunogenicity to the given antigen by western blot and by antigen pre-absorption of the Mitf antibody control staining (Fig.2).

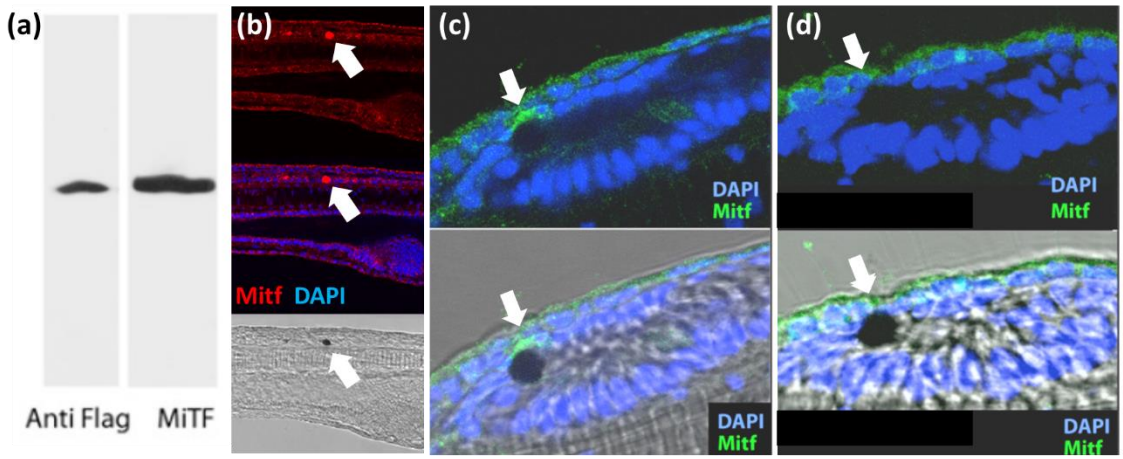

Fig. 2: *B. floridae* Mitf antibody verification.

a) Western blot analysis of the Mitf antibody. HEK293T cells were transfected with an expression vector carrying a Flag-tagged partial coding sequence of the Mitf, cultured for two days and used for whole-cell extract preparation. The extract was subjected to western blotting. Rabbit antibody raised against the *B. floridae* Mitf recognizes the same band as anti-Flag antibody when tested with Flag-Mitf fusion antigen. b) Specificity of the Mitf antibody signal was further confirmed by specific nuclear stainings (white arrowhead) in the pigment cells of the dorsal ocelli, where Mitf expression was reported previously (Yu et al. 2008). Top panel – Mitf signal in red; middle panel – Mitf in red merged with DAPI in blue; bottom panel – bright field of the inspected area to visualise the pigment spots of the dorsal ocelli. c) Specific signal of the Mitf antibody *in situ* obtained by IHC is lost after pre-adsorption of the antibody with the Mitf antigen as seen in d). c-d) Top panels Mitf in green merged with DAPI in blue; bottom panels – Mitf merged with DAPI in bright field. Adapted from Vopalensky et al. (2012).

Whole-mount immunohistochemistry.

For immunohistochemistry, all fixed larvae were washed 3x20 minutes in 1x PBT (1x PBS, 0.1% Tween 20), followed by blocking in blocking solution (10% BSA in 1x PBS) for 1 hour at room temperature and incubated with the primary antibody diluted in Blocking solution (1:200) overnight at 4 °C. After blocking, larvae were washed 3-4 times for 20 minutes in 1x PBT at room temperature and incubated with secondary antibodies (diluted in blocking solution) for 2 hours. Secondary antibodies were washed away three times for 20 minutes in 1x PBT. For nuclear visualisation the larvae were incubated with DAPI (1µg/ml) in 1x PBS and washed 3x 5 minutes with 1xPBT.

For confocal microscopy, stained larvae were mounted in Vectashield (Vector Laboratories) using small coverslips as spacers between microscopy slide and the coverslip, to prevent squashing of the animal. Single cell resolution analysis was obtained using Leica Inverted and Upright TCS SP5 Confocal Microscopy System, with a four fluorescent channel detection system. Images were captured and processed in Leica Application Suite 1.8.0 software.

RESULTS AND DISCUSSION

Fluorescent signal was apparent in the melanin expressing pigment cells of the frontal eye (Fig. 3).

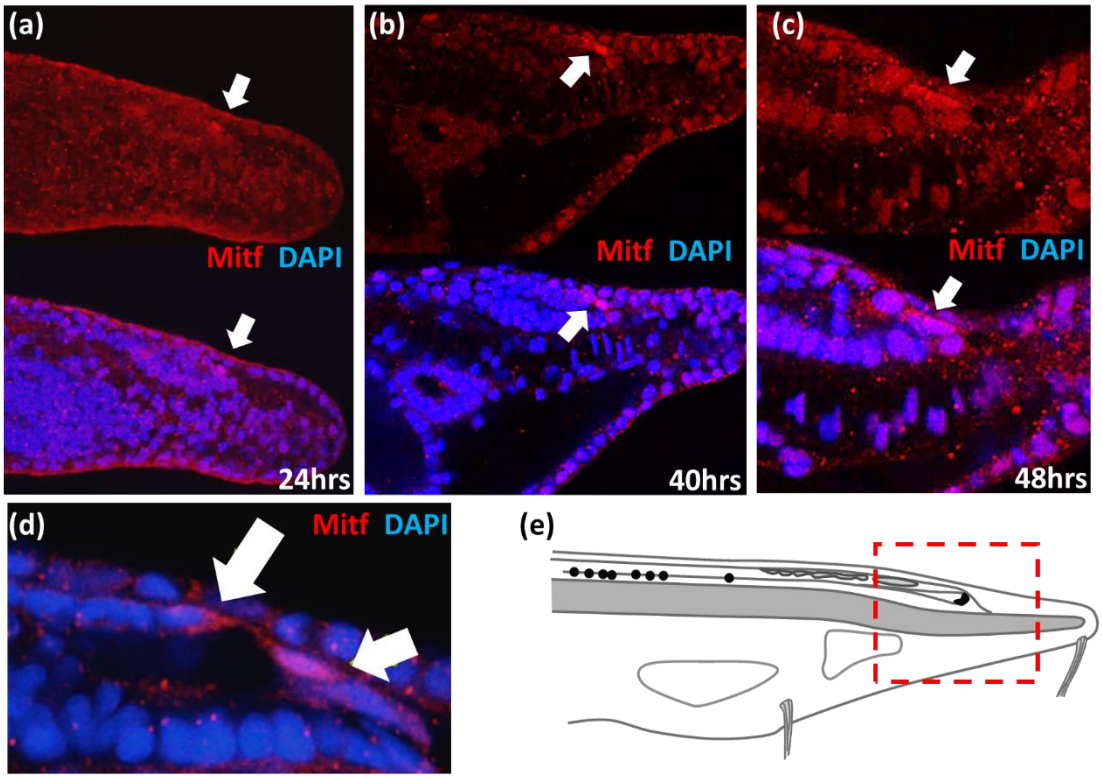

Fig. 3: Expression of Mitf in the frontal eye region.

a) In the frontal eye region Mitf specific signal starts to be visible in 24 hours old larvae. The Mitf antibody labelled the nucleus (white arrows) of the developing frontal eye pigment cell. b-c) Mitf signal in 40 and 48 hours old larvae. In Addition to the nuclear signal, partial localization in the pigment cell cytoplasm was observed (situation documented in vertebrates as well; see Lu et al. 2010) a-c) Top panels - Mitf in red; bottom panels - Mitf merged with DAPI in blue. d) Detail of the Mitf signal localization in the pigment cells. Large white arrow – cytoplasmic signal; small white arrow nuclear signal. e) Red box shows the visualised area of the animal.

Additionally, the vertebrate Otx2 paralogue was mapped into these same pigment cells, which is known to acts in cooperation with Mitf during RPE differentiation and development (Martinez-Morales et al. 2003). The presence of melanin in these cells was then confirmed, using melanin synthesis specific inhibitor phenylthiourea (PTU) to abolish melanin synthesis in the frontal eye (Karlsson et al. 2001).

CONCLUSION

Combined, the data indicate that the only shielding pigment of *B. floridae* frontal eye pigment cells is melanin and that the molecular fingerprint of these cells closely

resembles the molecular fingerprint of vertebrate retinal pigmented epithelium. In both *B. floridae* and vertebrates, the pigmented cells are adjacent to the ciliary photoreceptor cells, further confirming the homology of amphioxus and vertebrate eyes.

LIST OF PUBLICATIONS

1) **Liegertová M,** Pergner J, Kozmiková I, Fabian P, Pombinho AR, Strnad H, Pačes J, Vlček Č, Bartůněk P, Kozmik Z. (2015). **Cubozoan genome illuminates functional diversification of opsins and photoreceptor evolution.** *Sci Rep.* 5:11885. (IF 5.578)

2) Vopalenský P, Pergner J, **Liegertová M**, Benito-Gutierrez E, Arendt D, Kozmik Z. (2012). **Molecular analysis of the amphioxus frontal eye unravels the evolutionary origin of the retina and pigment cells of the vertebrate eye.** *Proc Natl Acad Sci U S A.* 109(38):15383-8. (IF 9.674)

3) Manuscript in preparation:

Marková K., Serekeš J., Goliáš V., **Liegertová M.**, Vlček Č., Kozmik Z.

The lenses of box jellyfish in space and time: Crystallins as lens creators.

APPENDIX

Table 1. List of primers used in this study.

Gene	Reverse primers for 5´end direction walking	Forward primers for 3´end direction walking
Tcop1	CCATTACCATCAGGAAGACCAACAAGG	CACAAAGTGCAAGAGAAATCGAGAGACA
Tcop2	TCGATTATCTCACGTGATACCCACTTGG	CCCAGTGCATACTGTCTCTTATATACTCG
Tcop3	GGTGCACAACCTACATGTTGACTTTCAG	ACCTACAAGAGTTCTCTCCTATCTGAAGG
Tcop4	GGACATACTATTCCAATCACCTGCTTTCC	CGAACCAGAACAGCTGTCGTAATCTT
Tcop5	CCAAAGTGACTCTTGGAGCGATGTC	TCATGTTCTACATCAGAAGCGAATTGACG
Tcop6	CCAACGACGATCTGGATTGCCAATTAATG	TGCTTACCCACTCTCAGCATATTCCA
Tcop7	CACCTGATTTCTAGTAGGATGCAGGCA	CAACTTCTAAGTAACAACAGGACTCGGT
Tcop8	CTAGGGCTGCATTGGATCCAAACTTTG	CCTCTCAACATTGTATCATGCTTTCAGC
Tcop9	AGGTCGTCCATAAAGAAAGAATGGCAT	GCACTCGACCGTTATATGACAGTGT
Tcop10	CAGATGCGAAGTTTGTCCTGGATATCA	GGGATCAGCAGAGATTAAGGATGCTACT
Tcop11	AAGCTGCTTGGAGGCTGATGAGATT	TACGATGGCACAGTGATGACAGCA
Tcop12	ACTGACTAAATTGCTGTCAATGGTCACG	ATCCTCGGTCTGCTATCTACCTGTTG
Tcop13	ATGGCGGCTAACTTGTCTGAAATACTTTC	GCAGTGGACATTTGGTATGGAGCTA
Tcop14	CCCTCTGTAGAATAACTTGAGAGTCCAGTA	CGCTATCAATATCGTCATCTTTTGCCAC
Tcop15	CTACATTGCCTGTGACGCTCTCATG	-
Tcop16	GCCTCTTTATTTCAGCTCTAAACTTATGATGC	-
Tcop17	CGGATATTTACATGACGTCGCATCATCC	AGTTATTGCCTATCGCCAGTGGAAG

Gene/PCR product	Forward primers for qRT-PCR	Reverse primers for qRT-PCR
Tcop1/212 bp	TATGCCCGTTGTTTGCCTATC	GGTGACATTTTGGCGATTGAT
Tcop2/119 bp	AGTTGCTGCCCAGATTGTGTT	TTGTAGTGGGCGAGTTCCTGT
Tcop3/217 bp	GACCCGCTCGATGTGTCTTAC	AGGGAAGCCAACAGAACACAA
Tcop4/228 bp	CAGTCTCTTCGGTGGCTCACT	TCCAATCACCTGCTTTCCAGT
Tcop5/205 bp	TTGACGCGCTCTACTTTGTCA	GACATAAGCATCACGGCAACA
Tcop6/170 bp	GCACGGGTCAAACTCTCAAAC	ATTCTGCTATTGGGCTCACGA
Tcop7/155 bp	TTGCTGGTCTTCCTCATTGGT	GGAAGCAGCAAACAAGAATGG
Tcop8/194 bp	TGCATATTAGGCGTCACAACG	AATTGGGTTTAATGGGCCTTG
Tcop9/150 bp	ACCCAAGAAAAACCGAAAGGA	CAGAGCAACGCACTTTCACAC
Tcop10/227 bp	CTTGGGCATCTGTTGATGGTT	CAGCCATCGTAGCCAAATCTC
Tcop11/211 bp	ACCTGGCTATTCGGAGATGGT	GTAGTGCTGCCCAGACAAACC
Tcop12/160 bp	GCAACCTCTTGCATGTCACAA	AAGCGATCAACTGCCAACAAT
Tcop13/224 bp	CTGCACAGCTGTTTGGTTCTG	GAACATGGCTGAGGACTTTGC
Tcop14/178 bp	GACTGGTCTTGCCTTTGATCG	GCTCACCTGGAGACCCTCTTT
Tcop15/238 bp	GGCTGAAAATGCGAGAGAAGA	ACCATAACCCCAATGATGCTG
Tcop16/232 bp	TATCCCGTCGCTGGAGTAAGA	TTACCGCCAAAGCATACATCC
Tcop17/193 bp	TATGGTTTTTGCGTGCATGTC	ACCATCCGAAGTAGGGAGGAA
Tcop18/176 bp	CCACTTTTGGGATCTCCACTG	CGCTTCAAGGGAAGTACGATG
Rpl32/146 bp	CTTGAAGCGACGCCTAACTCT	AATGGTTGTCCCCACGGTAAAG

Gene	Forward primers for anti-Tcop antibody preparatio	Reverse primers for anti-Tcop antibody:
Tcop1	CGCGGATCCAACCCTATCATTTACTGTTGT	CCCAAGCTTTTACTGACCTTCCTCTCCCG
Tcop13	CGCGGATCCAACCCGATCATTTACTGCTTCCTT	CCCAAGCTTTTAACTCTCTGCAGCCCCTC

Gene	Forward primers for degenerate PCR:	Reverse primers for degenerate PCR:
Arrestin	CARCCNGCNCCNGGNGAYAC	TCRTGYTTNARYTTNCCRTC
CNG channel	ATHATHCAYTGGAAYGCNTG	TARTCRAACCAYTTDATNAC

Gene	Forward primers for 3´RACE	Forward nested primers for 3´RACE
GNAI	TGGCCCTTAGTGGCTACG ATCTTGTGC	GCATGAAGCTCTTCGATTCCATCTGCA
GNAS	GGATCCAGCTTATGTACCGAACGACCA	GTTGGAGGACAGCGCGATCAACGTCGA
GNAG	GGAAGATCTATCATCTACTCTCATTTCACATG	-
Crystallin J1D	GATGCAGCAGCTCAACCCTTACAGTG	CGTATTGAACAATCTCATTCCCACGGAC
Crystallin J1E	ACTGGATCTACAGCCTACCCAAACTG	GGAGGCAATTAAAGTTTGGTCGATCCAC
Crystallin J2B	CAAGAGGCAGAGCGAGTTAGGGAAGTG	-

Table 2. List of peptide sequences used for generation of the polyclonal antibodies.

Antibody	Sequence of the peptide used for imunization	Host organism
anti-Tcop1	- NPIIYCFLHKQFRRAVLRGVCGRIVGGNAIAPSSTGVEPGQTLGGGAAES*	mouse
anti-Tcop13	- NPIIYCLLNKQFRTLLFRATRVSPGEEGQ*	mouse
anti-Mitf	- MDDVIDDIISLESSFDDSFNFLDAPMQQISSTMPLTSSLLDGFGTVGSLTPM	rabbit
	VTANTSASCPADLTNIKKEPVQMSESELKALAKDRQKKDNHNMNEWGYS	
	EMVGWIGGVPEQAMALAKDRQKKDNHNIIERRRRFNINDRIKELGTLLPKT	
	ADPDMRWNKGTILKASVDYIRRLKKEHERMRHMEERQKQMEQMNRKMLLR -	

Publication: **Cubozoan genome illuminates functional diversification of opsins and photoreceptor evolution. *Sci Rep.* 5:11885.**

SCIENTIFIC REPORTS

OPEN

Cubozoan genome illuminates functional diversification of opsins and photoreceptor evolution

Received: 10 February 2015
Accepted: 05 June 2015
Published: 08 July 2015

Michaela Liegertová[1,*], Jiří Pergner[1,*], Iryna Kozmiková[1], Peter Fabian[1], Antonio R. Pombinho[2], Hynek Strnad[3], Jan Pačes[3], Čestmír Vlček[3], Petr Bartůněk[2] & Zbyněk Kozmik[1]

Animals sense light primarily by an opsin-based photopigment present in a photoreceptor cell. Cnidaria are arguably the most basal phylum containing a well-developed visual system. The evolutionary history of opsins in the animal kingdom has not yet been resolved. Here, we study the evolution of animal opsins by genome-wide analysis of the cubozoan jellyfish *Tripedalia cystophora*, a cnidarian possessing complex lens-containing eyes and minor photoreceptors. A large number of opsin genes with distinct tissue- and stage-specific expression were identified. Our phylogenetic analysis unequivocally classifies cubozoan opsins as a sister group to c-opsins and documents lineage-specific expansion of the opsin gene repertoire in the cubozoan genome. Functional analyses provided evidence for the use of the Gs-cAMP signaling pathway in a small set of cubozoan opsins, indicating the possibility that the majority of other cubozoan opsins signal via distinct pathways. Additionally, these tests uncovered subtle differences among individual opsins, suggesting possible fine-tuning for specific photoreceptor tasks. Based on phylogenetic, expression and biochemical analysis we propose that rapid lineage- and species-specific duplications of the intron-less opsin genes and their subsequent functional diversification promoted evolution of a large repertoire of both visual and extraocular photoreceptors in cubozoans.

Many animals sense light cues for vision and nonvisual photoreception. Light is captured by an opsin-based photopigment in a photoreceptor cell and leads to a cellular light response through a G protein-mediated phototransduction cascade[1,2]. Opsins are members of the G protein-coupled receptor (GPCR) superfamily; proteins with seven transmembrane helices that are involved in a diverse set of signaling functions. Within the GPCR superfamily, the opsins form a large monophyletic subclass of proteins characterized by a lysine in the seventh transmembrane helix that serves as the attachment site for the chromophore. Functional opsin proteins covalently bind a chromophore, gaining photosensitivity. Opsins are essential molecules in mediating the ability of animals to detect and use light for diverse biological functions and have been discovered in a wide variety of tissue and cell types, signaling through multiple pathways, and carrying out functions beyond image formation[1,3].

Phylogenetic analysis has indicated that four major opsin monophyletic groups can be recognized[1,3–5]. The first group, is comprised of the c-type opsins, the vertebrate visual (transducin-coupled) and non-visual opsin subfamily, the encephalopsins, pinopsins, paprapinopsins, parietopsins and tmt-opsin subfamily and the invertebrate ciliary opsins. The second group, Cnidopsins, is a group consisting of all cnidarian opsins, except for so called Nematostella group 1 and Nematostella group 4 opsins, whose phylogenetic position is still unresolved[4,6]. Cnidopsins are exclusively found among cnidarians and not

[1]Department of Transcriptional Regulation, Institute of Molecular Genetics, Videnska 1083, Prague, CZ-14220, Czech Republic. [2]Department of Cell Differentiation, Institute of Molecular Genetics, Videnska 1083, Prague, CZ-14220, Czech Republic. [3]Department of Genomics and Bioinformatics, Institute of Molecular Genetics, Videnska 1083, Prague, CZ-14220, Czech Republic. *These authors contributed equally to this work. Correspondence and requests for materials should be addressed to Z.K. (email: kozmik@img.cas.cz)

present in any other phyla. The third so-called 'r-type' group consists of Gq-coupled invertebrate visual opsins and vertebrate and invertebrate melanopsins and Group 4 opsins contain an assortment of relatively poorly characterized opsin types including, neuropsins, peropsins, and a mixed group of RGRs (retinal G-protein coupled receptors)[7–10]. The distribution of the opsins into these four major groups is supported by analyses of intron arrangements and insertion/deletion events[3] and all groups contain genes found in multiple tissue locations (*e.g.* photoreceptor cells (PRCs) and/or other tissues). Two recently published analyses of opsin phylogeny by Feuda *et al.*[6,11] have shown that in contrast to the findings of a majority of other studies[3,5,10], Cnidarian opsins, including the Nematostella group 1 and Nematostella group 4 opsins, might not be of monophyletic origin, but rather can be divided into three groups, each more closely related to either the c-, r- or Group 4 opsins.

One of the defining characteristics of opsins are the presence of covalently bound chromophores, most commonly 11-cis retinal, that confer light sensitivity to the visual pigment. The chromophore is attached via a Schiff base linkage to a universally conserved lysine in the seventh transmembrane helix. Upon exposure to light, the chromophore undergoes a photoisomerization event to form all-trans retinal, that in turn drives the activation of the photopigment. Aside from this universally conserved lysine, other important amino acid residues can also be found in opsin primary structures. One example is the so-called 'counterion', typically a negatively charged amino acid that is required to interact with and thus raise the pKa of the protonated Schiff base linkage between retinal and lysine, stabilizing the binding of a proton at physiological pH. While vertebrate visual pigments use amino acid-113 as the counterion, position 181 can also be used by a diverse group of opsins containing photoisomerases and Gi/o-coupled pigments, whereas vertebrate melanopsins utilize amino acid position 83[3]. Multiple lines of evidence support the hypothesis that amino acid substitutions in the fourth cytoplasmic loop of duplicated opsins were involved in the origins of novel opsin-G protein interactions[5]. Residues 310-312, encompassing the so-called tripeptide region, were formerly demonstrated by site-directed mutagenesis to mediate opsin-G protein interactions in ciliary opsins[12] and these data were later supported by correlation analyses[5].

Box jellyfish belong to the phylum Cnidaria, arguably the most basal phylum containing a well-developed visual system. It is well known that light affects many behavioral activities of cnidarians, including diel vertical migration, responses to rapid changes in light intensity and reproduction[13]. Their phylogenetic position, simple nervous system and elaborate set of eyes[14] make their visual system of key importance for understanding the early evolution of vision, and also for understanding the biology of box jellyfish[15–18]. The eyes of box jellyfish share many features with those of vertebrates. Morphologically, they are similar by overall design (lens, retina, ciliary photoreceptors)[14,19], and recently, characterization of some molecular components has suggested that the box jellyfish visual system is more closely related to vertebrate than to invertebrate visual systems[20–23]. Photoreceptive organs in Cnidaria have diverse structures, not only between species[24] but within the same species. The cubozoan jellyfish investigated in this study, *Tripedalia cystophora*, has four equally spaced sensory structures called rhopalia, dangling from a stalk and situated within open cavities surrounding the bell. Each rhopalium has six separate eyes. There are two complex, lens-containing eyes (upper lens eye – ULE, and lower lens eye – LLE), one larger than the other, situated at right angles to each other, and two pairs (one pit-shaped, one slit-shaped) of simple ocelli comprising photoreceptors on either side of the complex eyes[25,26]. As the visual fields of individual eyes of the rhopalium partly overlap, *T. cystophora* (as well as other Cubomedusae) has an almost complete view of its surroundings. The lens-containing *T. cystophora* eyes have sophisticated visual optics, similar to molluscs and vertebrates[14,19]. Two opsin genes have so far been identified in cubozoans, one in *T. cystophora*[22], and one in the related species *Carybdea rastonii*[27]. Expression of both these opsins has been detected in eyes of the corresponding species[22,27]. *C. rastonii* opsin was furthermore shown to transfer the light stimulus via the Gs signaling pathway[27].

In the present work, we characterize a complement of 18 opsin genes identified in cubozoan jellyfish *T. cystophora* by the whole-genome analysis. Based on phylogenetic, expression and biochemical analysis we propose that rapid lineage- and species-specific duplications of the intron-less opsin genes and their subsequent functional diversification promoted evolution of both visual and extraocular photoreception in cubozoans.

Results

A large complement of opsin genes are present in *T. cystophora* genome. In addition to previously annotated *T. cystophora* c-opsin[22] we identified 17 other *Tripedalia* opsins (Tcops) sequences. Among those novel sequences, we were able to identify the ortholog (93% sequence identity) of the previously investigated *C. rastonii* opsin (Caryb)[27], designated here in *T. cystophora* as Tcop13 (Fig. S1). Complete coding sequences for all these opsins were obtained by Genome Walking (GenomeWalker, Clontech). All of the eighteen *T. cystophora* opsins are intron-less genes, which show overall sequence homology with other cnidarian opsins as well as to bilaterian rhodopsins. The conserved lysine to which the chromophore 11-cis-retinal binds was found in each of the cloned opsins, suggesting that they are indeed used for photoreception. Next, we investigated the three potential counterion sites at amino-acid position 83, 113, 181 (numbered according to bovine rhodopsin) within the cnidopsins (Fig. S2). Negatively charged amino acids (either glutamic acid/E or aspartic acid/ D) at position 83 was found in more than 50% of the identified cnidopsins, with more than 95% having E/D at position 181. Intriguingly, E/D residues at position 113 were only found in four of the identified *T. cystophora* opsins.

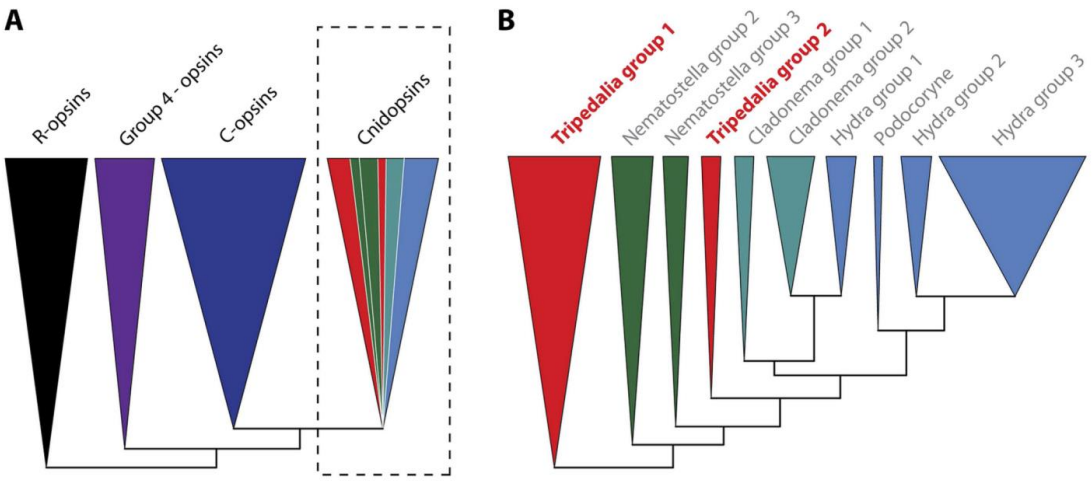

Figure 1. Schematic representation of the opsin phylogenetic analysis of a large set of opsin genes including the cubozoan dataset. A) Phylogenetic analysis performed in this study recovered previously described four major opsin lineages – r-opsins, c-opsins, group 4 opsins and cnidopsins. Herein the C-opsins and cnidopsins form sister groups. (For details see Fig. S3), **B)** Detailed inspection of cnidopsin branch indicates extensive gene duplication and lineage-specific expansion of cnidarian opsins. (For details see Fig. S4).

These were, Tcop8, Tcop12, Tcop15, and Tcop16 (Fig. S2 – red box). However, it is important to note that E/D counterions at position 113 have, to date, not been found in any opsins identified outside of chordates. Next, we investigated the identity of residues 310–312 within all the Tcop sequences. The tripeptides tended to be conserved among closely related cnidopsin groups of each species (Fig. S2) but are apparently not conserved across the cnidarian lineages. In summary, our collective data indicate that a large repertoire of diverse opsins is present in the cubozoan genome, some of which have some intriguing sequence similarities to vertebrate opsins.

Phylogenetic relationships of cubozoan opsins within the opsin gene family. To investigate the relationship between the newly identified Tcops and other known metazoan opsins, we inferred a molecular phylogenetic tree by the maximum likelihood method from a set of 779 opsin protein sequences. Our phylogenetic analysis of this large and diverse set of opsin sequences recovered the four major lineages described in earlier studies[3–5,10], *i.e.* the c-type opsins, the cnidopsins, the r-type opsins, and group 4 opsins. The relationships among the four major lineages in our analyses correlated with those proposed in other recent studies of opsin evolution[4,5,10], however, the statistical support for some of the relationships was weak. Due to such weak branch support, we were unable to exclude the possibility that group 4 and r-type opsins cluster together as sister groups, opposing the c-type opsin and cnidopsin subgroups as has been suggested by Porter *et al.*[3] (based on their phylogeny and the presence of functional unity as bistable pigments of arthropod/cephalopod visual r-type opsins and chicken group 4 neuropsin[28,29]). We found that the relationship between cnidopsins and the c-type opsin subfamily was most strongly supported. All cnidarian opsins except for *Nematostella* group 1 and *Nematostella* group 4 opsins fell within the cnidopsins, group and as was shown by Suga *et al.*[4], the phylogenetic positions of these two groups remained unclear even after more precise Maximum-Likelihood analyses. In the phylogenetic tree of the opsin family, all identified Tcops fell into the cnidopsins subfamily (Fig. 1A, Fig. S3), consistently clustering with the hydrozoan opsins[30]. The cnidopsin group, composed entirely of cnidarian opsins, is the only group lacking representation of broad taxonomic diversity from the major animal phyla. The phylogenic trees presented here (Fig. 1B, Fig. S4) and elsewhere[3,4] are indicative of extensive gene duplications (and diversifications) in each of the cnidarian lineages after their initial split. This latter point is exemplified by the case of Tcops that form two distinct phylogenetic groups: Tc-group 1 and Tc-group 2 (Fig. 1B).

In summary, our phylogenetic analysis unequivocally classifies cubozoan opsins as a sister group to c-type opsins and documents lineage-specific expansion of the opsin gene repertoire in the cubozoan genome.

Functional diversification of opsins in *T. cystophora*: evidence of an apparent dichotomy in G protein-coupled signaling. Sequence analysis and phylogenetic classification provided an important insight into the evolutionary history and possible relationships among opsins. However, these sequence-based approaches do not answer the question whether one or more signaling pathways are being used by *T. cystophora* opsins and do not permit the drawing of conclusions regarding which signaling pathway is coupled to any particular opsin. In order to get a deeper insight into the functional diversification of opsins identified in *T. cystophora* we used a GloSensor™ cAMP HEK293 cell based Gs protein-coupled signaling assay[31] to investigate biochemical properties of all Tripedalia opsins (for description see Material and methods). We used *C. rastonii* opsin (Caryb), shown to activate the Gs-cAMP pathway[27], as a positive control. As heterologous protein expression in cell lines may sometimes prove difficult or even impossible[32], we first checked the expression of the individual opsin genes in GloSensor™ cAMP HEK293 cells by immunofluorescent labeling. The staining revealed that all examined opsins were expressed in GloSensor™ cAMP HEK293 cells and at comparable levels. Moreover the sub-cellular fluorescent signal for opsin was consistently detectable on the cell membranes (Fig. S5 and data not shown), thus confirming successful expression of the Tcop genes. The luciferase activity in GloSensor™ cAMP HEK293 cells, transfected with individual opsin constructs and pre-incubated in the dark with 9-cis retinal, was determined before and after repeated light stimulations (Fig. 2). Light stimulation of cells was in specific cases immediately followed by increased luciferase activity reaching a maximum after several minutes (Tcop5) or 10 minutes (Tcop13, Caryb) and remaining constant for several minutes before decreasing to the basal levels observed prior to illumination (Tcop5) or slightly higher (Caryb; Tcop13). Comparison of the previously characterized Caryb with its ortholog from *T. cystophora*, Tcop13, revealed that both opsins show similar light responses (Fig. 2A). In contrast, medaka (*Oryzias latipes*) opsin RH1, expected to signal via a distinct G protein-coupled pathway (Gi, leading to a cGMP decrease), elicited no increase of luciferase activity in our assay (Fig. 2A), being expressed at comparable levels to those of *T.cystophora* opsins (Fig. S5). Furthermore, no light-dependent stimulation of the Gs protein-coupled assay was detected using the invertebrate r-opsin gene, expected to function via Gq signaling (data not shown). Our assay was, therefore, highly specific for opsins signaling via the Gs-cAMP pathway, but was insensitive to signaling via Gi or Gq. We performed the light response assay several times for the entire set of *T. cystophora* opsins. Of all the opsins examined, only Tcop5 and Tcop13 activated the Gs-cAMP signaling pathway (Fig. 2B–E and data not shown). No convincing light induced opsin-Gs-cAMP response, similar to that of Caryb, Tcop5 and Tcop13, was detected for other Tcops. Tcop5 and Tcop13 sustained enhancement of G protein-coupled pathway signaling after repeated light stimulation. However, we noticed a conspicuous difference in the light response between these two opsins. Tcop5 responded to light faster but with lower intensity (Fig. 2C), whereas the response of Tcop13 was considerably slower, ultimately reaching higher signaling values (Fig. 2D).

To better understand the molecular features of cnidopsins, we focused on the role of the tripeptide in cnidopsin signaling. As stated above, the tripeptide is important for the contact between bovine rhodopsin and its G protein[12]. Accordingly, we replaced the HKQ tripeptide region in Tcop13 with either the tripeptides NKQ, SKS and NRS, originally found in Tcop1 (or bovine rhodopsin), Tcop14 and Tcop18, respectively, none of which activated the Gs signaling cascade in our assay. We expected to observe a loss of Gs cascade activation resulting from the tripeptide mutation. Surprisingly, we found that the tripeptide mutation in Tcop13 did not disrupt Gs activation; rather, it influenced the dynamics of the response to the light stimulation. Specifically, the introduction of the tripeptides NKQ and SKS led to an enhanced and prolonged response, while the introduction of NRS variant caused a massive light response after both single and repeated stimulation (Fig. 2F). Our data show that tripeptide mutation in cnidopsins contributes to subtle tuning of the opsin response to light stimulation, rather than influencing Tcop-G protein coupling *per se*.

In summary, Gs-cAMP signaling characterized only a small set of *T. cystophora* opsins, indicating that the majority of cubozoan opsins likely signal by a distinct and as of yet unidentified signaling pathway. Moreover, the highly sensitive two-dimensional functional assay used here (measuring time response as well as response intensity) uncovered subtle differences among individual opsins, suggesting possible fine tuning for specific photoreceptor tasks.

Phototactic behavior of *T. cystophora* medusa is dependent on Gs signaling. Caryb opsin present in retinas of lensed eyes of *C. rastonii* was previously shown to transfer the light stimulus via the Gs signaling pathway[27]. To investigate whether Tc-group 2 (especially Tcop13), that signal via Gs (see above), serve as important visual pigments in *T. cystophora*, we performed a phototaxis behavioral assay in the absence or presence of the pharmacological compound NF449. NF449 was originally identified as a selective suppressor of the Gs signaling pathway, with limited effect on the prototypical Gi/Go- and Gq-coupled receptors pathways[33]. Positive phototaxis in *T. cystophora* medusa was significantly decreased after treatment with NF449. Although, a variable response was detected in response to white light depending on NF449 concentration and timing of the treatments (Fig. 3 + video), most probably due to reversible inhibition of the Gs signaling pathway by NF449. The number of treated animals exhibiting a phototactic response 5 minutes after the treatment was: $5 \pm 5\%$ in samples treated with 100 μM NF449 and 0% in samples treated with 1 mM. The number of responding medusae treated with 100 μM NF449 after 3 h rose to $95 \pm 5\%$ and the number of medusae treated with 1 mM NF449 rose to 10%.

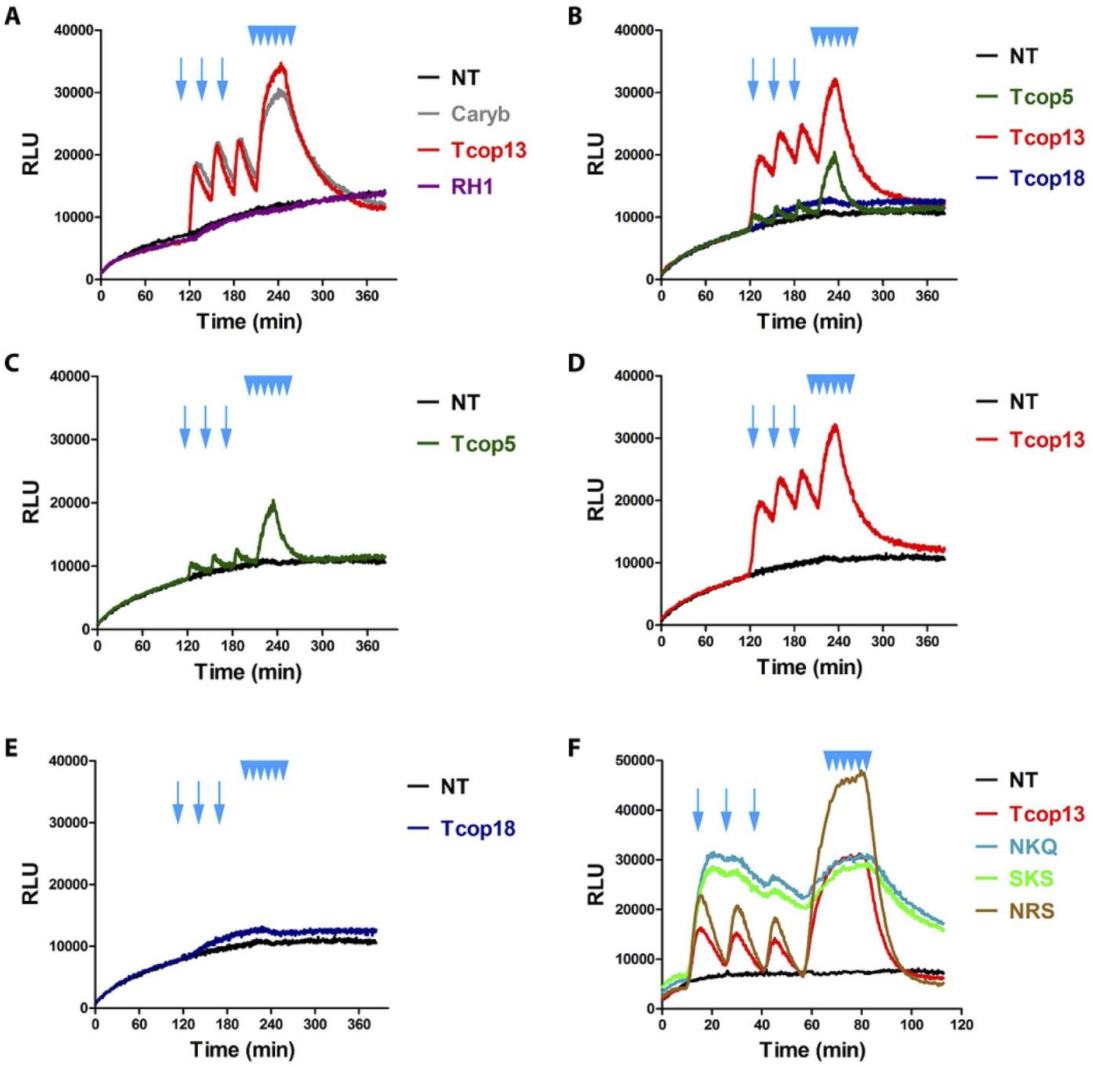

Figure 2. Opsin-Gs-cAMP assay. Light activation of opsin-Gs-cAMP pathway by selected opsins. GloSensor™-20F cAMP HEK293 cells (Promega) were transfected with expression vectors encoding genes for different opsins, treated and stimulated with light, as described in Materials and Methods. Arrows represent simple light pulses, multiple arrowheads represent repeated stimulation. Each graph represents a mean of triplicates for every sample. **A)** Previously reported Gs-cAMP pathway stimulating opsin from *C. rastonii* (Caryb)[27] showed ability to increase the cAMP level in our setup (visualized with cAMP-dependent luciferase activity). The exact homolog of Caryb from *T. cystophora* Tcop13 showed a highly similar response in our assay. Opsin RH1 from medaka, expected to signal via Gt leading to cGMP decrease, showed no change in luciferase activity. **B)–E)** Examples of different Tcop light responses. Tcop5 showed faster and weaker activation of the Gs-cAMP pathway than Tcop13. Tcop18 did not activate the Gs-cAMP pathway. **F)** Analysis of tripeptide activity in Tcop13 was performed. Tcop13 tripeptide HKQ was replaced with tripeptides NKQ, SKS and NRS (originally found in opsins Tcop1 or bovine rhodopsin, Tcop14 and Tcop18 – none of which activated the Gs cascade). Tripeptide mutation did not disrupt Gs activation by Tcop13, but influenced length or sensitivity of Tcop13 response to light stimulation. NT – non-transfected cells used as negative control; Caryb – signal for cells transfected with a vector expressing opsin from *C. rastonii*, used as positive control; RH1 – signal for cells transfected with a vector expressing opsin RH1 from medaka fish *Oryzias latipes*, used as negative control; Tcop5, Tcop13, Tcop18 – signal for cells transfected with vectors expressing opsins from *T. cystophora* - Tcop5, Tcop13 or Tcop18, respectively; NKQ, SKS, NRS – Tcop13 original tripeptide HKQ replaced with tripeptides NKQ, SKS or NRS.

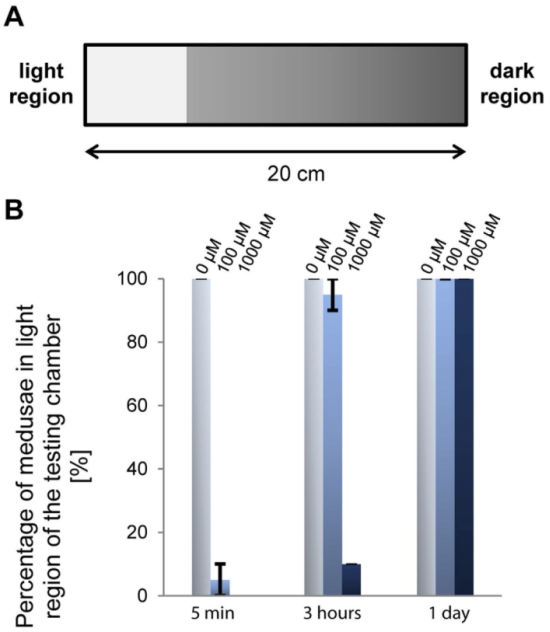

Figure 3. Test of *T. cystophora* medusa phototaxis after NF449 treatment. A) Schematic representation of the testing chamber. **B)** Statistical analysis of the light response of *T. cystophora* after NF449 (Gαs inhibitor) treatments (0 µM, 100 µM, 1 mM). Bars represent the percentage of phototactic medusae in given time point.

However, after 24 hours the decrease in photosensory response was no longer present. We observed 100% phototactic response in untreated animals (0 µM NF449) after 5 min, 3 h, 24 h intervals (Fig. 3B). Thus, the pharmacological inhibition of Tc-group 2 opsins abrogates positive phototactic movement of cubozoan medusa.

Opsin gene expression analysis reveals both redundancy and specialization. The large complement of opsins found in the *T. cystophora* genome raises the possibility of their differential tissue-specific or stage-specific utilization. To investigate the expression patterns of *T. cystophora* opsins, we first analyzed mRNA isolated from different jellyfish life stages and dissected adult tissues by real-time qRT-PCR analysis. The normalized expression levels, relative to Rpl32 levels, of specific opsin genes in each dissected adult body part was calculated relative to that observed in the rhopalium (set at 1.0) and plotted (Fig. 4). Relevant opsin expression data were also represented as a heat map showing z-score of Tcops expression in different *T. cystophora* body parts. (Fig. S6A). All Tcop genes were found to be expressed at the mRNA level in the rhopalium. Moreover, for the majority of opsins (Tcop1, Tcop3–7, Tcop9, Tcop11, Tcop13, Tcop16, Tcop18), the rhopalium was the tissue exhibiting the highest detected expression. Other opsins were most highly expressed in the male gonads (Tcop2, Tcop10, Tcop17), tentacles (Tcop12, Tcop14) or manumbrium (Tcop8, Tcop15). For a better gene-to-gene comparison within the rhopalium, the results were plotted separately (Fig. S7). The expression data in the adult tissues identified common/over-lapping sites of expression most probably reflecting a common gene origin. Nevertheless, a clear tendency for specialization was apparent as very large differences in relative expression levels and/or unique sites of expression were detected.

Next, we investigated opsin gene expression during the life cycle of *T. cystophora*. To this end, mRNAs from non-pigmented larva, pigmented larva (larval eye-containing stage), vegetatively grown polyp, four stages of a metamorphosing polyp (stages 3 and 4 containing a developing rhopalia) and medusae were isolated and subjected to qRT-PCR. The expression levels of all individual opsins for each *T. cystophora* life stage relative to the juvenile medusa expression (set as 1.0) were then calculated (Fig. 5 and Fig. S6B). The results revealed two consistent features. Firstly, opsins whose expression was detected in the adult rhopalium, sharply increased their expression during the polyp metamorphosis, coincident with the emergence of the developing rhopalia structure. Secondly, many Tc-group 1 opsins were highly expressed in the pigmented (eye-containing) larval stage, contrasting with the expression of Tc-group 2 opsins (established as Gs-coupled receptors with a major functional role in the adult lens-containing eye, see above), that were notably absent at this stage.

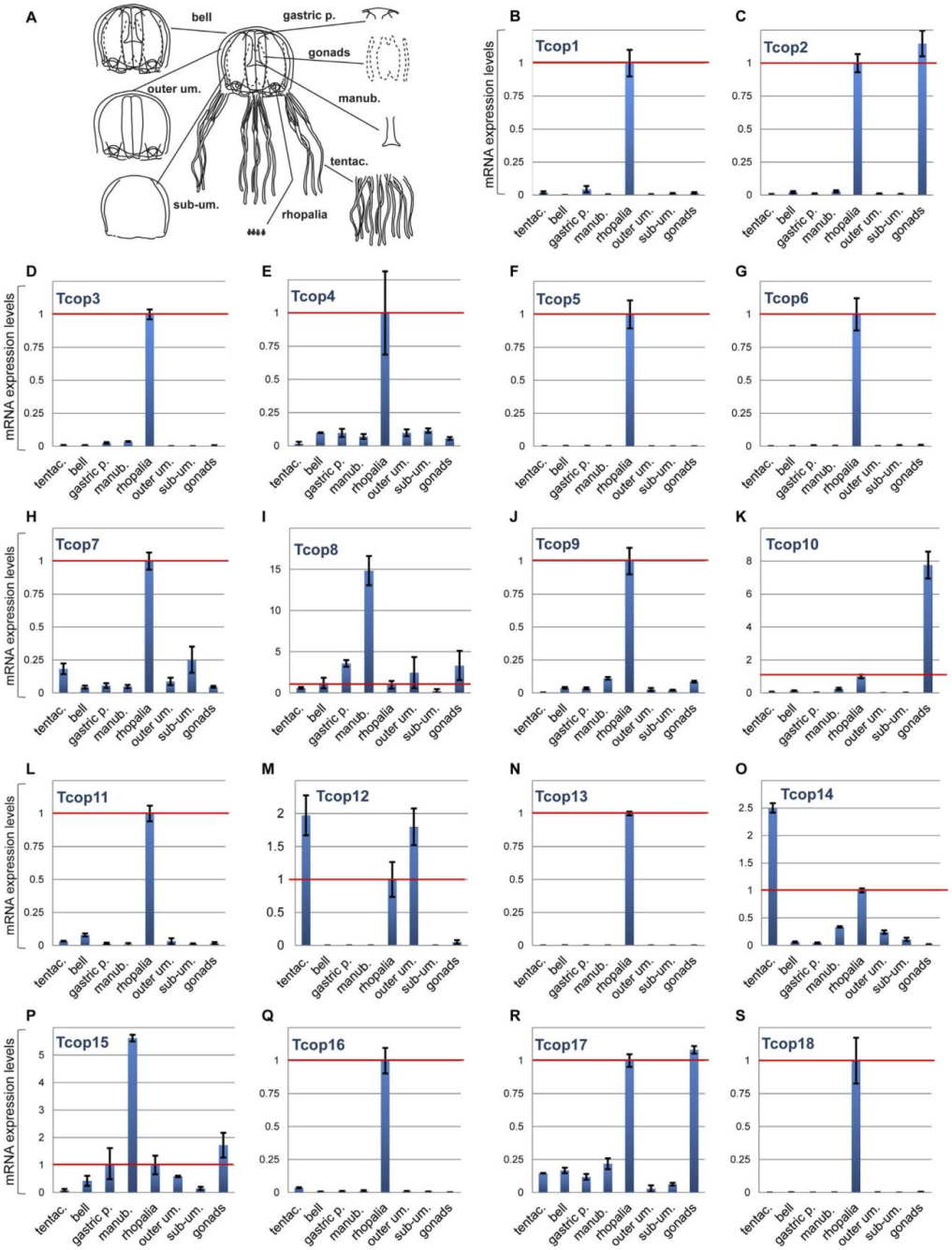

Figure 4. mRNA expression levels of *T. cystophora* opsins in dissected body parts of adult jellyfish. A) For real-time PCR analysis, medusae were dissected into eight body parts: tentacles (tentac.), manubrium (manb.), male gonads, gastric pouch (gastric p.), bell, outer umbrella (outer um.), sub-umbrella (sub-um.) and rhopalia. **B–S)** mRNA expression level of opsins for each dissected body part relative to the rhopalium expression (1.0 – red line). y – axis: relative mRNA expression level, x – axis: analyzed body parts.

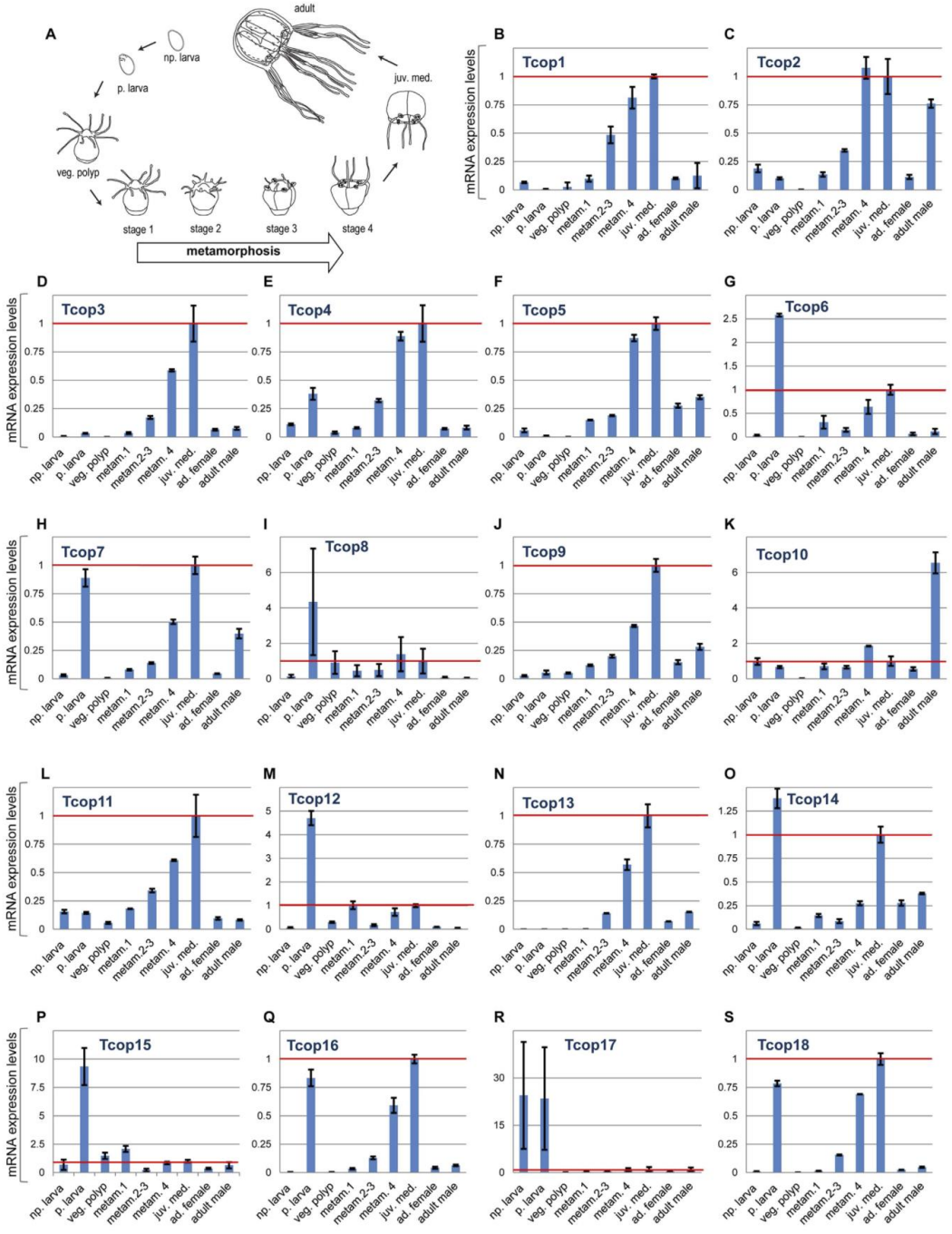

Figure 5. mRNA expression levels of *T. cystophora* opsins in different life stages . **A)** For real-time PCR analysis, animals of nine subsequent life stages were collected: non-pigmented larva (np. larva), pigmented larva (p. larva), vegetative polyp (veg.polyp), three polyp-to-medusa metamorphosing stages (metam1, 2–3, 4), juvenile medusa (juv. med.), adult female (ad. female) and adult male. **B-S)** mRNA expression levels of opsins for each life stage relative to the juvenile medusa expression (1.0 – red line). x – axis: analyzed stages, y – axis: relative mRNA expression level.

To gain further insight into the possibly diverse roles of Tc-group 1 and Tc-group 2 opsins in the various cubozoan eyes (Fig. 6A–C), we also analyzed the expression of key representatives of each opsin type by immunohistochemical staining (IHC) *in situ*. Accordingly, we generated a specific antibody against Tcop13 and performed co-staining with another antibody raised against Tcop18[22] on cryo-sectioned rhopalia. We found that both Tcop13 and Tcop18 were found to be co-expressed in the retinas of *T. cystophora* ULE and LLE in distinct patterns (Fig. 6D–P). We also discovered that *T. cystophora* retinas contain at least two distinct photoreceptor types: ciliary photoreceptor type-A that express Tcop18 not restricted only to the cilia but rather expressed more broadly within the whole cell body (Fig. S8) plus ciliary photoreceptor type-B (expressing Tcop13 in the receptor cell cilia). Both opsins were also distinctly expressed in the developing lens eyes of the newly metamorphosed *T. cystophora* medusae; however, only Tcop18 was detected in the developing eyes of another Carybdeid jellyfish, *Alatina marsupialis* (Fig. S9). Another difference in the apparent utilization of Tc-group 1 and Tc-group 2 opsins was revealed by further analysis of their expression in the two lesser eye types, slit and pit eyes, whose morphology has been thoroughly studied[26]. Only Tcop18 (but not Tcop13) was found to be expressed in the pit and slit ocelli of *T. cystophora*; both types of ocelli thus seem to be formed exclusively from type-A photoreceptors based on the opsin type expression (Fig. S10). However, some molecular features are shared by the PRCs of lesser eye types with those of complex lensed eyes. For example, all PRCs in *T. cystophora* contain two different screening pigments, dark pigment and a white pigment, first described in *Chiropsella bronzie*[24], that becomes conspicuous in polarization microscopy (Fig. S11). It is important to stress that the Tc-group 1 opsin Tcop18 is the only known opsin to be expressed in the lesser eyes thus far. All phylogenetic, biochemical and gene expression data are schematically summarized in Fig. 7.

Discussion

A Scenario for intron-less retrogene-derived cnidarian opsin expansion. The current results highlight distinct features of intron-less genes in vertebrates. It appears that many intron-less genes are evolutionary innovations, so their formation, at least in part, via reverse transcription-mediated mechanisms, could be an important route of evolution of tissue-specific functions in animals[34,35].

The lack of introns is typical for most members of the giant GPCR gene family and it has been proposed that many G-protein-coupled receptors are derived and amplified from a single intron-less common progenitor that was encoded by a retrogene (a DNA gene copied into genome by reverse transcription of an RNA transcript)[36,37]. Interestingly the vertebrate rhodopsin GPCRs, that are widespread phylogenetically and abundantly expressed, contain four introns in highly conserved positions[38]. However, most of the cnidarian opsins thus far annotated are intron-less genes, although at least one opsin in anthozoan *Acropora digitifera*, CNOP2, has been characterized with two introns[39]. Astonishingly, the first of these intron matches, in position and phase, with the first intron of bovine rhodopsin (Fig. S12). Such examples of the first introns to be located in cnidarian opsins are moderately short and have conventional GT-AG donor and acceptor splice sites and thus it appears that this intron was already present in an opsin gene present in the last common ancestor of eumetazoa. Accordingly, intron-less opsin genes appear to be a Cnidarian feature, with the original variant of the gene most probably being lost in medusozoans. Similarly, intron-less opsin genes were previously identified in two cephalopod species[40] and in genome of teleost fish[41], in both cases probably derived from introns containing opsin genes by retrotransposition. Based on these facts and our data, we propose the scenario (Fig. S13) that cnidarian intron-less opsins are retrogenes derived from an ancient eumetazoan ciliary-like opsin with introns. This hypothesis is supported by the phylogenetic relationship of c-like opsins and cnidopsins (Fig. 1A) and by the fact that both variants of the opsin gene (with or without introns) are still present in basal anthozoa (Fig. S12). Once an intron-less opsin gene was present in cnidarian genome, subsequent rapid lineage- and species-specific duplications resulted in a variety of opsins. This process provided the substrate for the evolution of cnidarian photoreception, be it either extraocularly or in sophisticated cubozoan eyes.

Gene duplications and their subsequent divergence play an important part in the evolution of novel gene functions[42]. Our data show that in *T. cystophora* genome, each of the opsins has been duplicated at least once, and several have undergone multiple rounds of duplication (Fig. S4). Theory suggests that duplicated genes can be lost rapidly[43], but the spectrally diverse aquatic environment (such as the margins of mangrove lagoons naturally inhabited by *T. cystophora*) could provide strong selective pressures on the opsin genes, and thus, photoreception evolution. Photoreception tuning through opsin sequence evolution might therefore be a result of sensory adaptation to this rich environment of spectral light.

In both medaka and zebrafish the opsin gene diversity in the genome is high, similarly as in the genome of *T. cystophora*. Subtype opsin genes in medaka and zebrafish are closely linked and are clearly products of local gene duplications[44]. Tandem duplication appears to be the most common mode of opsin gene family expansion in fishes[45]. Gene duplication followed by amino acid substitutions at key tuning sites played an important role in generating a diverse set of fish opsin genes. It is probable that similar mechanisms of opsin gene repertoire expansion occurred in the case of cnidaria (evolutionary convergence), where the opsin genes, being relatively short and intron-less, were even more rapidly duplicated and subsequently functionally diversified (see Fig. 8 for schematical representation).

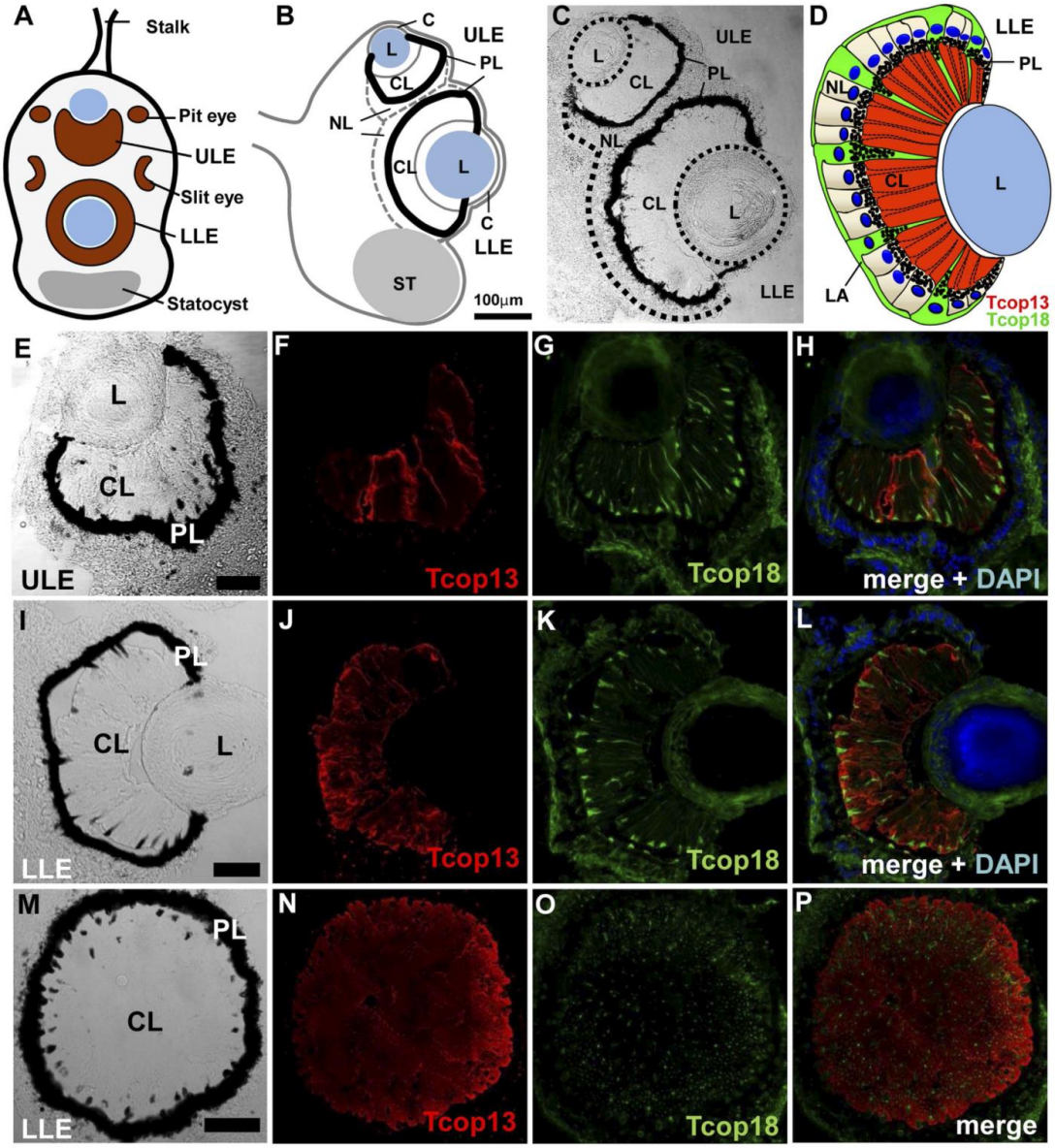

Figure 6. Visual organs of *T. cystophora* and immunohistochemical localization of Tcop13 and Tcop18. **A)** Schematic diagram of the rhopalium. The large (LLE) and small (ULE) complex eyes lie along the medial line, while the pit and slit ocelli are paired laterally. **B)** Schematic diagram of rhopalium sagittal plane (adapted from O´Connor 2009). **C)** Sagittal section through the rhopalium. Upper (ULE) and lower (LLE) lens eyes contain the typical components of camera-type eyes: a cornea (C), a lens (L), and a retina consisting of a ciliary layer (CL), a pigment layer (PL) and a neural layer (NL). St – statocyst, S – stalk. **D)** Schematic representation of the lens eye retina. The ciliary layer (CL) is dominated by the ciliary segments of type-B receptor cells (red). Scattered among the type-B receptor cells are the cone-shaped projections of type-A photoreceptor cells (green). In the neural layer (NL), both receptors types have their cell bodies with nuclei (dark blue); only type-A receptor cell bodies are positive for opsin signal. Projections of type-A photoreceptor cell bodies create a compact layer (LA) surrounding the whole retina. **E–H)** Confocal images of immuno-histochemical staining for Tcop13 (red), Tcop18 (green), DAPI (blue) in the upper lens eye (ULE). **I-L)** Large camera-type eye (LLE) retina longitudinal section. **M–P)** Large camera-type eye retina transverse section. (Scale bars: 50 µm).

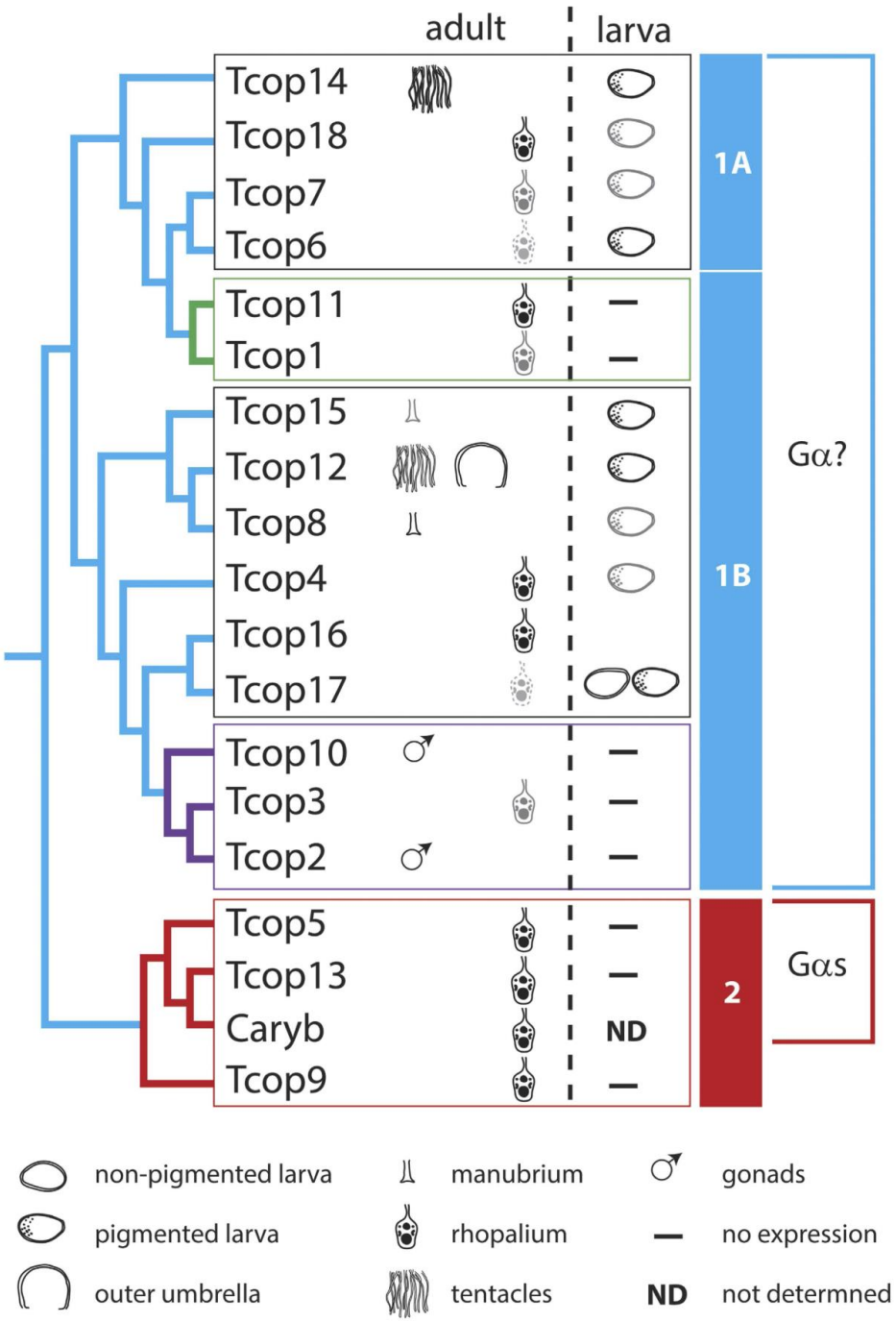

Figure 7. Schematic representation of opsin expression patterns according to their phylogenetic relationship. *T. cystophora* opsins can be classified into two groups, a probable more ancient Tc-group 1 opsin, with a broader expression pattern, and Tc-group 2 – rhopalium-specific opsins. The size and shade intensity of the symbols corresponds with the level of expression. Green coloured box and branches represent rhopalia specific Tc group 1A opsins. Purple coloured box and branches represent male specific Tc group 1B opsins. Red coloured box and branches represent rhopalia specific Tc-group 2 opsins.

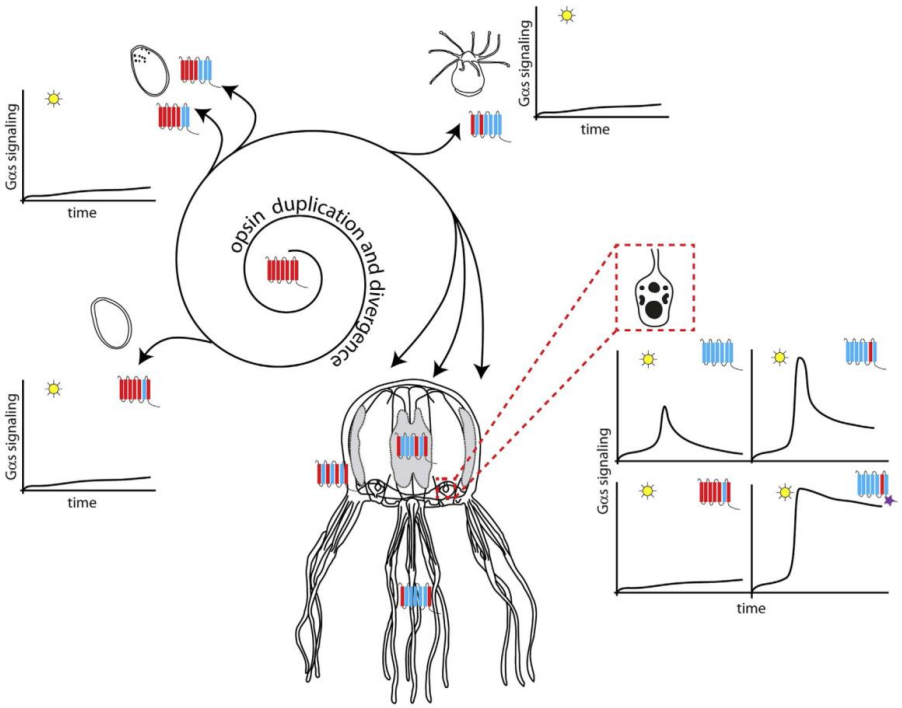

Figure 8. Possible scenario for expansion and functional diversification of opsins in *T. cystophora*. Our data and data from other studies[39,60] show that Cnidarian intron-less opsins might have been derived from an ancient eumetazoan ciliary-like opsin containing introns by retro-transposition. Once anchored in the genome the ancient cnidopsin gene underwent several rounds of duplication, diversification and sensitivity tuning. Individual opsins were thus accommodated for distinct functions in diverse tissue photoreceptors - ocular, extraocular and larval. These opsins differ in stage- or tissue-expression, primary structure and also in subsequent cellular signaling – either via Gs-cAMP pathway or other G-protein pathways. For further information see Discussion.

Rhopalia-specific opsin expression in *T. cystophora*. Cubozoa have relatively simple nervous systems consisting of a nerve net and a ring nerve. The latter has extensions forming ganglia and connections with the radial nerves and rhopalia. Morphological and electrophysiological studies have shown that a significant part of the CNS of cubomedusae is situated within the rhopalia[25,46,47]. In addition to numerous ciliated photoreceptors within the retinas of all six eyes, each rhopalium houses over 1,000 neurons of which approximately 500 are retina-associated. Each rhopalium also contains a group of pacemaker neurons that regulate swimming movements through the direct control of neuronal activity in the motor nerve net, and thus individual rhopalium facilitates various behaviors such as obstacle avoidance or light-shaft attraction enabling them to remain in close proximity to prey gathered in beams of light passing through open parts of the mangrove canopy. This behavioral regulation is most probably influenced by the visual input received by each rhopalium[48].

Based on our mRNA (Fig. 4) and protein (Fig. 6) expression profiles, many of the opsin genes identified here are expressed in rhopalia. Since it is not easy to determine the physiological relevance of a given gene just based on the level of its mRNA expression, we appreciated the finding that Tcop18, with 100 times lower level of mRNA transcripts compared to Tcop13 (Fig. S7), is significantly expressed on protein level (Fig. 6). Based on this fact, we suggest that all Tc-group 2 opsins, plus at least one opsin from each subclass of Tc-group 1 is rhopalium-specific. Moreover, the real-time PCR analysis has revealed that all of the rhopalium-expressed opsins are dramatically up-regulated when the rhopalia are formed during the polyp-to-medusa metamorphosis (Fig. 5). We thus propose that the *Tripedalia* rhopalium is a complex organ integrating and processing multiple light cues, gained though a diverse set of opsins, and transforming these signals into various behavioral responses.

Retina-specific opsin expression in *T. cystophora*. In addition to the extensive real-time PCR expression analysis, we paid special attention to the IHC analysis of retina specific opsins expression in *Tripedlia* rhopalia. The cubozoan lens-containing eyes have a thin cornea (made of monociliated

epithelial cells), a spherical cellular lens, a thin vitreous space, and a hemisphere-shaped everse retina with pigmented photoreceptors of the ciliary type, as judged from their ultra-structural morphology[24,49,50].

A previous study identified three types of photoreceptors in the lensed eyes of *T. cystophora* on the basis of differences in the morphology of their sensory cilium and microvillar organization[50]. In contrast, other studies[51–53] supported the interpretation that there was only a single basic morphological type of photoreceptor in cubozoan lensed eyes. Our IHC data support the first interpretation, showing that there are at least two types of PRC (each with markedly different opsin expression profiles) in the lensed eyes of *T. cystophora*. Both cell types have three distinct segments, giving rise to three retinal layers: 1. a thick layer of receptor-cell cilia formed from type-B PRCs (expressing Tcop13) and cone-shaped projections from type-A PRCs (expressing Tcop18), creating the ciliary layer; 2. a thin pigment layer where both receptor cells types are densely pigmented; 3. a neural layer containing nucleated cell bodies of both types of receptor cells.

The ciliary layer is dominated by the ciliary segments of type-B receptor cells. The cilia extend from the pigment layer to the vitreous space. From the ciliary membrane, microvilli extend, partly as bundles of parallel microvilli and partly as a disorganized tangle (as shown in another cubozoan jellyfish *Ch. bronzie*[24]). The microvilli make up the majority of the volume of the ciliary layer. Scattered among the type-B receptor cells are the cone-shaped projections of type-A photoreceptor cells partially filled with screening pigment granules. These cones run parallel to the ciliary trunks of the type-B sensory cells. In the neural layer, the type-A receptor cells have their cell bodies with nuclei, and they are also positive for Tcop18 protein expression (Fig. 6E–P). Projections of type-A photoreceptor cell bodies create a compact layer surrounding the whole retina.

It has been previously suggested that the lens eye photoreceptors utilize a different photopigment from those of the pit eyes and slit eyes[52]. According to dominant mRNA and protein levels and strict retinal specificity, we consider Tcop13 the main visual opsin of *T. cystophora* complex lens eyes. On the other hand, Tcop18 (also expressed in lens eyes) appears to be the main visual opsin in the lesser eyes. Our IHC data show, that retinas of both eye types (lens and lesser eyes) express different opsin combinations (various combinations of Tcop13 and Tcop18) according to their task (another level of visual tuning). The expression of rhopalium-specific opsins surely does not only involve photoreceptors of the retina, as some of the retina-associated neurons will most probably prove to be photosensitive as well, given our qRT-PCR analysis. This possibility should be resolved in the future by detailed IHC analysis assaying other Tcops expression.

Tissue-specific and larval opsins. Eyes are not the only means of photoreception in the Cnidarians, as many species lack distinct ocular structures yet exhibit specific photic behaviors. In these animals, photosensitivity is mediated through extraocular PRCs. Extraocular photosensitivity, is widespread throughout the animal kingdom, in both invertebrates and vertebrates[54,55]. The extraocular photosensitive cells are not organized into a complex organ such as ocelli or lens eyes. Instead, these cells are solitary or grouped and are scattered or localized throughout the animal body. Identification of the cells involved in extraocular photodetection has often proved difficult, but in some animals, neurons, epithelial cells, and muscle cells have been shown to be photosensitive[54,56–58]. Intriguingly, an ancient opsin-mediated phototransduction pathway and a previously unknown layer of sensory complexity in the control of cnidocyte discharge in cnidarian *Hydra magnipapillata* was reported very recently[59]. These various extraocular photoreceptors function as light detectors, informing the animal of the presence of light, measuring light intensity, and activating rhythmic behaviors as well as other physiological processes.

Our extensive qRT-PCR analysis (Figs 4, 5, S6, S7) (with support from the phylogenetic data) of different developmental stages and tissues revealed that the *T. cystophora* opsins can be classified into two groups, the probably more ancient Tc-group 1 opsins and Tc-group 2 rhopalium-specific opsins (Fig. 7). Tc-group 1 opsins tend to have broader expression. The broadest tissue- and stage-specific expression distribution is visible in Tc-group 1B, with Tcop2 and Tcop10 being male gonad-specific and other Tcops expressed in tissues such as bell, tentacles or manubrium. Both sub-groups 1A and 1B show a trend for increasing tissue/organ specificity of opsins after subsequent duplications.

More than a half of the opsins from those two subgroups were detected (at least in small amounts) in planula larvae, with Tcop17 (and probably Tcop6) being larva-specific. Such a variety of larval opsins is astonishing considering that to date only three larval opsins have been reported from reef corals[60]. Planula larvae have an extremely simple organization with no nervous system at all. Their only advanced feature is the presence of 10–15 pigment-cup ocelli, evenly spaced across the posterior half of the larval ectoderm. The ocelli are single-cell structures containing a cup of screening pigment filled with presumably photosensory microvilli. These morphologically rhabdomeric-like photoreceptors have no neural connections to any other cells, but each has a well-developed motor-cilium, appearing to be the only means by which light can control the behavior of the larva[61].

Our analysis implies that Cnidarians extensively utilize opsins not only for visual but also for extraocular photosensitivity. Revisiting the possible diversity of Tcops tissue/stage specific expression by IHC protein expression analysis and physiological studies could shed more light on their use for various behavioral tasks.

Phototransduction by cubozoan opsins. To investigate the coupling partner of *T. cystophora* opsins we performed an opsin-Gs-cAMP coupling assay. Our data revealed that the Gs-cAMP pathway[27] is used by opsin genes from Tc-group 2. Moreover our behavioral test showed for the first time that the opsin-Gs-cAMP cascade is functionally connected with vision guided behaviour. However, we were unable to obtain any light-mediated activation of signal transduction via this pathway for Tc-group 1 opsins. We propose that opsins that did not signal in our assay either use different G-protein pathways, as recently proposed in reef corals[60], act as photoisomerases or for unknown reason do not signal in our cell-line based assay, but nonetheless use Gs signaling cascade under natural conditions. The later possibility is, however, in our opinion very unlikely, because we saw comparable expression of all Tcops on the cell membranes of our test cell system and moreover not even a repeated flash stimulation lead to any response. However, we do acknowledge the possibility, that some of examined Tcops did not fold properly in mammalian cells used in the assay and thus were unable to signal. In some cases we did record slight increases in luciferase signal (like the one in Fig. 2E for Tcop18), however this phenomenon also appeared in some wells containing cells transfected with control opsins (not signaling though Gs-cAMP cascade) or non-transfected cells. This slight increase in luciferase activity was probably connected with non-opsin-specific changes in cellular metabolism during experiment (note that increase in luciferase activity in Fig. 2E starts 140 minutes from the beginning of the experiment and does not seem to be connected with light stimulation). Clearly the future identification of the actual Gα subunit coupled to Tc-group 1 opsins is going to be necessary to understanding if *T. cystophora* possess at least two independent photosystems, thus providing another level for the functional divergence of the identified opsins. Another interesting feature of our assay is the time-course of response of Tcop5, Tcop13 and Caryb transfected cells to light stimulus, reaching the peak in the order of minutes. This phenomenon is probably not caused by the slow light response of the opsins themselves, but rather indicative of the slow kinetics of the recombinant cAMP-sensitive luciferase expression in GloSensor™ cAMP HEK293 cells. In a study by Koyanagi *et al.*[62], the use of a similar assay led to peak of response in order of minutes even in the case of bovine rhodopsin, which is known to respond to light stimuli in other direct assay systems within millisecond time periods[63].

Future structure-function studies of prototypical cubozoan group 2 opsin is highly warranted. It would be interesting to find out whether any of the proposed E/D counterions are indeed used by *T. cystophora* opsins. Likewise, the significance of various tripeptide variants found among *T. cystophora* opsins awaits further experimental interrogation. Our data so far point to variable sensitivity and bleaching properties of individual opsins depending on their primary amino acid sequence. Based on their expression and conserved amino acid sequence at key positions, we assume that all Tcops described here are functional opsins, but as mentioned earlier, this remains to be confirmed by other analysis (IHC expression, identification of Tc-group 1 signalling cascade).

In summary, our data suggest that the expansion and diversification of the opsin gene family in cubozoans has allowed fine tuning and optimal photopigment function.

In summary, a detailed expression analysis uncovered both redundancy and specialization in the utilization of the opsin gene repertoire. On the one hand, multiple opsins with presumably similar molecular characteristics are apparently utilized in the same stage/tissue. On the other hand, a clear tendency to establish unique expression patterns exists both within the opsin subfamilies (Tc-group 1 and Tc-group 2) and between the two subfamilies. Remarkably, retina photoreceptors of lens-containing eyes express opsins most probably utilizing at least two distinct signaling pathways.

Materials and Methods

Jellyfish collection and culture. Adult *T. cystophora* were collected from the mangroves of La Parguerra, Puerto Rico. Laboratory cultures were established using settling larvae and artificial seawater. Settled larvae metamorphosed into young polyps. Young polyps were transformed into budding (asexually reproducing) polyps by feeding with Artemia once a week. Polyps were stimulated into metamorphosis (transformation into free swimming medusa) by incubation at 28°C. Polyps and young medusa were both maintained at 26 °C. All stages were collected for (opsin) expression pattern analysis (RT-PCR) and juvenile medusa also for rhopalium IHC.

Isolation of *Tripedalia cystophora* opsin genes. *Tripedalia cystophora* genomic DNA shotgun sequencing was performed on the GS FLX Titanium platform (454 Life Sciences, Roche). Pyrosequencing resulted in 1,952,068 reads (about 7×10^8 bases) with average read length of 360 bp. Assembly generated 134,683 of all contigs containing 790,111 (40.5%) reads. Assembly was done by program Newbler, version 2.3 (Roche). Resulting contigs were combined with singleton reads to produce a complete contig database. The database was subjected to similarity search by the FASTA[64] program using a wide range of homologous opsin proteins from other cnidarian and bilaterian species. FASTA search provided hits corresponding to short stretches of assumed Tripedalia opsin protein sequences. Full opsin genes sequences were obtained by using the Genome Walking strategy (Genome Walker, Clontech). Opsin sequences were deposited in GeneBank (accession numbers: JQ968416 -JQ968432).
(Primers in Supplement -T1)

Molecular phylogeny. To investigate the relationship between the cnidarian opsins and bilaterian opsins, we inferred a molecular phylogenetic tree by the maximum likelihood (ML) method implemented in PhyML 3.0[65] with LG substitution model[66]. Support for internal nodes was assessed using Approximate Likelihood-Ratio Test for Branches[67].

Dataset. Opsin protein sequences were acquired as described by Porter *et al.*[3]; however, incomplete sequences were discarded from the analysis and other 26 *Nematostella vectensis* annotated opsins were added to the dataset. In order to root the phylogenetic tree, 22 non-opsin GPCRs from the human genome were used as outgroups. The resulting dataset of 801 (779 opsin plus 22 non-opsin) transcripts plus genome trace opsin sequences was aligned using ClustalX[68] under default parameters and trimmed by eye in BioEdit. For phylogenetic analyses, only the 7-transmembrane region including intervening inter- and extra-cellular domains was included, as it was difficult to ascertain homology of N- and C- termini due to sequence length variation and lack of conservation across genes. The molecular phylogenetic tree of the opsin family was inferred from an alignment of 226 amino acids long (after N- and C-termini exclusion) opsin sequences. (Sequences in Supplement -T2)

Quantitative RT-PCR. RNA from indicated stages or dissected adult *T. cystophora* tissues was isolated using TRIZOL reagent (Invitrogen). Contaminating genomic DNA was removed by DNAse digestion and RNA repurification on RNeasy Micro columns (Qiagen) according to the manufacturer's protocol. The same amounts of RNA from each sample were used for reverse transcription using VILO cDNA kit (Invitrogen). Primers for qPCR were designed using Primer 3 software (see Supplementary Table 1 for sequences of primers). The qPCR was performed in LightCycler 2.0 System using LightCycler® 480 DNA SYBR Green I Master kit (Roche Diagnostics, Germany) according to the standard manufacturer's protocol. Target genes (Tcop1-Tcop18) and the housekeeping gene (Rpl32) were measured under the same conditions from the same cDNA. Results were analyzed by LightCycler software and crossing point values (Cp) were further determined as an average of Cp values from all replicates and normalized by Cp values of the housekeeping gene (so called deltaCp values). The results show relative normalized gene expression. Statistical significance of changes in the mRNA level of target genes between different samples were calculated by a Student´s t-test. For other data reproduction, heat map from z-scores (Standard scores) of deltaCp values for target genes (Tcop1-Tcop18) expression in different *T. cystophora* tissues was constructed. Z-score representation was obtained in R statistical environment with Bioconductor package.

Generation and verification of antibodies. An antibody directed against Tcop13 c-opsin was prepared by immunization of mice as follows. The C-terminal region of *c-opsin* corresponding to amino acids 281-330 (*NPIIYCFLHKQFRRAVLRGVCGRIVGGNAIAPSSTGVEPGQTLGGGAAES*; primers in Supplement -T1) was cloned into the expression vector pET42, expressed in BL21(DE3)RIPL cells (Stratagene), and purified by *Ni*-NTA Agarose Beads (QIAGEN). Purified protein was used as antigen for mouse immunization. Human kidney HEK293 cells were transfected with EGFP_C1-c-opsin (amino acids 281–330) expression vector by using FuGENE®6 reagent (Roche). Total extracts were prepared from c-opsin-transfected cells and mock-transfected cells and were analyzed by Western blotting by using anti-c-opsin mouse serum and chemiluminescent detection kit (Pierce).

Tissue collection and histology. Jellyfish were fixed in 4% paraformaldehyde (PFA), cryoprotected in 30% sucrose overnight at 4°C, and embedded and frozen in OCT (Tissue Freezing Medium, Jung). Horizontal frozen sections were prepared with a 8–12 μm thickness. The cryosections were washed three times in PBS and subsequently immuno-stained with an antibody.

Immunohistochemistry. The cryosections were refixed in 4% PFA for 10 min, washed three times with PBS, permeabilized with PBT (PBS + 0.1% Tween 20) for 15 min, and blocked in 10% BSA in PBT for 30 min. The primary antibodies were diluted in 1% BSA in PBT (1:500), incubated overnight at 4 °C, washed three times with PBS, and incubated with secondary antibodies in 1% BSA in PBT (1:500). The sections were counterstained with DAPI and mounted. Primary antibodies used were: anti-Tcop18[22], anti-Tcop13, and anti-acetylated tubulin (Sigma). The following secondary antibodies were used: Alexa Fluor 488- or 594-conjugated goat anti-mouse or anti-rabbit IgG (Molecular Probes).

Construction of opsin-expressing vectors. The expression vector pcDNA3.1 + 1D4 for opsin gene production in mammalian cells was prepared as follows. The sequence for BamHI restriction site followed by the sequence of 1D4 epitope tag from bovine rhodopsin was introduced into multiple cloning site of pcDNA 3.1+ vector (Clontech) through KpnI and EcoRI sites. Opsin cDNA of box jellyfish *C. rastonii* (GeneBank AB435549), kindly provided Dr. Koyanagi, was amplified from the vector by PCR and cloned into pcDNA3.1 + 1D4 vector using BamHI and HindIII cloning sites. The opsins of box jellyfish *T. cystophora*, which are all intron-less, were amplified by PCR from genomic DNA and cloned

into pcDNA 3.1 + 1D4 vector either via BamHI and HindIII or BamHI and KpnI cloning sites. All the constructs were verified by standard sequencing techniques before use.

Immunofluorescent staining of GloSensor™ cAMP HEK293 cells. GloSensor™ cAMP HEK293 cells (Promega) ($2.5*10^3$) were seeded onto coverslips and transfected with FuGene HD (ROCHE). The next day, cells were washed with PBS and fixed with 4% paraformaldehyde (PFA) for 10 minutes. Fixed cells were permeabilized with 0.1% Triton X-100 for 10 minutes and blocked with 10% BSA in 1x PBS with 0.1% Tween 20 for 1 hour. A mouse monoclonal antibody raised against 1D4 epitope (Millipore Chemicon MAB5356), at a concentration of 1:250, was used in conjunction with a secondary antibody conjugated with Alexa Fluor 488 to immuno-stain expressed opsins. Cells were mounted in Mowiol®. Fluorescent images were captured using a Leica SP5 confocal microscope.

Light response assays. GloSensor™ cAMP HEK293 cells (Promega) ($10*10^3$) were plated into a solid white 96-well plate in L15 CO_2-independent medium with phenol red (Gibco) and 10% serum and incubated overnight at 37 °C, 0.3% CO_2. The cells were transfected the next day with plasmids expressing opsin genes using FuGENE® HD Transfection Reagent (ROCHE). Immuno-fluorescent staining revealed a transfection efficiency of 50% using this method. All procedures following transfection of the cells with the various opsin receptors were carried out in dim red light. Six hours post transfection 9-cis retinal (Sigma-Aldrich) was added to a final concentration of 10 mM. The cells were then kept overnight in an incubator (37 °C; 0.3% CO_2). Next day the cells were removed from the incubator and left to equilibrate for 30 minutes at room temperature. Beetle luciferin potassium salt (Synchem) reconstituted in 10 mM HEPES buffer was added to the cells to a final concentration of 3 mM. The cells were then placed in a top-read Envision plate reader with ultra-sensitive luminescence model. Luciferase activity was measured for 2 hours with 0.1 second resolution and cycles of every 1 minute to determine the luciferin uptake. Cells were then subjected to three pulses of light stimulation using repeated flashes from a Nikon speedlight SB-600 electronic camera flash (5 flashes, 1 flash/ second in each pulse, ~40000 lumen/m2 per flash) followed by recovery periods of 30 minutes when Raw Luminescence Units (RLU) were recorded. After the third measurement, the cells were stimulated with seven light pulses with periods of 3 minutes (5 flashes, 1 flash/ second in each pulse). Luminescence was recorded between pulses (0.1 second resolution, 15 seconds per cycle) and another 120 minutes after the last pulse (0.1 seconds resolution, 30 seconds per cycle). The experiment for the tripeptide mutation was performed in a similar way with minor changes. The entire experiment was performed at 37 °C, which led to faster response of cells to the light stimulation. Three pulses (5 flashes, 1 flash/ second in each pulse) followed by recovery of 15 minutes were applied. The following repeated stimulation was done with 30 light pulses (1 flash) with periods of 30 seconds. Luminescence was measured another 30 minutes after the last pulse. Luminescence recordings were analyzed with Microsoft Office Excel. All experiments comprised cells plated and treated in triplicate. Prism (Graphpad) software was used for all statistical analyses.

***T. cystophora* phototaxis test.** All behavioral tests were performed at room temperature (22 °C). Phototaxis experiments were performed in an aquarium-like testing chamber (20 × 5 × 5 cm) with one illuminated side (Fig. 7a). To test the effect of suramin analog 4,4‘,4“,4“‘-(carbonylbis(imino-5,1,3-benzenetriylbis (carbonylimino)))tetrakis-benzene-1,3-disulfonic acid (NF449 - Calbiochem) on the *T. cystophora* phototactic behavior, we incubated 3-day-old medusae in 1 ml of artificial seawater with NF449 at a final concentration of either 0 μM, 100 μM, and 1 mM for 30 minutes under artificial day light. Medusae were then washed with artificial seawater, placed into the dark part of the testing chamber and tested for phototactic behavior. The number of medusae that reached the light region after 5 minutes, 3 hours and 24 hours was counted and compared to the number of animals from the untreated control group.

References

1. Terakita, A. The opsins. *Genome Biol* **6,** 213, doi: 10.1186/gb-2005-6-3-213 (2005).
2. Sakmar, T. P., Menon, S. T., Marin, E. P. & Awad, E. S. Rhodopsin: insights from recent structural studies. *Annual Review of Biophysics and Biomolecular Structure* **31,** 443-484, doi: 10.1146/annurev.biophys.31.082901.134348 (2002).
3. Porter, M. L. *et al.* Shedding new light on opsin evolution. *Proc Biol Sci* **279,** 3–14, doi: 10.1098/rspb.2011.1819 (2012).
4. Suga, H., Schmid, V. & Gehring, W. J. Evolution and functional diversity of jellyfish opsins. *Current Biology* **18,** 51–55, doi: 10.1016/j.cub.2007.11.059 (2008).
5. Plachetzki, D. C., Degnan, B. M. & Oakley, T. H. The origins of novel protein interactions during animal opsin evolution. *PLoS One* **2,** e1054, doi: 10.1371/journal.pone.0001054 (2007).
6. Feuda, R., Hamilton, S. C., McInerney, J. O. & Pisani, D. Metazoan opsin evolution reveals a simple route to animal vision. *Proceedings of the National Academy of Sciences of the United States of America* **109,** 18868–18872, doi: 10.1073/pnas.1204609109 (2012).
7. Kojima, D. *et al.* A novel Go-mediated phototransduction cascade in scallop visual cells. *Journal of Biological Chemistry* **272,** 22979–22982 (1997).
8. Koyanagi, M., Terakita, A., Kubokawa, K. & Shichida, Y. Amphioxus homologs of Go-coupled rhodopsin and peropsin having 11-cis- and all-trans-retinals as their chromophores. *FEBS Letters* **531,** 525–528 (2002).
9. Hara, T. & Hara, R. Rhodopsin and retinochrome in the squid retina. *Nature* **214,** 573–575 (1967).
10. Plachetzki, D. C., Fong, C. R. & Oakley, T. H. The evolution of phototransduction from an ancestral cyclic nucleotide gated pathway. *Proc Biol Sci* **277,** 1963–1969, doi: 10.1098/rspb.2009.1797 (2010).
11. Feuda, R., R.-S. O., Oakley, T. H. & Pisani, D. The comb jelly opsins and the origins of animal phototransduction. *Genome Biology and Evolution* **6,** 1964-*1971*, doi: 10.1093/gbe/evu154 (2014).

12. Marin, E. P. *et al.* The amino terminus of the fourth cytoplasmic loop of rhodopsin modulates rhodopsin-transducin interaction. *Journal of Biological Chemistry* **275,** 1930–1936 (2000).
13. Martin, V. J. Photoreceptors of cnidarians. *Can. J. Zool.* **80,** 1703–1722, doi: 10.1139/Z02-136 (2002).
14. Nilsson, D. E., Gislen, L., Coates, M. M., Skogh, C. & Garm, A. Advanced optics in a jellyfish eye. *Nature* **435,** 201–205, doi: 10.1038/nature03484 (2005).
15. Coates, M. M. Visual ecology and functional morphology of cubozoa (cnidaria). *Integr Comp Biol* **43,** 542–548, doi: 10.1093/icb/43.4.542 (2003).
16. O'Connor, M., Nilsson, D. E. & Garm, A. Temporal properties of the lens eyes of the box jellyfish Tripedalia cystophora. *J Comp Physiol A Neuroethol Sens Neural Behav Physiol* **196,** 213–220, doi: 10.1007/s00359-010-0506-8 (2010).
17. Garm, A., Oskarsson, M. & Nilsson, D. E. Box jellyfish use terrestrial visual cues for navigation. *Current Biology* **21,** 798–803, doi: 10.1016/j.cub.2011.03.054 (2011).
18. Petie, R., Garm, A. & Nilsson, D. E. Visual control of steering in the box jellyfish Tripedalia cystophora. *Journal of Experimental Biology* **214,** 2809–2815, doi: 10.1242/jeb.057190 (2011).
19. Land, M. F. & Nilsson, D. E. Animal eyes. *Oxford, Oxford University Press* (2002).
20. Kozmik, Z. *et al.* Role of Pax genes in eye evolution: a cnidarian PaxB gene uniting Pax2 and Pax6 functions. *Dev Cell* **5,** 773–785 (2003).
21. Piatigorsky, J. & Kozmik, Z. Cubozoan jellyfish: an Evo/Devo model for eyes and other sensory systems. *International Journal of Developmental Biology* **48,** 719-729, doi: 10.1387/ijdb.041851jp (2004).
22. Kozmik, Z. *et al.* Assembly of the cnidarian camera-type eye from vertebrate-like components. *Proceedings of the National Academy of Sciences of the United States of America* **105,** 8989–8993, doi: 10.1073/pnas.0800388105 (2008).
23. Kozmik, Z. *et al.* Cubozoan crystallins: evidence for convergent evolution of pax regulatory sequences. *Evol Dev* **10,** 52–61, doi: 10.1111/j.1525-142X.2007.00213.x (2008).
24. O'Connor, M., Garm, A. & Nilsson, D. E. Structure and optics of the eyes of the box jellyfish Chiropsella bronzie. *J Comp Physiol A Neuroethol Sens Neural Behav Physiol* **195,** 557–569, doi: 10.1007/s00359-009-0431-x (2009).
25. Parkefelt, L., Skogh, C., Nilsson, D. E. & Ekstrom, P. Bilateral symmetric organization of neural elements in the visual system of a coelenterate, Tripedalia cystophora (Cubozoa). *Journal of Comparative Neurology* **492,** 251–262, doi: 10.1002/cne.20658 (2005).
26. Garm, A., Andersson, F. & Nilsson, D. E. Unique structure and optics of the lesser eyes of the box jellyfish Tripedalia cystophora. *Vision Research* **48,** 1061–1073, doi: 10.1016/j.visres.2008.01.019 (2008).
27. Koyanagi, M. *et al.* Jellyfish vision starts with cAMP signaling mediated by opsin-G(s) cascade. *Proceedings of the National Academy of Sciences of the United States of America* **105,** 15576–15580, doi: 10.1073/pnas.0806215105 (2008).
28. Panda, S. *et al.* Illumination of the melanopsin signaling pathway. *Science* **307,** 600–604, doi: 10.1126/science.1105121 (2005).
29. Yamashita, T. *et al.* Opn5 is a UV-sensitive bistable pigment that couples with Gi subtype of G protein. *Proceedings of the National Academy of Sciences of the United States of America* **107,** 22084–22089, doi: 10.1073/pnas.1012498107 (2010).
30. Bridge, D., Cunningham, C. W., Schierwater, B., DeSalle, R. & Buss, L. W. Class-level relationships in the phylum Cnidaria: evidence from mitochondrial genome structure. *Proceedings of the National Academy of Sciences of the United States of America* **89,** 8750–8753 (1992).
31. Bailes, H. J., Z. L. & Lucas, R. J. Reproducible and sustained regulation of Gαs signalling using a metazoan opsin as an optogenetic tool. *PLOS one* **7,** doi: 10.1371/journal.pone.0030774 (2012).
32. Koyanagi, M., Kubokawa, K., Tsukamoto, H., Shichida, Y. & Terakita, A. Cephalochordate melanopsin: evolutionary linkage between invertebrate visual cells and vertebrate photosensitive retinal ganglion cells. *Current Biology* **15,** 1065–1069, doi: 10.1016/j.cub.2005.04.063 (2005).
33. Hohenegger, M. *et al.* Gsalpha-selective G protein antagonists. *Proceedings of the National Academy of Sciences of the United States of America* **95,** 346–351 (1998).
34. Shabalina, S. A. *et al.* Distinct patterns of expression and evolution of intronless and intron-containing mammalian genes. *Molecular biology and evolution* **27,** 1745–1749, doi: 10.1093/molbev/msq086 (2010).
35. Zou, M., Guo, B. & He, S. The roles and evolutionary patterns of intronless genes in deuterostomes. *Comparative and functional genomics* **2011,** 680673, doi: 10.1155/2011/680673 (2011).
36. Gentles, A. J. & Karlin, S. Why are human G-protein-coupled receptors predominantly intronless? *Trends in genetics : TIG* **15,** 47–49 (1999).
37. Brosius, J. Many G-protein-coupled receptors are encoded by retrogenes. *Trends in genetics : TIG* **15,** 304–305 (1999).
38. Fridmanis, D., Fredriksson, R., Kapa, I., Schioth, H. B. & Klovins, J. Formation of new genes explains lower intron density in mammalian Rhodopsin G protein-coupled receptors. *Molecular phylogenetics and evolution* **43,** 864–880, doi: 10.1016/j.ympev.2006.11.007 (2007).
39. UCSC, G. B. G. *Opsin evolution: update blog http://genomewiki.ucsc.edu, (Date of acces: 20/05/2012).*
40. Morris, A. B. J. & Hunt, D. M. The molecular basis of a spectral shift in the rhodopsin of two species of squid from different photic enviroments. *Proceedings of the Royal Society of London B* **254,** 233–240 (1993).
41. Fitzgibbon, J., H. A., Slobodvanyuk, S. J., Bellingham, J., Bowmaker, J. K. & Hunt, D. M. The rhodopsin-encoding gene of bony fish lacks introns. *Gene* **164,** 273–277 (1995).
42. Innan, H. & Kondrashov, F. The evolution of gene duplications: classifying and distinguishing between models. *Nature reviews. Genetics* **11,** 97–108, doi: 10.1038/nrg2689 (2010).
43. Lynch, M. & Conery, J. S. The evolutionary fate and consequences of duplicate genes. *Science (New York, N.Y.)* **290,** 1151–1155 (2000).
44. Matsumoto, Y., Fukamachi, S., Mitani, H. & Kawamura, S. Functional characterization of visual opsin repertoire in Medaka (Oryzias latipes). *Gene* **371,** 268–278, doi: 10.1016/j.gene.2005.12.005 (2006).
45. Rennison, D. J., Owens, G. L. & Taylor, J. S. Opsin gene duplication and divergence in ray-finned fish. *Molecular phylogenetics and evolution* **62,** 986–1008, doi: 10.1016/j.ympev.2011.11.030 (2012).
46. Skogh, C., Garm, A., Nilsson, D. E. & Ekstrom, P. Bilaterally symmetrical rhopalial nervous system of the box jellyfish Tripedalia cystophora. *Journal of Morphology* **267,** 1391–1405, doi: 10.1002/jmor.10472 (2006).
47. Garm, A., Ekstrom, P., Boudes, M. & Nilsson, D. E. Rhopalia are integrated parts of the central nervous system in box jellyfish. *Cell Tissue Res* **325,** 333–343, doi: 10.1007/s00441-005-0134-8 (2006).
48. Stockl, A. L., Petie, R. & Nilsson, D. E. Setting the pace: new insights into central pattern generator interactions in box jellyfish swimming. *PLoS One* **6,** e27201, doi: 10.1371/journal.pone.0027201 (2011).
49. Yamasu, T. & Yoshida, M. Fine structure of complex ocelli of a cubomedusan, Tamoya bursaria Haeckel. *Cell and Tissue Research* **170,** 325–339 (1976).
50. Laska, G., Hundgen, M. Morphologie und ultrastruktur der lichtsinnesorgane von Tripedalia cystophora Conant (Cnidaria, Cubozoa). *Zool Jb Anat* **108,** 107–123 (1982).
51. O'Connor, M. *et al.* Visual pigment in the lens eyes of the box jellyfish Chiropsella bronzie. *Proc Biol Sci* **277,** 1843–1848, doi: 10.1098/rspb.2009.2248 (2010).

52. Ekstrom, P., Garm, A., Palsson, J., Vihtelic, T. S. & Nilsson, D. E. Immunohistochemical evidence for multiple photosystems in box jellyfish. *Cell and Tissue Research* **333,** 115–124, doi: 10.1007/s00441-008-0614-8 (2008).
53. Garm, A. & Ekstrom, P. Evidence for multiple photosystems in jellyfish. *Int Rev Cell Mol Biol* **280,** 41–78, doi: 10.1016/s1937-6448(10)80002-4 (2010).
54. Yoshida, M. Extraocular photoreception. *Handbook of sensory physiology* **VII/6A**, 582–640 (1979).
55. Taddei-Ferretti, C. & Musio, C. Photobehaviour of Hydra (Cnidaria, Hydrozoa) and correlated mechanisms: a case of extraocular photosensitivity. *Journal of Photochemistry and Photobiology. B, Biology* **55,** 88–101 (2000).
56. Arkett, S. A. & Spencer, A. N. Neuronal mechanism of a hydromedusan shadow reflex. I. Identified reflex components and sequence of events *J. Comp. Physiol. A* **159,** 201–213 (1986).
57. Sawyer, S. J., D. H. B. & Shick, M. Neurophysiological correlates of the behavioral response to light in the sea anemone Anthopleura elegantissima. *Biol. Bull. (Woods Hole, Mass.)* **186,** 195–201 (1994).
58. Musio, C. *et al.* First identification and localization of a visual pigment in Hydra (Cnidaria, Hydrozoa). *J Comp Physiol A* **187,** 79–81 (2001).
59. Plachetzki, D. C., Fong, C. R. & Oakley, T. H. Cnidocyte discharge is regulated by light and opsin-mediated phototransduction. *BMC Biol* **10**, 17, doi: 10.1186/1741-7007-10-17 (2012).
60. Mason, B. *et al.* Evidence for multiple phototransduction pathways in a reef-building coral. *PLoS One* **7,** e50371, doi: 10.1371/journal.pone.0050371 (2012).
61. Nordstrom, K., Wallen, R., Seymour, J. & Nilsson, D. A simple visual system without neurons in jellyfish larvae. *Proc Biol Sci* **270,** 2349–2354, doi: 10.1098/rspb.2003.2504 (2003).
62. Koyanagi, M.T. E., Nagata, T., Tsukamoto, H. & Terakita, A. Homologs of vertebrate Opn3 potentially serve as a light sensor in nonphotoreceptive tissue. *Proceeding of the National Academy of Sciences of the United States of America* **110,** 4998–5003, doi: 10.1073/pnas.1219416110 (2013).
63. Heck, M. S. S., Maretzki, D., Bartl, F. J., Ritter, E., Palczewski, K. & Hofmann, K. P. Signaling States of Rhodopsin: FORMATION OF THE STORAGE FORM, METARHODOPSIN III, FROM ACTIVE METARHODOPSIN II. *Journal of Biological Chemistry* **278,** 3162–3169 (2003).
64. Pearson, W. R. & Lipman, D. J. Improved tools for biological sequence comparison. *Proceedings of the National Academy of Sciences of the United States of America* **85,** 2444–2448 (1988).
65. Guindon, S. *et al.* New algorithms and methods to estimate maximum-likelihood phylogenies: assessing the performance of PhyML 3.0. *Syst Biol* **59,** 307–321, doi: 10.1093/sysbio/syq010 (2010).
66. Le, S. Q. & Gascuel, O. An improved general amino acid replacement matrix. *Molecular Biology and Evolution* **25,** 1307–1320, doi: 10.1093/molbev/msn067 (2008).
67. Anisimova, M. & Gascuel, O. Approximate likelihood-ratio test for branches: A fast, accurate, and powerful alternative. *Syst Biol* **55,** 539–552, doi: 10.1080/10635150600755453 (2006).
68. Larkin, M. A. *et al.* Clustal W and Clustal X version 2.0. *Bioinformatics* **23,** 2947–2948, doi: 10.1093/bioinformatics/btm404 (2007).

Acknowledgements
We are grateful to Dr. Koyanagi for providing cDNA encoding *C. rastonii* opsin and Sarka Takacova and Dr. Alex Bruce for manuscript proofreading. This study was supported by the Grant Agency of the Czech Republic (P305/10/2141) to Z.K. by the Ministry of Education, Youth and Sports of the Czech Republic (LM2011022) to P.B. and by IMG institutional support RVO68378050.

Author Contributions
Conceived and designed the experiments: M.L., J.P., I.K., P.F., P.B., C.V. and Z.K. Performed the experiments: M.L., J.P., I.K., P.F., A.P. and Z.K. Analyzed the data: M.L., J.P., I.K., P.F., A.P., H.S., J.P.a. and Z.K. Wrote the paper: M.L., J.P. and Z.K.

Additional Information
Supplementary information accompanies this paper at http://www.nature.com/srep

Competing financial interests: The authors declare no competing financial interests.

How to cite this article: Liegertová, M. *et al.* Cubozoan genome illuminates functional diversification of opsins and photoreceptor evolution. *Sci. Rep.* **5**, 11885; doi: 10.1038/srep11885 (2015).

The supplementary information (87 pages) is available on-line:

http://www.nature.com/articles/srep11885#supplementary-information

SCIENTIFIC REPORTS

OPEN

Corrigendum: Cubozoan genome illuminates functional diversification of opsins and photoreceptor evolution

Michaela Liegertová, Jiří Pergner, Iryna Kozmiková, Peter Fabian, Antonio R. Pombinho, Hynek Strnad, Jan Pačes, Čestmír Vlček, Petr Bartůněk & Zbyněk Kozmik

Scientific Reports **5**:11885; doi: 10.1038/srep11885; published online 08 July 2015; updated on 24 September 2015

This Article contains a typographical error in the grant number in the Acknowledgements section.

"This study was supported by the Grant Agency of the Czech Republic (P305/10/2141) to Z.K. by the Ministry of Education, Youth and Sports of the Czech Republic (LM2011022) to P.B. and by IMG institutional support RVO68378050".

should read:

"This study was supported by the Grant Agency of the Czech Republic (P305/10/2141) to Z.K. by the Ministry of Education, Youth and Sports of the Czech Republic (LO1220) to P.B. and by IMG institutional support RVO68378050".

Publication: **Molecular analysis of the amphioxus frontal eye unravels the evolutionary origin of the retina and pigment cells of the vertebrate eye. Proc Natl Acad Sci U S A. 109(38):15383-8.**

Molecular analysis of the amphioxus frontal eye unravels the evolutionary origin of the retina and pigment cells of the vertebrate eye

Pavel Vopalensky[a,1], Jiri Pergner[a], Michaela Liegertova[a], Elia Benito-Gutierrez[b], Detlev Arendt[b,c], and Zbynek Kozmik[a,2]

[a]Department of Transcriptional Regulation, Institute of Molecular Genetics, CZ-14220 Prague, Czech Republic; [b]Developmental Biology Unit, European Molecular Biology Laboratory, Heidelberg, 69117 Heidelberg, Germany; and [c]Animal Evolution Department, COS Heidelberg, 69120 Heidelberg, Germany

Edited by Sean B. Carroll, University of Wisconsin, Madison, WI, and approved August 3, 2012 (received for review May 10, 2012)

The origin of vertebrate eyes is still enigmatic. The "frontal eye" of amphioxus, our most primitive chordate relative, has long been recognized as a candidate precursor to the vertebrate eyes. However, the amphioxus frontal eye is composed of simple ciliated cells, unlike vertebrate rods and cones, which display more elaborate, surface-extended cilia. So far, the only evidence that the frontal eye indeed might be sensitive to light has been the presence of a ciliated putative sensory cell in the close vicinity of dark pigment cells. We set out to characterize the cell types of the amphioxus frontal eye molecularly, to test their possible relatedness to the cell types of vertebrate eyes. We show that the cells of the frontal eye specifically coexpress a combination of transcription factors and opsins typical of the vertebrate eye photoreceptors and an inhibitory Gi-type alpha subunit of the G protein, indicating an off-responding phototransductory cascade. Furthermore, the pigmented cells match the retinal pigmented epithelium in melanin content and regulatory signature. Finally, we reveal axonal projections of the frontal eye that resemble the basic photosensory-motor circuit of the vertebrate forebrain. These results support homology of the amphioxus frontal eye and the vertebrate eyes and yield insights into their evolutionary origin.

evolution | vision | cephalochordate

The evolutionary origin of vertebrate eyes is enigmatic. Charles Darwin appreciated the conceptual difficulty in accepting that an organ as complex as the vertebrate eye could have evolved through natural selection (1). Part of the problem lies in the paucity of extant phyla with useful gradations that occurred during eye evolution, thus providing a scenario that led to the emergence of the vertebrate eye. For example, the eye of the adult lamprey (a jawless vertebrate) is remarkably similar to the eye of jawed vertebrates in the overall design, retina cell types, and multiple classes of opsins (2). Given these similarities, it is likely that the last common ancestor of jawless and jawed vertebrates already possessed an elaborate camera-type lens eye. To understand the seemingly sudden origin of the vertebrate eye, its evolutionary precursor must be identified within the non-vertebrate chordates lacking elaborated eye structures. Because of its basal phylogenetic position within the chordates (3), its slowly evolving genome (4), and its ancestral morphology, the cephalochordate amphioxus represents a traditional model organism for understanding the origin of vertebrate organs. Extensive electron microscopy studies of the cerebral vesicle of the basal chordate amphioxus revealed several putative photoreceptive organs—dorsal ocelli, Joseph cells, lamellar body, and the unpaired "frontal eye" (5). The pigmented dorsal ocelli and the Joseph cells are morphologically and molecularly related to invertebrate eye photoreceptors (6, 7), whereas the frontal eye and the lamellar body traditionally have been homologized to the vertebrate eyes and pineal gland, respectively, based on their position and morphological features. However, these statements of homology have been a matter of debate (8), and the lack of adequate comparative molecular evidence has not allowed any firm conclusion to be drawn.

In this work we focus specifically on the functional molecules (c-opsin, melanin, and serotonin) and on transcription factors (Rx, Otx, Pax4/6, Mitf) playing crucial roles during vertebrate eye development. Unlike the majority of published amphioxus expression studies, we use a set of amphioxus-specific antibodies in combination with confocal microscopy to gain cellular resolution and coexpression information and to track axonal projections of the frontal eye. Our data provide evidence that the amphioxus frontal eye is an opsin-based photoreceptive organ and that the frontal eye photoreceptors and pigment cells are homologous to rods/cones and pigment cells of the vertebrate eyes, respectively.

Results

Developmental Patterning of the Amphioxus Frontal Eye. Vertebrates have two separate sets of eyes, the lateral visual eyes and the dorso-medial pineal and parietal "eyes" that play a role in the detection of ambient light and, in some groups, convey a fast response to predator shadows (9–11). Previous studies have revealed a small set of transcription factors that specify photoreceptor cells in both retina and pineal gland. Expression of retinal homeobox (*Rx*) is an early marker for the developing retina and pineal gland and is required for eye vesicle morphogenesis (12–14). We cloned the amphioxus *rx* gene (Fig. S1 for the phylogenetic tree) and determined its expression in the developing cerebral vesicle. We found that *rx* demarcates the anterior end of the cerebral vesicle from the 24-hours postfertilization (hpf) stage onwards (Fig. 1 *A*–*C*). This location is where the frontal eye will start to differentiate at later stages, as evidenced by the presence of cells with long dendrites and cilia that exit the neuropore (15) and by the presence of a spot of dark pigment (Fig. 1 *D* and *E*). However, *rx* expression has not been detected in the area of the lamellar body (Fig. 1 *D* and *F*), the previously proposed homolog of the vertebrate pineal gland (16). During differentiation stages *rx* expression becomes restricted to the cells lying behind the most anterior tip of the cerebral vesicle.

To determine further whether any of the differentiating cells of amphioxus frontal eye would resemble the vertebrate

Author contributions: P.V., D.A., and Z.K. designed research; P.V., J.P., and M.L. performed research; P.V., J.P., M.L., and E.B.-G. contributed new reagents/analytic tools; P.V., J.P., E.B.-G., D.A., and Z.K. analyzed data; and P.V., E.B.-G., D.A., and Z.K. wrote the paper.

The authors declare no conflict of interest.

This article is a PNAS Direct Submission.

Freely available online through the PNAS open access option.

Data deposition: The sequences reported in this paper have been deposited in the GenBank database [accession nos. JX101655 (Rx), JX101656 (Go-alpha); JX101657 (Gi-alpha); JX101658 (c-opsin1); JX101659 (c-opsin2); and JX101660 (c-opsin3)].

[1]Present address: Animal Evolution Department, COS Heidelberg, 69120 Heidelberg, Germany.

[2]To whom correspondence should be addressed. E-mail: Kozmik@img.cas.cz.

This article contains supporting information online at www.pnas.org/lookup/suppl/doi:10.1073/pnas.1207580109/-/DCSupplemental.

EVOLUTION

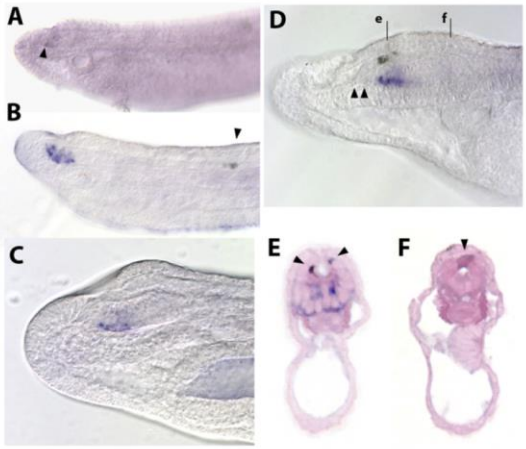

Fig. 1. Developmental expression of amphioxus *rx*. (*A*) The earliest trace of *rx* expression was detected in late neurula (24 hpf) in the anterior part of the cerebral vesicle (arrowhead). (*B*) In early larva (30 hpf), the expression becomes stronger and demarcates the anterior ventral half of the cerebral vesicle. The arrowhead points to the first Hesse eyecup. (*C*) At later stages, the expression is more restricted to the most anterior ventral part of the cerebral vesicle but excluding its very anterior-most tip. (*D*) In the 3.5-d-old larva with pigment cells and Row1 (arrowheads) cells already differentiated, the expression is restricted to the area of Row3/Row4 cells. (*E*) Plastic-embedded cross-section at the level of 'e' in *D*, showing the expression of *rx* in ventral cells of the cerebral vesicle. The arrowheads point to the posterior-most projections of the pigment deposits. (*F*) Expression of *rx* in the lamellar body was not observed at any stage of development. A more detailed inspection performed on the cross-section (at level 'f' in *D*) did not reveal the signal in cells of the lamellar body; the weak signal observed in the membrane protrusions (arrowhead) of the lamellar body is attributed to non-specific probe trapping caused by the large surface area of the structure.

photoreceptors molecularly, we produced antibodies against the amphioxus Otx, Pax4/6, and Rx transcription factors (Table S1). The antibodies showed the ability to recognize their respective antigens (Fig. S2 *A–C* and Fig. S3), recapitulated the RNA in situ expression patterns, and provided robust signal clearly distinguishable from nonspecific epidermal signal that we attribute to endogenous GFP expression (17) and secondary antibody trapping (Fig. 2*E*).

Expression of the single amphioxus *otx* and *pax4/6* orthologs has been detected previously in the anterior portion of the amphioxus cerebral vesicle (18, 19), but whole-mount RNA in situ hybridization analysis has not provided cellular resolution. Fluorescent confocal immunohistochemistry of amphioxus larvae with antibodies directed against amphioxus Otx and Pax4/6 proteins revealed colabeling of a single row of cells in the very anterior of the frontal eye (Fig. 2 *C–F*), termed "Row 1" by Lacalli et al (15). These cells are adjacent to the cells containing the dark pigment and thus are the most likely candidates for photoreceptor cells (15). Pax4/6 protein expression also was detected more posteriorly in cells scattered in the floor of the cerebral vesicle (Fig. 2 *F*) in a pattern similar to that of Rx (Fig. 2 *G–I* and Fig. S4). Interestingly, in addition to the differentiated cells bearing the apical extension, a small subset of Rx-positive cells buried deeper in the cerebral vesicle floor retained a rounded shape (Fig. 2*H*), suggesting a possible undifferentiated state.

Row1 Cells of the Frontal Eye Express *C-Opsin* Genes and the Gi-Alpha Protein Subunit. To challenge the possible photosensitive nature of Row1 cells in the amphioxus frontal eye (15), we set out to identify cells expressing the amphioxus *c-opsin* genes. Sixteen opsins have been detected in the amphioxus genome, four of which are related to the vertebrate rod, cone, and pineal opsins (20, 21). Phylogenetic analysis revealed that ancestral chordates possessed one *c-opsin* gene that by repeated and independent duplications gave rise to four paralogs in amphioxus and to numerous paralogs in the vertebrate lineage (20). We could not detect expression of any of the amphioxus *c-opsin* genes by RNA whole-mount in situ hybridization and subsequent RT-PCR analysis revealed a low mRNA expression level of these opsins, suggesting a low mRNA expression level; therefore we produced antibodies against all four c-opsin proteins (Table S1). Antibody staining indeed revealed specific expression of c-opsin1 and c-opsin3 in the Row1 (15, 22) cells of the amphioxus frontal eye (Fig. 3 *A* and *B*). The specificity of each antibody was confirmed by the loss of specific signal after preadsorption with the respective antigen (Fig. S3). We further noted that the c-opsin1 and c-opsin3 antibodies labeled morphologically distinct cells within Row 1 (compare Fig. 3 *A* and *B* and Fig. S5), consistent with possible differential responses to distinct wavelengths. None of the other rows of the frontal eye was positive for any of the other c-opsins. To characterize phototransduction in the amphioxus frontal eye further, we cloned the proteins of the amphioxus G-alpha subunit see Fig. S6 for the phylogenetic tree). The proteins of the G-alpha subunit are specific for distinct phototransductory cascades in vertebrates and invertebrates (23). In vertebrate rods and cones, transducin signals to phosphodiesterase that hydrolyses cGMP and shuts down the dark current, mediating an "off response" to light (23). The activity of such phosphodiesterase is stimulated by transducins, which arose by gene duplication of a more ancestral *Gi* gene encoding the inhibitory Gi-alpha subunit (23). Because the amphioxus genome predates the duplication events that generated transducins later in evolution, we investigated the expression of their more ancestral counterpart *Gi*. The only amphioxus *Gi* gene that we found is expressed in the most anterior cells of the amphioxus frontal eye (Fig. 3*C*). We also investigated expression of the Go-alpha subunit, which is active in the photoreceptors of vertebrate pineal eyes (11) and in the ciliary photoreceptors of mollusks (24). The amphioxus *Go* gene is expressed more broadly in the amphioxus cerebral vesicle (Fig. 3*D*); however, the most anterior portion of the frontal eye appeared to be specifically excluded from the *Go* expression domain, indicating that it is unlikely that the Row1 cells also signal via the Go-alpha subunit. Notably, the Gq-alpha subunit characteristic for invertebrate rhabdomeric photoreceptor cells has not been detected in the amphioxus frontal eye (6). This result suggests that the Row1 cells of the frontal eye couple to an inhibitory G-alpha subunit protein mediating the off response.

Pigmented Cells of the Amphioxus Frontal Eye. Cells of the vertebrate retinal pigmented epithelium (RPE) are specified by the *Mitf* transcription factor and use melanin as a shading pigment (25). We investigated expression of amphioxus *mitf* within the cerebral vesicle and found it restricted to the pigment cells of the frontal eye (Fig. 4 *A* and *B*). In addition, the vertebrate *Otx2* paralog acts in tight cooperation with *Mitf* during RPE development and differentiation (26). This might also be the case in amphioxus, where *mitf* is expressed concomitantly with *otx* in the pigment cells of the frontal eye (Fig. 2 *D–F*). Furthermore, we exposed developing amphioxus embryos and larvae to phenylthiourea (PTU), a specific inhibitor of melanin synthesis causing the absence of melanin pigment in the vertebrate eye (27). After PTU exposure, the dark pigment of the frontal eye was abolished completely (Fig. 4 *C–E*), indicating that melanin is indeed the only dark pigment of the frontal eye.

Projections. Finally, we analyzed axonal projections from frontal eye cells. Previous transmission electronic microscopy studies revealed only short projections to the laterally adjacent frontal

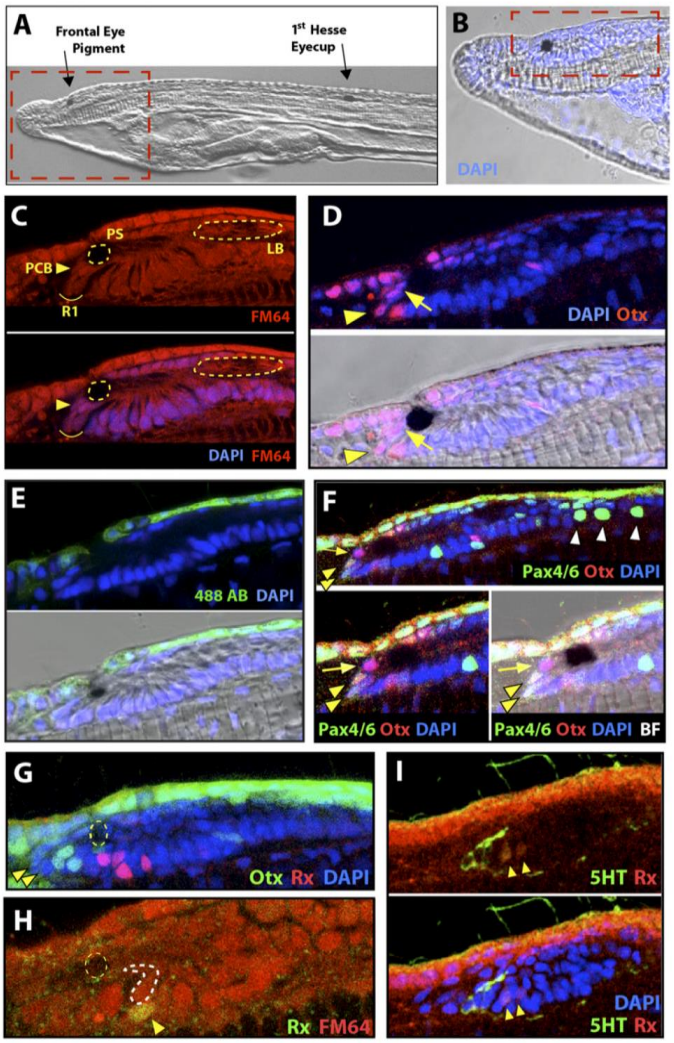

Fig. 2. Expression of *otx*, *pax4/6*, and *rx* in the amphioxus cerebral vesicle. (*A*) Overview of the anterior part of a larva at the 2.5–gill-slit stage typically used in this study. (*B*) Detailed view of the most anterior part of the larva (defined by red dashed box in *A*) with nuclei stained with DAPI. (*C–I*) The area of the cerebral vesicle defined by the red dashed box in *B*. (*C*) The cerebral vesicle was stained with FM64 stain to visualize the cell bodies and with DAPI to stain the nuclei to address the comparability of this stage with previous studies (22). The Row1 cells (R1) are positioned ventro-anteriorly to the pigment spot. Note the shapes of the cell bodies in the cerebral vesicle; the presence of apical cilium projecting to the lumen of the cerebral vesicle suggests that these cells already have differentiated at this developmental stage (compare with figure 2 in ref. 49). LB, lamellar body; PCB, pigment cell body; PS, pigment spot; R1, Row1 cells. (*D*) Otx protein is present in the nuclei of the most anterior cells of the cerebral vesicle, including the Row1 cells (arrowhead) and the more dorso-posteriorly positioned pigment cells (arrow). (*E*) Endogenous amphioxus GFP expression (17) and nonspecific trapping of the secondary antibody causes the presence of epidermal signal when green-fluorescent secondary antibodies are used (Alexa 488 is shown). For easy orientation, the *Lower* panel shows the same image including the brightfield. (*F*) (*Upper*) The broad *pax4/6* expression in the amphioxus cerebral vesicle and epidermis (19) includes Row1 cells, in which *pax4/6* is coexpressed with *otx* (yellow arrowheads). Furthermore, Pax4/6 is observed in scattered cells within the ventral floor of the cerebral vesicle (Fig S4C), in cells of the lamellar body, and the large cells of the PMC (white arrowheads). A detailed view of the frontal eye region is shown in the *Lower Left* panel and the brightfield channel for easy orientation is included in the *Lower Right* panel. (*G*) Consistent with the RNA in situ hybridization result (Fig. 1*D*), the antibody raised against Rx protein stained several nuclei positioned posterior to Row1 cells (arrowheads), and *rx* expression did not overlap with the most posterior nuclei expressing *otx*. The dashed circle demarcates the pigment spot. (*H*) A subset of *rx*-positive nuclei (yellow arrowhead) belonged to cells lacking apical projections and positioned deeper in the cerebral vesicle floor. Yellow dashed circle demarcates the pigment spot, and the white dashed line follows the cell shape of a cell possessing the apical projection. (*I*) To see whether *rx*-positive nuclei might belong to serotonergic Row2 cells (22), we performed coimmunolabeling with Rx and anti-serotonin antibody. The Rx signal (yellow arrowheads) was posterior to Row2 cells, suggesting possible expression in Row3 or Row4 cells. The high background staining in the red channel comes from the double sequential protocol used to perform staining with two primary antibodies raised in the same species (rabbit). The *Lower* panel includes the DAPI staining to visualize the extend of the cerebral vesicle.

nerves (22). We took advantage of the serotoninergic nature of the Row2 cells of frontal eye, which are in direct contact with the Row1 cells (22, 28), and detected long basal axonal projections from the frontal eye Row2 cells toward the posterior cerebral vesicle (Fig. 5 *A* and *B*), where we observed massive serotonin varicosities within the tegmental neuropil (22).

Discussion

The thorough immunohistochemical study presented in this work defines, at least in part, a molecular fingerprint for the amphioxus frontal eye at cellular resolution (summarized in Fig. 5*C*) and thus provides important insight into the evolutionary origin of the vertebrate eyes. The expression profile of vertebrate eye-specific regulatory (*Rx*, *Otx*, *Pax4/6*, and *Mitf*) genes and differentiation markers (c-opsins, Gi, melanin) in the amphioxus cerebral vesicle strongly supports the homology of photoreceptor and pigmented cells of the amphioxus frontal eye and the corresponding cell types in the vertebrate retina and retinal pigmented epithelium, respectively.

Regulatory Signature. The early developmental patterning of the amphioxus frontal eye is performed by the same set of transcription factors (Otx, Rx, and Pax4/6) as the vertebrate retina. In vertebrates, *Otx2* controls the development of both the retina and the pineal gland (29) and another vertebrate paralogue of *Otx*, cone rod homeobox (*Crx*) transcription factor, is crucial for

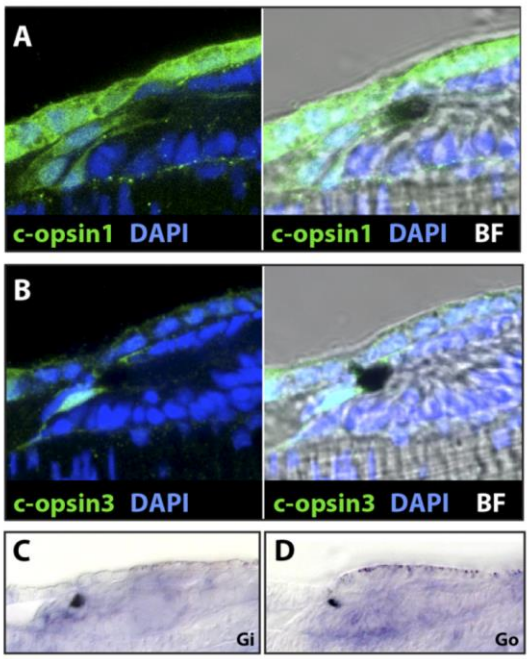

Fig. 3. Expression of amphioxus c-opsins and G-alpha subunits in the cerebral vesicle. Amphioxus larvae were stained with mouse polyclonal sera raised against the C-terminal portion of amphioxus c-opsins. For easy orientation, the bright-field (BF) images of the confocal plane are included on the right in *A* and *B*. (*A*) The expression of *c-opsin1* in several cells positioned at the most anterior tip of the frontal eye, corresponding to Row1 cells (22). (*B*) *c-opsin3* is expressed most dorsally, in the *Row1* cells ventrally adjacent to the pigment-producing cells (compare with figure 17 in ref. 22). (*C*) Expression of the Gi-alpha subunit in the cerebral vesicle revealed by RNA in situ hybridization. The cells with the strongest labeling are localized in the very anterior tip of the vesicle in the position corresponding to the photoreceptor cells. (*D*) The Go-alpha subunit is expressed throughout the cerebral vesicle, except in the very anterior tip, suggesting that it is excluded from the Row1 cells.

the terminal differentiation of the rods and cones (30). Likewise, vertebrate *Pax6* is necessary for proper eye development (31, 32), and the expression of *pax4* is characteristic for differentiated rods and cones (33, 34). During later stages, *otx* and *pax4/6* remain expressed in the differentiated Row1 photoreceptors, albeit at lower levels that suffice for maintenance of the differentiated state of the given cell type. This situation exemplifies the division of labor of the chordate single-copy orthologs (such as amphioxus *pax4/6* and *otx*) after gene duplication in the vertebrates, where *Pax6* and *Otx2* are active during early eye/pineal gland development, and their paralogs *Pax4* and *Crx* act during the terminal differentiation stages. Although the transient expression of *rx* in the precursors of ciliary photoreceptors (Fig. 1*B*) seems to be evolutionarily conserved (35), the absence of *rx* in the differentiated photoreceptors of Row1 cells contrasts with its expression in vertebrate differentiated photoreceptors and its involvement in the regulation of phototransduction genes (36). The overlapping expression of *rx* and ci-opsin1 in the ciliary photoreceptor of tunicates (37, 38) suggests either the acquisition of *rx* for the direct regulation of photoreceptor genes such as opsins at the base of Olfactores or amphioxus-specific loss of *rx* role for maintaining the differentiated ciliary photoreceptor program. The small population of *rx*-positive cells lacking the apical cilium might represent, as in vertebrates (39–41), a progenitor subpopulation needed for further growth of the frontal eye later in development. The absence of expression of *otx* and *rx* in the lamellar organ challenges its proposed homology with the vertebrate pineal gland, but the currently available data are too sparse to allow any conclusions. To resolve this issue, further molecular characterization of the lamellar organ will be rewarding.

Evolutionary Precursor of the Vertebrate Phototransduction Cascade. The expression of two ciliary opsins and the proteins of the G_i-alpha subunit in the amphioxus frontal eye provides molecular evidence of the photosensory nature of Row1 cells and corroborates the homology of these amphioxus cells and vertebrate rods, cones, and/or pinealocytes. Because c-opsin and Gi-alpha also are coexpressed in tunicate ciliary photoreceptors (38, 42), the amphioxus frontal eye photoreceptors using ciliary opsin

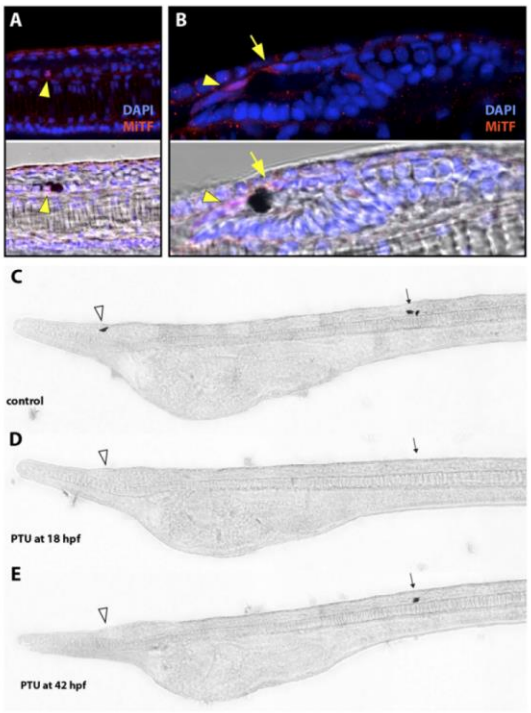

Fig. 4. Characterization of the frontal eye pigment cells. The *Lower* panels in *A* and *B* include the brightfield channel to visualize the pigment spot. (*A*) The specificity of Mitf antibody has been confirmed by specific nuclear staining (yellow arrowhead) in the pigment cell of the Hesse eyecup in which *mitf* expression was reported previously (57). (See also Fig. S2*E* for Western blot and Fig. S3 *E* and *F* for loss of signal after antigen preadsorption.) (*B*) The Mitf antibody labeled the nuclei (yellow arrowhead) and cytoplasm (yellow arrow) of the frontal eye pigment cells. The cytoplasmic localization of Mitf also was observed in vertebrates (58). (*C–E*) PTU treatment blocks pigment synthesis in both frontal eye and first Hesse eyecup in *B. lanceolatum*. (*C*) Control animals treated only with ethanol developed both pigmented structures, the first Hesse eyecup (black arrow) and pigment of the frontal eye (arrowhead). (*D*) Animals treated with 0.22 mM PTU from 18 hpf (before developing the first Hesse eyecup pigment) lack both pigmented structures. (*E*) Addition of PTU at 42 hpf (after the first Hesse eyecup has developed), results in animals lacking only the frontal eye pigment. This experiment shows that the pigment in both the Hesse eyecup and the frontal eye is melanin.

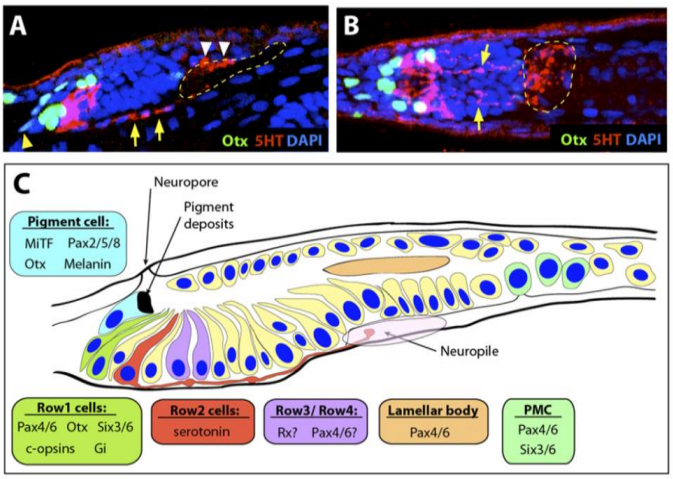

Fig. 5. The projections of the frontal eye region. (*A*) Serotonergic Row2 cells project axons to the neuropil (dashed outline), where the axons terminate by many varicosities (white arrowheads). A few varicosities are also encountered along the axons (yellow arrows). This double labeling also revealed that the Row2 cells do not express Otx, because its nuclear signal is never present in the cells expressing serotonin. Yellow arrowhead points to a Row1 cell. (*B*) Dorsal view of the same specimen showing the trajectory of the serotonergic axons with varicosities (yellow arrows) terminating in the neuropil area (dashed outline). (*C*) A schematic drawing summarizing the molecular data available for the frontal eye region at the differentiated state. The expression data for Pax2/5/8 (46) and Six3/6 (47) are based on previous studies.

coupled to Gi-alpha represent the ancestral chordate condition and an evolutionary forerunner of more sophisticated vertebrate visual photoreceptors. In early vertebrate evolution the two rounds of genome duplication giving rise to the vertebrate visual opsin subclass (by duplicating ancestral chordate ciliary opsin genes) and a new subclass of Gi-derived Gt-alpha protein subunits provided enough genetic material to allow biochemical evolution (43) to provide the highly efficient phototransductory system operating in today's vertebrate rods and cones.

Frontal Eye Pigment Cells Are Homologous to the Cells of the Vertebrate RPE. Unlike previous observations based on morphological and chemical properties (44, 45), our data provide biochemical evidence that the only shielding pigment of amphioxus pigment cells is melanin. The molecular fingerprint of the amphioxus frontal eye pigment cells, expressing *mitf*, *otx*, and *pax2/5/8* (46, 47), resembles the fingerprint of the vertebrate retinal pigmented epithelium (48). In both amphioxus and vertebrates, the pigmented cells are located directly adjacent to the ciliary photoreceptor cells (Row1 cells in amphioxus and rods and cones in the vertebrates), further corroborating the homology of amphioxus and vertebrate eyes.

Neural Circuitry of the Frontal Eye. The Row2 cells projecting axons to the tegmental neuropil provide further evidence for the homology of the frontal eye and the vertebrate retina. As projection neurons, Row2 cells would correspond to retinal ganglion cells [and to horizontal and amacrine cells, the presumed sister cell types of the ganglion cells (7)]. However, more information about Row2-specific expression will be needed to substantiate this issue and to test for any relationship to the rhabdomeric photoreceptor lineage (7). The tegmental neuropil has been compared with locomotor control regions of the vertebrate hypothalamus, where paracrine release modulates locomotor patterns such as feeding and swimming (49). Consistent with this idea, *FoxD* (50) and *Brn1/2/4* (51), whose vertebrate orthologs are expressed in the hypothalamus, also are expressed in the tissue apposed the tegmental neuropil in amphioxus. In addition, the retinohypothalamic tract in vertebrates projects to the anterior hypothalamic area involved in the control of basic behaviors (52) and also the pineal fibers connect bilaterally to the rostral hypothalamus (53). The amphioxus tegmental neuropil in the posterior cerebral vesicle receives not only projections from the frontal eye area but also bilateral afferents from the giant cells located in the primary motor center (PMC) (49). The PMC, positioned immediately beyond the caudal end of the cerebral vesicle, likewise is connected to the frontal eye region via an asymmetrical lateral dendrite of one of the abovementioned giant cells (49). Given that the PMC cells lie in the *gbx* expression region (54), and some of them also are positive for *pax4/6* (Fig. 2*F*), their molecular identity resembles that of the vertebrate interpeduncular nucleus located in the hindbrain and involved in locomotor control (55). Taken together, these findings indicate that in amphioxus the frontal eye projects to the neurosecretory/tegmental neuropil and to the locomotor center, like the eye and the pineal gland in vertebrates.

The study highlights the advantage of cellular resolution, gene coexpression, and structural analyses using molecular markers to define the neuronal circuitry in the amphioxus cerebral vesicle. Our data reveal direct innervation and indicate paracrine release of serotonin from Row2 cells in the tegmental neuropil in the posterior cerebral vesicle, reminiscent of retinohypothalamic projections in the vertebrates. Also, the frontal eye directly innervates locomotor control regions in the primary motor center, again reminiscent of more complex vertebrate circuits of the retina and pineal. The amphioxus frontal eye circuit thus represents a very simple precursor circuit that, by expansion, duplication, and divergence, might have given rise to photosensory-locomotor circuits as found in the extant vertebrate brain.

Experimental Procedures

Animals. *Branchiostoma floridae* larvae were obtained in Tampa Bay (Florida), during the spawning season in August 2010. At the 2.5–gill-slit stage, the animals were fixed with 3-(N-morpholino)propanesulfonic acid (MOPS) fixative (0.1 M MOPS, 2 mM $MgSO_4$, 1 mM EGTA, 0.5M NaCl, pH 7.5) for 30 min at room temperature and then were transferred to 100% methanol. Larvae for RNA in situ hybridization were kindly provided by Linda Z. Holland (Scripps Institution of Oceanography, University of California at San Diego, La Jolla, CA). *B. lanceolatum* larvae for the PTU experiment were provided by the amphioxus facility of the Arendt group, European Molecular Biology Laboratory, Heidelberg.

Immunohistochemistry. If not otherwise stated, all incubation steps were carried out at room temperature. Specimens were transferred to 1× PBS, 0.1% (vol/vol) Tween 20 (PBT) through 50% (vol/vol) and 25% (vol/vol) methanol in PBS. Specimens were washed three times (20 min each washing) in PBT, blocked in block solution [10% (wt/wt) BSA in PBS] for 1 h, and incubated with preadsorbed sera (dilutions are given in Table S1) overnight at 4 °C. On the next day, specimens were washed three or four times in PBT (20 min each washing) and were incubated with secondary antibodies for 2 h. Secondary antibodies were washed away with three washings in PBT (20 min

each washing). Nuclear counterstaining was carried out by incubation with 1 μg/mL DAPI in PBS and washing three times (5 min each washing). For FM4-64FX (Invitrogen) staining, the larvae were incubated in the dye (10 μg/mL) for 10 min in PBS and were washed twice with PBS.

For fluorescence/confocal microscopy, the specimens were mounted in VECTASHIELD (Vector Laboratories, Inc.) using small coverslips as spacers between the coverslip and the slide. The confocal images were taken using a Leica SP5 confocal microscope and were processed (contrast, brightness, and histogram adjustment) with FIJI free image analysis software (http://fiji.sc).

RNA in Situ Hybridization. Whole-mount RNA in situ hybridization to amphioxus larvae was performed according to a standard protocol (56). The only modification was the omission of levamisole in washes on day 3 (step vi).

PTU Treatment. *B. lanceolatum* embryos raised at 20 °C were treated in the dark with 0.22 mM PTU (stock solution 100 mM PTU in 96% EtOH) either from the 18-hpf stage onwards or from the 42-hpf stage onwards. Ethanol at the same dilution was used as a negative control. The drug was changed every 24 h. At 66 hpf the specimens were fixed and documented.

ACKNOWLEDGMENTS. We thank Nicholas and Linda Holland for providing fixed animals for whole-mount in situ hybridization and help with RNA in situ hybridization, Jitka Lachova for immunization of mice, and Cestmir Vlcek for excellent help in sequencing. This study was supported by the Grant Agency of the Czech Republic Grants P305/10/2141 and P305/10/J064 (to Z.K.) and DFG AR 387/2-1 (to D.A.) and the Grant Agency of the Charles University, Grant GAUK 91808 (to P.V.) and by IMG institutional support RVO 68378050.

1. Darwin C (1859) *On the Origin of Species by Means of Natural Selection* (Murray, London) 1st Ed.
2. Lamb TD, Collin SP, Pugh EN, Jr. (2007) Evolution of the vertebrate eye: Opsins, photoreceptors, retina and eye cup. *Nat Rev Neurosci* 8:960–976.
3. Delsuc F, Brinkmann H, Chourrout D, Philippe H (2006) Tunicates and not cephalochordates are the closest living relatives of vertebrates. *Nature* 439:965–968.
4. Putnam NH, et al. (2008) The amphioxus genome and the evolution of the chordate karyotype. *Nature* 453:1064–1071.
5. Lacalli TC (2004) Sensory systems in amphioxus: A window on the ancestral chordate condition. *Brain Behav Evol* 64:148–162.
6. Koyanagi M, Kubokawa K, Tsukamoto H, Shichida Y, Terakita A (2005) Cephalochordate melanopsin: Evolutionary linkage between invertebrate visual cells and vertebrate photosensitive retinal ganglion cells. *Curr Biol* 15:1065–1069.
7. Arendt D (2003) Evolution of eyes and photoreceptor cell types. *Int J Dev Biol* 47: 563–571.
8. Satir P (2000) A comment on the origin of the vertebrate eye. *Anat Rec* 261:224–227.
9. Solessio E, Engbretson GA (1993) Antagonistic chromatic mechanisms in photoreceptors of the parietal eye of lizards. *Nature* 364:442–445.
10. Vigh B, et al. (2002) Nonvisual photoreceptors of the deep brain, pineal organs and retina. *Histol Histopathol* 17:555–590.
11. Su CY, et al. (2006) Parietal-eye phototransduction components and their potential evolutionary implications. *Science* 311:1617–1621.
12. Rohde K, Klein DC, Møller M, Rath MF (2011) Rax: Developmental and daily expression patterns in the rat pineal gland and retina. *J Neurochem* 118:999–1007.
13. Furukawa T, Kozak CA, Cepko CL (1997) rax, a novel paired-type homeobox gene, shows expression in the anterior neural fold and developing retina. *Proc Natl Acad Sci USA* 94:3088–3093.
14. Bailey TJ, et al. (2004) Regulation of vertebrate eye development by Rx genes. *Int J Dev Biol* 48:761–770.
15. Lacalli T, Holland N, West J (1994) Landmarks in the anterior central nervous system of amphioxus larvae. *Philos Trans R Soc Lond B Biol Sci* 344(1308):165–185.
16. Ruiz S, Anadón R (1991) The fine structure of lamellate cells in the brain of amphioxus (Branchiostoma lanceolatum, Cephalochordata). *Cell Tissue Res* 263:597–600.
17. Deheyn DD, et al. (2007) Endogenous green fluorescent protein (GFP) in amphioxus. *Biol Bull* 213:95–100.
18. Williams NA, Holland PWH (1996) Old head on young shoulders. *Nature* 383:490.
19. Glardon S, Holland LZ, Gehring WJ, Holland ND (1998) Isolation and developmental expression of the amphioxus Pax-6 gene (AmphiPax-6): Insights into eye and photoreceptor evolution. *Development* 125:2701–2710.
20. Holland LZ, et al. (2008) The amphioxus genome illuminates vertebrate origins and cephalochordate biology. *Genome Res* 18:1100–1111.
21. Albalat R (2012) Evolution of the genetic machinery of the visual cycle: A novelty of the vertebrate eye? *Mol Biol Evol* 29:1461–1469.
22. Lacalli TC (1996) Frontal eye circuitry, rostral sensory pathways and brain organization in amphioxus larvae: Evidence from 3D reconstructions. *Philos Trans Roy Soc Lond B, Biol Sci* 351(1337):243–263.
23. Yau KW, Hardie RC (2009) Phototransduction motifs and variations. *Cell* 139:246–264.
24. Kojima D, et al. (1997) A novel Go-mediated phototransduction cascade in scallop visual cells. *J Biol Chem* 272:22979–22982.
25. Nguyen M, Arnheiter H (2000) Signaling and transcriptional regulation in early mammalian eye development: A link between FGF and MITF. *Development* 127: 3581–3591.
26. Martínez-Morales JR, et al. (2003) OTX2 activates the molecular network underlying retina pigment epithelium differentiation. *J Biol Chem* 278:21721–21731.
27. Karlsson J, von Hofsten J, Olsson PE (2001) Generating transparent zebrafish: A refined method to improve detection of gene expression during embryonic development. *Mar Biotechnol (NY)* 3:522–527.
28. Holland ND, Holland LZ (1993) Serotonin-Containing Cells in the Nervous-System and Other Tissues during Ontogeny of a Lancelet, Branchiostoma-Floridae. *Acta Zoologica* 74(3):195–204.
29. Nishida A, et al. (2003) Otx2 homeobox gene controls retinal photoreceptor cell fate and pineal gland development. *Nat Neurosci* 6:1255–1263.
30. Furukawa T, Morrow EM, Li T, Davis FC, Cepko CL (1999) Retinopathy and attenuated circadian entrainment in Crx-deficient mice. *Nat Genet* 23:466–470.
31. Hill RE, et al. (1991) Mouse small eye results from mutations in a paired-like homeobox-containing gene. *Nature* 354:522–525.
32. Estivill-Torrús G, Vitalis T, Fernández-Llebrez P, Price DJ (2001) The transcription factor Pax6 is required for development of the diencephalic dorsal midline secretory radial glia that form the subcommissural organ. *Mech Dev* 109:215–224.
33. Rath MF, et al. (2009) Developmental and daily expression of the Pax4 and Pax6 homeobox genes in the rat retina: Localization of Pax4 in photoreceptor cells. *J Neurochem* 108:285–294.
34. Rath MF, et al. (2009) Developmental and diurnal dynamics of Pax4 expression in the mammalian pineal gland: Nocturnal down-regulation is mediated by adrenergic-cyclic adenosine 3′,5′-monophosphate signaling. *Endocrinology* 150:803–811.
35. Arendt D, Tessmar-Raible K, Snyman H, Dorresteijn AW, Wittbrodt J (2004) Ciliary photoreceptors with a vertebrate-type opsin in an invertebrate brain. *Science* 306: 869–871.
36. Kimura A, et al. (2000) Both PCE-1/RX and OTX/CRX interactions are necessary for photoreceptor-specific gene expression. *J Biol Chem* 275:1152–1160.
37. D'Aniello S, et al. (2006) The ascidian homolog of the vertebrate homeobox gene Rx is essential for ocellus development and function. *Differentiation* 74:222–234.
38. Kusakabe T, et al. (2001) Ci-opsin1, a vertebrate-type opsin gene, expressed in the larval ocellus of the ascidian Ciona intestinalis. *FEBS Lett* 506:69–72.
39. Casarosa S, et al. (2003) Xrx1 controls proliferation and multipotency of retinal progenitors. *Mol Cell Neurosci* 22:25–36.
40. Nelson SM, Park L, Stenkamp DL (2009) Retinal homeobox 1 is required for retinal neurogenesis and photoreceptor differentiation in embryonic zebrafish. *Dev Biol* 328: 24–39.
41. Chen CM, Cepko CL (2002) The chicken RaxL gene plays a role in the initiation of photoreceptor differentiation. *Development* 129:5363–5375.
42. Yoshida R, Kusakabe T, Kamatani M, Daitoh M, Tsuda M (2002) Central nervous system-specific expression of G protein alpha subunits in the ascidian Ciona intestinalis. *Zoolog Sci* 19:1079–1088.
43. Sato K, Yamashita T, Ohuchi H, Shichida Y (2011) Vertebrate ancient-long opsin has molecular properties intermediate between those of vertebrate and invertebrate visual pigments. *Biochemistry* 50:10484–10490.
44. Franz V (1927) Morphologie der Akranier. *Ergeb Anat Entwicklungsgesch* 27:464–692.
45. Tenbaum E (1955) Polarisationsoptische Beiträge zur Kenntnis der Gewebe von Branchiostoma Lanceolatum (P). *Cell and Tissue Research* 42(3):149–192.
46. Kozmik Z, et al. (1999) Characterization of an amphioxus paired box gene, AmphiPax2/5/8: Developmental expression patterns in optic support cells, nephridium, thyroid-like structures and pharyngeal gill slits, but not in the midbrain-hindbrain boundary region. *Development* 126:1295–1304.
47. Kozmik Z, et al. (2007) Pax-Six-Eya-Dach network during amphioxus development: Conservation in vitro but context specificity in vivo. *Dev Biol* 306:143–159.
48. Martínez-Morales JR, Rodrigo I, Bovolenta P (2004) Eye development: A view from the retina pigmented epithelium. *Bioessays* 26:766–777.
49. Lacalli TC, Kelly SJ (2000) The infundibular balance organ in amphioxus larvae and related aspects of cerebral vesicle organization. *Acta Zoologica* 81(1):37–47.
50. Yu JK, Holland ND, Holland LZ (2002) An amphioxus winged helix/forkhead gene, AmphiFoxD: Insights into vertebrate neural crest evolution. *Dev Dyn* 225(3):289–297.
51. Candiani S, Castagnola P, Oliveri D, Pestarino M (2002) Cloning and developmental expression of AmphiBrn1/2/4, a POU III gene in amphioxus. *Mech Dev* 116:231–234.
52. Canteras NS, Ribeiro-Barbosa ER, Goto M, Cipolla-Neto J, Swanson LW (2011) The retinohypothalamic tract: Comparison of axonal projection patterns from four major targets. *Brain Res Brain Res Rev* 65:150–183.
53. Yáñez J, Busch J, Anadón R, Meissl H (2009) Pineal projections in the zebrafish (Danio rerio): Overlap with retinal and cerebellar projections. *Neuroscience* 164:1712–1720.
54. Castro LF, Rasmussen SL, Holland PW, Holland ND, Holland LZ (2006) A Gbx homeobox gene in amphioxus: Insights into ancestry of the ANTP class and evolution of the midbrain/hindbrain boundary. *Dev Biol* 295:40–51.
55. Lorente-Cánovas B, et al. (2012) Multiple origins, migratory paths and molecular profiles of cells populating the avian interpeduncular nucleus. *Dev Biol* 361:12–26.
56. Holland LZ, Holland PW, Holland ND (1996) *Whole Mount in Situ Hybridization Applicable to Amphioxus and Other Small Larvae*, Molecular Zoology, Advances, Strategies, and Protocols, eds Ferraris JD, Palumbi SR (Wiley-Liss Inc., New York), pp 474–483.
57. Yu JK, Meulemans D, McKeown SJ, Bronner-Fraser M (2008) Insights from the amphioxus genome on the origin of vertebrate neural crest. *Genome Res* 18:1127–1132.
58. Lu SY, Wan HC, Li M, Lin YL (2010) Subcellular localization of Mitf in monocytic cells. *Histochem Cell Biol* 133:651–658.

Supporting Information

Vopalensky et al. 10.1073/pnas.1207580109

SI Experimental Procedures

Expression and Purification of Proteins for Immunization. For overexpression of protein fragments, the pET system (Novagen) was used. Selected coding sequences were cloned into the pET42a(+) vector to create proteins containing 6xHis-GST fused to the protein fragment of interest. A total volume of 500 mL fresh LB medium without antibiotics was inoculated by culture grown overnight in LB medium supplemented with 12.5 μg/mL chloramphenicol and 30 μg/mL kanamycin. Bacteria were grown at 37 °C at 200 rpm until OD_{600} 0.6, and subsequently induced by 0.5 mM IPTG for 3 more hours. Cells were harvested at 6,000 × *g* for 20 min and the pellet wa stored at −80 °C until further processing. The pellet was resuspended in lysis buffer (6 M guanidine hydrochloride, 0.1M NaH_2PO_4, 0.01M Tris·Cl, pH 8.0, supplemented with fresh β-mercaptoethanol to a final concentration of 20 mM). The suspension was sonicated six times for 20 s and was incubated for 3 h at room temperature. The resulting lysate was centrifuged at 10 000 × *g* for 10 min, and the supernatant was mixed with Ni-NTA agarose beads (Qiagen) previously equilibrated with urea buffer (8 M urea, 20 mM Tris·Cl, 50 mM NaH_2PO_4, 100 mM NaCl, pH 8.0, supplemented with fresh β-mercaptoethanol to a final concentration of 20 mM). The suspension was incubated on a rotating platform overnight at room temperature. The beads with bound proteins were washed two times with 40 mL urea buffer and were loaded onto a disposable chromatographic column (Bio-Rad). The column was washed with urea buffer with decreasing pH (8.0–6.8), and His-tagged protein was eluted by urea buffer (pH 4.2) into several 1-mL aliquots. After elution, pH was adjusted immediately to 7.5 by 1 M Tris·Cl (pH 8). Protein concentration was estimated using Protein Assay Reagent (Bio-Rad).

Immunization of Rabbits and mice. For rabbit immunization, unbred female New Zealand White rabbits (Charles Rivers Laboratories) were used. Rabbits were immunized three or four times at 1-month intervals with 300–500 μg of purified protein mixed with Freund's Adjuvant (F5506; Sigma) in each immunization step. The final sera were tested for the ability to recognize a given antigen by Western blot. For mouse immunization, mice of the B10A-H2xBALB/CJ strain were immunized three or four times in 3-weeks interval with 30 μg purified protein mixed with Freund's Adjuvant (Sigma). Animal research complied with established protocols and was approved by the Animal Committee of the Institute of Molecular Genetics.

Preabsorbtion of Antibodies to Animal Powder. Before immunohistochemical staining, the sera were preadsorbed to amphioxus powder. Two frozen adult animals were ground in liquid nitrogen. Then 1 mL of acetone was added, and the mixture was left 30 min on ice. The powder was washed twice with acetone, dried and stored at −20 °C. To 1.5 mg powder, 1 mL of 10% BSA in 1× PBT (1× PBS, 0.1% Tween 20) was added and incubated for 30 min at 70 °C. After cooling, the crude serum was added to a final concentration of 1:100, and the solution was incubated overnight at 4 °C on a rotating platform. The next day the solution was centrifuged 5 min at 16,000 × *g*, and the supernatant containing the preadsorbed antibody was aliquoted and stored at −80 °C.

The rabbit polyclonal anti-5-HT antibody (20080; ImmunoStar) and mouse anti-acetylated β-tubulin (T6793; Sigma-Aldrich) were diluted 1:200 and 1:500, respectively.

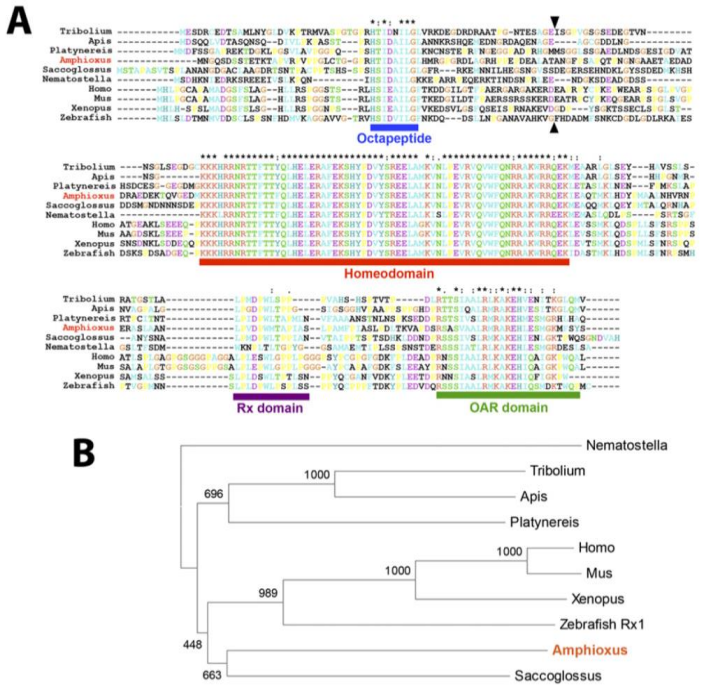

Fig. S1. Amino acid sequence alignment and phylogenetic tree of amphioxus Rx. (*A*) Amphioxus Rx contains the features characteristic for Rx proteins: the octapeptide, the Q50 homeodomain, the Rx domain, and the C-terminal otp, aristaless, and rax (OAR) domain. For brevity, a part of the amino acid sequence has been excluded (in the position of black arrowheads). (*B*) Neighbor-joining (NJ) phylogenetic tree of Rx protein sequences. The nonalignable regions have been excluded from the analysis. Numbers at the nodes represent the bootstrap support with 1,000 replicates. Accession nos.: *Nematostella*, XP_001634210.1; *Tribolium*, XP_973468.1; *Apis*, XP_001119966.1; *Platynereis*, AAU20320.1; *Homo sapiens* (Homo) Rx, NP_038463.1; *Mus* Rx, NP_038861.2; *Xenopus* Rx, AAB70267.1; Zebrafish Rx1, NP_571300.2; *Saccoglossus*, AAP79282.1.

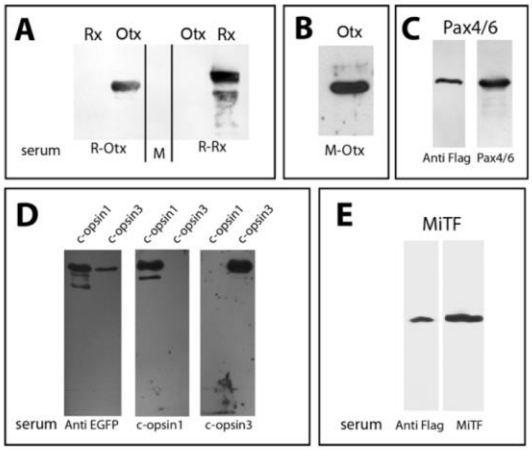

Fig. S2. Western blot analysis of antibodies generated in this work. HEK293T cell lines were transfected with an expression vector carrying Flag- (*A*–*C* and *E*) or EGFP-tagged (*D*) full-length coding sequences of the proteins indicated above each lane. Two days after transfection a whole-cell extract was prepared and subjected to Western blotting. The specificity of anti-Otx, -Rx, and -Pax4/6 antibodies was confirmed independently by recapitulating the whole-mount in situ hybridization patterns in immunohistochemical staining. (*A*) Rabbit antibodies against amphioxus Rx and Otx were tested on a double-lane blot containing the appropriate protein and another protein as a negative control. The lower band in the N-Rx–detected AmphiRx lane likely is caused by protein degradation. (*B*) Mouse polyclonal antibody against amphioxus Otx was generated to perform double immunohistochemical staining. (*C*) The rabbit antibody raised against amphioxus Pax4/6 recognizes the same band size as M2 anti-Flag (F1804; Sigma-Aldrich) antibody when tested with Flag-Pax4/6 fusion antigen. (*D*) Flag-tagged opsin antigens are recognized by anti-EGFP antibody as well as by mouse antibodies against amphioxus c-opsins. To exclude the possible cross-reactivity of anti–c-opsin antibodies, the antisera were tested with both c-opsin1 and c-opsin3 protein, showing specificity to the respective antigen. (*E*) Rabbit antibody raised against amphioxus Mitf recognizes the same band as M2 anti-Flag antibody when tested with Flag-Mitf fusion antigen.

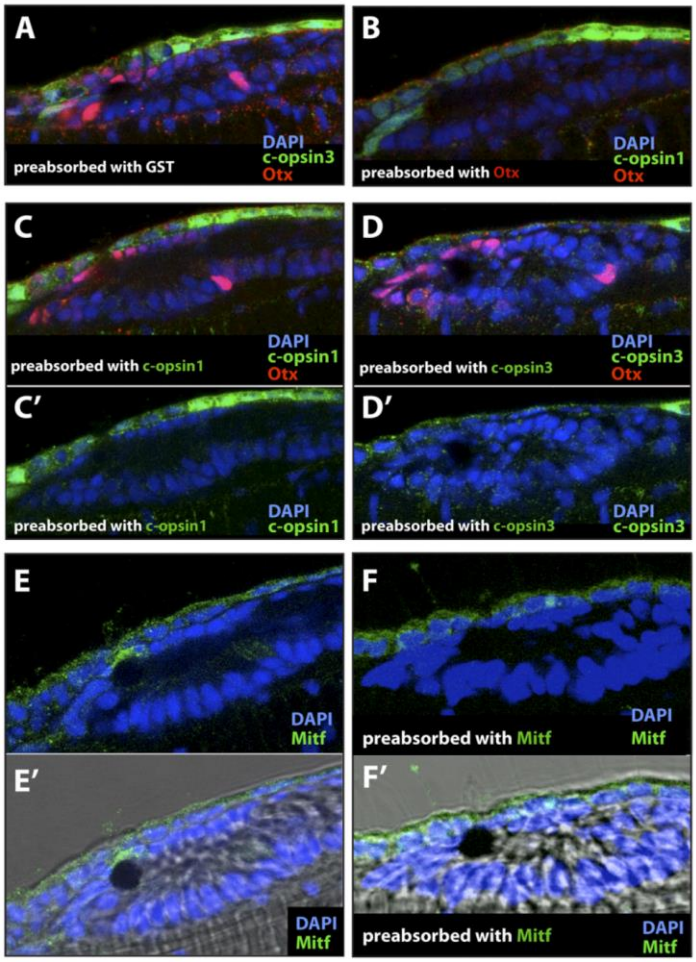

Fig. S3. Testing the specificity of c-opsin and Mitf antibodies. To test the specificity of antibodies for gene products with an unknown pattern of whole-mount in situ hybridization expression, we tested for the loss of specific signal after preadsorption of the antibody with its respective antigen used for immunization. Purified antigen was separated by SDS/PAGE, blotted to a nitrocellulose membrane, washed three times in PBT, and blocked with 10% BSA. Afterwards, the membranes with bound antigen were incubated for 4–6 h with the antibodies diluted to working concentration in 10% BSA. Following this preadsorption, the antibodies were used for immunohistochemical staining as described in *Experimental Procedures*. (*A*) As a negative control, the mixture of Otx and c-opsin3 antibodies was preadsorbed with GST not fused with any antigen. After such control preadsorption, the antibodies do not show any loss of specific immunohistochemical signal. (*B*) As a proof of principle, the preadsorption of the mixture of Otx and c-opsin1 antibodies with Otx antigen results in the specific loss of Otx but not c-opsin1 signal. (*C* and *C*′) Preadsorption of Otx/c-opsin1 antibody mixture with c-opsin1 antigen leads to specific loss of c-opsin1 staining. (*D* and *D*′) Likewise, only the signal of c-opsin3 is lost after preadsorbtion with c-opsin3 antigen. (*E*–*F*′) The signal of Mitf (*E* and *E*′) is lost when Mitf antibody is preadsorbed with Mitf antigen (*F* and *F*′).

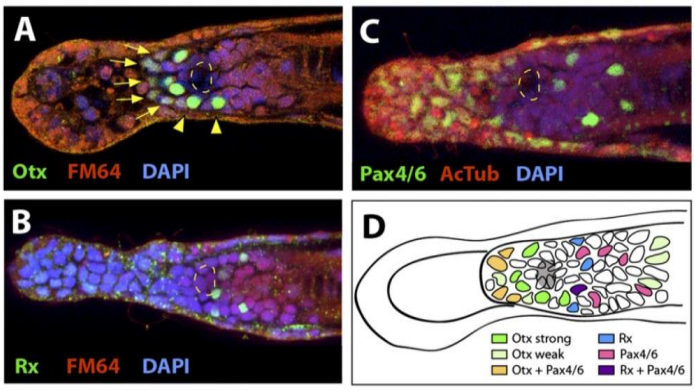

Fig. S4. Dorsal views on the cerebral vesicle floor plate. (*A*) *Otx* is expressed at two levels in the anterior tip of the cerebral vesicle: at a lower level in the very anterior row of cells (Row 1) and at a higher level in the adjacent more posterior row. The dashed yellow line demarcates the pigment spot. (*B*) *Rx* is expressed in few scattered cells in the anterior cerebral vesicle corresponding to the Row3/4 area. The mediolateral distribution of *rx*-positive nuclei varies among specimens. (*C*) Pax4/6 expression within the floor of the cerebral vesicle also is scattered, with the most anterior *pax4/6*-positive nuclei possibly overlapping some of the *rx*-positive nuclei. However, double immunohistochemistry could not be performed because the primary antibodies were from the same host species. (*D*) A schematic representation of the anterior part of an amphioxus larva showing the nuclei of the floor of the cerebral vesicle. The expression of *otx*, *rx*, and *pax4/6* is color-coded based on observations of multiple specimens. The coexpression of *rx* and *pax4/6* (purple) is only putative, based on position, and was not confirmed experimentally by double immunohistochemistry. The gray area represents the position of the pigment spot, which lies above the plane of the cerebral vesicle floor.

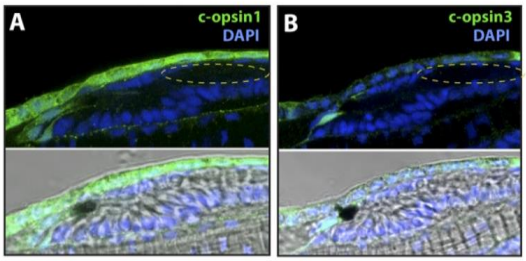

Fig. S5. Expression of *c-opsin1* and *c-opsin3* within the cerebral vesicle. The expression of *c-opsin1* (*A*) and *c-opsin3* (*B*) is restricted to Row1 cells in the anterior tip of the neural tube. No expression is observed within the lamellar body (marked with yellow dashed line). For easy orientation, the brightfield channels are included in the *Lower* panels.

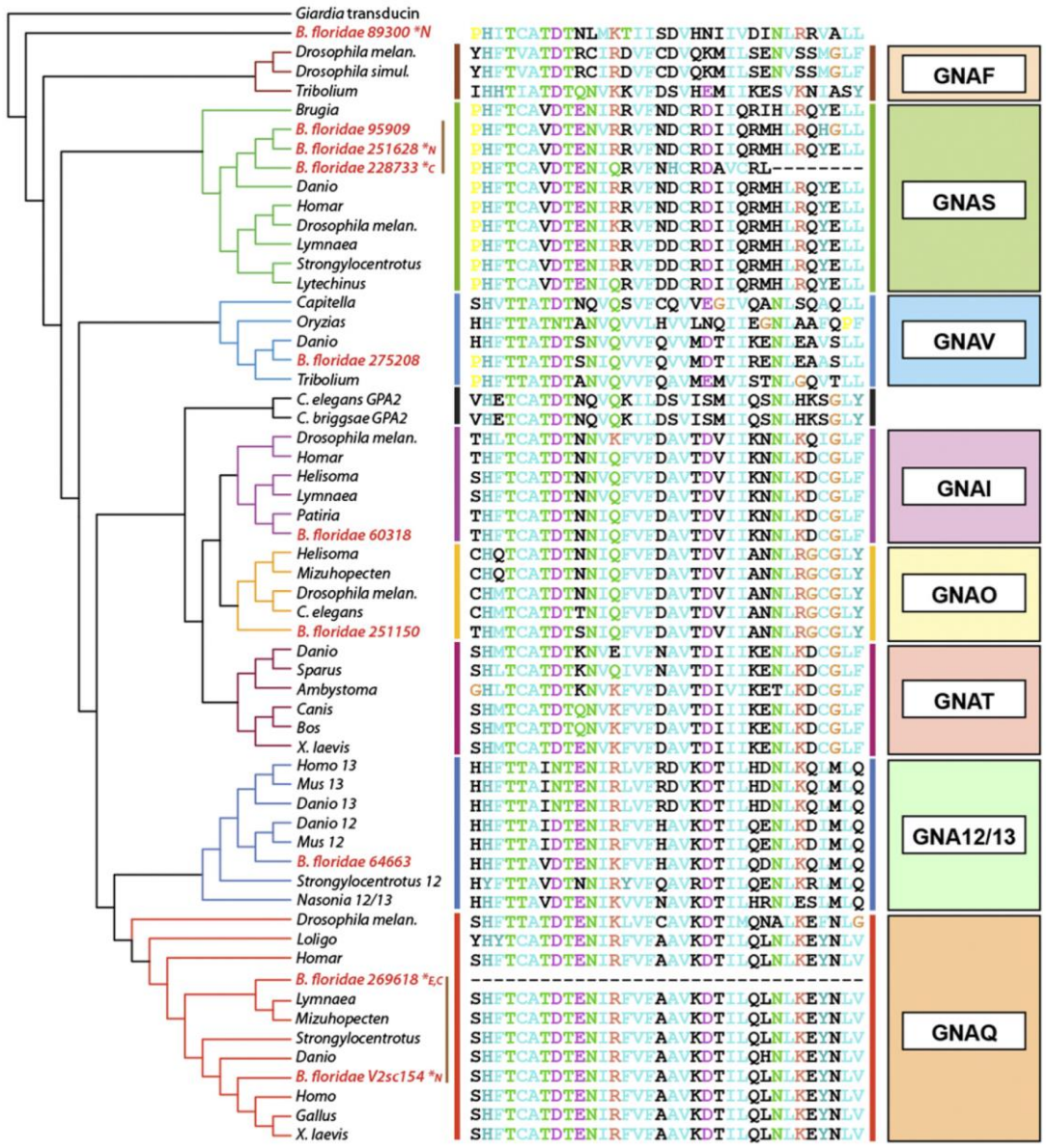

Fig. S6. Amino acid sequence alignment of Gα subunit C termini. The phylogenetic tree was inferred by the NJ method using *Giardia* transducin as an outgroup sequence. The missing sequence at either N or C termini did not allow all sequences of the phylogenetic tree to be inferred simultaneously. Therefore the tree shown here is based on two separate reconstructions. For this reason, the bootstrap support values are not shown; however, the tree reflects the topology of the two separate trees. In addition, the 12-amino acid C-terminal section is highly conserved in different subclasses and also supports the classification. Missing sequence information in the predicted amphioxus Gα subunits is marked by asterisks and a letter denoting the missing section (C, C-terminal portion; E, exon; N, N-terminal portion). The V1.0 predicted models mapping to the same genomic position in the V2.0 assembly are marked with a brown vertical bar. The gene model 251628 (GNAS subfamily) does not map to the same position; however, the overall sequence similarity suggests its identity with model ID 95909. The red-highlighted numbers of *B. floridae* sequences correspond to JGI *B. floridae* gene models V.1, except for V2sc154 referring to scaffold 154 in JGI *B. floridae* genome V2.0. Accession numbers: *Giardia* "transducin" - XP_001709656.1; *Drosophila melanogaster* GNAF - Q05337.1; *Drosophila simulans* GNAF - XP_002085174.1; *Tribolium* GNAF - XP_970742.1; *Brugia* GNAS - XP_001901198.1; *Danio* GNAS - XP_971664.2; *Homarus* GNAS - O16118.1; *Drosophila* GNAS - P20354.1; *Lymnaea* GNAS - CAA78808.1; *S. purpuratus* GNAS - NP_001001474.1; *Lytechinus* GNAS - AAS38583.1; *Capitella* GNAV - JGI Capca1:227716;

Legend continued on following page

Oryzias GNAV - (Oka et al, 2009); *Danio* GNAV - XP_699972.2; *Tribolium* GNAV - (Oka et al, 2009); *C. elegans* GPA2 - P22454.1; *C. briggsae* GPA2 - Q4VT35.1; *Drosophila* GNAI - P20353.2; *Homarus* GNAI - P41776.2; *Helisoma* GNAI - P51876.2; *Lymnaea* GNAI - P30682.3; *Patiria* GNAI - P30676.3; *Helisoma* GNAO - AAC41539.1; *Mizuhopecten* GNAO - O15976.3; *Drosophila* GNAO - P16378.1; *C. elegans* GNAO - P51875.3; *Danio* GNAT - AAL05601.1; *Sparus* GNAT - AAB41887.1; *Ambystoma* GNAT - AAC67569.1; *Canis* GNAT - NP_001003068.1; *Bos* GNAT - P04695.3; *X. laevis* GNAT - NP_001084030.1; *Homo* GNA13 - NP_006563.2; *Mus* GNA13 - NP_034433.3; *Danio* GNA13 - AAR25617.1; *Danio* GNA12 - NP_001013295.1; *Mus* GNA12 - NP_034432.1; *S. purpuratus* GNA12 - NP_001001476.1; *Nasonia* GNA12/13 - XP_001600076.1; *Drosophila* GNAQ - P23625.2; *Loligo* GNAQ - P38412.1; *Homarus* GNAQ - AAB49314.1; *Lymnaea* GNAQ - P38411.1; *Mizuhopecten* GNAQ - O15975.1; *S. purpuratus* GNAQ - NP_999835.1; *Danio* GNAQ - CAK04448.1; *Homo* GNAQ - NP_002063.2; *Gallus* GNAQ - NP_001026598.1; *X. laevis* GNAQ - AAH81126.1.

Table S1. Antibodies prepared in this work

Gene	Antigen amino acid sequence[†]	Host	Note[‡]	Dilution[§]
c-opsin1	NPLVYFAMNNQFRRYFQDLLCCGRRLFDA SASVNTCNTSAMPRHSPVFQKPDSDQYN GIQKSREPQMRTTGQNAPYRQWIEMQTIA VVVKADEVNNKFGEVKT*	Mouse	124039	1:200
c-opsin2	MNNQFRKCFLRSLNCRSQPRDPSSQQYTLK VGMSTSGSQAARTADRIKTVHVATANPQ DHRSSSGQAVEDNGGFRKSLTHSLPLN SISTLLEAEK*	Mouse	70446	1:200
c-opsin3	RVCCRQQAVPRVTPMDDNVHVRLGGEG PSQSQQFLPAGENVENVDMLEYVQE NCKPKADSLSTISE*	Mouse	74631	1:200
Otx	MAYMKSPYGMNGLSLSNPSIDLMTHHHH PGVGVSQYYNPTSAYTVTGQCPPPP*	Rabbit	275923	1:500
Otx	MAYMKSPYGMNGLSLSNPSIDLMTHHHH PGVGVSQYYNPTSAYTVTGQCPPPP*	Mouse	275923	1:500
Pax4/6	KLRNQRRSQDSDSSSPSRIPISSSFSTA TMYQPIAPPSAPVMSRSSHAGLTDSYS SLPPVPRWENFSVPGNMAPMPSMQQS RDQTSYSCMIPHSTAMTPRGYDSLALG SYNPTHAGHHVTTTHPSHMQAPSMPGH SHMSHANGGSAGLISPGVSVPVQVPG AVTEEMTSQPYWPRIQ*	Rabbit	69411	1:500
Rx	MNGQSDSSTETKTAPVRPVPPGLCT GGPRHTIDAILGLHMRGPGRDLAG RHPPEPDEALATYGDDDGQDQSEA LNLVVDILNASDDENRTVKPVTHS ANGFPSAPQTPNGNGAAETAEDADD RAEDEKT*	Rabbit	78608	1:250
MiTF	MDDVIDDIISLESSFDDSFNFLDAPM QQISSTMPLTSSLLDGFGTVGSLTP MVTANTSASCPADLTNIKKEPVQMS ESELKALAKDRQKKDNHNMNEWGYS EMVGWIGGVPEQAMALAKDRQKKDN HNIIERRRRFNINDRIKELGTLLPK TADPDMRWNKGTILKASVDYIRRLK KEHERMRHMEERQKQMEQMNRKMLLR IQELEMHCRAH*	Rabbit	247501	1:200

The asterisks in the protein sequence here denote the STOP codon, which has been always included in the plasmid.
[†]Amino acid sequence of the antigen used for immunization of the host species.
[‡]The protein ID in the JGI Amphioxus genome V1.0 (http://genome.jgi-psf.org/Brafl1/Brafl1.home.html).
[§]The dilution of antibodies for immunohistochemical staining.

REFERENCES

Abrahams, I. W. and D. S. Gregerson (1983). "Longitudinal study of serum antibody responses to bovine retinal S-antigen in endogenous granulomatous uveitis." Br J Ophthalmol 67(10): 681-684.

Adijanto, J., J. J. Castorino, Z. X. Wang, A. Maminishkis, G. B. Grunwald and N. J. Philp (2012). "Microphthalmia-associated transcription factor (MITF) promotes differentiation of human retinal pigment epithelium (RPE) by regulating microRNAs-204/211 expression." J Biol Chem 287(24): 20491-20503.

Agarwal, S. M. and J. Gupta (2005). "Comparative analysis of human intronless proteins." Biochem Biophys Res Commun 331(2): 512-519.

Anisimova, M. and O. Gascuel (2006). "Approximate likelihood-ratio test for branches: A fast, accurate, and powerful alternative." Syst Biol 55(4): 539-552.

Arendt, D. (2003). "Evolution of eyes and photoreceptor cell types." International Journal of Developmental Biology 47(7-8): 563-571.

Arendt, D. and J. Wittbrodt (2001). "Reconstructing the eyes of Urbilateria." Philosophical Transactions of the Royal Society of London. Series B: Biological Sciences 356(1414): 1545-1563.

Arendt, D., K. Tessmar, M. I. de Campos-Baptista, A. Dorresteijn and J. Wittbrodt (2002). "Development of pigment-cup eyes in the polychaete Platynereis dumerilii and evolutionary conservation of larval eyes in Bilateria." Development 129(5): 1143-1154.

Arendt, D., K. Tessmar-Raible, H. Snyman, A. W. Dorresteijn and J. Wittbrodt (2004). "Ciliary photoreceptors with a vertebrate-type opsin in an invertebrate brain." Science 306(5697): 869-871.

Arikawa, K., E. Eguchi, A. Yoshida, K. Aoki (1980). "Multiple extraocular photoreceptive areas on genitalia of butterfly, Papilio xuthus." Nature (288): 700-702.

Arkett, S. A., and A.N. Spencer (1986). "Neuronal mechanism of a hydromedusan shadow reflex. I. Identified reflex components and sequence of events " J. Comp. Physiol. A 159(159): 201–213.

Ausubel, F. M., R. Brent, R. E . Kingston, D. D. Moore, J. G. Seidman, J. A. Smith and K. Struhl (2003). Current Protocols in Molecular Biology. USA, John Wiley & Sons, Inc.

Bailes, H. J., L. Y. Zhuang and R. J. Lucas (2012). "Reproducible and sustained regulation of Galphas signalling using a metazoan opsin as an optogenetic tool." PLoS One 7(1): e30774.

Baldwin, J. M. (1993). "The probable arrangement of the helices in G protein-coupled receptors." Embo j 12(4): 1693-1703.

Beckmann, H., L. Hering, M. J. Henze, A. Kelber, P. A. Stevenson and G. Mayer (2015). "Spectral sensitivity in Onychophora (velvet worms) revealed by electroretinograms, phototactic behaviour and opsin gene expression." J Exp Biol 218(Pt 6): 915-922.

Belcastro, M., H. Song, S. Sinha, C. Song, P. H. Mathers and M. Sokolov (2012). "Phosphorylation of phosducin accelerates rod recovery from transducin translocation." Invest Ophthalmol Vis Sci 53(6): 3084-3091.

Bertrand, S. and H. Escriva (2011). "Evolutionary crossroads in developmental biology: amphioxus." Development 138(22): 4819-4830.

Betran, E., K. Thornton and M. Long (2002). "Retroposed new genes out of the X in Drosophila." Genome Res 12(12): 1854-1859.

Bielecki, J., A. K. Zaharoff, N. Y. Leung, A. Garm and T. H. Oakley (2014). "Ocular and extraocular expression of opsins in the rhopalium of Tripedalia cystophora (Cnidaria: Cubozoa)." PLoS One 9(6): e98870.

Bownds, D., J. Dawes, J. Miller and M. Stahlman (1972). "Phosphorylation of frog photoreceptor membranes induced by light." Nat New Biol 237(73): 125-127.

Breer, H. (1991). "Molecular reaction cascades in olfactory signal transduction." J Steroid Biochem Mol Biol 39(4b): 621-625.

Breer, H. (1993). "Second messenger signalling in olfaction." Ciba Found Symp 179: 97-109; discussion 109-114, 147-109.

Bridge, D., C. W. Cunningham, B. Schierwater, R. DeSalle and L. W. Buss (1992). "Class-level relationships in the phylum Cnidaria: evidence from mitochondrial genome structure." Proceedings of the National Academy of Sciences of the United States of America 89(18): 8750-8753.

Brosius, J. (1999). "Many G-protein-coupled receptors are encoded by retrogenes." Trends Genet 15(8): 304-305.

Brosius, J. and S. J. Gould (1992). "On "genomenclature": a comprehensive (and respectful) taxonomy for pseudogenes and other "junk DNA"." Proc Natl Acad Sci U S A 89(22): 10706-10710.

Bryson-Richardson, R. J., D. W. Logan, P. D. Currie and I. J. Jackson (2004). "Large-scale analysis of gene structure in rhodopsin-like GPCRs: evidence for widespread loss of an ancient intron." Gene 338(1): 15-23.

Burns, M. E. and V. Y. Arshavsky (2005). "Beyond counting photons: trials and trends in vertebrate visual transduction." Neuron 48(3): 387-401.

Carosa, E., Z. Kozmik, J. E. Rall and J. Piatigorsky (2002). "Structure and expression of the scallop Omega-crystallin gene. Evidence for convergent evolution of promoter sequences." J Biol Chem 277(1): 656-664.

Castellano, S., A. V. Lobanov, C. Chapple, S. V. Novoselov, M. Albrecht, D. Hua, A. Lescure, T. Lengauer, A. Krol, V. N. Gladyshev and R. Guigo (2005). "Diversity and functional plasticity of eukaryotic selenoproteins: identification and characterization of the SelJ family." Proc Natl Acad Sci U S A 102(45): 16188-16193.

Chatterjee, D., C. E. Eckert, C. Slavov, K. Saxena, B. Furtig, C. R. Sanders, V. V. Gurevich, J. Wachtveitl and H. Schwalbe (2015). "Influence of Arrestin on the Photodecay of Bovine Rhodopsin." Angew Chem Int Ed Engl 54(46): 13555-13560.

Chen, C. K., J. Inglese, R. J. Lefkowitz and J. B. Hurley (1995). "Ca(2+)-dependent interaction of recoverin with rhodopsin kinase." J Biol Chem 270(30): 18060-18066.

Cho, Y. K. and D. Li (2016). "Optogenetics: Basic Concepts and Their Development." Methods Mol Biol 1408: 1-17.

Coates, M. M. (2003). "Visual ecology and functional morphology of cubozoa (cnidaria)." Integr Comp Biol 43(4): 542-548.

Conant, F. (1897). "Notes on the cubomedusae." Johns Hopkins University Circulars (No. 132).

Cortesi, F., Z. Musilova, S. M. Stieb, N. S. Hart, U. E. Siebeck, M. Malmstrom, O. K. Torresen, S. Jentoft, K. L. Cheney, N. J. Marshall, K. L. Carleton and W. Salzburger (2015). "Ancestral duplications and highly dynamic opsin gene evolution in percomorph fishes." Proc Natl Acad Sci U S A 112(5): 1493-1498.

D'Alessio, G. (2002). "The evolution of monomeric and oligomeric betagamma-type crystallins. Facts and hypotheses." Eur J Biochem 269(13): 3122-3130.

Davies, W. L., J. A. Cowing, L. S. Carvalho, I. C. Potter, A. E. Trezise, D. M. Hunt and S. P. Collin (2007). "Functional characterization, tuning, and regulation of visual pigment gene expression in an anadromous lamprey." Faseb j 21(11): 2713-2724.

Davies, W. L., M. W. Hankins and R. G. Foster (2010). "Vertebrate ancient opsin and melanopsin: divergent irradiance detectors." Photochem Photobiol Sci 9(11): 1444-1457.

de Jong, W. W., J. A. Leunissen and C. E. Voorter (1993). "Evolution of the alpha-crystallin/small heat-shock protein family." Mol Biol Evol 10(1): 103-126.

Deming, J. D., J. S. Pak, J. A. Shin, B. M. Brown, M. K. Kim, M. H. Aung, E. J. Lee, M. T. Pardue and C. M. Craft (2015). "Arrestin 1 and Cone Arrestin 4 Have Unique Roles in Visual Function in an All-Cone Mouse Retina." Invest Ophthalmol Vis Sci 56(13): 7618-7628.

Eakin, R. M. (1982). "Morphology of invertebrate photoreceptors." Methods Enzymol 81: 17-25.

Ekstrom, P., A. Garm, J. Palsson, T. S. Vihtelic and D. E. Nilsson (2008). "Immunohistochemical evidence for multiple photosystems in box jellyfish." Cell and Tissue Research 333(1): 115-124.

Fernald, R. D. (2006). "Casting a genetic light on the evolution of eyes." Science 313(5795): 1914-1918.

Fernandez, A., Y. H. Tzeng and S. B. Hsu (2011). "Subfunctionalization reduces the fitness cost of gene duplication in humans by buffering dosage imbalances." BMC Genomics 12: 604.

Feuda, R., O. Rota-Stabelli, T. H. Oakley and D. Pisani (2014). "The comb jelly opsins and the origins of animal phototransduction." Genome Biol Evol 6(8): 1964-1971.

Feuda, R., S. C. Hamilton, J. O. McInerney and D. Pisani (2012). "Metazoan opsin evolution reveals a simple route to animal vision." Proceedings of the National Academy of Sciences of the United States of America 109(46): 18868-18872.

Finn, J. T., E. C. Solessio and K. W. Yau (1997). "A cGMP-gated cation channel in depolarizing photoreceptors of the lizard parietal eye." Nature 385(6619): 815-819.

Fitzgibbon, J., A. Hope, S. J. Slobodyanyuk, J. Bellingham, J. K. Bowmaker and D. M. Hunt (1995). "The rhodopsin-encoding gene of bony fish lacks introns." Gene 164(2): 273-277.

Foster, R. G. and M. W. Hankins (2002). "Non-rod, non-cone photoreception in the vertebrates." Prog Retin Eye Res 21(6): 507-527.

Foster, R. G., M. S. Grace, I. Provencio, W. J. Degrip and J. M. Garcia-Fernandez (1994). "Identification of vertebrate deep brain photoreceptors." Neurosci Biobehav Rev 18(4): 541-546.

Fredriksson, R., M. C. Lagerstrom, L. G. Lundin and H. B. Schioth (2003). "The G-protein-coupled receptors in the human genome form five main families. Phylogenetic analysis, paralogon groups, and fingerprints." Mol Pharmacol 63(6): 1256-1272.

Fridmanis, D., R. Fredriksson, I. Kapa, H. B. Schioth and J. Klovins (2007). "Formation of new genes explains lower intron density in mammalian Rhodopsin G protein-coupled receptors." Mol Phylogenet Evol 43(3): 864-880.

Garen-Fazio, S., E. J. Neer and C. J. Schmidt (1991). "Identification of a retinal protein in Drosophila with antibody to the alpha subunit of bovine brain G(o) protein." J Comp Neurol 309(1): 17-26.

Garm, A. and J. Bielecki (2008). "Swim pacemakers in box jellyfish are modulated by the visual input." J Comp Physiol A Neuroethol Sens Neural Behav Physiol 194(7): 641-651.

Garm, A. and P. Ekstrom (2010). "Evidence for multiple photosystems in jellyfish." Int Rev Cell Mol Biol 280: 41-78.

Garm, A. and S. Mori (2009). "Multiple photoreceptor systems control the swim pacemaker activity in box jellyfish." J Exp Biol 212(Pt 24): 3951-3960.

Garm, A., F. Andersson and D. E. Nilsson (2008). "Unique structure and optics of the lesser eyes of the box jellyfish Tripedalia cystophora." Vision Research 48(8): 1061-1073.

Garm, A., I. Hedal, M. Islin and D. Gurska (2013). "Pattern- and contrast-dependent visual response in the box jellyfish Tripedalia cystophora." J Exp Biol 216(Pt 24): 4520-4529.

Garm, A., M. O'Connor, L. Parkefelt and D. E. Nilsson (2007). "Visually guided obstacle avoidance in the box jellyfish Tripedalia cystophora and Chiropsella bronzie." J Exp Biol 210(Pt 20): 3616-3623.

Garm, A., M. Oskarsson and D. E. Nilsson (2011). "Box jellyfish use terrestrial visual cues for navigation." Curr Biol 21(9): 798-803.

Garm, A., P. Ekstrom, M. Boudes and D. E. Nilsson (2006). "Rhopalia are integrated parts of the central nervous system in box jellyfish." Cell Tissue Res 325(2): 333-343.

Gentles, A. J. and S. Karlin (1999). "Why are human G-protein-coupled receptors predominantly intronless?" Trends Genet 15(2): 47-49.

Gloriam, D. E., T. K. Bjarnadottir, Y. L. Yan, J. H. Postlethwait, H. B. Schioth and R. Fredriksson (2005). "The repertoire of trace amine G-protein-coupled receptors: large expansion in zebrafish." Mol Phylogenet Evol 35(2): 470-482.

Gomez Mdel, P., J. M. Angueyra and E. Nasi (2009). "Light-transduction in melanopsin-expressing photoreceptors of Amphioxus." Proc Natl Acad Sci U S A 106(22): 9081-9086.

Gomez, M. P. and E. Nasi (2000). "Light transduction in invertebrate hyperpolarizing photoreceptors: possible involvement of a Go-regulated guanylate cyclase." J Neurosci 20(14): 5254-5263.

Graham, D. M., K. Y. Wong, P. Shapiro, C. Frederick, K. Pattabiraman and D. M. Berson (2008). "Melanopsin ganglion cells use a membrane-associated rhabdomeric phototransduction cascade." J Neurophysiol 99(5): 2522-2532.

Guindon, S., J. F. Dufayard, V. Lefort, M. Anisimova, W. Hordijk and O. Gascuel (2010). "New algorithms and methods to estimate maximum-likelihood phylogenies: assessing the performance of PhyML 3.0." Syst Biol 59(3): 307-321.

Hall, T. A. (1999). "BioEdit: a user-friendly biological sequence alignment editor and analysis program for Windows 95/98/NT." Nucleic Acids Symposium Series 41 95-98.

Hardie, R. C. (2014). "Photosensitive TRPs." Handb Exp Pharmacol 223: 795-826.

Hardie, R. C. and M. Juusola (2015). "Phototransduction in Drosophila." Curr Opin Neurobiol 34: 37-45.

Henderson, B. and A. C. Martin (2014). "Protein moonlighting: a new factor in biology and medicine." Biochem Soc Trans 42(6): 1671-1678.

Hill, A. E. and E. J. Sorscher (2006). "The non-random distribution of intronless human genes across molecular function categories." FEBS Lett 580(18): 4303-4305.

Hofmann, C. M., N. J. Marshall, K. Abdilleh, Z. Patel, U. E. Siebeck and K. L. Carleton (2012). "Opsin evolution in damselfish: convergence, reversal, and parallel evolution across tuning sites." J Mol Evol 75(3-4): 79-91.

Hohenegger, M., M. Waldhoer, W. Beindl, B. Boing, A. Kreimeyer, P. Nickel, C. Nanoff and M. Freissmuth (1998). "Gsalpha-selective G protein antagonists." Proc Natl Acad Sci U S A 95(1): 346-351.

Holland, L. Z., V. Laudet and M. Schubert (2004). "The chordate amphioxus: an emerging model organism for developmental biology." Cell Mol Life Sci 61(18): 2290-2308.

Hurles, M. (2004). "Gene duplication: the genomic trade in spare parts." PLoS Biol 2(7): E206.

Innan, H. and F. Kondrashov (2010). "The evolution of gene duplications: classifying and distinguishing between models." Nat Rev Genet 11(2): 97-108.

Jagger, W. S. and P. J. Sands (1999). "A wide-angle gradient index optical model of the crystalline lens and eye of the octopus." Vision Res 39(17): 2841-2852.

Jeffery, C. J. (1999). "Moonlighting proteins." Trends Biochem Sci 24(1): 8-11.

Jonasova, K. and Z. Kozmik (2008). "Eye evolution: lens and cornea as an upgrade of animal visual system." Seminars in Cell and Developmental Biology 19(2): 71-81.

Kabza, M., J. Ciomborowska and I. Makalowska (2014). "RetrogeneDB--a database of animal retrogenes." Mol Biol Evol 31(7): 1646-1648.

Kang, S. W. and W. J. Kuenzel (2015). "Deep-brain photoreceptors (DBPs) involved in the photoperiodic gonadal response in an avian species, Gallus gallus." Gen Comp Endocrinol 211: 106-113.

Karlsson, J., J. von Hofsten and P. E. Olsson (2001). "Generating transparent zebrafish: a refined method to improve detection of gene expression during embryonic development." Mar Biotechnol (NY) 3(6): 522-527.

Kaupp, U. B. (2010). "Olfactory signalling in vertebrates and insects: differences and commonalities." Nat Rev Neurosci 11(3): 188-200.

Kawamura, S. and S. Tachibanaki (2008). "Rod and cone photoreceptors: molecular basis of the difference in their physiology." Comp Biochem Physiol A Mol Integr Physiol 150(4): 369-377.

Koch, K. W. and D. Dell'Orco (2015). "Protein and Signaling Networks in Vertebrate Photoreceptor Cells." Front Mol Neurosci 8: 67.

Kojima, D., A. Terakita, T. Ishikawa, Y. Tsukahara, A. Maeda and Y. Shichida (1997). "A novel Go-mediated phototransduction cascade in scallop visual cells." Journal of Biological Chemistry 272(37): 22979-22982.

Koop, D. and L. Z. Holland (2008). "The basal chordate amphioxus as a simple model for elucidating developmental mechanisms in vertebrates." Birth Defects Res C Embryo Today 84(3): 175-187.

Koyanagi, M. and A. Terakita (2008). "Gq-coupled rhodopsin subfamily composed of invertebrate visual pigment and melanopsin." Photochemistry and Photobiology 84(4): 1024-1030.

Koyanagi, M. and A. Terakita (2014). "Diversity of animal opsin-based pigments and their optogenetic potential." Biochim Biophys Acta 1837(5): 710-716.

Koyanagi, M., A. Terakita, K. Kubokawa and Y. Shichida (2002). "Amphioxus homologs of Go-coupled rhodopsin and peropsin having 11-cis- and all-trans-retinals as their chromophores." FEBS Letters 531(3): 525-528.

Koyanagi, M., K. Kubokawa, H. Tsukamoto, Y. Shichida and A. Terakita (2005). "Cephalochordate melanopsin: evolutionary linkage between invertebrate visual cells and vertebrate photosensitive retinal ganglion cells." Current Biology 15(11): 1065-1069.

Koyanagi, M., K. Ono, H. Suga, N. Iwabe and T. Miyata (1998). "Phospholipase C cDNAs from sponge and hydra: antiquity of genes involved in the inositol phospholipid signaling pathway." FEBS Lett 439(1-2): 66-70.

Koyanagi, M., K. Takano, H. Tsukamoto, K. Ohtsu, F. Tokunaga and A. Terakita (2008). "Jellyfish vision starts with cAMP signaling mediated by opsin-G(s) cascade." Proceedings of the National Academy of Sciences of the United States of America 105(40): 15576-15580.

Kozmik, Z. (2008). "The role of Pax genes in eye evolution." Brain Research Bulletin 75(2-4): 335-339.

Kozmik, Z., J. Ruzickova, K. Jonasova, Y. Matsumoto, P. Vopalensky, I. Kozmikova, H. Strnad, S. Kawamura, J. Piatigorsky, V. Paces and C. Vlcek (2008a). "Assembly of the cnidarian camera-type eye from vertebrate-like components." Proceedings of the National Academy of Sciences of the United States of America 105(26): 8989-8993.

Kozmik, Z., M. Daube, E. Frei, B. Norman, L. Kos, L. J. Dishaw, M. Noll and J. Piatigorsky (2003). "Role of Pax genes in eye evolution: a cnidarian PaxB gene uniting Pax2 and Pax6 functions." Dev Cell 5(5): 773-785.

Kozmik, Z., S. K. Swamynathan, J. Ruzickova, K. Jonasova, V. Paces, C. Vlcek and J. Piatigorsky (2008b). "Cubozoan crystallins: evidence for convergent evolution of pax regulatory sequences." Evol Dev 10(1): 52-61.

Krupnick, J. G., O. B. Goodman, Jr., J. H. Keen and J. L. Benovic (1997). "Arrestin/clathrin interaction. Localization of the clathrin binding domain of nonvisual arrestins to the carboxy terminus." J Biol Chem 272(23): 15011-15016.

Kuhn, H., N. Bennett, M. Michel-Villaz and M. Chabre (1981). "Interactions between photoexcited rhodopsin and GTP-binding protein: kinetic and stoichiometric analyses from light-scattering changes." Proc Natl Acad Sci U S A 78(11): 6873-6877.

Kuhn, H., S. W. Hall and U. Wilden (1984). "Light-induced binding of 48-kDa protein to photoreceptor membranes is highly enhanced by phosphorylation of rhodopsin." FEBS Lett 176(2): 473-478.

Kumbalasiri, T. and I. Provencio (2005). "Melanopsin and other novel mammalian opsins." Exp Eye Res 81(4): 368-375.

Lacalli, T. C. (2004). "Sensory systems in amphioxus: a window on the ancestral chordate condition." Brain Behav Evol 64(3): 148-162.

Land, M. F. and D-E. Nilsson (2002). "Animal eyes." Oxford: Oxford University Press.

Land, M. F. and R. D. Fernald (1992). "The evolution of eyes." Annu Rev Neurosci 15: 1-29.

Larkin, M. A., G. Blackshields, N. P. Brown, R. Chenna, P. A. McGettigan, H. McWilliam, F. Valentin, I. M. Wallace, A. Wilm, R. Lopez, J. D. Thompson, T. J. Gibson and D. G. Higgins (2007). "Clustal W and Clustal X version 2.0." Bioinformatics 23(21): 2947-2948.

Laska, G. and M. Hundgen (1982). "Morphologie und ultrastruktur der lichtsinnesorgane von Tripedalia cystophora Conant (Cnidaria, Cubozoa)." Zool Jb Anat(108): 107–123.

Laska-Mehnert, G. (1985). "Cytologishe veranderungen wahrend der metamorphose des cubopolypen Tripedalia cystophora (Cubozoa, Carybdeidae) in die medusae." Helgolander wiss. Meeresunters 39: 129-164.

Le, S. Q. and O. Gascuel (2008). "An improved general amino acid replacement matrix." Molecular Biology and Evolution 25(7): 1307-1320.

Liegertova, M., J. Pergner, I. Kozmikova, P. Fabian, A. R. Pombinho, H. Strnad, J. Paces, C. Vlcek, P. Bartunek and Z. Kozmik (2015). "Cubozoan genome illuminates functional diversification of opsins and photoreceptor evolution." Sci Rep 5: 11885.

Lu, S. Y., H. C. Wan, M. Li and Y. L. Lin (2010). "Subcellular localization of Mitf in monocytic cells." Histochem Cell Biol 133(6): 651-658.

Luo, D. G., T. Xue and K. W. Yau (2008). "How vision begins: an odyssey." Proc Natl Acad Sci U S A 105(29): 9855-9862.

Lynch, M. and A. Force (2000). "The probability of duplicate gene preservation by subfunctionalization." Genetics 154(1): 459-473.

Lynch, M. and J. S. Conery (2000). "The evolutionary fate and consequences of duplicate genes." Science 290(5494): 1151-1155.

Magadum, S., U. Banerjee, P. Murugan, D. Gangapur and R. Ravikesavan (2013). "Gene duplication as a major force in evolution." J Genet 92(1): 155-161.

Marin, E. P., A. G. Krishna, T. A. Zvyaga, J. Isele, F. Siebert and T. P. Sakmar (2000). "The amino terminus of the fourth cytoplasmic loop of rhodopsin modulates rhodopsin-transducin interaction." Journal of Biological Chemistry 275(3): 1930-1936.

Marks, P. S. (1976). "Nervous control of light responses in the sea anemone, Calamactis praelongus." J Exp Biol 65(1): 85-96.

Martin, V. J. (2002). "Photoreceptors of cnidarians." Can. J. Zool. 80: 1703-1722.

Martinez-Morales, J. R., V. Dolez, I. Rodrigo, R. Zaccarini, L. Leconte, P. Bovolenta and S. Saule (2003). "OTX2 activates the molecular network underlying retina pigment epithelium differentiation." J Biol Chem 278(24): 21721-21731.

Mason, B. M. and J. H. Cohen (2012). "Long-wavelength photosensitivity in coral planula larvae." Biol Bull 222(2): 88-92.

Mason, B., M. Beard, M. W. Miller (2011). "Coral larvae settle at a higher frequency on red surfaces." Coral Reefs(30): 667-676.

Mason, B., M. Schmale, P. Gibbs, M. W. Miller, Q. Wang, K. Levay, V. Shestopalov and V. Z. Slepak (2012). "Evidence for multiple phototransduction pathways in a reef-building coral." PLoS One 7(12): e50371.

Matsumoto, Y., S. Fukamachi, H. Mitani and S. Kawamura (2006). "Functional characterization of visual opsin repertoire in Medaka (Oryzias latipes)." Gene 371(2): 268-278.

Maximov, V. V. (2000). "Environmental factors which may have led to the appearance of colour vision." Philos Trans R Soc Lond B Biol Sci 355(1401): 1239-1242.

Milligan, G. and E. Kostenis (2006). "Heterotrimeric G-proteins: a short history." Br J Pharmacol 147 Suppl 1: S46-55

Molday, R. S. and O. L. Moritz (2015). "Photoreceptors at a glance." J Cell Sci 128(22): 4039-4045.

Morris, A., J. K. Bowmaker and D. M. Hunt (1993). "The molecular basis of a spectral shift in the rhodopsins of two species of squid from different photic environments." Proc Biol Sci 254(1341): 233-240.

Mundy, B. (1998). "Role of light intensity and spectral quality in coral settlement: implications for depth-dependent settlement." Journal of Experimental Marine Biology and Ecology (223): 235-255.

Musio, C., S. Santillo, C. Taddei-Ferretti, L. J. Robles, R. Vismara, L. Barsanti and P. Gualtieri (2001). "First identification and localization of a visual pigment in Hydra (Cnidaria, Hydrozoa)." J Comp Physiol A 187(1): 79-81.

Nathans, J. (1990). "Determinants of visual pigment absorbance: identification of the retinylidene Schiff's base counterion in bovine rhodopsin." Biochemistry 29(41): 9746-9752.

Newman, T. and B. J. Trask (2003). "Complex evolution of 7E olfactory receptor genes in segmental duplications." Genome Res 13(5): 781-793.

Nickle, B., S. E. Wilkie, J. A. Cowing, D. M. Hunt and P. R. Robinson (2006). "Vertebrate opsins belonging to different classes vary in constitutively active properties resulting from salt-bridge mutations." Biochemistry 45(23): 7307-7313.

Nilsson, D. E. and S. Pelger (1994). "A pessimistic estimate of the time required for an eye to evolve." Proc Biol Sci 256(1345): 53-58.

Nilsson, D. E., L. Gislen, M. M. Coates, C. Skogh and A. Garm (2005). "Advanced optics in a jellyfish eye." Nature 435(7039): 201-205.

Nordstrom, K., R. Wallen, J. Seymour and D. Nilsson (2003). "A simple visual system without neurons in jellyfish larvae." Proc Biol Sci 270(1531): 2349-2354.

Nordstrom, K., T. A. Larsson and D. Larhammar (2004). "Extensive duplications of phototransduction genes in early vertebrate evolution correlate with block (chromosome) duplications." Genomics 83(5): 852-872.

O'Connor, M., A. Garm and D. E. Nilsson (2009). "Structure and optics of the eyes of the box jellyfish Chiropsella bronzie." J Comp Physiol A Neuroethol Sens Neural Behav Physiol 195(6): 557-569.

O'Connor, M., A. Garm, J. N. Marshall, N. S. Hart, P. Ekstrom, C. Skogh and D. E. Nilsson (2010a). "Visual pigment in the lens eyes of the box jellyfish Chiropsella bronzie." Proc Biol Sci 277(1689): 1843-1848.

O'Connor, M., D. E. Nilsson and A. Garm (2010b). "Temporal properties of the lens eyes of the box jellyfish Tripedalia cystophora." J Comp Physiol A Neuroethol Sens Neural Behav Physiol 196(3): 213-220.

Palczewski, K., J. H. McDowell, S. Jakes, T. S. Ingebritsen and P. A. Hargrave (1989). "Regulation of rhodopsin dephosphorylation by arrestin." J Biol Chem 264(27): 15770-15773.

Panda, S., S. K. Nayak, B. Campo, J. R. Walker, J. B. Hogenesch and T. Jegla (2005). "Illumination of the melanopsin signaling pathway." Science 307(5709): 600-604.

Parkefelt, L. and P. Ekstrom (2009). "Prominent system of RFamide immunoreactive neurons in the rhopalia of box jellyfish (Cnidaria: Cubozoa)." J Comp Neurol 516(3): 157-165.

Parkefelt, L., C. Skogh, D. E. Nilsson and P. Ekstrom (2005). "Bilateral symmetric organization of neural elements in the visual system of a coelenterate, Tripedalia cystophora (Cubozoa)." Journal of Comparative Neurology 492(3): 251-262.

Pearson, W. R. (2016). "Finding Protein and Nucleotide Similarities with FASTA." Curr Protoc Bioinformatics 53: 3.9.1-3.9.25.

Pearson, W. R. and D. J. Lipman (1988). "Improved tools for biological sequence comparison." Proceedings of the National Academy of Sciences of the United States of America 85(8): 2444-2448.

Petie, R., A. Garm and D. E. Nilsson (2011). "Visual control of steering in the box jellyfish Tripedalia cystophora." Journal of Experimental Biology 214(Pt 17): 2809-2815.

Pfister, C., M. Chabre, J. Plouet, V. V. Tuyen, Y. De Kozak, J. P. Faure and H. Kuhn (1985). "Retinal S antigen identified as the 48K protein regulating light-dependent phosphodiesterase in rods." Science 228(4701): 891-893.

Piatigorsky, J. (2003). "Gene sharing, lens crystallins and speculations on an eye/ear evolutionary relationship." Integr Comp Biol 43(4): 492-499.

Piatigorsky, J. (2007). Gene Sharing and Evolution: The Diversity of Protein Functions. Cambridge, Massachusetts, Harvard University Press.

Piatigorsky, J. and G. J. Wistow (1989). "Enzyme/crystallins: gene sharing as an evolutionary strategy." Cell 57(2): 197-199.

Piatigorsky, J. and G. Wistow (1991). "The recruitment of crystallins: new functions precede gene duplication." Science 252(5009): 1078-1079.

Piatigorsky, J. and Z. Kozmik (2004). "Cubozoan jellyfish: an Evo/Devo model for eyes and other sensory systems." International Journal of Developmental Biology 48(8-9): 719-729.

Piatigorsky, J., B. Norman, L. J. Dishaw, L. Kos, J. Horwitz, P. J. Steinbach and Z. Kozmik (2001). "J3-crystallin of the jellyfish lens: similarity to saposins." Proc Natl Acad Sci U S A 98(22): 12362-12367.

Piatigorsky, J., J. Horwitz and B. L. Norman (1993). "J1-crystallins of the cubomedusan jellyfish lens constitute a novel family encoded in at least three intronless genes." J Biol Chem 268(16): 11894-11901.

Piatigorsky, J., J. Horwitz, T. Kuwabara and C. E. Cutress (1989). "The cellular eye lens and crystallins of cubomedusan jellyfish." J Comp Physiol A 164(5): 577-587.

Pichaud, F., A. Briscoe and C. Desplan (1999). "Evolution of color vision." Curr Opin Neurobiol 9(5): 622-627.

Plachetzki, D. C., B. M. Degnan and T. H. Oakley (2007). "The origins of novel protein interactions during animal opsin evolution." PLoS One 2(10): e1054.

Plachetzki, D. C., C. R. Fong and T. H. Oakley (2010). "The evolution of phototransduction from an ancestral cyclic nucleotide gated pathway." Proc Biol Sci 277(1690): 1963-1969.

Plachetzki, D. C., C. R. Fong and T. H. Oakley (2012). "Cnidocyte discharge is regulated by light and opsin-mediated phototransduction." BMC Biol 10(1): 17.

Porter, M. L., J. R. Blasic, M. J. Bok, E. G. Cameron, T. Pringle, T. W. Cronin and P. R. Robinson (2012). "Shedding new light on opsin evolution." Proc Biol Sci 279(1726): 3-14.

Pugh, E. N., Jr., S. Nikonov and T. D. Lamb (1999). "Molecular mechanisms of vertebrate photoreceptor light adaptation." Curr Opin Neurobiol 9(4): 410-418.

Rando, R. R. (2001). "The biochemistry of the visual cycle." Chem Rev 101(7): 1881-1896.

Rennison, D. J., G. L. Owens and J. S. Taylor (2012). "Opsin gene duplication and divergence in ray-finned fish." Mol Phylogenet Evol 62(3): 986-1008.

Robinson, P. R., G. B. Cohen, E. A. Zhukovsky and D. D. Oprian (1992). "Constitutively active mutants of rhodopsin." Neuron 9(4): 719-725.

Roy, S. W. (2004). "The origin of recent introns: transposons?" Genome Biol 5(12): 251.

Roy, S. W. and W. Gilbert (2005a). "Complex early genes." Proc Natl Acad Sci U S A 102(6): 1986-1991.

Roy, S. W. and W. Gilbert (2005b). "Rates of intron loss and gain: implications for early eukaryotic evolution." Proc Natl Acad Sci U S A 102(16): 5773-5778.

Roy, S. W., A. Fedorov and W. Gilbert (2003). "Large-scale comparison of intron positions in mammalian genes shows intron loss but no gain." Proc Natl Acad Sci U S A 100(12): 7158-7162.

Rozen, S. and H. Skaletsky (2000). "Primer3 on the WWW for general users and for biologist programmers." Methods Mol Biol 132: 365-386.

Ruiz, S. and R. Anadon (1991). "The fine structure of lamellate cells in the brain of amphioxus (Branchiostoma lanceolatum, Cephalochordata)." Cell Tissue Res 263(3): 597-600.

Sakmar, T. P., S. T. Menon, E. P. Marin and E. S. Awad (2002). "Rhodopsin: insights from recent structural studies." Annual Review of Biophysics and Biomolecular Structure 31: 443-484.

Sakurai, K., J. Chen, S. C. Khani and V. J. Kefalov (2015). "Regulation of mammalian cone phototransduction by recoverin and rhodopsin kinase." J Biol Chem 290(14): 9239-9250.

Sawyer S. J., H. B. Dowse, and J. M. Shick (1994). "Neurophysiological correlates of the behavioral response to light in the sea anemone Anthopleura elegantissima." Biol. Bull. (Woods Hole, Mass.) 186(186): 195-201.

Shabalina, S. A., A. Y. Ogurtsov, A. N. Spiridonov, P. S. Novichkov, N. A. Spiridonov and E. V. Koonin (2010). "Distinct patterns of expression and evolution of intronless and intron-containing mammalian genes." Mol Biol Evol 27(8): 1745-1749.

Shinzato, C., E. Shoguchi, T. Kawashima, M. Hamada, K. Hisata, M. Tanaka, M. Fujie, M. Fujiwara, R. Koyanagi, T. Ikuta, A. Fujiyama, D. J. Miller and N. Satoh (2011). "Using the Acropora digitifera genome to understand coral responses to environmental change." Nature 476(7360): 320-323.

Skogh, C., A. Garm, D. E. Nilsson and P. Ekstrom (2006). "Bilaterally symmetrical rhopalial nervous system of the box jellyfish Tripedalia cystophora." Journal of Morphology 267(12): 1391-1405.

Soto, F., G. Lambrecht, P. Nickel, W. Stuhmer and A. E. Busch (1999). "Antagonistic properties of the suramin analogue NF023 at heterologously expressed P2X receptors." Neuropharmacology 38(1): 141-149.

Steele, R. E., C. N. David and U. Technau (2011). "A genomic view of 500 million years of cnidarian evolution." Trends Genet 27(1): 7-13.

Stockl, A. L., R. Petie and D. E. Nilsson (2011). "Setting the pace: new insights into central pattern generator interactions in box jellyfish swimming." PLoS One 6(11): e27201.

Strader, M. E., S. W. Davies and M. V. Matz (2015). "Differential responses of coral larvae to the colour of ambient light guide them to suitable settlement microhabitat." R Soc Open Sci 2(10): 150358.

Strauss, O. (2005). "The retinal pigment epithelium in visual function." Physiol Rev 85(3): 845-881.

Suga, H., V. Schmid and W. J. Gehring (2008). "Evolution and functional diversity of jellyfish opsins." Current Biology 18(1): 51-55.

Sun, H., D. J. Gilbert, N. G. Copeland, N. A. Jenkins and J. Nathans (1997). "Peropsin, a novel visual pigment-like protein located in the apical microvilli of the retinal pigment epithelium." Proceedings of the National Academy of Sciences of the United States of America 94(18): 9893-9898.

Sweeney, A. M., D. L. Des Marais, Y. E. Ban and S. Johnsen (2007). "Evolution of graded refractive index in squid lenses." J R Soc Interface 4(15): 685-698.

Taddei-Ferretti (1997). Biophysics of Photoreception: Molecular and Phototransductive Events. Singapore, World Scientific.

Taddei-Ferretti, C. and C. Musio (2000). "Photobehaviour of Hydra (Cnidaria, Hydrozoa) and correlated mechanisms: a case of extraocular photosensitivity." Journal of Photochemistry and Photobiology. B, Biology 55(2-3): 88-101.

Tarttelin, E. E., J. Bellingham, M. W. Hankins, R. G. Foster and R. J. Lucas (2003). "Neuropsin (Opn5): a novel opsin identified in mammalian neural tissue." FEBS Letters 554(3): 410-416.

Terakita, A. (2005). "The opsins." Genome Biol 6(3): 213.

Terakita, A., M. Koyanagi, H. Tsukamoto, T. Yamashita, T. Miyata and Y. Shichida (2004). "Counterion displacement in the molecular evolution of the rhodopsin family." Nat Struct Mol Biol 11(3): 284-289.

Terakita, A., T. Yamashita and Y. Shichida (2000). "Highly conserved glutamic acid in the extracellular IV-V loop in rhodopsins acts as the counterion in retinochrome, a member of the rhodopsin family." Proceedings of the National Academy of Sciences of the United States of America 97(26): 14263-14267.

Thompson, J. D., T. J. Gibson, F. Plewniak, F. Jeanmougin and D. G. Higgins (1997). "The CLUSTAL_X windows interface: flexible strategies for multiple sequence alignment aided by quality analysis tools." Nucleic Acids Res 25(24): 4876-4882.

Travis, G. H., M. Golczak, A. R. Moise and K. Palczewski (2007). "Diseases caused by defects in the visual cycle: retinoids as potential therapeutic agents." Annu Rev Pharmacol Toxicol 47: 469-512.

Tsukamoto, H., A. Terakita and Y. Shichida (2005). "A rhodopsin exhibiting binding ability to agonist all-trans-retinal." Proc Natl Acad Sci U S A 102(18): 6303-6308.

Untergasser, A., I. Cutcutache, T. Koressaar, J. Ye, B. C. Faircloth, M. Remm and S. G. Rozen (2012). "Primer3--new capabilities and interfaces." Nucleic Acids Res 40(15): e115.

van Straalen, N. M., Roelofs, D. (2012). “An Introduction to Ecological Genomics”. Oxford: Oxford University Press. Second edition.

Velarde, R. A., C. D. Sauer, K. K. Walden, S. E. Fahrbach and H. M. Robertson (2005). "Pteropsin: a vertebrate-like non-visual opsin expressed in the honey bee brain." Insect Biochem Mol Biol 35(12): 1367-1377.

Vopalensky, P. and Z. Kozmik (2009). "Eye evolution: common use and independent recruitment of genetic components." Philosophical Transactions of the Royal Society of London. Series B: Biological Sciences 364(1531): 2819-2832.

Vopalensky, P., J. Pergner, M. Liegertova, E. Benito-Gutierrez, D. Arendt and Z. Kozmik (2012). "Molecular analysis of the amphioxus frontal eye unravels the evolutionary origin of the retina and pigment cells of the vertebrate eye." Proc Natl Acad Sci U S A 109(38): 15383-15388.

Watanabe, Y., K. Kawasaki, N. Miki and C. H. Kuo (1990). "Isolation and analysis of the human MEKA gene encoding a retina-specific protein." Biochem Biophys Res Commun 170(2): 951-956.

Wistow, G. J. and J. Piatigorsky (1988). "Lens crystallins: the evolution and expression of proteins for a highly specialized tissue." Annu Rev Biochem 57: 479-504.

Xiong, W. H., E. C. Solessio and K. W. Yau (1998). "An unusual cGMP pathway underlying depolarizing light response of the vertebrate parietal-eye photoreceptor." Nat Neurosci 1(5): 359-365.

Yamada, E. (1982). "Morphology of vertebrate photoreceptors." Methods Enzymol 81: 3-17.

Yamashita, T., H. Ohuchi, S. Tomonari, K. Ikeda, K. Sakai and Y. Shichida (2010). "Opn5 is a UV-sensitive bistable pigment that couples with Gi subtype of G protein." Proceedings of the National Academy of Sciences of the United States of America 107(51): 22084-22089.

Yamasu, T. and M. Yoshida (1976). "Fine structure of complex ocelli of a cubomedusan, Tamoya bursaria Haeckel." Cell and Tissue Research 170(3): 325-339.

Yang, G. Q., T. Chen, Y. Tao and Z. M. Zhang (2015). "Recent advances in the dark adaptation investigations." Int J Ophthalmol 8(6): 1245-1252.

Yau, K. W. (1994). "Phototransduction mechanism in retinal rods and cones. The Friedenwald Lecture." Invest Ophthalmol Vis Sci 35(1): 9-32.

Yau, K. W. and R. C. Hardie (2009). "Phototransduction motifs and variations." Cell 139(2): 246-264.

Yoshida, M. (1979). "Extraocular photoreception." Handbook of sensory physiology VII/6A: 582-640.

Yoshida, R., T. Kusakabe, M. Kamatani, M. Daitoh and M. Tsuda (2002). "Central nervous system-specific expression of G protein alpha subunits in the ascidian Ciona intestinalis." Zoolog Sci 19(10): 1079-1088.

Yu, J. K., D. Meulemans, S. J. McKeown and M. Bronner-Fraser (2008). "Insights from the amphioxus genome on the origin of vertebrate neural crest." Genome Res 18(7): 1127-1132.

Zang, J., J. Keim, E. Kastenhuber, M. Gesemann and S. C. Neuhauss (2015). "Recoverin depletion accelerates cone photoresponse recovery." Open Biol 5(8).

Zhong, Z., L. Yang, Y. E. Zhang, Y. Xue and S. He (2016). "Correlated expression of retrocopies and parental genes in zebrafish." Mol Genet Genomics 291(2): 723-737.

Zhou, K., M. Zou, M. Duan, S. He and G. Wang (2015). "Identification and analysis of retrogenes in the East Asian nematode Caenorhabditis sp. 5 genome." Genome 58(7): 349-355.

Zou, M., B. Guo and S. He (2011). "The roles and evolutionary patterns of intronless genes in deuterostomes." Comp Funct Genomics 2011: 680673.

Zylka, M. J., X. Dong, A. L. Southwell and D. J. Anderson (2003). "Atypical expansion in mice of the sensory neuron-specific Mrg G protein-coupled receptor family." Proc Natl Acad Sci U S A 100(17): 10043-10048.